



City Research Online

City, University of London Institutional Repository

Citation: Pacheco Cutillas, M. (2004). The relative loss of chromatic and achromatic sensitivity in primary open angle glaucoma and the normal ageing process. (Unpublished Doctoral thesis, City, University of London)

This is the accepted version of the paper.

This version of the publication may differ from the final published version.

Permanent repository link: <https://openaccess.city.ac.uk/id/eprint/30734/>

Link to published version:

Copyright: City Research Online aims to make research outputs of City, University of London available to a wider audience. Copyright and Moral Rights remain with the author(s) and/or copyright holders. URLs from City Research Online may be freely distributed and linked to.

Reuse: Copies of full items can be used for personal research or study, educational, or not-for-profit purposes without prior permission or charge. Provided that the authors, title and full bibliographic details are credited, a hyperlink and/or URL is given for the original metadata page and the content is not changed in any way.

City Research Online:

<http://openaccess.city.ac.uk/>

publications@city.ac.uk

**The Relative Loss of Chromatic and Achromatic
Sensitivity in Primary Open Angle Glaucoma and
the Normal Ageing Process**

Mireia Pacheco Cutillas

**Submitted in fulfilment of the requirements for
the degree of Doctor of Philosophy**

**Applied Vision Research Centre,
Department of Optometry and Visual Science,
City University, London**

December, 2004

Table of Contents

Table of Contents	3
List of Figures.....	11
List of Tables	19
Acknowledgements.....	23
Abstract.....	27
Key of abbreviations:	28
1 Introduction.....	29
1.1 Aims of the thesis.....	29
1.2 Structural and physiological aspects of the visual system relevant to glaucoma.....	30
1.2.1 Retina.....	31
1.2.1.1 Topography of the retina: Central versus peripheral regions.....	31
1.2.1.2 Cells and synaptic connections in the retina	33
1.2.2 Optic Nerve	45
1.2.2.1 Intraocular optic nerve: retinal nerve fibre layer and the optic disc..	46
1.2.2.2 Lamina cribrosa and the retrobulbar portion of the optic nerve	47
1.2.2.3 Blood supply	48

1.2.3	The central visual pathways.....	48
1.2.3.1	Optic chiasm: Semidecussation of optic nerve fibres	48
1.2.3.2	Lateral Geniculate Nucleus.....	49
1.2.3.3	Primary visual cortex	53
1.2.3.4	Prestriate cortex	55
1.2.4	Parallel processing of the visual system	56
1.3	Introduction to the disease. Limitations in its diagnosis and treatment	59
1.4	Clinical changes in glaucomatous optic neuropathy.....	61
1.5	Mechanisms of damage in the pathogenesis of glaucomatous optic neuropathy	62
1.5.1	Mechanical damage.....	62
1.5.2	Poor vascular function	63
1.5.3	Abnormal axonal transport.....	64
1.5.4	Selective cell loss	66
1.6	POAG: a disease of the elderly. Ageing factors	67
1.7	Loss of visual function in POAG	69
1.7.1	Perimetry in glaucoma	70
1.7.2	Contrast Sensitivity.....	71
1.7.2.1	Spatial contrast sensitivity.....	72
1.7.2.2	Temporal contrast sensitivity: Flicker sensitivity.....	72
1.7.2.3	Frequency-doubling perimetry	73

1.7.3	Chromatic discrimination in Glaucoma.....	74
1.7.3.1	Colour vision processing in primates	74
1.7.3.2	Colour vision deficiencies: congenital versus acquired defects.....	75
1.7.3.3	Classification of acquired colour vision deficiencies.....	77
1.7.3.4	Assessment of colour vision defects in glaucoma.....	79
1.7.3.5	Acquired colour vision deficiencies in glaucoma.....	85
1.7.4	Motion discrimination in Glaucoma.....	88
1.7.5	Parallel pathway isolating studies.....	89
2	Research outline.....	91
2.1	Rationale behind the study.....	91
2.1.1	Selective stimulation of the visual parallel pathways.....	91
2.1.2	Luminance and colour channels	92
2.1.3	Glaucomatous damage	92
2.1.3.1	Preferential damage and reduced redundancy theories.....	93
2.1.3.2	Functional defects	93
2.1.3.3	Colour vision testing in glaucoma	93
2.2	Objectives of the study	94
2.3	Logistics	95
3	Experimental methods.....	97
3.1	Summary	97
3.2	Random luminance modulation (RLM)	97
3.3	Description of equipment	98

3.4	Experimental conditions	100
3.5	Measurement procedure	101
3.6	Visual Stimuli	104
3.6.1	Measurement of Chromatic Discrimination Ellipses	104
3.6.2	Measurement of Luminance or Chromatic Motion Discrimination Direction 106	
3.7	Subjects	112
3.7.1	Assessment and diagnosis	112
3.7.2	Primary open angle glaucoma (POAG) subjects.....	113
3.7.3	Subjects at risk of developing POAG	113
3.7.4	Control group.....	114
4	Characterisation of chromatic sensitivity in POAG.....	115
4.1	Introduction.....	115
4.2	Aims of the study.....	116
4.3	Subjects and method.....	116
4.3.1	Subjects.....	116
4.3.2	Methods.....	120
4.4	Results	121
4.4.1	Chromatic discrimination ellipses.....	121
4.4.1.1	Control group.....	121
4.4.1.2	POAG group.....	122

4.4.1.3	At risk group	124
4.4.1.4	Comparison of CD ellipses for the three groups	125
4.4.1.5	Characterisation of the CD loss (CD ellipses' changes) with progression of the disease	130
4.4.2	Patterns of chromatic discrimination loss in glaucoma.....	140
4.4.3	Chromatic sensitivity loss along R/G and B/Y colour opponent channels 153	
4.4.3.1	R/G and B/Y chromatic discrimination loss as a function of severity of the disease	158
4.4.3.2	Relative loss of chromatic discrimination in glaucoma	165
4.4.4	Validation of the CD sensitivity measurements as a method for detecting glaucoma.....	170
4.5	Summary of results	176
4.6	Discussion	177
5	Chromatic and achromatic loss of sensitivity in POAG.....	187
5.1	Introduction	187
5.2	Aim	188
5.3	Subjects and method	188
5.3.1	Subjects	188
5.3.2	Methods	191
5.4	Results	191
5.4.1	Effect of background noise level.....	192
5.4.2	Effect of glaucoma on chromatic and achromatic sensitivity	194

5.4.2.1	Relative loss of sensitivity with glaucoma	197
5.4.2.2	Loss of chromatic and achromatic sensitivity and its relation to severity of visual field loss	201
5.5	Summary of main results	210
5.6	Discussion	211
6	Chromatic and achromatic loss of sensitivity in ageing	219
6.1	Introduction.....	219
6.2	Aim.....	220
6.3	Subjects and methods.....	220
6.3.1	Subjects.....	220
6.3.2	Methods.....	220
6.4	Results	221
6.4.1	Effect of background noise level	221
6.4.2	Relative loss of sensitivity with age	224
6.4.3	Effect of age across the span of life	233
6.4.4	Effect of age on regional sensitivity.....	239
6.4.4.1	Regional sensitivity in younger subjects.....	239
6.4.4.2	Regional sensitivity in older subjects	243
6.4.4.3	Differential effect of ageing on regional sensitivity	243
6.5	Summary of results	248
6.6	Discussion	249

6.6.1	Rate of chromatic and achromatic sensitivity loss with ageing	251
6.6.2	Regional sensitivity	252
7	Summary of results and conclusions	255
7.1	Summary of results	256
7.2	Overview and conclusions	259
7.3	Perspective	261
8	Appendices	263
8.1	Appendix of supporting publications.	263
8.1.1	Peer-reviewed published papers.	263
8.1.2	Conference abstracts	263
8.1.3	Other publications.....	263
8.2	Individual CD ellipses' cases.....	265
9	Reference list	273

List of Figures

- Figure 1.1: Three- dimensional diagram of the organisation of the human retina (from the Webvision <http://webvision.med.utah.edu>) 34
- Figure 1.2: Structure of a rod and a cone and connections with the RPE layer..... 36
- Figure 1.3: Diagram showing examples of spontaneous activity, an on response, an off response and plots a typical retinal ganglion cell receptive field. A ganglion cell receives excitatory connections from a number of photoreceptors and lateral inhibitory connections from a number of horizontal cells which receive input from the surrounding photoreceptors (Bruce & Green, 1990)..... 42
- Figure 1.4: Histological section through the primate lateral geniculate nucleus (LGN) to show the layering of the neurons into 4 parvocellular layers, 2 magnocellular layers and 6 koniocellular layers (from the Webvision <http://webvision.med.utah.edu>). 51
- Figure 1.5: Schematic diagram of the visual pathways from retinal ganglion cells to the higher visual areas (adapted from Merigan & Maunsell (1993)) 59
- Figure 1.6: Mechanisms of damage in the pathogenesis of glaucoma leading to apoptosis of ganglion cells (adapted from Flammer (2001)). 65
- Figure 3.1: Square array of achromatic checks forming the stimulus template..... 100
- Figure 3.2: CIE (x,y) chromaticity diagram showing the phosphor limits used for the motion discrimination direction experiment with the CAD test (Colour Assessment and Diagnosis Test) for a 12 cd/m² luminance background field..... 103
- Figure 3.3: An example of a frame of the stimulus used to measure chromatic discrimination ellipses showing the fixation target in the centre (foveal measurement)..... 105
- Figure 3.4: Effect of dynamic noise on the detection of luminance contrast defined motion. Mean luminance contrast thresholds for static and temporally modulated noise. Bars indicate 1 SE of the mean. 108

Figure 3.5: Simulation of a frame intended for foveal measurement.....	109
Figure 3.6: Simulation of a frame intended for the eccentric measurement.	110
Figure 3.7: An example of a frame of the stimulus used to measure motion direction discrimination thresholds for colour contrast defined signals.	110
Figure 3.8: An example of a frame of the stimulus used to measure motion direction discrimination thresholds for luminance contrast defined signals.....	111
Figure 3.9: Schematic drawing of the response button box.....	112
Figure 4.1: Ellipses fitted to the average chromatic discrimination thresholds, measured in the control group, along 12 directions in chromatic space. Measurements for fovea and 7 deg eccentricity are shown.	122
Figure 4.2: Ellipses fitted to the average chromatic discrimination thresholds, measured in the POAG group, along 12 directions in chromatic space. Measurements for fovea and 7 deg eccentricity are shown.	123
Figure 4.3: Ellipses fitted to the average chromatic discrimination thresholds, measured in the group at risk of developing glaucoma, along 12 directions in chromatic space. Measurements for foveal and 7 deg eccentricity are shown.	124
Figure 4.4: Box-and-whisker plots of the areas of the fitted ellipses, for foveal and 7 deg measurements, in each group tested.....	127
Figure 4.5: Box-and-whisker plots of the elongation of the fitted ellipses, for foveal and 7 deg measurements, in each group tested.....	127
Figure 4.6: Box-and-whisker plots of the orientation (in deg) of the fitted ellipses, for foveal and 7 deg measurements, in each group tested.	128
Figure 4.7: Ellipses fitted to the average CD thresholds, measured in the Early glaucoma group (AGIS=2-4). Measurements for foveal and 7 deg eccentricity are shown.	132

Figure 4.8: Ellipses fitted to the average CD thresholds, measured in the Moderate glaucoma group (AGIS=5-9). Measurements for foveal and 7 deg eccentricity are shown.	133
Figure 4.9: Ellipses fitted to the average CD thresholds, measured in the Advanced glaucoma group (AGIS>9). Measurements for foveal and 7 deg eccentricity are shown.	134
Figure 4.10: Box-and-whisker plots of the areas of the fitted ellipses, for foveal and 7 deg measurements, in each group tested.	137
Figure 4.11: Box-and-whisker plots of the elongation of the fitted ellipses, for foveal and 7 deg measurements, in each group tested.	137
Figure 4.12: Box-and-whisker plots of the orientation of the fitted ellipses, for foveal and 7 deg measurements, in each group tested.	138
Figure 4.13: An example of a POAG subject (PR) classified in stage 1 of CD loss. Red shows foveal and eccentric measurements for this subject compared to the average measurements in the control group (blue). Notice the similarity of the size and shape of the measurements in the control group.	141
Figure 4.14: An example of an At risk subject (RB) classified in stage 2 of CD loss. Red shows foveal and eccentric measurements for this subject compared to the average measurements in the control group (blue). Notice the enlargement of the eccentric measurements compared to the control group.	142
Figure 4.15: An example of a POAG subject (VF) classified in stage 3 of CD loss. Red shows foveal and eccentric measurements for this subject compared to the average measurements in the control group (blue). Notice the enlargement of the foveal and eccentric measurements compared to the control group.	143
Figure 4.16: An example of a POAG subject (EC) classified in stage 4 of CD loss. Red shows foveal and eccentric measurements for this subject compared to the average measurements in the control group (blue). Both foveal and eccentric measurements are large compared to the control group. However, the eccentric to foveal area ratio is less than 5.7 due to the relative increase in size of the foveal area.	144

Figure 4.17: An example of a POAG subject (EB) classified in stage 5 of CD loss. Red shows foveal and eccentric measurements for this subject compared to the average measurements in the control group (blue). This case shows an elongated foveal ellipse compared to the control group. 145

Figure 4.18: An example of a POAG subject (JD) classified in stage 6 of CD loss. Red shows foveal and eccentric measurements for this subject compared to the average measurements in the control group (blue). This case shows massive areas for both foveal and 7 deg measurements compared to the control group. 146

Figure 4.19: Distribution of CD loss stage with severity of VF damage as measured by the AGIS score in POAG and At risk subjects. 148

Figure 4.20: Mean log thresholds along the 60 deg and 240 deg directions and along the 150 deg and 330 deg direction for foveal and 7 deg eccentricity measurements in each group tested..... 154

Figure 4.21: Box plots of the B/Y and R/G thresholds for foveal and 7 deg eccentricity measurements in each group tested. 155

Figure 4.22: Box plots of the B/Y and R/G thresholds for foveal and 7 deg eccentricity measurements are shown for each POAG subgroup classified according to the severity of VF damage (AGIS score)..... 159

Figure 4.23: Comparison of foveal measurements of R/G and B/Y chromatic log threshold increases in the POAG and At risk subjects as a function of visual field loss (AGIS score). Linear functions are fitted to the data..... 160

Figure 4.24: Comparison of 7 deg measurements of R/G and B/Y chromatic log thresholds increases in the POAG and At risk subjects as a function of visual field loss (AGIS score)..... 161

Figure 4.25: A comparison of threshold differences for B/Y with those for R/G sensitivities (log threshold units), for each individual subject. The triangles represent differences for individual POAG subjects, from the control mean. The X symbols represent differences for individual At risk subjects from the control mean. The circles represent differences for each control subject compared to the

- mean for control subjects (the point (0,0) represents the “mean control value”). POAG cases are classified according to the severity of glaucomatous damage. 166
- Figure 4.26: Threshold differences for B/Y sensitivity compared with those for R/G sensitivities (log threshold units), for each individual POAG, At risk and control subject. For details see caption to Figure 4.25. 167
- Figure 4.27: Same data as Figure 4.25 above. The mean regression line and the confidence intervals for the control group have been plotted instead of the individual data ($R^2=0.60$). Point (0,0) is the mean for the control group. Continuous lines along the x and y axes show the upper limit for the reference range in the control group. 168
- Figure 4.28: Same data as Figure 4.26 above. The mean regression line and the confidence intervals for the control group have been plotted instead of the individual data ($R^2=0.17$). Point (0,0) is the mean for the control group. Continuous lines along the x and y axes show the upper limit for the reference range in the control group. 169
- Figure 4.29: Plot of discriminant function 1 and 2 for the control, POAG and At risk groups. 172
- Figure 5.1: Mean chromatic (R/G and B/Y) and achromatic motion discrimination thresholds (log units) of the control and POAG observers, as a function of the three levels of background LC noise (12, 24 and 48%) at foveal and 7 deg eccentricity locations. Bars indicate 2 SE of the mean. 193
- Figure 5.2: Box-plots of the log thresholds for chromatic (R/G and B/Y) and achromatic sensitivity allow a comparison of the POAG (N=13) and control (N=17) groups. The box contains the middle 50% of the cases. 195
- Figure 5.3: A comparison of the threshold differences (log units) for B/Y to those for R/G sensitivity for each individual subject. The triangles represent the difference for each POAG subject from the control group mean. The colour code represents the severity of visual field loss (AGIS score sub-classification section 5.3.1) for each POAG subject. The circles represent differences for individual control observers compared to the mean value for control observers (the point (0,0)

represents the mean control value). The mean regression line and the confidence intervals for the control group have been plotted ($R^2=0.85$ and $R^2=0.85$, for foveal and 7 deg data, respectively). Continuous lines along the x and y axes show the upper limit for the reference range in the control group (+1.96 SD). 199

Figure 5.4: Threshold differences for B/Y sensitivity plotted against those for achromatic sensitivity (log units), for each individual POAG and control subject. For details see caption to Figure 5.3. 200

Figure 5.5: Threshold differences for R/G sensitivity compared to those for achromatic sensitivity (log units), for each individual POAG and control subject. For details see caption to Figure 5.3. 200

Figure 5.6: Foveal and 7 deg eccentricity stimulus locations. The stimulus presentation at the fovea and at one of the four possible eccentric (sup temporal, sup nasal, inf temporal and inf nasal) measurements is shown overlapping the distribution of locations on the 24-2 Humphrey visual field program to demonstrate the area coverage in the visual field. The light sensitivity loss (dB) for the foveal and 7 deg locations was the average of the four corresponding HFA stimuli locations in the total deviation probability plot. 202

Figure 5.7: Achromatic and chromatic (R/G and B/Y) contrast log thresholds plotted as a function of severity of visual field loss (AGIS score) for the POAG subjects. ... 204

Figure 5.8: Comparison of foveal measurements of R/G and B/Y chromatic log threshold increases in the POAG subjects as a function of visual field loss (AGIS score). A quadratic function gave a statistically significant fit with the R/G threshold data, whereas the B/Y thresholds are equally well described by a linear function. This highlights the differential effect of the severity of the disease on B/Y and R/G thresholds. 205

Figure 5.9: Comparison of 7 deg measurements of R/G and B/Y chromatic log threshold increases in the POAG subjects as a function of visual field loss (AGIS score). 206

-
- Figure 5.10: Increase in achromatic and chromatic (R/G and B/Y) contrast log threshold as a function of the loss of light sensitivity (in dB) at the locus tested given by the HFA total probability plot for the POAG subjects. 208
- Figure 6.1: Mean log thresholds of the older and younger normal subjects for chromatic (R/G and B/Y) and achromatic sensitivity, as a function of the three LC background noise levels (12, 24 and 48%) used, at each location. Bars indicate 2 SE of the mean. 223
- Figure 6.2: Box-plots of the log thresholds for chromatic (R/G and B/Y) and achromatic sensitivity allow a comparison of the younger (N=13) and older (N=17) groups. The box contains the middle 50% of the cases. 226
- Figure 6.3: A comparison of threshold differences for R/G sensitivity to those for B/Y sensitivity (log units), for each subject. The circles represent the differences in log threshold units for each old observer from the young mean log threshold value. The triangles represent differences in log threshold values for each young observer compared to the mean log threshold value for young observers. Point (0,0) represents the mean young value. The solid line corresponds to the linear regression for the younger group ($R^2=0.31$ and $R^2=0.72$, for foveal and 7 deg data, respectively). The dotted lines correspond to the reference range for the younger group (+1.96 SD). 230
- Figure 6.4: Threshold differences for B/Y sensitivity compared to those for achromatic sensitivity (log units), for each individual subject. For details see caption to Figure 6.3. 231
- Figure 6.5: Threshold differences for R/G sensitivity compared to those for achromatic sensitivity (log units), for each individual subject. For details see caption to Figure 6.3. 232
- Figure 6.6: Distribution of achromatic log thresholds as a function of age. Each point represents data from a single observer. At the eccentric location each young subject displays 4 measurements, one for each quadrant. The solid line is the best fitting regression line for the data. 234

Figure 6.7: Distribution of R/G chromatic log thresholds as a function of age. For details see caption to Figure 6.6.....	234
Figure 6.8: Distribution of B/Y chromatic log thresholds as a function of age. For details see caption to Figure 6.6.....	235
Figure 6.9: Distribution of R/G chromatic motion discrimination log thresholds as a function of age. At the eccentric location each young subject displays 4 measurements, one for each quadrant. The solid line is the best fit for the quadratic model (Equation 1).	237
Figure 6.10: Distribution of B/Y chromatic motion discrimination log thresholds as a function of age. For details see caption to Figure 6.9.	237
Figure 6.11: Average and ± 2 SE for motion discrimination log thresholds of chromatic (R/G and B/Y) and achromatic sensitivities, measured for the fovea and four eccentric locations, in younger and older subjects.....	242
Figure 6.12: Effect of age on regional sensitivity. Mean threshold differences (in log units), between older and younger groups, for the fovea and each of the four eccentric locations tested, for chromatic (R/G and B/Y) and achromatic stimuli. All differences are statistically significant at the $p < 0.001$ level, apart from those marked (n.s.= not significant).	244

List of Tables

Table 1: Physiological differences comparing receptive field properties of cells in magnocellular and parvocellular layers.	52
Table 1.2: A comparison between the characteristics of congenital and acquired colour vision defects (from Birch, 1993).....	77
Table 1.3: Verriest's classification of acquired colour vision anomalies (Verriest, 1963).	78
Table 4.1: Summary of clinical characteristics of the twenty POAG eyes. *AGIS score for severity of visual field loss (section 3.7.1).....	118
Table 4.2: Details of clinical characteristics of eyes at risk of developing POAG. *AGIS score for severity of visual field loss (section 3.7.1).....	119
Table 4.3: Summary of the parameters of the ellipses fitted to the average CD thresholds, along 12 directions in chromatic space, for each of the groups tested.	125
Table 4.4: Mean values and SD for the area, elongation and orientation of the fitted ellipses in each group tested.....	126
Table 4.5: Mean values and SD for Log of the area, elongation and orientation of the fitted ellipses in each group tested.....	130
Table 4.6: Summary of the parameters of the fitted ellipses and mean areas for the At risk, Early, Moderate and Advanced glaucoma sub-groups.....	131
Table 4.7: Mean values and SD for the area, elongation and orientation of the fitted ellipses in each sub-group tested.....	136
Table 4.8: Mean values and SD for Log of the area, elongation and orientation of the fitted ellipses in each sub-group tested.	139
Table 4.9: Results for the POAG eyes.....	150

Table 4.10: Results for the eyes at risk of developing POAG	151
Table 4.11: B/Y and R/G average log thresholds and SD for control, POAG and At risk groups at each location tested.....	155
Table 4.12: Pairwise comparisons of R/G and B/Y sensitivity of the Control, POAG and At risk group means for LSD post hoc test, measured at the fovea.	157
Table 4.13: Pairwise comparisons of R/G and B/Y sensitivity of the Control, POAG and At risk group means for Tamhane post hoc test, measured at 7 deg eccentricity.	158
Table 4.14: B/Y and R/G log thresholds mean and SD for control, and each of the POAG subgroups tested.	159
Table 4.15: Pairwise comparisons of R/G and B/Y sensitivity of the Control, At risk and POAG subgroups means for LSD post hoc test, measured at the fovea.	163
Table 4.16: Pairwise comparisons of R/G and B/Y sensitivity of the Control, At risk and POAG subgroups means for Tamhane post hoc test, measured at 7 deg eccentricity.....	164
Table 4.17: Structure matrix table for control, At risk and POAG groups showing correlations between discriminating variables and discriminant functions.....	171
Table 4.18: Discriminant analysis classification results for control, POAG and At risk groups. The number and percentage of cases correctly classified and misclassified are displayed.....	173
Table 4.19: Discriminant analysis classification results for control and POAG groups. The number and percentage of cases correctly classified and misclassified are displayed.....	174
Table 4.20: Structure matrix table for control and POAG group showing correlations between discriminating variables and discriminant functions.....	174

Table 4.21: Discriminant analysis classification results for control, At risk and all POAG subgroups. The number and percentage of cases correctly classified and misclassified are displayed.	175
Table 5.1: Summary of clinical characteristics of the thirteen POAG eyes. *AGIS score for severity of visual field loss (see section 3.7.1).	189
Table 5.2: The mean log thresholds, for the three levels of noise used, for achromatic and chromatic (R/G and B/Y) conditions for the control and the glaucoma (POAG) groups, at both locations tested.	195
Table 5.3: Achromatic, B/Y and R/G mean log threshold differences between POAG and control groups for the foveal and eccentric locations tested.	196
Table 5.4: Spearman's rho correlation coefficients for the rank correlation between chromatic (R/G and B/Y) and achromatic log thresholds, and AGIS score and loss of light sensitivity at the locus tested.	209
Table 6.1: The mean and SD for the log thresholds for young and old normal groups are shown for achromatic and chromatic (R/G and B/Y colour confusion axes) conditions, at both locations tested.	225
Table 6.2: Independent samples t-test for Achromatic, B/Y and R/G log thresholds between older and younger group for both foveal and eccentric locations tested.	227
Table 6.3: Pearson's correlation coefficients for the achromatic and chromatic (R/G and B/Y) log threshold differences in the older group.	233
Table 6.4: Coefficients of determination (R^2) and increase in mean log threshold (reduction in sensitivity) for the linear regression model fitted to the data, for each condition tested.	236
Table 6.5: Summary of parameter fits for quadratic function fitted to the chromatic measurements.	236

Table 6.6: Average and SD for motion discrimination of chromatic (R/G and B/Y) and achromatic log thresholds measured for younger and older subjects at the fovea and all eccentric locations. 241

Table 6.7: Independent samples t-test for chromatic (R/G and B/Y) and achromatic mean log threshold differences between older and younger groups, measured at the fovea and four eccentric locations. 245

Table 6.8: Effect of age on regional sensitivity. Mean log thresholds differences, between the older and younger groups, for the fovea, and the superior and inferior eccentric locations tested, for chromatic (R/G and B/Y) and achromatic conditions. 246

Table 6.9: Independent samples t-test for mean log threshold differences with age, for achromatic, B/Y and R/G sensitivities measured at the fovea and the superior and inferior locations. 247

Acknowledgements

I would like to gratefully acknowledge the invaluable help of my supervisors J.L. Barbur and D.F. Edgar. My special thanks to David Edgar for his close guidance throughout. I sincerely thank them for all their involvement in directing my research.

To the College of Optometrists for their financial support, which was much appreciated.

To Arash Sahraie for all his help in those early times of ignorance.

To David Crabb and Miquel Ralló for their statistical advice.

To Mr Philip Bloom, consultant ophthalmologist, who granted me access to his glaucoma clinic at the Western Eye Hospital and allowed me to collect data from his patients.

To my colleagues in Spain at the Departament d'Optica i Optometria (Universitat Politecnica de Catalunya, UPC) for their support, encouragement and patience over these years.

To my friends and family for their constant source of support and encouragement. In particular to my Mother, Francesca, for her endless help and constant backing in difficult times. To David, who more than anyone knows about the sacrifices and determination required to complete a project like this. His encouragement and support in the pursuit of this project never failed.

Finally, my tribute to all those willing volunteers and patients who generously gave up their valuable time to participate in this study, without them this project would have not been possible.

Declaration

I grant powers of discretion to the University Librarian to allow this thesis to be copied in whole or in part without further reference to me. This permission covers only single copies made for study purposes, subject to normal conditions of acknowledgement.

"Life is short, and Science is long; the occasion fleeting, experiment fallacious,
and judgement difficult"

(Hippocrates of Kos, circa 400 B.C.)

Abstract

Primary open angle glaucoma is a progressive and relatively common disease. Damage to the retinal ganglion cells causes characteristic structural changes in the optic nerve head, progressive loss of visual function and eventually blindness. Early detection of this disease is therefore desirable. It has been suggested that the assessment of impaired visual function in glaucoma can be made more sensitive by the selective isolation of specific stimulus attributes. An important aim of this investigation was to establish how the processing of colour or luminance contrast signals is affected differently in glaucoma.

Chromatic sensitivity was measured using a computerised colour display that employs isoluminant colour-defined stimuli buried in dynamic luminance contrast noise, stimulus conditions that isolate the use of colour signals and reveal loss of chromatic sensitivity. The characterisation of chromatic sensitivity loss in a group of POAG and at risk subjects was determined by measuring chromatic displacement (CD) thresholds along 12 directions in CIE - xy chromaticity chart, which allowed fitting CD ellipses. The analysis of the pattern of CD loss at different stages of the disease, both at the fovea and 7 deg, reveals the earliest signs of damage to be found at the paracentral location (7 deg). A non-selective CD loss with a characteristic increase in variance is observed early in the disease. As damage progresses foveal sensitivity is also progressively affected showing a greater B/Y relative loss, which becomes similar and even exceeded by the R/G loss when the disease is established. For moderate and advanced stages of the disease, the relative loss becomes greater for the R/G thresholds at both foveal and 7 deg. The test showed an overall success rate of 71% in identifying cases correctly.

In addition, moving, colour-defined stimuli designed to isolate either the transient luminance channel or the R/G and B/Y chromatic colour opponent mechanisms were used to find evidence of preferential damage for detection of one or the other of these stimulus attributes. Findings in patients with POAG and normal subjects of similar and younger age were compared. The relative increase of chromatic (R/G and B/Y) and achromatic thresholds was determined with ageing and glaucomatous damage. Although both mechanisms were significantly affected by POAG damage, the chromatic thresholds showed greater relative increase. The R/G and B/Y chromatic thresholds increased differently as a function of the severity of visual field loss. The B/Y sensitivity showed the greatest loss in early glaucoma subjects, however the R/G mechanism showed a faster rate of threshold increase and a better correlation with severity of field loss than B/Y thresholds. Ageing affected significantly both the chromatic (R/G and B/Y) and achromatic mechanisms. Chromatic threshold increases were on average twice the increase observed in the achromatic mechanism for foveal and parafoveal measurements. The rate of increase, as a function of age, in chromatic thresholds (along R/G and B/Y mechanisms) showed an accelerated fashion from the 5th-6th decade onwards. Meanwhile the achromatic thresholds increased at a slower, linear rate throughout life. In spite of the initial, more rapid increase along the B/Y colour opponent system (particularly for foveal thresholds), there were no significant differences between the rate of ageing for R/G and B/Y mechanisms. The largest age-related loss of chromatic sensitivity occurs in the lower hemifield for the B/Y mechanism.

In conclusion, both the glaucomatous damage and the ageing process lead to reduction in both R/G and B/Y chromatic sensitivity. The relative B/Y versus R/G chromatic loss in POAG depends on the severity of glaucomatous damage. The first signs of chromatic discrimination loss in the patients at risk of suffering POAG appear in the paracentral locations (7 deg) and are characterised by a non-selective loss of chromatic sensitivity and an increased inter- and within-subject variability. The relative age-related loss of R/G and B/Y sensitivity is mostly non-selective and independent of stimulus location.

Key of abbreviations:

AGIS: Advanced Glaucoma Intervention Study
B/Y: Blue/ yellow
CAD test: Colour Assessment and Diagnosis test
CC: Chromatic contrast
CD: Chromatic displacement
CIE: Commission Internationale de l'Eclairage
CO: Carbon monoxide
FDT: Frequency Doubling Perimetry
F-M 100 Hue test: Farnsworth- Munsell 100 Hue test
HFA: Humphrey Field Analyser
IN: Inferior Nasal
IOP: intra-ocular pressure
IT: Inferior Temporal
L- cone: Long Wavelength cone
LC: Luminance contrast
LGN: Lateral geniculate nucleus
LOCS: Lens Opacity Classification System
M- cone: Medium Wavelength cone
NRR: Neuroretinal rim
OH: Ocular hypertensive
POAG: Primary Open Angle Glaucoma
R/G: Red/ green
RLM: Random Luminance Modulation
RPE: Retinal Pigment Epithelium
SAP: Standard Automated Perimetry
S-cone: Short Wavelength cone
SN: Superior Nasal
ST: Superior Temporal
SWAP: Short-wavelength automated perimetry
VEP: Visual Evoked Potentials

1 Introduction

This chapter begins by stating the aims of this thesis together with a brief description of the factors motivating this research. An overview of the anatomy and physiology of the visual pathways from retina to brain follows. Emphasis will be placed on the structural and functional organisation of the retina, optic nerve and higher visual pathways to help our understanding of the vision processing, particularly colour perception, and the pathogenesis of glaucomatous neuropathy. Then, the limitations in the diagnosis of glaucomatous optic neuropathy, the mechanisms of damage in its pathogenesis and the most relevant histopathological studies of primate and human glaucoma related to the selective cell loss theories are discussed. Next, the neurological and optical ageing related factors that usually accompany the disease and can also contribute to visual function loss are revised. Finally, the results of conventional and non-conventional psychophysical tests relevant to glaucoma are summarised, focusing further on chromatic discrimination and the isolation of functional parallel visual mechanisms.

1.1 Aims of the thesis

There is a current controversy in glaucoma research on the relative level of damage to the visual mechanisms. Histological evidence of preferential damage to large optic nerve fibres in human and experimental glaucoma has provided the enthusiasm for developing new psychophysical tests aimed at detecting magnocellular dysfunction. However, these results have been challenged (Harwerth *et al.*, 2002; Morgan *et al.*, 2000). Evidence for parvocellular function deficits in glaucoma has also been provided by studies aimed to isolate the B/Y mechanism (Johnson *et al.*, 1993a; Johnson *et al.*, 1993b; Sample *et al.*, 1994) or even the R/G mechanisms (Alvarez *et al.*, 1997; Feliuss *et al.*, 1995b; Greenstein *et al.*, 1996; Kalloniatis *et al.*, 1993). Thus, size-dependent vulnerability cannot be sustained as the only basis for damage in glaucoma. The important question is whether there are visual functional channels that are relatively

more susceptible to glaucomatous insult. If that were the case the development of a test able to isolate its function would facilitate the early detection of the disease. On the other hand, the relative loss of sensitivities may vary through the course of the disease, or as a function of the eccentricity. Therefore, this information will help to select the best stimulus parameters in order to enhance the specificity and sensitivity of the test.

The present thesis' main objective is twofold. First, to characterise the total loss of chromatic discrimination ability of POAG subjects by determining the pattern of loss at different stages of the disease. It is widely accepted that colour vision is diminished in glaucoma. However, there is some controversy regarding the degree of B/Y and R/G deficit/ involvement and whether the underlying mechanisms of sensitivity loss differ at different stages or at different retinal eccentricities. It is important to establish the relative loss since a test designed to detect early damage might not necessarily be equally effective at monitoring progression of the disease.

Secondly, we aimed to determine the relative loss of chromatic and achromatic sensitivity in POAG subjects using tests designed to isolate the responses of the colour (R/G and B/Y) and luminance mechanisms.

In addition, a normal database obtained from a group of healthy younger and older control subjects was examined and compared with the POAG subjects. This not only allowed us to establish whether POAG subjects were within a normal or abnormal range of responses, but also extended the knowledge of how chromatic and achromatic sensitivities change as a function of age and the differential effect of ageing on different visual mechanisms.

1.2 Structural and physiological aspects of the visual system relevant to glaucoma

In order for any visual function to take place visible light from the outside world has to traverse the transparent media of the eye and reach the retina. The retina is composed of cells that can transform this physical energy into a neural signal, which can be sent to the brain where visual sensation takes place.

This section describes how this takes place by outlining the anatomy and physiology of the visual pathway from retina to brain. Emphasis will be placed on the structural and functional organisation of the retina, optic nerve and higher visual pathways to help our understanding of the pathogenesis of glaucomatous neuropathy. The mechanisms of glaucomatous damage to these structures will be discussed in section 1.5.

1.2.1 Retina

The retina is a thin layer, which lines the back of the eye. Ganglion cells lie innermost in the retina, and the photoreceptors (the rods and cones) lie outermost in the retina against the pigment epithelium and choroid. A description of its layers and components are given in section 1.2.1.2.

The job of the retina is to detect the light first, and secondly to inform the brain about the features of the image to allow the construction of a mental picture of the external objects. Light travels through the thickness of the retina and finally reaches and activates the photoreceptors. The visual pigment in the photoreceptors processes the absorption of photons by means of photochemical reactions, which are finally translated into an electrical message able to stimulate succeeding neurones of the retina. At the end of this neural processing the ganglion cells will transmit the retinal message to the brain along the optic nerve.

1.2.1.1 Topography of the retina: Central versus peripheral regions.

The adult retina has about 80 to 110 million rods and 4 to 5 million cones (Curcio *et al.*, 1990; Farber *et al.*, 1985). The differences in the relative concentration of the varieties of receptors give rise to two functionally specialised areas: the central and the peripheral retina.

The central retina is richer in cones since it contains both thinner cones and more of them as well as more ganglion cells. This gives rise to a region of high spatial resolution. On the other hand, the peripheral retina is rod-dominated which means a high sensitivity to detecting light but poor form discrimination. Physiologically, the central area is free of major blood vessels.

Cone density peaks in the fovea and then falls off sharply in all directions, although there is some concentration of cones along the horizontal meridian, particularly in the nasal retina. The rod density peaks in an elliptical ring around 15-20 deg. The highest rod concentration occurs in the superior retina (Curcio *et al.*, 1990; Farber *et al.*, 1985). The extent of the cone-rich area is about 5.5 mm in diameter and is marked by the presence of variable amounts of a yellow carotenoid-type pigment, which lies in the photoreceptor axons and the inner retinal cells, and gives the name to the region, the macula lutea. The intensity of the yellow pigment varies considerably from individual to individual and can have some effect on colour perception (see section 1.6).

At the centre of the macula is the fovea, which occupies about 5 degrees of the retina. Here the ganglion cells are piled into six layers so making this area the thickest portion of the entire retina. In the centre of the fovea there is a region of 54 mins of arc, termed the foveola, with the highest concentration of cones and free of rods (Cohen, 1992). Williams *et al.* (1981) demonstrated that the central 25 min are also free of blue cones. The foveola consists entirely of the outer, the inner segments and the cell bodies of the photoreceptors, and the glial cell processes. The axons of the photoreceptors are pushed out of the foveal area. In the same way, the horizontal and bipolar neurones and those amacrine and ganglion cells with which they interact and from which they receive information, are displaced. So, in the foveolar regions all these elements are missing, making it the thinnest portion of the retina. In contrast, the region of the optic nerve head has no retina or photoreceptors, producing a blind spot in the visual field.

In the central retina, the cones have oblique axons displacing their cell bodies from their synaptic pedicles in the outer plexiform layer (OPL). These oblique axons with accompanying Muller cell processes form a pale-staining fibrous-looking area termed as the Henlé nerve fibre layer (section 1.2.1.2.b). The latter layer is absent in the peripheral retina.

Throughout the retina the major blood vessels of the retinal vasculature supply the capillaries that run into the neural tissue. Capillaries are found running through all parts of the retina from the nerve fibre layer to the outer plexiform layer and even occasionally as high as in the outer nuclear layer (see section 1.2.1.2 for description). Nutrients from the vasculature of the choriocapillaris behind the pigment epithelium layer supply the delicate photoreceptor layer.

1.2.1.2 Cells and synaptic connections in the retina

The retina is composed of a layer of epithelial cells, three layers of nerve cell bodies and two layers of synapses (Figure 1.1). The outer nuclear layer (ONL) contains cell bodies of the rods and cones, the inner nuclear layer (INL) contains the somal of the bipolar cells and also those of the horizontal, amacrine, interplexiform, some "displaced" ganglion cells and the somal regions of the glial cells of Muller. The ganglion cell layer contains the cell bodies of most of the ganglion cells, displaced amacrine cells and the cell bodies of some astroglial cells (Cohen, 1992).

Dividing these nerve cell layers two synaptic contacts occur. The first area of synapses is the outer plexiform layer (OPL), between the ONL and the INL, where photoreceptors, horizontal cells and bipolar neurons synapse. The second synapsis of the retina is in the inner plexiform layer (IPL), situated between the INL and the ganglion cell layer. This is where synaptic interactions involving bipolar neurones, amacrine cells and ganglion cells take place.

The photoreceptors' signals are conveyed through the retina by what is called a vertical, or direct, pathway. The cone direct pathway consists of cones, bipolar and ganglion cells, together with horizontal cells (OPL) and amacrine cells (IPL), which transmit lateral inhibitory signals. The rod direct pathway is the same, but also has a relay stage at the amacrine cell level before the synapsing ganglion cells. There are also lateral pathways at two levels of the retina. One is the lateral connection between photoreceptors by means of horizontal cells. The other interconnects ganglion cells by means of different varieties of amacrine cells, which somehow interact to influence and integrate the ganglion cell signals. These lateral connections mean that signals supplied to vertical pathways from one or more photoreceptors are influenced indirectly by signals from neighbouring photoreceptors. It is by virtue of the lateral connections within the retina and the fact that several photoreceptors input to a bipolar cell, and several bipolars to a ganglion cell, that a great deal of data processing takes place already in the retina (Oyster C.W, 1999).

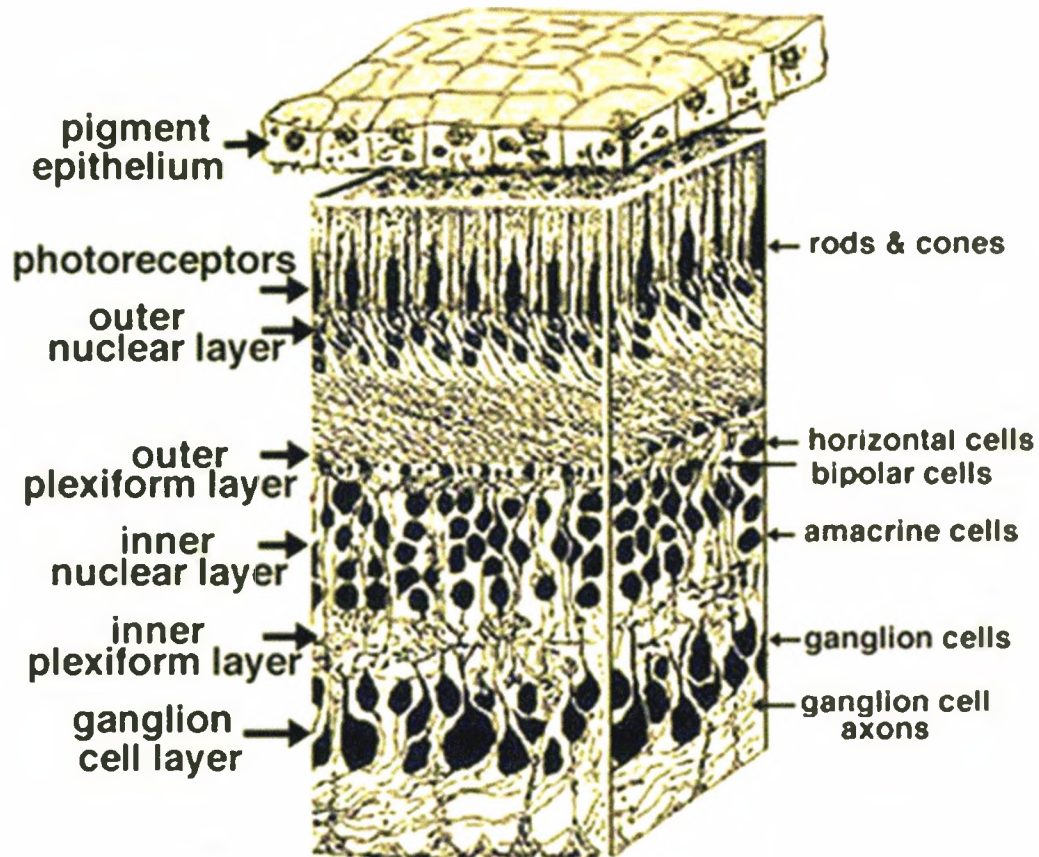


Figure 1.1: Three- dimensional diagram of the organisation of the human retina (from the Webvision <http://webvision.med.utah.edu>)

1.2.1.2.a Retinal Pigment Epithelium

The retinal pigment epithelium is implicated in the ocular transport of vitamin A, vital for the most efficient regeneration of visual pigment. It also has phagocytic functions, where portions of the tips of the outer segments are ingested and digested in the pigment epithelium, allowing for regeneration. The pigment in the cells also absorbs all the extra light, preventing it from scattering back into the eye. Finally, the epithelium forms an important blood-retinal barrier between the retina and the vascular system of the choroid and guards the special ionic environment of the retina (Ruskell, 1988).

1.2.1.2.b Visual Photoreceptors

Photoreceptors are highly specialised sensory neurones in which the different cellular components are stratified along the length of the cell. There are four types of photoreceptors: the rods, and three types of cones. The latter differ in spectral sensitivity and are referred to as L-, M-, and S-cones as their peak sensitivities are in the long (563 nm), middle (534 nm) and short- wavelength (420 nm) of the visible spectrum (Bowmaker & Dartnall, 1980), respectively.

The major elements of the photoreceptors are: the outer segment, the inner segment, the nucleus and the synaptic body. In cones the outer segment is conical and smaller than the inner segment, whereas the rods have inner and outer cylindrical segments of similar diameter (Figure 1.2). The outer segments of both rods and cones produce and contain the visual pigments, which capture the photons to begin the visual process. The pigments are combinations of the aldehyde of vitamin A and various proteins (Saari, 1992). The outer segment is adjacent to the pigment epithelium, portions of the tips of outer segment are ingested and digested. The inner segment is the photoreceptor's metabolic centre. At the apex of the inner segment there is a large collection of mitochondria.

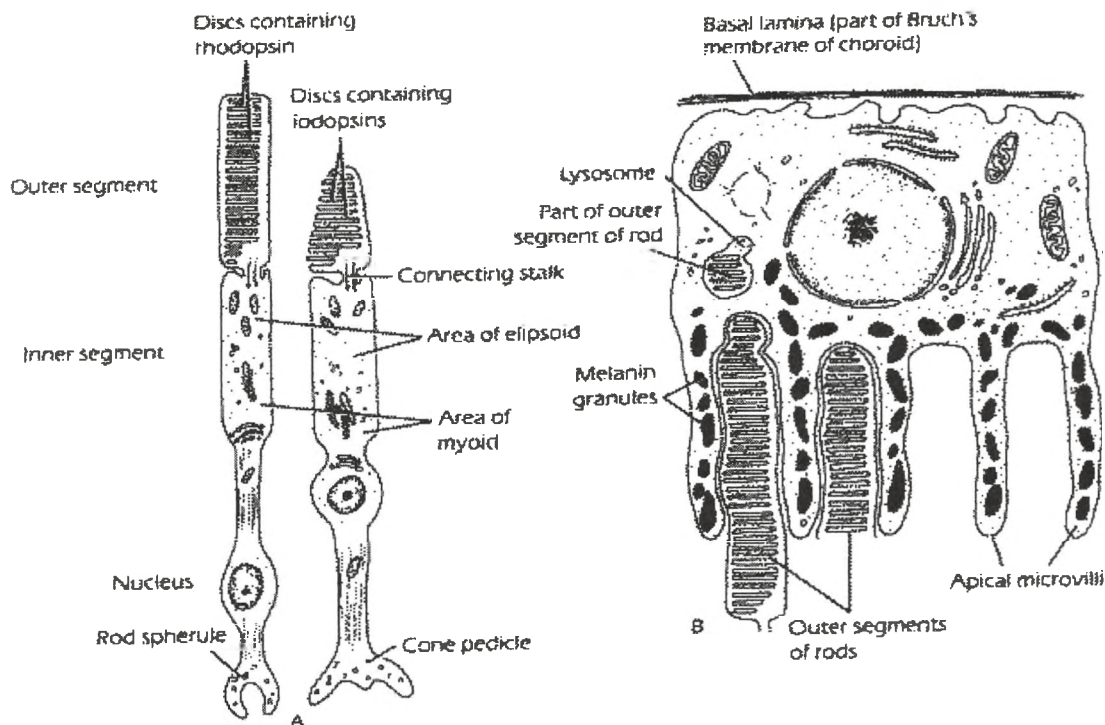


Figure 1.2: Structure of a rod and a cone and connections with the RPE layer.

Outer and inner segments are joined by a narrow connecting cilium. The inner segment is continuous with the nucleus and an axon ending as the synaptic terminal. The terminal contains synaptic vesicles with the neurotransmitter glutamate; the release of glutamate when the terminal's membrane depolarises is the mode of communication with other retinal neurones.

Rod cells make synaptic contact with adjacent cells via a rod spherule, and cones via a cone pedicle. Spherule and pedicle are connected to the cell body by a narrow process called the internal fibre. These internal fibres are elongated and almost horizontally layered in the fovea (see 1.2.1.1), and are known as the fibres of Henlé. The axis formed by the aligned inner and outer segments to the plane of the retina at the external limiting membrane is often not perpendicular. An analysis of the optical aspects revealed that the receptor axes are so tipped as to orient them to the exit of

the eye (Laties & Enoch, 1971) rather than to the centre of the ocular sphere (Stiles-Crawford effect). This maximises the ability of any one photoreceptor to capture light.

Rods are extremely sensitive to light and provide monochrome sensitivity to a wide range of intensities. They have poor spatial and temporal resolution. Scotopic vision is mediated by rods. Cones are not as sensitive as rods but provide high spatial resolution and colour vision under good lighting conditions. Cone initiated activity can dominate neuronal signalling even where rods outnumber cones in the retina.

One important role for the retina is to maintain the perception of contrast over the 12 log unit range of illumination in which vision is possible. This is possible since the photoreceptor's sensitivity is proportional to the antilogarithm of the pigment concentration, and thus it can be altered enormously by very small changes in the pigment concentrations. Although this ability to adapt to a range of light intensities in the environment is faster in cones, it is greater, in the long run, in rods (due to the convergence of many rods to one only ganglion cell). That way, the sensitivity to low intensity light in the peripheral retina is greater than in the central retina. Changes in pupil size help to achieve this adaptation process, by regulating the amount of light that falls in the retina.

The spatial distribution of the three different types of cones differs. S-cones constitute only about 10-18% of the cone population (Wassle & Boycott, 1991). The average spacing between the S-cones is 10 min of visual angle (Curcio *et al.*, 1991; Williams *et al.*, 1981). This wide spacing is consistent with the strong blurring of the short-wavelength component of the image due to chromatic aberration. This spatial defocus also implies that signals initiated by S-cones will vary slowly over time (a blurred boundary moving across on the retina will produce a gradual change in light sensitivity), so the S-cones will generally be coding slower temporal variations than the L- and M- cones (Wandell B.A., 1995). S-cones are absent from the central fovea and they have their peak sensitivity at 1 deg from the fovea (De Monasterio *et al.*, 1985).

L- and M- cones have a higher sampling density and form a regular pattern grid. This also matches the quality of the image in the portion of the wavelength spectrum where they have their peak sensitivity. It has not yet proved possible to distinguish between red and green cones, and there are conflicting reports of their relative frequencies, since there are larger inter-individual variations depending upon the nature of the

experimental method employed (Kremers *et al.*, 2000). According to Cicerone and Nerger (1989) there are about twice as many L- as M- cones. Calkins *et al.* (1995) found that the "non-blue" cones could be divided into two roughly equal groups according to the number of synapses subsequently made between bipolar and ganglion cells, and they hypothesise that these two groups correspond to red and green cones. Otherwise these two types show similar spatial distributions, and appear to be randomly intermingled.

1.2.1.2.c Cells and interactions of the inner nuclear layer

The inner nuclear layer, sometimes called the bipolar layer, not only has the somal bodies of the bipolar cells but also those of the horizontal, amacrine, interplexiform cells, some "displaced" ganglion cells and some somal regions of the glial cells of Muller. Their synaptic contacts are found in the inner plexiform layer. Cells depolarising to "light off" appear to have their connections in the outer half of the IPL, while those depolarising to "light on" appear to have their connection in the inner half. Cells responding both at on and off have terminals in both regions.

1.2.1.2.c.1 Bipolar cells

Photoreceptors synapse on to bipolar cells, in the outer plexiform layer, and send outputs to amacrine or ganglion cells. Bipolar cells receive inputs from either rods or cones. A rod bipolar cell may be in contact with between 15 and 40 rod terminals in primates (Kolb, 1991; Wässle & Boycott, 1991). Rod bipolar cells do not contact ganglion cells directly but synapse onto amacrine cells, which also link this information to the cone pathway. Thus, convergence in the rod system not only takes place at this level but also at the rod-bipolar synapse. This is the reason why the rod system has such a high sensitivity to light but poor resolution.

Cone bipolars may be divided into diffuse, midget and S-cone types. The diffuse collect information from several cones, whereas the midget type only contact with one cone and are found at the fovea, thus preserving the potential for high spatial resolution at the fovea. There is also a cone bipolar which is specific for S-cones only (Kolb,

1991; Mariani, 1984) creating a unitary pathway between S-cones and S-cone ganglion cells.

Bipolar cells have antagonistic centre-surround receptive fields and a further distinction may be made between ON- and OFF-cells, which are depolarised and hyperpolarized respectively by light falling on their receptive field centres.

1.2.1.2.c.2 Horizontal cells

Horizontal cells are also found in the outer plexiform layer. These are inhibitory interneurons, which laterally connect bipolars and photoreceptors. Three morphologically different types have been distinguished, HI, HII and HIII (Kolb, 1991). From the many lateral connections they form, horizontal cells contribute to the inhibitory receptive field surrounds of bipolar and ganglion cells, so that when light depolarises an on-bipolar, the horizontal cell dendrites cause inhibition at the edge of the illuminated area which sharpens contrast and enhances spatial resolution.

1.2.1.2.c.3 Interplexiform cells

Interplexiform cells should be mentioned here, as they synapse on to bipolar cells and horizontal cells in the outer plexiform layer (Dowling, 1990). However, their input occurs in the inner plexiform layer. The function of these cells is unclear, but they appear to be dopaminergic, and may therefore decrease the responsiveness of horizontal cells to light and decrease the electrical coupling between horizontal cells.

1.2.1.2.c.4 Amacrine cells

Amacrine cells are inter-neurons, which help in analysing the visual signal. They serve to integrate, modulate and interpose a temporal domain to the visual message presented to the ganglion cell (Kolb, 1991). They are unique in the retina because they have no morphologically definable axon, and their dendrites function as axons making incoming and outgoing synapses. They make contact with bipolar cells, other amacrine cells and the cell bodies and dendrites of ganglion cells.

There are at least 25 types of amacrine cell in the human retina, and these can be classified in terms of the stratification of their dendrites in the inner plexiform layer, their size, branching characteristics (Kolb, 1991) and the neurotransmitters they use (Wassle & Boycott, 1991).

1.2.1.2.d Ganglion cell layer

The ganglion cell layer has ganglion cells and displaced amacrine cells, as well as astroglial nuclei. Ganglion cell bodies form a single stratum in most of the retina, except in the macula where they are ranked in 6 to 8 rows, and in the fovea where they are virtually absent. Ganglion cell axons course towards the optic nerve forming the nerve fibre layer. It is estimated that there are about 1.2 million ganglion cells in the human retina (Jonas *et al.*, 1990).

There are different types of ganglion cells. Since the nerve fibres of the ganglion cells are believed to be damaged primarily in early glaucoma, the notion of the existence of different types of retinal ganglion cells can be of importance in understanding functional damage caused by the disease.

1.2.1.2.d.1 *Classification and functional characteristics of ganglion cells*

Most ganglion cells are either midget or parasol cells. Both are found at all retinal locations from fovea to periphery, but midget cells are smaller and more numerous than parasol. They come in ON and OFF varieties, based on the different levels at which their dendrites ramify in the IPL. Together, they account for more than 80% of all ganglion cells.

Midget ganglion cells receive information from a rather small group of cones. In fact near the fovea each midget cell makes contact with a single M- or L- cone via a single cone bipolar (Cohen, 1992), thus originating a one-to-one wiring channel. They have relatively small cell bodies and are much more common than parasol ganglion cells.

Parasol ganglion cells instead make contact with diffuse bipolars or, via amacrine cells, with rod bipolars. Parasol ganglion cells are relatively strongly represented towards the

peripheral retina (Schein & De Monasterio, 1987) and are about 3 to 5 times larger than midget ganglion cells. They make up only about 4 - 10% of the ganglion cells (Rodieck, 1998).

There is also another group of ganglion cells termed bistratified, which have terminals in both ON and OFF strata of the INL. They are in the minority, accounting for 10% or less of all ganglion cells and differ mainly in size, forming small- and large-field bistratified ganglion cells. Other types of ganglion cells have been described (Peterson & Dacey, 2000), but little is shown about them. So, a small portion of the retinal output (10%) and the supplied information to the brain is not completely known.

The retinal area from where a ganglion cell receives input determines the spatial extent of the receptive field of that cell, reflecting the amount of convergence onto it. It can range in size from that of one cone, to several degrees in diameter in the peripheral retina. However, in any given retinal region there is a wide spread of sizes of the receptive fields of ganglion cells. The midget cells tend to have a smaller receptive field, at any given area of the retina, than the parasol cells, which collect inputs from many receptors (Leventhal *et al.*, 1981).

Many ganglion cells have receptive fields with a concentric "centre-surround" organisation, as has been shown in monkey retina (De Monasterio & Gouras, 1975). In this case the receptive field centre responds antagonistically to the input signals as compared to the surround (Figure 1.3).

The retina can be considered as having parallel depolarising (ON-centre) and hyperpolarising (OFF-centre) informational pathways. The co-existence of both types of neurones provides for a very sharp mechanism to separate contrast edges in the visual image. There are also ON-OFF ganglion cells, which respond with a burst of impulses at stimulus onset and offset, and some of these are direction-sensitive (Dowling, 1987). They are thought to connect to both information streams. These are far less common than ON-centre and OFF-centre cells in the human and primate retina.

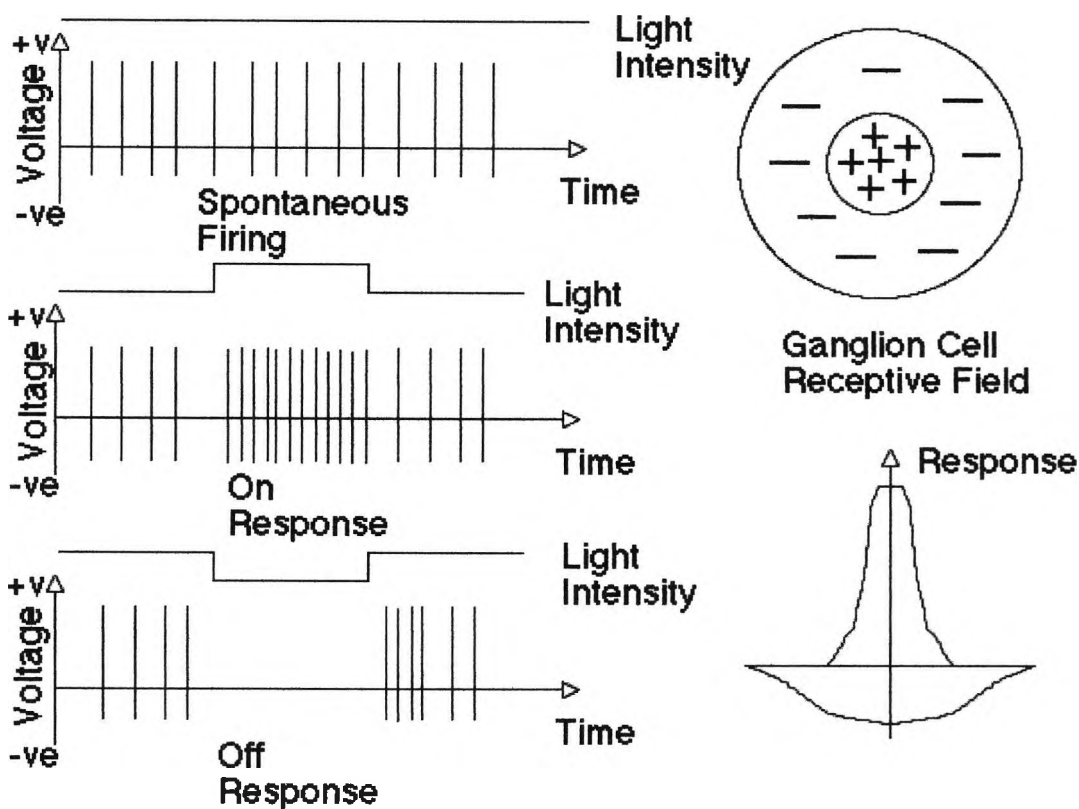


Figure 1.3: Diagram showing examples of spontaneous activity, an on response, an off response and plots a typical retinal ganglion cell receptive field. A ganglion cell receives excitatory connections from a number of photoreceptors and lateral inhibitory connections from a number of horizontal cells which receive input from the surrounding photoreceptors (Bruce & Green, 1990).

Another difference among ganglion cells is the way they signal intensity change. Gouras (1969) classified monkey ganglion cells as tonic cells, which fire all the time the stimulus is on, and phasic cells which only fire at stimulus onset. The latter having generally faster axonal conduction than tonic cells. In a similar way, Cleland *et al.* (1971) classified ganglion cells in the cat and described them as sustained (tonic) and transient (phasic). Sustained cells are not responsive to the rearrangement of dark and bright elements in their receptive fields provided that the net illumination is constant, whereas the transient ganglion cells would respond to each such change. In other

words, cells with sustained responses are signalling the magnitude of an intensity change, whereas those with transient responses report specially about the rate of contrast change.

Parasol ganglion cells have transient response properties since most of their synapses are from amacrine cells, which tend to respond with transient potentials. On the other hand, midget ganglion cells only receive 20% or less of their input from amacrine cells, and they reflect the more sustained character of their direct bipolar cells inputs (Dowling, 1987).

Retinal ganglion cells send continuous and spontaneous action potential signals. They fire a steady stream of impulses when no stimulus is present and then spike type discharges on top of this background noise when there is a visual stimulus.

Ganglion cells either respond to broadband (black versus white) portions of the spectrum or are excited (or inhibited) by relatively narrow portions of the spectrum, thus showing colour opponency. The first type receives signals from 2 cone varieties whose activation transiently excites the receptive field centre of the ganglion cell and inhibits its surround (Gouras & Link, 1966). Most of the midget ganglion cells show colour opponency, except for the midget ganglion cells in the peripheral retina. Most of the parasol cells get additive input from all receptor types, thus do not carry any chromatic information.

Colour opponent ganglion cells typically have sustained responses and fall into 2 major physiological classes.

First, the blue-yellow, which receive input from S- cones, opposed by combined M- and L- cone input. They have spatially overlapping ON and OFF receptive fields (Dacey, 1999). This ganglion cell is relatively rare, only 3% of the foveal ganglion cells (Calkins *et al.*, 1998a), and has been identified by Dacey and Lee (1994) as the small bistratified ganglion cell, which responds to increasing blue light (blue-ON) and decreasing yellow light (yellow-OFF; the additive combination of L- and M- cone signals) even when iso-luminant conditions are present. Most probably the blue-ON component is due to input from S-cone photoreceptors, via S-cone bipolars cells, whereas the yellow-OFF inputs are from diffuse bipolar and these in turn from L- and

M- cones. It has been hypothesised that this pathway forms a phylogenetically ancient colour system (Silveira *et al.*, 1999).

The second class is the red-green opponent cells, which receive antagonistic input from M- and L- sensitive cones, but they lack significant s-cone input. They have a centre-surround organisation. Red-green spectral opponency has long been linked to the midget ganglion cells in the central retina, but an underlying mechanism remains unclear. Midget ganglion cells receive input from a single midget bipolar cell, which in turn receives input from just one cone type. Thus, chromatic discrimination is not possible with a single cone type and another opposing input is required. A possible colour-opposing signal could come from lateral connections through amacrine cells, which would provide yellow (additive red and green) antagonism (Calkins & Sterling, 1996; Dacey, 1996; Dacey, 1999). Although less than optimal this would be a form of colour opponency. This colour contrast mechanism represents a first step in the analysis of colour signals within the retina.

Ganglion cells have also traditionally been classified according to their axonal targets in the lateral geniculate nucleus (LGN). Those projecting to the parvocellular layers of the LGN have been termed parvo- or P- cells, and similarly ganglion cells projecting to magnocellular layers of the LGN have been known as magno- or M- cells (Figure 1.4). There has been a tendency in the literature to associate midget ganglion cells with P- cells and parasol ganglion cells with M- cells. But other ganglion cell types must project to either the magno- or the parvo- layers (Oyster C.W, 1999). Finally, the small ganglion cells project to the koniocellular interlaminar region of the LGN (Dacey & Lee, 1994; Dacey, 1996; Martin *et al.*, 1997; Lee, 1996).

The functional properties of ganglion cells have been studied in the rhesus monkey (De Monasterio & Gouras, 1975). Fast, transient responding ganglion cells predominantly project to the magnocellular layers of the LGN and slower, sustained responding cells to the parvocellular layers of the LGN (Calkins & Sterling, 1996; De Monasterio, 1978; Derrington & Lennie, 1984; Schiller & Malpeli, 1978). This means that the P- pathway mainly carries sustained responses, with good resolution of different wavelength, shape, fine stereopsis, and moderate resolution of contrast to the LGN, whereas the M- pathway has good temporal resolution and excellent spatial contrast sensitivity, as required for discerning movement, direction of movement and fast flicker

(Livingstone & Hubel, 1987), but poor colour sensitivity and a cruder ability than the P systems for responding to textures and subtle patterns. Both systems are reactive to dark versus dark and can indicate brightness. These functional differences between P- and M- cells are maintained along 2 segregated parallel pathways, which extend from the retina to visual cortex and beyond (section 1.2.4).

Kaplan and Shapley (1986) investigated the contrast sensitivity of macaque retinal ganglion cells and found that cells projecting to M- layers are much more sensitive to luminance contrast than cells projecting to parvocellular layers. Purpura *et al.* (1988) showed that the contrast gain of cells projecting to M- layers is higher than that of cells projecting to parvocellular layers even at low levels of retinal illumination. They suggested that scotopic vision is mediated by cells projecting to M- layers, which must therefore indicate a high rod input into the M system.

Lee *et al.* (1990) also found that cells projecting to M- layers are more sensitive to luminance modulation, while cells projecting to parvocellular layers of the LGN are more sensitive to chromatic modulation under most conditions. Under isoluminant conditions, then, it would be expected that M- cells would have a minimum response. Experiments have shown that this is the case for two different techniques for finding isoluminance between two colours. Using heterochromatic flicker photometry, minimum flicker is seen between two colours at the same ratio as cells projecting to M- layers have their minimum response (Lee *et al.*, 1988). Kaiser *et al.* (1990) found that phasic (transient) cells show a minimum response near equal luminance as defined by the minimally distinct border technique.

1.2.2 Optic Nerve

Once all the neural processing in the retina has culminated the message concerning the visual image is transmitted to the brain along the axons of the ganglion cells. They course across the retina to the optic nerve head where they turn and leave the globe forming the optic nerve, which can be divided into the intraocular part and the retrobulbar part.

The number of fibres in monkey and human studies has been estimated to be on average 1,200,000 axons, with a range of about 800,000 to 1,500,000 (Jonas *et al.*,

1990). There is considerable variation from person to person, and even between two fellow eyes (Jonas *et al.*, 1999; Repka & Quigley, 1989; Sanchez *et al.*, 1986). This large range in the fibre count and variability has been suggested to indicate the anatomical reserve capacity of different individuals, which could account for differing susceptibility in progressive nerve disease like glaucoma and partly, for the variability of the psychophysical test results (Jonas J.B. & Nauman G.O.H., 1993).

1.2.2.1 Intraocular optic nerve: retinal nerve fibre layer and the optic disc.

The retinal nerve fibre layer is composed primarily of ganglion cell axons and some astrocytes, retinal vessels, and Muller cells processes. Ganglion cell axons run across the retina and converge towards the optic nerve head, which is about 3 mm nasal to the posterior pole of the eye and about 1 mm below the horizontal plane. They enter the optic nerve in an orderly and systematic way. Axons from retinal locations nasal, superior, and inferior to the optic nerve head follow direct paths to the nerve. Those on the nasal side of the fovea also have axons running directly to the nerve, known as the papillomacular bundle. Axons from all other ganglion cells follow arcuate paths around the fovea. Temporal to the fovea, the horizontal raphe divides them into those running below and above the fovea.

Axons from ganglion cells in neighbouring areas are grouped into adjacent fibre bundles separated by glial tissue, the Muller cells processes (Radius & de Bruin, 1981). The axon bundles preserve a considerable degree of spatial order in the nerve head. Those around the perimeter of the nerve head are coming from ganglion cells in the far peripheral retina while those in the centre of the nerve head are from the central parafoveal retina (Minckler, 1980). This retinotopical arrangement holds until the axons pass through the lamina cribrosa into the optic nerve, where significant reordering occurs.

The nerve fibre layer is thickest just around the optic disc, with regional differences. It is thickest at the vertical optic disc poles and thinnest at the temporal and nasal optic disc borders. This arrangement is responsible for the characteristic shape and thickness of the neuroretinal rim (NRR) in the optic disc, which is broadest at the inferior pole and progressively narrower at the superior, nasal and finally, the temporal disc region.

The ophthalmoscopic view of the optic nerve head shows just its surface, which is known as the optic disc. The mean optic disc diameter has been found to be between 1.47 and 1.89 mm (Sing *et al.*, 2000). It is slightly vertically oval with its horizontal diameter being about 7 to 10% shorter (Jonas *et al.*, 1999). Some studies have indicated a high inter-individual variability (Sing *et al.*, 2000; Jonas *et al.*, 1990), which corresponds to the inter-individual variability of the scleral canal.

The area inside the optic disc consists of the NRR and the optic cup. The shape of the latter is determined by the different thickness of the NRR as described above. The cup is horizontally oval, with a diameter 7.7% longer than the vertical (Jonas, 1990). Since the optic disc is vertically oval and the optic cup is horizontally oval, the cup-disc ratio is significantly larger in the horizontal meridian, in normal eyes.

The size of the optic disc is correlated with the size of the cup and the cup-disc ratio. Thus, eyes with small discs tend to have small cups and vice-versa (Sing *et al.*, 2000). This feature is important when evaluating for glaucomatous optic nerve change, since early damage in an eye with a small cup-disc ratio could be missed unless other abnormalities of the disc were to be detected. The cup-disc ratio in the normal population ranges from 0.0-0.84 (Jonas *et al.*, 1988).

1.2.2.2 Lamina cribrosa and the retrobulbar portion of the optic nerve

The lamina cribrosa is a sieve-like structure made of collagen fibres. The holes are channels through which the bundles of ganglion cell axons and retinal blood vessels pass. It is the most complex and densely packed structure in the optic nerve. Axonal bundles branch and rejoin extensively along their course through the optic nerve head, interchanging large numbers of axons. This subdivision of bundles is maximal at the lamina cribrosa (Minckler D.S., 1996).

The lamina cribrosa preserves intraocular pressure against a gradient between the intraocular and extraocular space. It is also the site for transition of the tissue surrounding the axon bundles. The prelaminar portion mostly consists of glial cells, whereas the postlaminar sheaths contain more connective tissue and oligodendrocytes, which are responsible for the characteristic myelination of the axons

back to the terminal nuclei in the brain. Behind the lamina cribrosa, the optic nerve is also surrounded by the meninges throughout its orbital course.

1.2.2.3 Blood supply

The central retinal artery provides some branches to the intra-orbital portion of the optic nerve, the core of the nerve, but its main function is to supply the retina. The main arterial supply to the optic nerve itself is from branches from arteries in the pia mater surrounding the nerve, which are derived from the short posterior ciliary arteries and supply the outer portion of the nerve. The lamina cribrosa and the pre-laminar portion of the optic nerve are supplied by branches from the circle of Zinn and from the choroid, both also derived from the short posterior ciliary arteries, with little or no contribution by central retinal artery branches (Cohen, 1992).

The optic nerve microvascular bed resembles anatomically the retinal and CNS (central nerve system) vessels, which have the physiologic properties of autoregulation (Weinstein *et al.*, 1982) and the presence of the blood-brain barrier.

The details of the arterial supply deserve considerable interest because of the presumed relevance to the pathophysiology of glaucomatous optic neuropathy.

1.2.3 The central visual pathways

After the two optic nerves pass through their respective canals and exit the sphenoid bone, they merge as the optic chiasm, from which the bilateral optic tracts arise, each tract containing fibres going to their central destinations in the brain.

1.2.3.1 Optic chiasm: Semidecussation of optic nerve fibres

Axons from the retina project through the optic chiasm, where fibres from the nasal half of each retina cross to the opposite side of the brain. The axons from the temporal hemiretina remain on the same side. Thus, each of the optic tracts contains a complete representation of the opposite hemifield of vision. This is known as semidecussation.

After axons pass through the chiasm, they are rearranged within the tract so that axons carrying the same sort of visual information cluster together, regardless of where they originate in the retina. This segregation by cell type rather than retinal location is in preparation for the projection to the lateral geniculate nucleus (LGN), since it has separate regions for inputs from different classes of retinal ganglion cells and for inputs from the two eyes.

1.2.3.2 Lateral Geniculate Nucleus

The majority of retinal axons terminate in the LGN, the principal subcortical region that processes visual information for perception, but about 10% of the ganglion cell axons have subsidiary projections. The pretectal nucleus of the midbrain uses inputs from the retina to control pupillary reflexes, whereas the superior colliculus is involved with eye movements (Mason C. & Kandel E.R., 1992).

The lateral geniculate nucleus (LGN) consists of six superimposed layers or coronal slices. Each layer receives inputs from the retinal hemifield of only one eye. They are numbered 1 through 6 beginning at the ventral side of the nucleus. Layers 1, 4 and 6 receive inputs from the contralateral eye, layers 2, 3 and 5 ipsilateral inputs. Since the left LGN receives axons from the left eye's temporal retina and the right eye's nasal retina it deals, therefore, with the information of the right visual field. Equally the right LGN deals with information of the left visual field. Thus, at the level of the LGN input from the two eyes has not yet been integrated.

One characteristic of the retinogeniculate projection is the retinotopic organisation, where the mapping of the retina on the LGN retains spatial order. Furthermore, since the layers of the nucleus are stacked on top of one another, the six maps are in precise vertical register, so that a given point in the visual world that is seen by both eyes projects to a line within the LGN, which passes through all layers. However, this mapping is distorted because the central retina is represented by more axons than the periphery. This "cortical magnification" persists in the primary visual cortex.

Cells in the LGN are functionally segregated in the different layers, to some extent by size. Layers 1 and 2 (each one from each eye) are the large-cell or magnocellular layers. Layers 3 to 6 (two each from each eye) are the small-cell or parvocellular

layers. In general, parasol ganglion cells terminate in the magnocellular layers and midget ganglion cells and other small ganglion cells terminate in the parvocellular layers (Leventhal *et al.*, 1981; Perry *et al.*, 1984) (Figure 1.4).

Wiesel and Hubel (1966) described 3 types of parvocellular cells in the LGN, most of them having colour-selective responses. Type I, the most common (80% of parvocellular units), had an opponent centre-surround receptive field organisation. Type II cells, less common, lack centre-surround organisation and have chromatically but not spatially opponent receptive fields. Type III, 10% of parvocellular units, have centre-surround organisation but no colour sensitivity. In the magnocellular layers they also found Type III cells together with a unique variety of cells, type IV. These have centre-surround organisation, where the centre responds to most wavelengths and the inhibition of the surround is supplied by long wavelength cones. They respond with dramatic, prolonged silence to a large red spot.

This classification has been revised by Derrington and Lennie (1984) and they concluded that parvocellular cells can be divided into two types; the Type I/Type III group that has a spatially and chromatically opponent receptive field, which is driven only by red and green cones, and another type which receives blue cone input opposed to some combination of red and green cone input, with more nearly spatially co-extensive mechanisms. In the magnocellular layers, Derrington *et al.* (1984) found that most cells have chromatically opponent receptive fields, with spatially segregated antagonistic mechanisms.

In addition, another division of the LGN has been identified (Hendry & Yoshioka, 1994). This consists of inter-laminar populations of cells below each of the six major layers, which receive input from small bistratified retinal ganglion cells.

Layers of the LGN

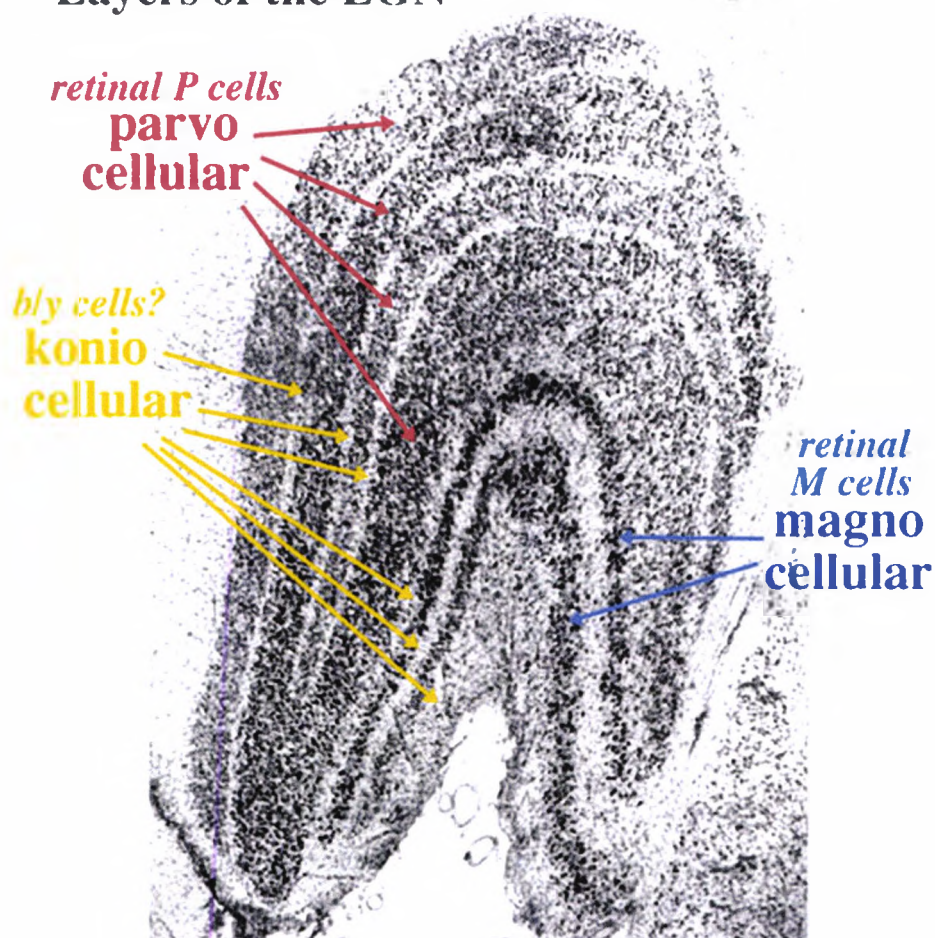


Figure 1.4: Histological section through the primate lateral geniculate nucleus (LGN) to show the layering of the neurons into 4 parvocellular layers, 2 magnocellular layers and 6 koniocellular layers (from the Webvision <http://webvision.med.utah.edu>).

The response properties of LGN cells are remarkably similar to those of the retinal ganglion cells that input to them (Hubel & Wiesel, 1962). The differences in colour opponency, contrast sensitivity and linearity between magno- and parvocellular ganglion cells also apply to magno and parvocellular cells in the LGN (Derrington & Lennie, 1984).

Table 1 is a summary of the physiological differences comparing receptive field properties of cells in magno- and parvo- layers.

Receptive field properties	Magnocellular	Parvocellular
Size	Larger	Smaller
Conduction speed	Faster	Slower
Contrast sensitivity	Higher (threshold < 2%)	Lower (threshold > 10%)
Response	Phasic (transient)	Tonic (sustained)
Spatial resolution	Low	High
Temporal resolution	Faster	Slower

Table 1: Physiological differences comparing receptive field properties of cells in magnocellular and parvocellular layers.

This seems to suggest that the LGN acts as a relay between the retina and the visual cortex with very little filtering taking place. However, axons also run from the visual cortex to the LGN and this feedback may have some influence on the activity of the LGN (Bruce & Green, 1990).

Schiller and Malpeli (1978) found that ON- and OFF- centre cells are segregated into separate laminae in the LGN. Layers 5 and 6 of the rhesus monkey contain predominantly ON-centre Type I cells, while layers 3 and 4 contain predominantly OFF-

centre Type I cells. However, ON- and OFF- centre cells are intermingled throughout magnocellular layers.

The existence of simultaneous ON- and OFF-channels as well as segregation of colour-opponent and broad-band channels, seems to point to the existence of parallel pathways, each with different kinds of information that is projected to different cells and even different regions in the central nervous system. Parallel processing of the visual information will be discussed in section 1.2.4

1.2.3.3 Primary visual cortex

The axons of the LGN neurones continue the primary visual pathway as the optic radiations projecting to the primary visual cortex in the occipital lobe. The primary visual cortex is also known as area 17 of Brodmann or area V1 (visual 1). It has a characteristic striped appearance in cross-section, which is due to the arrangement of cells in six layers of different densities. For this reason it is also known as the striate cortex. It occupies the region within the depth of, and around, the calcarine fissure (Ruskell, 1988).

1.2.3.3.a Functional architecture of the primary visual cortex

The primary visual cortex has the function of integrating the activity of an intricate pattern of input and output connections with an exquisite organisation, which will be discussed in this section.

As in the laminae of the LGN, the striate cortex contains a precise topographic map of the retina, and just like in the LGN (section 1.2.3.2) the cortical area devoted to the central part is much larger than the one devoted to the periphery.

Of the six cellular layers in the primary visual cortex, layer IV is greatly expanded and receives most of the terminating fibres of the optic radiations. It is subdivided into layers IVA, IVB and IVC. Both, M- and P- cells from LGN terminate in IVC, but in separate sub-layers. Magno-cellular axons terminate in layer IVC α , whereas parvo-cellular axons innervate layer IVC β , and so segregation of these two pathways is

maintained. Inter-laminar cells from the LGN terminate in layers II and III (Bruce & Green, 1990). Also, axons carrying inputs from right and left eye are segregated in precise regular alternating columns, known as ocular dominance columns (Hubel & Wiesel, 1972). In fact the columns, so defined, extend through the cortex for considerable distances constituting slabs (Ruskell, 1988).

As well as the laminar and columnar structure described above, cells in the visual cortex may also be classified according to receptive field properties and histochemical staining. Hubel and Wiesel provided the first coherent description of the receptive field properties of cells in the striate cortex (Hubel & Wiesel, 1962; Hubel & Wiesel, 1968). They classified the various types of cells as simple, complex and hypercomplex.

Simple cells, which are similar to the centre-surround cells of the LGN, exhibit summation within their separate excitatory (ON-) and inhibitory (OFF-) regions and antagonism when both areas are stimulated simultaneously. However, the simple cells' receptive field has elongated ON- and OFF- subfields, which lie adjacent and parallel to each other (Bruce & Green, 1990). They respond best to slits of light along a particular orientation and in a particular position in their receptive field. The majority are selective for wavelength (Thorell *et al.*, 1984); others have more complex properties such as "double-opponency", in which different regions of the receptive field show opposite colour-opponent responses (this physiology appears to play a role in discerning borders of colour contrast) (Ts'o & Gilbert, 1988). They often have direction-selective responses to moving patterns. Finally, some show "end-inhibition" and respond more strongly to a short slit that ends within their receptive field than to one that is longer (Bruce & Green, 1990).

Complex cells have many properties in common with simple cells including the orientation preference, direction and wavelength selectivity, and end-inhibition. Complex cells showing end-inhibition were the cells originally termed hypercomplex cells by Hubel and Wiesel (Bruce & Green, 1990). Contrary to simple cells, the complex cells' receptive field does not possess easily definable ON- and OFF regions. Their optimal response is often to an appropriately orientated line, no matter where it lies in the receptive field that is swept across the receptive field. Many complex cells respond better to one direction of movement across the receptive field than the opposite, and therefore show direction selectivity (Hubel David H., 1998).

Cells with the same preference for orientation of the stimulus are organised, again into columns (Hubel *et al.*, 1978). This orientation changes systematically across the visual cortex. Cells in adjacent columns have orientation preferences that differ only slightly (10°), but in a continuing progressive fashion, in the same clockwise or anti-clockwise direction.

Recent studies (Obermayer & Blasdel, 1993) using optical imaging to detect the patterns of activation in response to gratings of different orientations, presented to right and left eyes separately, have shown a relationship between ocular dominance bands and the organisation of orientation selectivity in the monkey's visual cortex. The whole pattern suggests that both a radial and a linear arrangement of orientation preferences are important, possibly for different visual functions (Bruce & Green, 1990).

Staining of visual cortex in primates to reveal levels of cytochrome oxidase (CO) (enzyme present in mitochondriae), which are greater in more metabolically active cells (Livingstone & Hubel, 1984), has shown a regular array of dark blobs, separated by non-stained regions, the interblobs. They are most clearly visible in layers II and III, but are also detectable in layers V and VI in line with the pattern in the upper layers. Horton and Hubel (1981) showed that the blobs are aligned in ocular dominance stripes. A staining pattern is also evident in V2, although the pattern is not one of blob-interblob variation but forms a pattern of stripes (see section 1.2.3.4).

1.2.3.4 Prestriate cortex

After completion of initial processing in the primary visual cortex, visual information is transmitted to other cortical areas for further interpretation. The prestriate cortex surrounds the primary visual cortex (V1) and is further sub-divided into two areas, area 18 or V2 and area 19 or V3.

V2, which is immediately adjacent to V1, receives a major input from V1 and is organised retinotopically in the same way as V1. CO stain reveals coarse parallel stripes different from the fine blobs in V1 (Horton, 1984). They alternate thickly and thinly across the full width of V2. The receptive field properties of cells in V2 correlate with the stripe-like pattern. They appear to be principally of the complex variety, and many of them show end-inhibition responses. Thus, properties of cells in V2 make

them even more specific in terms of feature extraction from the visual scene. This increasing specificity of the tuning of visual cortical cells is also applicable to area V3, which surrounds V2 (Baker, 2000).

The functional segregation evident in V1 seems to be maintained at the level of V2. Connections with other extrastriate areas suggest that this division of labour is perpetuated at even higher levels of cortical processing (Horton, 1992).

Zeki (1973) discovered V4, a cortical area within the parietal lobe. V4 cells are mostly colour selective, and respond better to an optimal coloured stimulus than to a white light. V4 receives most of its input from the colour-coded cells located within the thin and pale CO stained stripes in V2. Most neurons in V4 have complex, oriented, and end-inhibition receptive fields (Desimone & Schein, 1987).

V5, also known as MT, is located in the middle temporal lobe. V5 neurons have been reported to be very sensitive to stimulus motion (Zeki, 1974). These cells have directional selectivity, responding to movement of the stimulus in a preferred direction and give no response to an opposite, null direction. Some units require a properly oriented slit moved in a certain direction (like complex cells in V1, but with much larger receptive fields). Cells in V5 with common directional preference show a tendency to cluster together within columns. V5 receives a direct projection from layer IVB in V1 and from the thick CO stripes in V2, both populated with directionally selective units. V5 is thought to govern smooth pursuit mechanisms and perception of visual motion (Horton, 1992).

1.2.4 Parallel processing of the visual system

The projection of the Magno cells (mostly parasol ganglion cells) in the retina to the M layers of the LGN forms the magnocellular pathway and similarly the projection of Parvo cells (mostly midget ganglion cells) in the retina to the P- layers of the LGN forms the parvocellular pathway. The axons of the magnocellular and parvocellular layers of LGN project to IVC α and IVC β of the primary visual cortex (Perry *et al.*, 1984). There is evidence that the small bistratified cells project to koniocellular layers of LGN (Dacey, 1999; Dacey, 2000) in parallel with the M- and P- cells. Thus, the M- and P-

visual pathways from the retina to the LGN remain clearly separated up to the level of V1.

Examination of the central connections and their physiological properties has revealed a highly specific organisation. CO staining studies (Horton & Hubel, 1981; Livingstone & Hubel, 1984) indicate that cells in layer IVC α of V1, (input from magnocellular-LGN cells) connect to cells in layer IVB. In contrast IVC β of V1, (input from parvo and koniocellular-LGN layers) send axons into the blob and interblob regions of layers II and III. The connections to the blob and interblob zones have very different physiological properties. Cells in the blobs do not display orientation preferences, like cells in layer IVC or in the LGN. However, they are colour sensitive. Inter-blobs have orientation specificity but they are not responsive to chromatic stimuli.

From V1, axons in the blobs project to the thin stripes in V2, whereas inter-blob cells project, via the thin and inter-stripe regions of V2, mainly to V4 (specialized in colour processing) and to areas of the inferotemporal (IT) cortex. It receives a major contribution from the P pathway (ventral visual pathway). The thick stripes of V2 receive their input from IVB, and proceed to the middle temporal (MT) area (specialized in motion processing) and to areas in the posterior parietal cortex. It receives a major contribution from the M pathway (dorsal visual pathway) (Merigan & Maunsell, 1993).

The dorsal visual pathway plays a prominent role in motion perception, spatial localization and sensory motor coordination, whereas the ventral visual pathway is involved in the visual identification of colours, patterns, or objects (Schiller & Logothetis, 1990).

In spite of this gross functional specialization, the dorsal and ventral visual pathways should not be considered as a simple prolongation of the M and P subcortical streams. For instance, there is evidence of a moderate P input to cortical area MT (Maunsell *et al.*, 1990). In addition, some aspects of visual motion perception are unaffected by M lesions of the LGN (Merigan WH & Byrne CE, 1991).

It has been suggested to analyse the functional characteristics of these cells by describing the frequency characteristics of the temporal and spatial patterns that they transmit to avoid identifying M and P pathways with psychologically distinct visual functions, as it seems that some can use both to transmit information (Schiller &

Logothetis, 1990). The P-pathway is then described as a channel carrying information about patterns of light at all spatial frequencies, but only at low to medium temporal frequencies, whereas the M-pathway is used to transmit in a region of high temporal and low spatial frequencies (Derrington & Lennie, 1984). In addition, the nature of colour-opponency implies that the P-pathway transmits information about luminance contrast at high spatial frequencies, and about chromatic contrast at low spatial frequencies (Bruce & Green, 1990).

In summary, the two major subcortical visual pathways (M and P), which proceed from the respective ganglion cells, show a clear segregation up to the LGN. Subsequently, the mapping of the subcortical to the cortical (dorsal and ventral) visual pathways is not one-to-one as there is mixing of the M and P streams within the visual cortex, thus the segregation is only partial (Merigan & Maunsell, 1993). Nevertheless, two pathways dominate the complex network of connections in the visual cortex: the dorsal and ventral visual pathways.

Figure 1.5. shows a diagram illustrating the organisation of the visual system. It summarizes the main current knowledge about the neural transmission in the visual system. The dorsal and ventral pathways are grossly parallel, but there are over 300 known connections between them (Merigan & Maunsell, 1993).

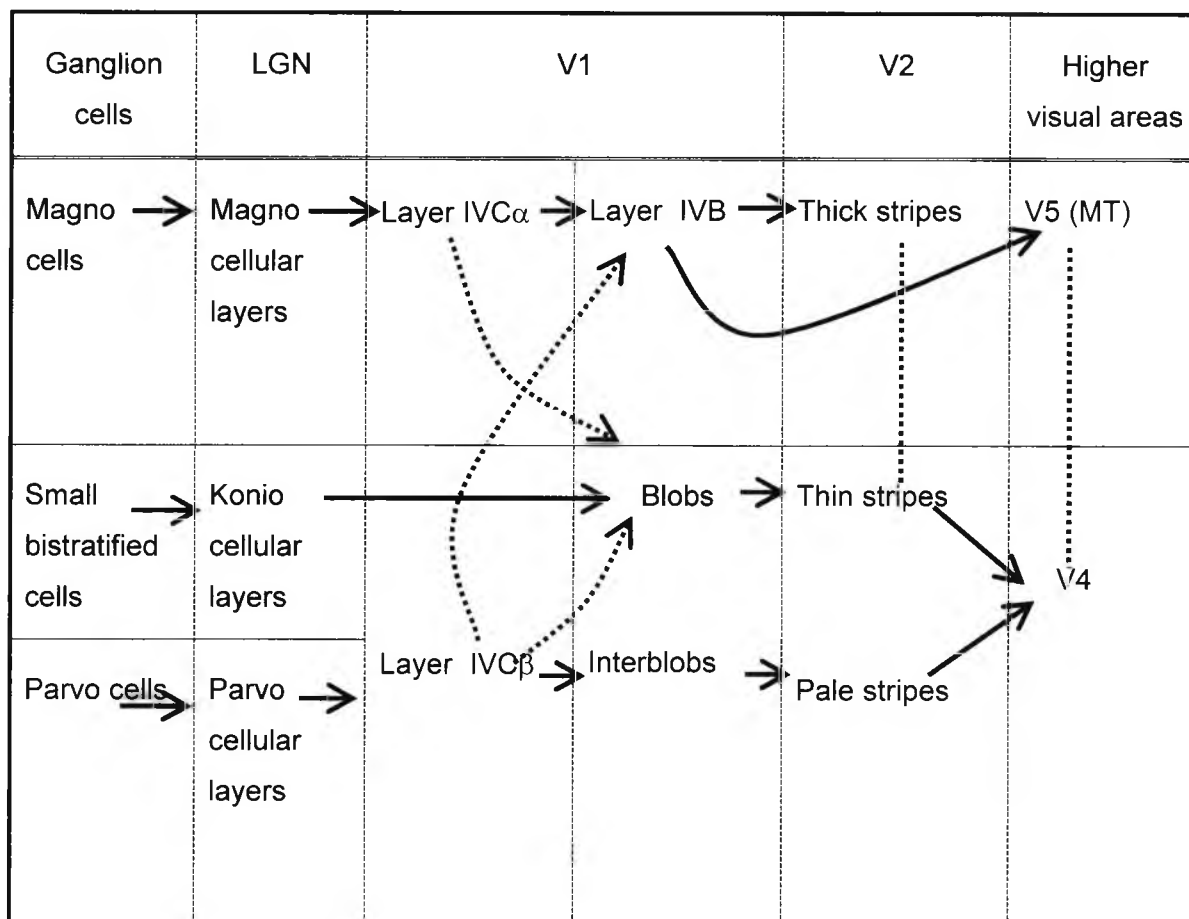


Figure 1.5: Schematic diagram of the visual pathways from retinal ganglion cells to the higher visual areas (adapted from Merigan & Maunsell (1993))

1.3 Introduction to the disease. Limitations in its diagnosis and treatment

Glaucoma is considered to be a progressive optic neuropathy whose pathogenesis, though unclear, is multifactorial (Drance, 1992; Drance, 1997). Damage to the retinal nerve fibres causes characteristic morphological abnormal changes of the optic nerve head, progressive loss of visual function and eventually blindness. Primary open angle glaucoma (POAG) is the most common form of glaucoma in Western countries and prevalence increases with advancing age (Tuck & Crick, 1998). The prevalence over the age of 40 has been estimated in a number of studies to be between 1.2 - 2.1% (Tuck & Crick, 1998; Sommer *et al.*, 1991; Dielemans *et al.*, 1994; Coffey *et al.*,

1993;Harwerth *et al.*, 2002;Klein *et al.*, 1992), increasing up to 4.7% in people 75 years of age or older (Coffey *et al.*, 1993;Harwerth *et al.*, 2002;Klein *et al.*, 1992). It is a chronic, insidious and slowly progressive condition that usually affects both eyes. Diagnosis is usually based on demonstration of pathological cupping of the disc, characteristic visual field loss, and of detection of raised intraocular pressure (IOP), which is a major risk factor (Sommer *et al.*, 1991). Other risk factors are age (Tuck & Crick, 1998), race (Tielsch *et al.*, 1991) and family history (Tielsch *et al.*, 1994).

In many cases progression can be prevented by reducing IOP, either medically or surgically. However, it has been estimated that a significant proportion of undiagnosed patients with glaucomatous damage, around 39%, have an IOP of 21mm Hg or lower (Dielemans *et al.*, 1994). Furthermore, some patients continue to suffer visual field loss after their IOP has been normalised (Brubaker, 1996). In addition, there is a large sector of the population who present with elevated IOP (5-8%) (Dielemans *et al.*, 1994;Klein *et al.*, 1992;Sommer *et al.*, 1991), but show no other signs of glaucoma. Thus, IOP is a poor predictor of development of glaucomatous damage.

On the other hand, considerable loss of optic nerve fibres has been shown to occur prior to functional impairment being detected with conventional automatic static threshold perimetry (Quigley *et al.*, 1989), which implies that the optic nerve has redundancy in its number of fibres in terms of function and that glaucoma does not give field defects as early signs of the disease.

A variety of patterns of inheritance have been observed in association with the different types of glaucoma. Both autosomal dominant and recessive patterns of inheritance have been observed with considerable variation in the clinical expression in different families and in degree of penetrance. Studies based on linkage analysis using mapping techniques have managed to establish the genetic locations of some types of glaucoma.

Eight major genetic loci have been linked to glaucoma. Six of these, designated GLC1A-F (mostly autosomal dominant), are associated with forms of POAG and two, GLC3A and GLC3B (which exhibit an autosomal recessive pattern of inheritance), with congenital glaucoma. Three genes have also been identified to date: MYOC/TIGR, CYP1B1 and OPTN. The discovery of the OPTN gene (Rezaie *et al.*, 2002), which

codes for the protein optineurin, is particularly important because it is considered the most significant glaucoma-related gene discovered thus far. The OPTN gene was identified on chromosome 10p14 in a study of 54 families with autosomal dominantly inherited adult-onset POAG. Sequence alterations in OPTN were found in 16.7% of families with hereditary POAG (compared to 4% in the MYOC gene (Stone *et al.*, 1997), including individuals with normal intraocular pressure. Optineurin is expressed in the trabecular meshwork, nonpigmented ciliary epithelium, retina, and brain, and is speculated to play a neuroprotective role.

Although much progress has been attained in the last decade in finding new genes, detecting disease-related mutations and determining allele frequencies within populations of different ethnic backgrounds, little is known about the function of the mutated gene products and the underlying pathogenic mechanisms.

1.4 Clinical changes in glaucomatous optic neuropathy

The progressive loss of the neurofibre layer leads to the characteristic excavation of the optic disc and axonal degeneration in the optic nerve, which manifests as a deepening of the disc floor, plus narrowing and undermining of the neuroretinal rim (Hartwick, 2001). Many studies have been performed to investigate the pattern of nerve fibre loss. Histological evidence was provided by Quigley *et al.* (1982) and later Airaksinen (1989) suggesting that axons can be damaged either focally in bundles or diffusely, across the entire population of fibres, or a combination of both.

Focal damage is seen anatomically as notching of the neuroretinal rim, or as damage to the superior and inferior poles of the optic nerve (Heron *et al.*, 1988) and ophthalmoscopically as defects in the striation pattern around the optic nerve head. Usually, these signs correlate with visual field defects such as arcuate and paracentral defects (Quigley *et al.*, 1987).

Diffuse damage is less specific. The optic cup enlarges concentrically due to damage to the neuroretinal rim (Drance *et al.*, 1987; Heron *et al.*, 1988). It is characterised by a generalised reduction in differential light sensitivity (Caprioli *et al.*, 1987), which can also be found in other conditions often found in patients with glaucoma, such as cataracts or ageing (Stamper, 1989; Motolko *et al.*, 1982).

Studies of both the nerve fiber layer of the retina and of perimetry suggest that glaucomatous damage may occur diffusely across the population of nerve fibers, focally in the arcuate portion of the nerve fiber layer, or in both places (Stamper, 1989).

1.5 Mechanisms of damage in the pathogenesis of glaucomatous optic neuropathy

Although IOP has always been consistently found to be one of the most important risk factors in glaucoma, visual loss and neuronal damage can also occur without elevated pressure (Drance *et al.*, 1987). Therefore, other mechanisms may play a role in damage occurring to the optic nerve (Bron & Caird, 1997). Two of the major theories that account for the mechanisms of damage in the pathogenesis of glaucoma include (1) mechanical dysfunction via cribriform plate compression of the axons and (2) onset of vascular dysfunction causing ischemia to the optic nerve.

In addition, contemporary hypotheses include excitotoxic damage from excessive retinal glutamate, deprivation of neuronal growth factors, peroxynitrite toxicity from increased nitric oxide synthase activity, immune-mediated nerve damage, and oxidative stress (Kaushik *et al.*, 2003; Morgan *et al.*, 1999).

1.5.1 Mechanical damage

The mechanical hypothesis is described as the changes happening to the lamina cribrosa when it is subjected to higher than normal IOP. Interference of axoplasmic flow caused by pressure-induced compression and misalignment of pores in the lamina has been demonstrated in monkeys and cats (Quigley & Addicks, 1980; Radius & Bade, 1981). Light microscopy studies of axonal transport alterations induced by brief (2-4 h), modest (30-50 mm Hg) elevation of IOP suggest that the initial triggering event leading to blockage in the lamina is the indentation of axons by glial-collagen beams along the edges of axonal bundles (Minckler D.S., 1993).

The susceptibility of damage at the level of the lamina is due to the congestion in that region with large amounts of interaxonal glial tissue and axon bundles, which are maximally subdivided (see 1.2.2) in their course to the brain. Superior and inferior

poles of the optic nerve head show an increased susceptibility to damage. These areas have larger holes and allow larger bundles of axons to go through, with less collagenous tissue supporting the individual bundles (Dandona *et al.*, 1990). These fibres correspond to the arcuate nerve fibres, which are known to lose function earliest in glaucoma.

Although higher than statistically normal pressure has been considered the main cause of lamellar deformation, conceivably a lamina less resistant than normal could undergo deformation at a lower pressure than the average eye. Reports in cases of low-tension glaucoma have shown that the greater damage tends to occur in the eye with the higher IOP (Cartwright & Anderson, 1988).

1.5.2 Poor vascular function

Normal blood flow in the optic nerve and the retina is little affected by elevation of IOP due to an auto-regulatory mechanism, which compensates for moderate alterations in perfusion pressure by changing the vascular resistance so, that blood flow is constant at constant metabolic demands (Bill, 1993). However, a disturbance of the auto-regulation system can cause ocular perfusion to vary depending on the IOP and blood pressure. Although an extremely high IOP will always produce a decrease in ocular blood flow, decreased blood flow can even occur with a moderate or normal level of IOP when auto-regulation is impaired. Similarly, a decrease in blood pressure will produce a reduction in ocular perfusion only when it is either excessive or in the presence of disturbed auto-regulation. Other factors like severe myopia may also reduce ocular perfusion (Flammer, 2001).

There is some evidence that eyes affected by glaucoma do not maintain normal blood flow in the retina in the face of elevated IOP as efficiently as normal eyes (Quigley, 1993). For instance, a nocturnal fall in blood pressure, which causes a reduction in optic nerve head perfusion, has been considered a factor in the pathogenesis of glaucoma (Gherghel *et al.*, 2001).

Fluctuations in IOP and blood pressure have been shown to greatly aggravate the maintenance of axoplasmic transport in the lamina (Minckler D.S., 1993), particularly in patients with disturbed auto-regulation (Flammer *et al.*, 1999).

Thus, the greater susceptibility to pressure-induced damage in some eyes could be explained not only by individual anatomical variations (e.g. weaker lamina), but also by possibly impaired auto-regulatory capacity in the optic disc, which could lead to poor nutrition. All these factors may play a role in the development of glaucomatous neuronal damage and their relative importance varies in individual cases.

1.5.3 Abnormal axonal transport

Axoplasmic flow can be halted either mechanically by high IOP or secondary to inadequate ocular perfusion in the region's blood flow. This leads to neurotrophin deprivation, caused by retrograde axonal transport blockage from periods of elevated IOP; glutamate toxicity caused by ischemia, and formation of free oxygen radicals, which results in oxidative damage, particularly to mitochondria and nucleus. All of these stimuli are believed to trigger cell atrophy through apoptosis (Quigley *et al.*, 1995). When the damage is too wide-spread, the cell breaks into fragments and is rapidly phagocytosed by adjacent cells without the inflammatory response found in necrosis (Nickells & Zack, 1996). Figure 1.6 shows a schematic drawing of the different factors contributing to the mechanisms of glaucomatous damage leading to apoptosis of the ganglion cells.

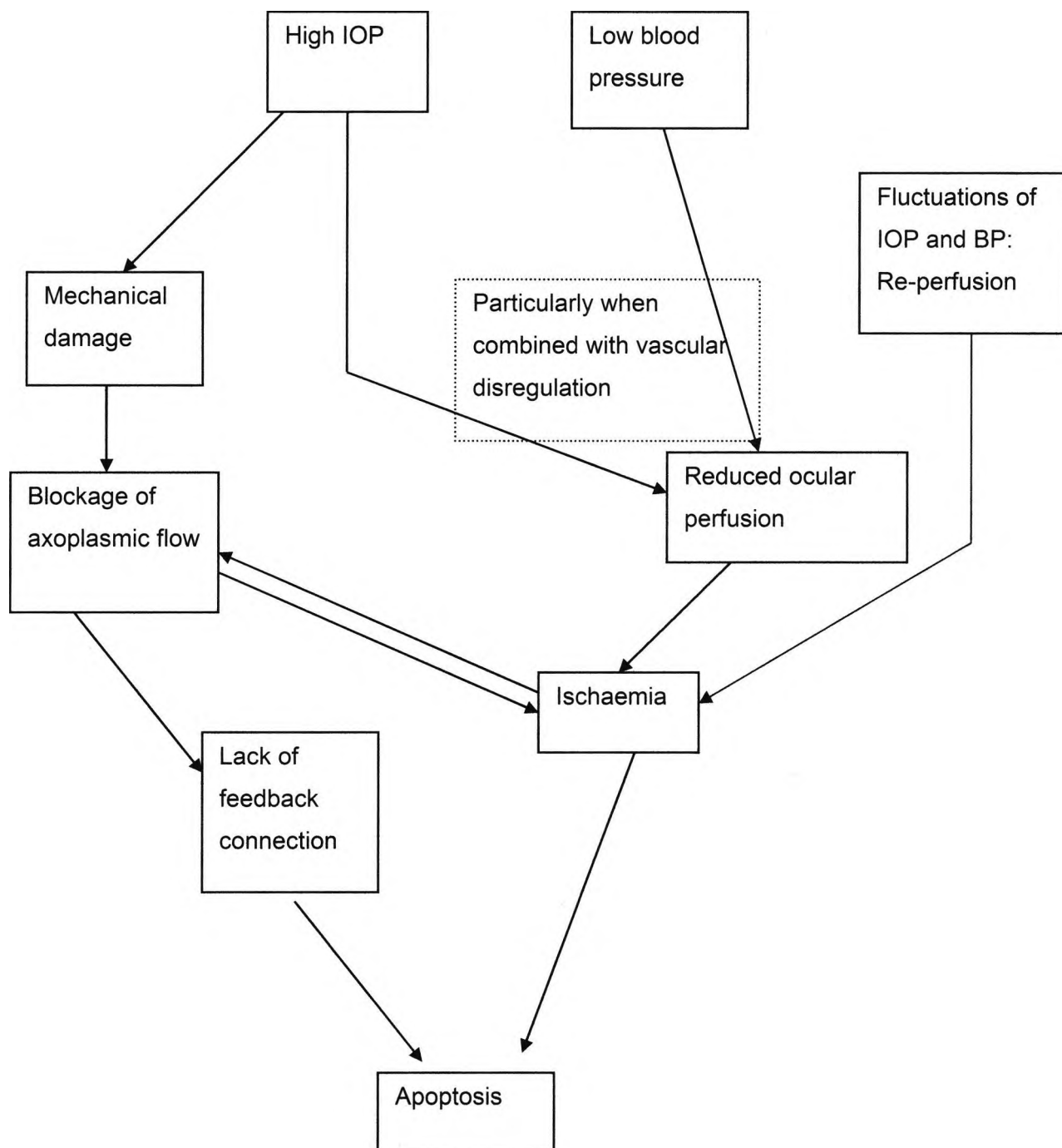


Figure 1.6: Mechanisms of damage in the pathogenesis of glaucoma leading to apoptosis of ganglion cells (adapted from Flammer (2001)).

1.5.4 Selective cell loss

The question whether specific types of ganglion cells or rather, fibres, are relatively more vulnerable to early glaucomatous damage has been debated for some time. Sanchez *et al.* (1986) managed to demonstrate statistically significantly different sized groups fibres (peak sizes: 0.5, 0.8 and 1.5 μm), corresponding to different ganglion cell classes. However, other authors have been unable to reproduce the same results (Jonas *et al.*, 1990).

Quigley *et al.* carried out a series of histological postmortem studies both in experimentally induced glaucoma in monkeys (Quigley *et al.*, 1987) and in human glaucomatous eyes (Quigley *et al.*, 1988) comparing axon loss. They found indications that fibres, with a larger than average diameter, were relatively more damaged, though no fibre size was spared from damage. These studies forged the basis for the early, selective damage to larger diameter axons hypothesis.

However, these results have been questioned subsequently since they may have been biased by shrinkage of the fibres after death. In fact, Morgan *et al.* (2000) found a 20% and 16% reduction in size for parasol and midget cells respectively, when comparing induced ocular hypertensive to fellow eyes in monkeys, which suggests that both types of ganglion cells undergo shrinkage before cell death. They also found no significant reduction in the proportion of parasol to midget cells with increasing cell loss. Oyster C.W. (1999) replotted Quigley's original data in the form of relative frequency histograms or cumulative frequency distributions and came to the conclusion that, although there was an axon loss throughout the range of axon diameters, the samples differ most widely in the middle of the axon diameter range.

CO reactivity studies have indicated a general reduction in neural metabolism, with increasing severity of glaucoma (Crawford *et al.*, 2000). However, this reduction did not appear to be any greater for P- and M- cell pathways in the LGN nor the visual cortex.

Recent histological work in the monkey model has failed to find evidence for selective losses of ganglion cell populations apart from a suggestion for a reduced parvo-cellular input to cortical centres (Harwerth *et al.*, 2002).

Johnson and other authors have suggested that selective losses of neurons are not needed to give improved detection when isolating specific neuronal populations (Johnson, 2001; Sample *et al.*, 2000; Yates *et al.*, 1998). The reduced redundancy theory suggests that tests that isolate the responses of a single class of ganglion cells (regardless of fiber size) are better able to detect glaucomatous damage than non-selective tests, such as standard perimetry, which may be mediated by several ganglion cell classes (Johnson, 1995). Isolating the detection process to a single attribute will remove such redundancy by activating a single neural system better reflecting the early onset of disease. Therefore, tests preferentially targeting functions subserved by these cells will provide higher sensitivity (Alvarez *et al.*, 1997).

There are many methods that can be used to minimise redundancy. Among others using a smaller stimulus, coloured targets, flickering targets or adopting a frequency doubling illusion can be included.

1.6 POAG: a disease of the elderly. Ageing factors

Because the prevalence of POAG increases with advancing age, it is important to distinguish between age-related functional loss deterioration and deterioration caused by the disease itself. Multiple factors are associated with the age-dependent decrease in visual performance, which can be classified into two broad groups: neurological attenuation and optical changes of the media.

Studies have revealed a statistically significant loss of nerve fibre bundles with increasing age, together with an increase in interbundle collagen (Minckler, 1986). Mean losses of 5,426 fibres per year of age have been reported Jonas *et al.* (1990). This age-related nerve fibre loss parallels the age-related reduction in the number of neurones in both the peripheral and central nervous system (Brody, 1955).

Optical radiation in the wavelengths between 400 and 1400 nm provides a stress to the retina, which generates oxidative changes in the tissue. Cones and RPE are more susceptible to the blue end of the spectrum. With age, there seems to be an accumulation of lipid waste products in the RPE and impairment of its phagocytic functions, with the consequent damage to the overlying Bruch's membrane. Drusen

may also appear in Bruch's membrane in the region of the macula and represent a risk factor for the development of macular degeneration (Bron & Caird, 1997).

The crystalline lens is also susceptible to age-related damage due to its unique properties and requirements (Bron & Caird, 1997). Sclerosis and yellowing of the ageing lens alters the spectral quality of the light reaching the retina, and fluorescence of the lens may affect vision in some lighting conditions by producing haze (Weale, 1995).

Macular pigment absorption particularly affects wavelengths in the region 420-500 nm. Inter-individual differences in colour vision are significantly affected by individual variations in the density of the macular pigment. Werner *et al.* (1987) used a psychophysical monochromatic flicker technique to measure the optical density of human macular pigment at the central 1 degree of the retina in 50 subjects aged between 10 and 90 years. Although substantial inter-individual differences were present, these variations were not systematically related to age.

Ageing has been reported to result in a loss of chromatic discrimination of a type similar to that found in tritan-like defects (Birch, 1993; Verriest, 1963; Francois & Verriest, 1959), the severity of which varies with the illumination level. Normative data for different age-groups have been established for the widely-used F-M 100 hue clinical test Verriest *et al.*, 1982; Kinnear & Sahraie, 2002). Differentiation between age-related and glaucomatous changes in colour vision was established when a group of POAG patients was compared to a control group, matched for age and lens density (Sample *et al.*, 1988). They found no significant correlation between the test results and lens density. However, the POAG group showed a significant difference in the F-M 100 hue error scores, not attributable to age, lens or pupil size, demonstrating that their colour vision loss is partly caused by the disease process.

Miosis is another contributing factor to the attenuation of visual performance in the elderly. It exacerbates the loss of blue/yellow chromatic sensitivity and contributes to the reduction of incoming light flux to the retina.

In summary, most measurable ocular functions, i.e. anatomical, biochemical and neurological functions, decline with age. However, substantial inter-individual differences are common.

1.7 Loss of visual function in POAG

The hypothesis of selective cell loss and Quigley's findings that up to 50% of optic nerve fibres may be atrophic before a visual defect can be detected (Quigley *et al.*, 1989) have promoted the development of numerous psychophysical tests searching for functional loss due to glaucomatous damage. These tests can contribute to the development of new and more sensitive strategies for clinical testing, and also can help to understand the mechanisms of loss of visual function.

Although clinical psychophysical tests provide a non-invasive assessment of the visual function and the quantitative investigation of the abnormality, some limitations have been described in their use (Fitzke, 1988; Ruben *et al.*, 1994; Bodis-Wollner & Brannan, 1994):

- As subjective tests they are influenced by non-visual aspects (motor, cognitive skills, etc.) of the patient's response.
- Require the patient's co-operation.
- Measure the function of the visual system as a whole (eye, visual pathway, visual cortex). Therefore potential contributions from different sources need to be carefully considered.
- There is usually a limited correlation of results with standard established psychophysical tests (e.g. automated perimetry).
- Effective isolation of a psychophysical channel often involves some adaptation or masking paradigm, which can be difficult or tiring for the subject.
- Selection of the method for threshold determination is complex. On one hand there is an inherent variability of the results when testing near threshold. On the other hand there is also variability of the observer's responses. The first problem can be counterbalanced by using a large number of observations, but this translates into an increased testing time which adversely affects the observer's variability.

The use of visual display units (VDU) has been of great benefit to the generation of visual stimuli. Computer generated moving or isoluminant colour stimuli, and "flashing" lights to trigger pupil responses or to measure scattered light are some examples. By selecting the characteristics of the stimulus (colour, temporal properties, etc) the isolation of visual functions can be attempted.

1.7.1 Perimetry in glaucoma.

The standard for assessment of functional vision defects in glaucoma is currently the subjective measurement of light sensitivity threshold across the visual field. White-light test targets are superimposed on a white background in computerised perimetry to detect the depth and extent of visual function loss (Heijl, 1985; Johnson, 1996). A map of the sensitivity across the visual field that is derived from light-sense thresholds measured at a number of locations across the retina is used in the diagnosis (Anderson, 1987).

The visual field defects from glaucoma are characterised by a progressive loss of sensitivity that typically begin in the mid-periphery of the nasal field and eventually extend to the central visual field (Drance, 1985; Mikelberg *et al.*, 1986; Quigley, 1993). This progression is an indication of progressive pathological losses of retinal ganglion cells with the extent of neural damage related to the amount of increase in light-sense thresholds (Katz *et al.*, 1997). A comprehensive, qualitative description of visual field defect progression has been given by Drance (1989).

However, the clinical interpretation of visual field defects is complicated due to the lack of precision and accuracy between the losses in visual sensitivity and retinal ganglion cell pathological loss (Harwerth *et al.*, 2002; Kerrigan-Baumrind *et al.*, 2000). Studies have shown in both humans (Quigley *et al.*, 1989) and monkeys with glaucoma (Harwerth *et al.*, 1999a) that a 10dB depression requires a 40-50% ganglion cell loss. More recently, a primate model of high-tension glaucoma (Harwerth *et al.*, 2002) determined that sensitivity depressions greater than 10 dB were proportional to ganglion cell losses at the rate of 0.4 dB per percentage loss. This work identified that a 70% ganglion cell loss produced a 15dB depression in sensitivity in the arcuate region.

Blue-on-yellow perimetry, also known as short-wavelength automated perimetry (SWAP), assesses the S-cone visual field under yellow adaptation. It has been reported to be superior to using conventional white targets (Johnson *et al.*, 1993a; Sample *et al.*, 1993), but it is not clear whether this advantage is related to relative scarcity of B-cones (reduced redundancy theory) or to some type of selective post-receptoral pre-ganglionic damage in early glaucoma (Bodis-Wollner & Brannan, 1994). The stimulus is allegedly detected by S-cones and processed by means of the small-bistratified B/Y ganglion cells, providing a dynamic range of isolation before the next most sensitive mechanism (R/G) can detect the target (Sample *et al.*, 2000).

Felius *et al.* (1995a) determined which channel was responsible for detection of B-on-Y thresholds, by measuring relative sensitivities of the colour and luminance channels under B-on-Y test conditions in normal and early glaucomatous patients. B-on-Y thresholds were determined by the B/Y colour opponent channel in normals and in most of the defective cases. However, as a result of larger threshold elevations (factor 1.8 relative to achromatic) in the colour channel, in some defects detection is taken over by the luminance channel. They concluded that these effects are more likely to occur when defects become deeper.

In a twelve year longitudinal evaluation SWAP has shown to be more effective than standard automated perimetry (SAP) for early detection. Although SWAP has slightly higher test-retest variability than SAP, it has consistently been found superior to SAP for identifying progression (Sample *et al.*, 2000).

Other aspects of visual function are also affected in the visual field before any change in sensitivity can be detected by conventional perimetry. Other stimuli that have been used in the visual field include: moving and flickering sine-wave gratings, moving lines, random dot kinematograms, acuity testing, etc. The following sections will discuss some of these methods.

1.7.2 Contrast Sensitivity

The minimum contrast required for an observer to detect a difference in average luminance between two visible areas is the measure of contrast threshold, which in turn is the reciprocal of contrast sensitivity. If the two areas are adjacent to one another in

space, the ability to detect a difference in luminance is called spatial contrast sensitivity. If the visual areas occur sequentially in time, the ability to detect a difference in luminance is called temporal contrast sensitivity.

Spatial and temporal contrast sensitivity have been found to be reduced in the peripheral visual field of glaucoma and ocular hypertensive patients, even in the absence of scotomas in the area tested (Falcao-Reis *et al.*, 1990).

1.7.2.1 Spatial contrast sensitivity

Contrast sensitivity measurements in glaucoma were first reported by Arden and Jacobson (1978) using printed charts of low to mid-range spatial frequency sinusoidal gratings which varied in contrast. Some follow-up studies using these stimuli suggested contrast sensitivity losses also exist in ocular hypertensives (Wood & Lovie-Kitchin, 1993). Other studies revealed little deficit (Sokol *et al.*, 1980), since the overlap between ocular hypertensives and normals was too large (Stamper *et al.*, 1982). In early glaucoma, contrast sensitivity is typically impaired for the middle-range spatial frequencies with less change at lower and higher frequencies. This indicates a diffuse loss in central visual function, which is not apparent when using high-contrast acuity targets. Such loss has been reported in 50-93% of glaucoma subjects (Ross *et al.*, 1984) and 20-70% of ocular hypertensives (Wood & Lovie-Kitchin, 1993). However, spatial contrast sensitivity testing has lacked specificity, with similar losses occurring in patients with a range of other ocular disorders.

1.7.2.2 Temporal contrast sensitivity: Flicker sensitivity

Temporal contrast sensitivity for middle and higher frequencies has shown deficits in glaucoma and ocular hypertension (Tyler, 1981). However, there has been no perfect agreement between various studies concerning the exact temporal frequency which provides optimal discrimination, and discrepancies between studies may be due to methodological differences (Holopigian *et al.*, 1990).

Atkin *et al.* (1978) compared different spatial and temporal frequencies using an oscilloscope display to produce flickering gratings and reported that low spatial frequency patterns modulated in time at about 8Hz provide the best statistical discrimination between glaucoma patients and normals. Furthermore, about 50% of ocular hypertensives showed significant sensitivity losses.

This specificity of spatial and temporal aspects in glaucoma has been related to the large ganglion cell selective damage theory (section 1.5.4). These cells are primarily responsible for detection of low spatial frequency, rapidly modulated patterns, which would suggest they are more vulnerable to glaucomatous damage.

Flicker sensitivity has also been applied for testing the visual field (Regan & Neima, 1984). Flicker fusion frequency measures the highest detectable flicker rate at many points in the central visual field. It is the maximum temporal resolution at very high contrast. Lachenmayr *et al.* (1991) found higher sensitivity but lower specificity for flicker than for static perimetry in glaucoma when comparing static, flicker and resolution perimetry. Flicker perimetry was also found to be largely independent from disturbances of the ocular media (Lachenmayr, 1994).

In temporal modulation perimetry, as designed by Casson *et al.* (1993), the modulation threshold was determined for frequencies of 2, 8 and 16 Hz. Their results suggest that defects in temporal modulation perimetry may precede the onset or progression of defects in standard perimetry (Lachenmayr, 1994).

1.7.2.3 Frequency-doubling perimetry

A variation of the flicker sensitivity method is the frequency-doubling technology (FDT), which has been described by Johnson and Samuels (1997). They reported measuring contrast thresholds for frequency-doubling at 16 locations within the visual field in glaucoma patients and normals. The test could be completed in 5 min and had a sensitivity of 93% and a specificity of 100%.

The low spatial frequency and high temporal frequency stimulus characteristics suggest that this illusion is mediated by mechanisms in the M-cell pathway. Furthermore, it has been attributed to a small subset of magno- ganglion cells, which

are non-linear in their response properties (Maddess *et al.*, 1998). There is some debate whether FDT measures this subset (approx. 3% of ganglion cells) (Maddess *et al.*, 2000) or whether the target is more likely to be detected, because of its flicker component, by the full complement of magno cells (still only 10% population).

FDT has been shown to be sensitive to early glaucomatous defects and to correlate well with standard automated perimetry (SAP) for determining mean defect (MD) (Johnson & Samuels, 1997); (Sponsel *et al.*, 1998). A preliminary study has reported FDT abnormalities in 46% of ocular hypertensive subjects, as opposed to 22% identified by SWAP and only 5% in SAP (Sample *et al.*, 2000). FDT requires approximately half the test time of standard perimetry and SWAP, due to the smaller number of locations tested, and the results are less likely to be affected by blur or pupil size given the low spatial frequency nature of the stimulus (Sample *et al.*, 2000).

1.7.3 Chromatic discrimination in Glaucoma

Colour vision defects in glaucoma have been described since 1883 (Grutzner, 1972) and although many early investigations indicated red-green defects (Köllner, 1912), later studies suggested that tritan defects predominate (Francois & Verriest, 1959; Drance *et al.*, 1981; Flammer & Drance, 1984; Hamill *et al.*, 1984). A summary of the early research can be found in Drance *et al.* (1981).

In recent years, computer-generated colour tests have provided the means for isolating the processing of chromatic signals from the accompanying achromatic cues (Fallowfield & Krauskopf, 1984; KingSmith *et al.*, 1983; Hart, Jr. *et al.*, 1984; Arden *et al.*, 1988; Barbur *et al.*, 1994; Regan *et al.*, 1994) as well as the design of a great variety of stimuli that can be presented at different retinal locations.

1.7.3.1 Colour vision processing in primates

Colour vision in humans and monkeys begins with the signals from three cone photoreceptor types, which have their maximal sensitivities in the short- (S), middle- (M) and long- (L) wavelength region of the visible spectrum. This is considered the first

stage of colour processing and is based on the Young-Helmholtz model. Signals from these three cone types are relayed to the retinal ganglion cells via cone-specific bipolar cell types, where the second processing stage of colour vision starts. This is based on the Hering model, which describes vision as comprising of two colour opponent channels and one luminance channel.

Contemporary descriptions formulate colour space as cardinal opponent axes (Krauskopf *et al.*, 1982; MacLeod & Boynton, 1979). They represent subtractive interactions between L- and M- sensitive cones (L-M), and between S-cones and an additive combination of L- and M-cones (S- (L+M)). Additionally, there is a luminance axis (L+M), an additive combination of L- and M-cone outputs with little if any contribution from the S-cone system. This experimental model explains well the responses from the retina and LGN, however indications exist that a transformation involving the spatial and temporal integration of chromatic information takes place between the LGN and V1 (Lennie *et al.*, 1990; Livingstone & Hubel, 1987).

Colour coding ganglion cells fall into three major physiological classes. The midget, that respond well to R/G chromatic stimuli (L-M), and project to the P- lamina of the dorsal LGN, which when lesioned dramatically reduces R/G sensitivity (Merigan *et al.*, 1991; Schiller & Logothetis, 1990). The small bistratified, the only retinal ganglion cell that has so far been shown to respond well to S-cone isolating stimuli and which comprises a blue-on pathway via the koniocellular interlamina region of the LGN (Dacey & Lee, 1994; Dacey, 1996; Martin *et al.*, 1997; Lee, 1996). Finally, the parasol that project to the M- lamina of the LGN, which converging evidence suggests mediates sensitivity to high-frequency luminance modulation (Lee *et al.*, 1990; Merigan *et al.*, 1991; Schiller & Logothetis, 1990).

A diagram illustrating the organisation of the visual system is shown in Figure 1.5. in section 1.2.4.

1.7.3.2 Colour vision deficiencies: congenital versus acquired defects

Whereas congenital colour deficiencies are generally due to alteration or loss of cone types, acquired colour deficiencies can be due to abnormalities anywhere along the visual pathways, from the cones to the visual cortex.

Congenital colour vision deficiencies result from inherited cone photopigment abnormalities. The most common form of deficiency is due to abnormal responses to red-green stimuli, originating from an abnormal or functionally absent long-wavelength sensitive photopigment (protan-type anomalies) or intermediate-wavelength sensitive photopigment (deutan-type). The prevalence of red/green deficiency is reported to be approximately 8% in males, made up of approximately 6% deutan- and 2% protan-type defects, and 0.4% in females (Birch, 1993).

A less frequent form of congenital chromatic anomaly is the tritan-type, caused by an absent or abnormal short-wavelength photopigment. Its estimated prevalence lies between 1 in 13,000 and 1 in 65,000 for tritanopia (Wright, 1952) and is approximately 1 in 1000 for tritanomalialia (van Norren & Went, 1981).

Unlike congenital defects, acquired colour vision anomalies are evenly distributed between males and females. They may present with symptoms (the subject may notice something wrong with his/her colour perception), may change in severity with time and differences in severity between eyes are often found. On the other hand, congenital defects are stable through life and affect both eyes equally. A summary of characteristic differences between congenital and acquired defects given by Birch (1993) is in Table 1.2.

Congenital defects	Acquired defects
Present at birth	Onset after birth
Type and severity of defect is stable throughout life	Type and severity of defect may fluctuate
Type of defect can be classified precisely	Type of defect may not be easy to classify. Combined or non-specific deficiencies frequently occur
Both eyes are equally affected	Monocular differences in the type and severity of the defect often occur
Visual acuity and visual fields are normal	Visual acuity is often reduced and visual field defects often occur
Predominantly protan or deutan	Predominantly "tritan-like"
Higher prevalence in males	Approximately equal prevalence in males and females

Table 1.2: A comparison between the characteristics of congenital and acquired colour vision defects (from Birch, 1993).

1.7.3.3 Classification of acquired colour vision deficiencies

Of the many attempts to classify acquired colour vision deficiencies, Verriest's classification, published in 1963 (Verriest, 1963), is the most widely-used, and a simplified version describing the three main types of anomaly is given in Table 1.3. More precise classifications (Hermes *et al.*, 1989) based on Table 1.3 and other classifications of acquired colour vision deficiencies (Krastel & Moreland, 1991) are available.

Name	Alternative names	Colour Discrimination defect	Visual Acuity
Type I	Acquired R/G, protan-like	Mild to severe confusion of R/G hues, little or no loss of B/Y	Moderate to severe reduction
Type II	Acquired R/G, deutan-like	Mild to severe confusion of R/G hues with a concomitant mild loss of B/Y	Moderate to severe reduction
Type III	Acquired B/Y, tritan-like	Mild to moderate confusion of B/Y hues with a lesser impairment of R/G	May be normal or moderately reduced.

Table 1.3: Verriest's classification of acquired colour vision anomalies (Verriest, 1963).

The relationship between the retinal distribution of chromatic mechanisms and the location and progress of the underlying pathology affecting or destroying the chromatic mechanism has been suggested as the key element defining the type of acquired chromatic discrimination defect (Hart, Jr., 1987). For example, a patient suffering from a disease resulting in early destruction of foveal function will normally present initially with a central scotoma, poor visual acuity and a Type I (red-green) defect. However, in patients with diseases of the macula where visual acuity is well-preserved, most will have Type III (blue-yellow or tritan-like) defects, at least in the early stages of the disease process.

Optic nerve disease often produces a Type II (red-green) deficiency, but if visual acuity is preserved then the predominant colour deficiency is Type III (blue-yellow). In moderate glaucomatous optic neuropathy, paracentral scotomas and a reduction of

sensitivity in the arcuate regions are common visual field defects, while visual acuity is spared, hence the most frequent chromatic anomaly associated with POAG is a Type III defect.

Congenital anomalies have served to enunciate and develop colour vision theories, therefore they have influenced subsequent studies, theories and focus given to the acquired colour vision anomalies. For this reason, the same terms employed to describe congenital anomalies have also been used in the many attempts to classify acquired anomalies, which is confusing. However, acquired anomalies are variable and less easy to classify. Non-specific or combined defects may occur, which have characteristics associated with more than one type of congenital colour deficiency.

1.7.3.4 Assessment of colour vision defects in glaucoma.

The assessment of colour vision in glaucomatous patients is of interest and relevant for the following reasons:

1. Colour vision is considered to be affected from the beginning of the course of the disease and so it can provide a useful tool in its early detection.
2. It can provide an indication of the treatment efficacy or it can be used to monitor its evolution.
3. It can help in differentiating types of glaucoma (Yamazaki *et al.*, 1989), and in differentiating those with glaucoma from ocular hypertensives, and so can help to decide the most appropriate treatment.

1.7.3.4.a Clinical tests

1.7.3.4.a.1 Arrangement tests

In general, these use a variety of Munsell hues of the same saturation and luminance. The hues are chosen to be distributed around a complete circle surrounding the equal-energy white point in the CIE (Commission Internationale de l'Eclairage) diagram. Arrangement tests are particularly useful for evaluating patients with eye disease

because their demands on acuity are low (Krastel & Moreland, 1991), and no specific colour confusions are predicted.

1. Farnsworth-Munsell 100-Hue test (F-M 100-Hue): Consists of 85 coloured caps, which the patient has to arrange in a natural colour order between two fixed colours (Farnsworth, 1943). The results are plotted on a polar chart. Correct ordering produces a perfect circle of points, and the numbers on the back of the caps will be consecutive. However, transpositional errors cause points to be further away from the centre of the chart, with some or all non-consecutive numbers. Congenital colour vision defects produce characteristic patterns, which have clusters of errors confined to restricted areas, localized at nearly diametrically opposite regions of the circle. The severity of the discrimination defect is quantified by the "Total Error Score" (TES), obtained by summing the error scores for each cap (Kinnear, 1970). Although the F-M 100-Hue test is particularly useful for monitoring progression in acquired deficiency, it is unable to distinguish subtle differences, such as between severe trichromatic anomalies and pure dichromacy.
2. Farnsworth-Munsell D-15: An abbreviated version of the former test, the D-15 is designed to identify moderate to severe colour vision defects (Farnsworth, 1947). The 15 caps are arranged in a natural colour order from one fixed colour. The plotted error pattern will indicate the type of defect. In moderate to severe colour defectives, the pattern consists of criss-crossing lines, which demonstrate isochromatic confusion axes. Although a quicker test than the F-M 100-Hue, the D-15 was not designed to be a screening test and is not considered to be very sensitive for screening for use in POAG. There are several versions of this test in circulation and the "desaturated" test introduced by Lanthony, using the same colours, but with low saturation, is often used.
3. The City University test: This is a derivative of the D-15 test (Fletcher, 1972). Each chart has a central colour and four surrounding colours, three of which are typical isochromatic confusions for protan, deutan and tritan congenital deficiency, while the fourth is an adjacent colour in the D-15 sequence and is the usual preference of those with normal colour vision. Although classification

of congenital protan and deutan deficiency is imprecise, the City test is useful for acquired defects (Heron *et al.*, 1994).

1.7.3.4.a.2 Pseudo-isochromatic Plates

These are the most widely-used clinical tests to assess colour vision, because they are portable and easy to use. In general, these tests are most useful for detection of congenital anomalies.

1. *Ishihara plates*: This is the most efficient pseudo-isochromatic test. The major disadvantages of the Ishihara plates are that they do not contain designs for the detection of tritan defects, and that patients require 6/18 visual acuity (Birch, 1993) to resolve the test. Consequently, the Ishihara test is not appropriate for the assessment of the majority of acquired anomalies, which are associated with tritan-type defects.
2. *The H-R-R test*: A series of plates designed for the detection of congenital, including tritan, deficiencies. The minimum visual acuity required for interpretation of the test is 6/60. Moderate and severe acquired Type III deficiencies are detected by the H-R-R plates.

Other pseudoisochromatic tests with tritan plates include the *Lanthony tritan album*, and the *F2 plate*, introduced by Farnsworth to detect congenital tritanopia.

The ability of quick, simple-to-apply clinical tests to detect Type III (tritan-like) deficiencies in POAG and ocular hypertensives has been assessed (Heron *et al.*, 1994), and the battery of tests consisted of the H-R-R, Lanthony and F2 plates, plus the D-15 and desaturated D-15, and the City University test. In general, individual tests showed poor sensitivity for the detection of glaucoma. Indeed the Farnsworth F2 test did not detect any Type III defects. Best validity was shown by the City University and the H-R-R tests, and the results suggested that a combination of these tests may be useful in glaucoma screening programs.

1.7.3.4.a.3 Anomaloscopes

These colour-matching instruments are more efficient than arrangement and pseudo-isochromatic tests for the discrimination between normal trichromats and the various types of colour defectives. The patient matches one half of a field, using a variable mixture of two colours of fixed luminance, with the test colour of variable luminance. Of particular importance in acquired colour deficiency is the "matching range" - the range of colour ratios over which the mixture of the two fixed-luminance colours appears to match the test colour. In Types I and II acquired deficiency, when red and green are mixed to match yellow, the matching range widens as the disease progresses. Patients with Type III (tritan-like) deficiencies, due to retinal disease, frequently exhibit pseudoprotanomaly, where the colour match is slightly displaced towards red.

In the *Nagel anomaloscope*, the spectral colours red and green are mixed to match monochromatic yellow. In addition to matching yellow with a red and green mixture, the *Pickford-Nicolson anomaloscope*, which uses broad-band glass filters, also matches blue-green with blue plus green. The Pickford-Nicolson anomaloscope has been used extensively by Lakowski and his co-workers in the study of acquired colour deficiency in glaucoma patients (Drance *et al.*, 1981; Lakowski *et al.*, 1972). However, the blue and green filters are not optimal, leading to high variance in the normal match due to variations in macular pigment (Moreland, 1984). This problem can be overcome by choosing blue and green wavelengths for which macular pigment absorbance is equal. A further slight modification of the wavelengths used allows them to lie on a tritanopic confusion line (Pokorny *et al.*, 1979), while retaining approximate equality of macular pigment absorbance. Patients suffering from glaucoma usually accept wide ranges of matching compared to normal subjects, but in general do not show complete tritanopia (Sample *et al.*, 1986).

Both red/green and blue/green matches are available on the Spectrum "Colour Vision Meter", from Interzeag. Although anomaloscopes have been widely-used in research into colour deficiency in POAG they have little place in screening procedures because the test procedure for the blue-green match is complicated.

1.7.3.4.a.4 *Clinical assessment of colour vision in glaucoma patients. How and when?*

It is recommended in patients with glaucoma that the tests used should allow assessment of tritan type defects as well as red-green defects, as in the case of the F-M 100 hue and its reduced version, the D15. During the examination it is essential to cover one eye to allow independent assessment, which may indicate different degrees of severity in each eye. Of course, it is essential to follow the illumination and distance testing norms for each test, otherwise results would be invalidated. It is not always possible to carry out colour vision assessment at an early stage of the disease, but at least it should be carried out as soon as the diagnosis is known since colour vision assessment can help with the subsequent follow up.

Like any other psychophysical vision test, the result obtained on a repeated test is usually more reliable, especially with elderly people who can feel confused.

1.7.3.4.b Psychophysical methods

Some of the most common clinical colour vision tests described above are simplified versions of psychophysical methods. They are usually based on pigment colours. The more sophisticated psychophysical methods used in research involve computerised and calibrated equipment, and allow a more detailed evaluation of the deficient chromatic mechanisms. A review of the earlier psychophysical techniques has been described in KingSmith (1991).

1.7.3.4.b.1 *Computerised methods*

The introduction, in the late 1980's, of high-resolution colour monitors under computer-control, paved the way for a new generation of techniques to assess colour vision. Often, the observer's task is to detect a stimulus whose chromaticity is modulated in different directions of chromatic space on a background of different chromaticity. Computer emulations of clinical colour vision tests (e.g. HRR, Ishihara, City) have also been introduced (Birch, 1991; Hoffmann & Menozzi, 1998; Ing *et al.*, 1994).

The most extensively used research methods to assess acquired colour vision defects are based on one of the following techniques:

1. Measurement of colour contrast sensitivity by means of flicker heterochromatic photometry (Devos *et al.*, 1995; Falcao-Reis *et al.*, 1991; Felius *et al.*, 1995b; Fristrom, 1997; Yu *et al.*, 1991). The chromatic threshold for detection of a striped pattern at constant luminance is determined, allowing the measurement of pure chromatic discrimination.
2. Measurement of computer-controlled colour-mixture thresholds, in order to estimate equiluminous chromatic thresholds and compare them with achromatic thresholds measured under the same conditions (Alvarez *et al.*, 1997).
3. Increment thresholds for detection of a target on a coloured background. The technique is similar in principle to the two-colour increment threshold developed by Stiles (1978) to probe the basic colour vision mechanisms. Coloured backgrounds are used to adapt two types of cone, so that the resulting spectral sensitivity curve is dominated by the third type. Blue on yellow perimetry uses this principle to study the loss of sensitivity of chromatic mechanisms (SW-cones) as a function of position in the visual field.
4. Determination of pure chromatic discrimination thresholds in the absence of possible additional luminance cues formed at the stimulus boundaries. Luminance masking techniques are used to eliminate the luminance cues. The stimuli are often formed by small elements, each one with its own profile and randomly set luminance (Birch *et al.*, 1992; Regan *et al.*, 1994). The mean luminance of the stimulus is always the same as that of the background, therefore, the observer is forced to use chromatic signals to solve the perceptual task presented. Chromatic sensitivity can be measured in any direction of chromatic space, allowing the determination of discrimination ellipses.

1.7.3.5 Acquired colour vision deficiencies in glaucoma

Colour vision defects in glaucoma have been described since the last century and although early investigations indicated that red-green defects accompanied glaucomatous optic neuropathy (Köllner, 1912), later studies suggested that tritan defects predominate (Francois & Verriest, 1959; Drance *et al.*, 1981; Flammer & Drance, 1984; Hamill *et al.*, 1984). A summary of the early research can be found in Drance *et al.* (1981).

Prevalence estimates for the different types of colour vision defect in POAG have been obtained using a variety of non-computerised tests. Based on these reports (Austin, 1974; Kalmus *et al.*, 1974; Lakowski *et al.*, 1972) typical prevalences are 20 - 40% for normal colour discrimination, 30 - 60% where the dominant defect is blue-yellow, 0 - 6% for red-green defects, and 10 - 30% for a general loss of chromatic discrimination.

Several possible explanations (Gunduz *et al.*, 1988) have been suggested for this predominance of blue-yellow (tritan-like) defects in POAG, including:

- short-wavelength cones or their neuronal connections are less able to resist the effects of raised IOP (Quigley *et al.*, 1987).
- selective damage to blue-yellow sensitive ganglion cells or their axons. Blue-yellow ganglion cells have larger receptive fields, are larger than red/green cells, and have a unique morphology and connectivity to second-order neurons (Kolb *et al.*, 1997), which may make blue-yellow ganglion cells more susceptible to IOP-related damage (Quigley *et al.*, 1987).
- relative scarcity of ganglion cells which code blue-yellow signals (Calkins *et al.*, 1998b), and a relatively little overlap between adjacent receptive fields of these ganglion cells. As a consequence, although only a few ganglion cells may cease to function, there is preferential impairment of the blue-yellow discrimination threshold compared with red-green, even if the proportion of damaged fibres is the same for both types. This has become known as the reduced redundancy theory (see section 1.5.4).

Specific losses of the red-green chromatic mechanism are usually associated with very advanced POAG cases (Pearson *et al.*, 2001). When chronically raised IOPs were

induced in monkeys, the greatest losses in the red-green opponent channel were found in those animals with the most advanced glaucoma (Kalloniatis *et al.*, 1993).

In many patients with POAG, colour vision defects precede the development of standard white-on-white visual field loss. However, some POAG patients never develop chromatic defects (Drance *et al.*, 1981; Drance & Lakowski, 1983) or only develop them in advanced disease. Several studies have found greater colour vision losses in high tension POAG compared with normal tension glaucoma (Lachenmayr & Drance, 1992; Trick, 1993; Yamagami *et al.*, 1995; Yamazaki *et al.*, 1988; Yamazaki *et al.*, 1989), suggesting that there may be two separate mechanisms for damage to visual function in glaucoma. One mechanism would operate as a result of elevated IOP and is responsible for central and paracentral visual function loss, including chromatic discrimination loss, and the second mechanism would be independent of the level of IOP.

There have been many attempts to correlate the severity of visual field defects in POAG with colour vision changes measured using clinical tests. Lakowski and Drance (1979) reported that 34% of those with early visual field defects, 54% with moderate visual field defects, and 74% with severe defects produced scores beyond the 95th percentile for normals on the F-M 100-Hue test. In a five year study, the percentage of ocular hypertensive patients with F-M 100-Hue error scores of >200 and/or a score of greater than 80 on the Pickford-Nicolson anomaloscope (blue-yellow and blue-green scores) who subsequently developed field defects were 77%, 80% and 55% respectively (Drance *et al.*, 1981; Drance & Lakowski, 1983). Surprisingly though, around 20% of those who developed visual field defects failed to show a colour vision defect initially. Although age, visual acuity and pupil size were not controlled in this study, it offers some pointers to the predictive ability of these clinical colour vision tests. In cases of POAG with suspicious visual fields, elevations of the differential threshold at the centre of the field were associated with high F-M 100-Hue error scores (Flammer & Drance, 1984). This demonstrates the existence of chromatic disturbance at the foveal level, even when field defects are not extensive. Breton and Krupin (1987), on the other hand, taking care to minimise the effects of age by applying a correction for age-related changes in F-M 100-Hue scores, in a sample of suspicious and glaucomatous patients, found a significant correlation between colour anomalies and visual field defects only in the 60 to 69 years age group. In addition, there was no

evidence that the overall loss of field was closely related to the severity of the colour vision deficit.

All these studies used tests that evaluate colour discrimination at the fovea only. Although foveal processing of colour is often affected in POAG, modern computerised techniques allow the determination of colour discrimination both at foveal and eccentric retinal locations, which can be analysed in conjunction with visual field data from the same locations. The following studies describe the use of such techniques.

Falcao-Reis *et al.* (1991) measured colour contrast sensitivity using an extra-macular stimulus, at 6 month intervals for a period of 2 years in POAG patients and ocular hypertensives. Colour contrast sensitivity thresholds were more than 2 SDs greater than the control group in 69% of POAG subjects and 32% of ocular hypertensive subjects.

All 84 patients with POAG examined by Yu *et al.* (1991)), using a colour-contrast heterochromic flicker technique, showed thresholds of more than 2 SDs above the normal mean. Their extra-macular stimulus was a 25 degree diameter annulus of thickness 1 degree, concentric with a central white fixation spot. The subjects' task was to identify the quadrant in which a 45 degree gap was introduced into the annulus, while the colour of the annulus was modulated. Furthermore, their 77 high-risk ocular hypertensive patients fell into two differentiated groups; one with thresholds similar to normals and one with elevated thresholds, which in 50% of cases were more than three SDs above the normal mean. Using a similar method, Felius *et al.* (1995b) measured cone contrast thresholds along L, M, S, L-M and L+M test directions at 12 degrees eccentricity in a group of POAG, at-risk patients and normals. Colour contrast defects in POAG and in at-risk subjects occurred in all five modulation directions, although abnormalities in the short wavelength (blue) direction were more pronounced.

Fristrom (1997) used the colour contrast threshold technique to compare groups of glaucomatous, normal, and ocular hypertensive subjects. The colours tested were varied along the protan, deutan and tritan colour confusion axes. At all axes there were significant differences in mean colour contrast threshold between the glaucomatous and normal groups. However, because values for colour contrast thresholds overlapped for all groups, it was difficult to determine a cut-off point, which achieved an adequate separation between normals and those with POAG.

Greenstein *et al.* (1996) studied the foveal effects of POAG on the colour opponent and luminance systems by measuring the chromatic modulation threshold necessary to discriminate a 3 degree disc from a white background. The equiluminance was determined by flicker photometry. Both, those with the disease and suspects demonstrated similar sensitivity losses for both the red-green and blue-yellow opponent systems, accompanied by decreased sensitivity to achromatic contrast, i.e. sensitivity losses were not restricted to the S-cone system.

Although these studies show that the progress of the disease can be monitored by measuring peripheral chromatic discrimination, whether it can be used as a predictor of those patients who will convert from ocular hypertension to glaucoma remains to be established in follow-up investigations with larger groups of patients.

1.7.4 Motion discrimination in Glaucoma

Motion processing has also been reported to be affected in a number of studies. Various aspects of motion processing can be assessed by varying the inter-stimulus interval, direction of displacement, or by measuring thresholds for the detection of motion.

Elevations of motion displacement threshold have been described using a 2° vertical line oscillating at 2.5 Hz at 15° eccentricity in the temporal field in areas of normal HFA visual field in glaucoma eyes (Westcott *et al.*, 1998) and above and below the blind spot in glaucoma and OH eyes (Fitzke *et al.*, 1989).

Random dot kinematograms have also demonstrated specific losses of motion sensitivity in these patients. Coherent motion thresholds for a large stimulus (60° width), with low dot density were elevated by 70% for a group of POAG patients and 44% for a group of ocular hypertensive relative to controls (Silverman *et al.*, 1990). Minimum, maximum displacement and coherence threshold were measured in POAG and low risk patients (Bullimore *et al.*, 1993; Giaschi *et al.*, 1996). Only minimum displacement thresholds were significantly affected in the POAG, but were not correlated with any indices of perimetric sensitivity. Glaucoma suspects did not show any abnormalities with any of the tests of motion perception. More complex procedures

for testing motion have also been described. Motion defined form recognition of letters was developed by Giaschi *et al.* (1996). The test revealed abnormalities in 80% of POAG and 38% of OHT patients. During a 3-year follow-up period, 50% of these OHT patients developed glaucoma.

Several studies have reported motion thresholds to be relatively little affected by moderate amounts of blur (Barton *et al.*, 1996; Trick *et al.*, 1995).

1.7.5 Parallel pathway isolating studies

As discussed above, many studies have proved a reduction in several aspects of visual perception in glaucoma. However, not all these studies have attempted to isolate psychophysical channels. Some were actually undertaken long before the idea of parallel channelling in the visual system had emerged. Although they still provide useful information about the types of visual processing information that is impaired in glaucoma, no relative comparison of damage along parallel visual mechanisms can be attained.

The preferential damage to larger than average axons hypothesis (Quigley *et al.*, 1987; Quigley *et al.*, 1988) and the reduced redundancy theory, which suggests that testing via selected functional channels can improve earlier recognition of damage (Johnson, 1995) have prompted the development of psychophysical strategies aiming to target the M- or the P- pathway. In some cases they have also targeted both pathways in the same patients, in order to reveal selective versus non-selective loss of sensitivity in glaucoma.

The most relevant glaucoma studies that, like the present one, have aimed to selectively stimulate the colour-opponent and luminance contrast mechanisms, separately, on the same subject are summarised below. They provide the evidence for current opinion about relative loss of chromatic (R/G and B/Y) and achromatic sensitivities in glaucoma.

Felius *et al.* (1995b) measured the heterochromatic flicker photometric match, using a 12° ring, in early glaucoma patients. They reported a uniform threshold elevation for

luminance and colour-opponent mechanisms. However, the B/Y mechanism showed a small but significant preference of elevation.

Greenstein *et al.* (1996) measured foveal discrimination thresholds along the R/G and B/Y colour axes and along an achromatic luminance axis in POAG and suspects. Although, they found that the greatest relative sensitivity loss was for the B/Y system, it was accompanied by significant reductions of R/G sensitivity. They concluded the loss was not selective for the B/Y channel.

Kelly *et al.* (1996) measured foveal isoluminant colour and luminance thresholds in POAG and found that both colour and luminance thresholds were increased. Glaucoma patients showed a non-selective defect in R/G and luminance sensitivity ($P < .05$), but a selective colour defect for B/Y stimuli ($P < .01$).

Alvarez *et al.* (1997) measured foveal colour mixture thresholds for early glaucomatous damage eyes. R/G sensitivity selective losses (versus achromatic) were represented by 55% of the cases and B/Y sensitivity selective losses were 42%. They concluded that R/G chromatic sensitivity was significantly more affected than achromatic sensitivity.

Pearson *et al.* (2001) selectively mediated detection by the R/G, blue-on chromatic mechanisms and the high-frequency flicker achromatic mechanism using a 3° stimulus to test perimetrically abnormal regions at eccentric locations (12 - 20 deg). They found larger chromatic losses in a greater number of POAG subjects of which, red and blue contrast sensitivity defects were similar in magnitude.

Beirne *et al.* (2003) measured peripheral (13 deg) resolution acuity using achromatic and blue-cone isolating gratings in eyes with early to moderate glaucoma. Acuity resolutions were significantly lower for mean chromatic and achromatic, however no selective loss of mean SWS acuity was shown. Some individuals with early glaucoma showed lower chromatic/achromatic ratio at certain locations.

Most of the studies above suggest a greater relative loss for chromatic compared to the achromatic mechanism induced by glaucomatous damage. However, the conclusions of these research studies about the relative loss of R/G and B/Y sensitivity are less unanimous.

2 Research outline

2.1 Rationale behind the study

The visual system has been conceptualised as consisting of a set of channels, which process in parallel different aspects of visual perception (section 1.2.4). The Magno- and Parvo-cellular pathways, which are segregated at the level of the retina and remain segregated up to the visual cortex, show different physiological response properties (section 1.2.3.2). The Magno-system responds to high temporal and low spatial frequencies, high luminance contrast and movement. The Parvo-system responds best to high spatial and low temporal frequencies and has colour opponency.

2.1.1 Selective stimulation of the visual parallel pathways

This functional dichotomy has led to the development of psychophysical tests that isolate the Magno- and Parvo-systems. This can be useful in order to study the properties of one channel without the intrusion of the other channel. For example, in a disease like glaucoma where retinal ganglion cells are affected, if a certain type of ganglion cell is more vulnerable and susceptible to damage it would be useful to develop a test that selectively isolates the function of the pathway associated with that type of cell. This would provide the basis for earlier detection of the disease.

Different paradigms have been used to effectively isolate psychophysical channels. A selective pre-adaptation or a masking technique applied to the other channel are some of the possibilities to enhance the sensitivity of the channel to be studied.

2.1.2 Luminance and colour channels

The channels that serve the perception of colour and luminance play a central role in this thesis and although we have referred to them in (section 1.2.4) a short summary is given below.

The first stage of the visual system comprises three independent cone mechanisms, the L-, M- and S-cones. The second stage is formed by the colour-opponent ganglion cells, the R/G and the B/Y, which play a role in the processing of the colour information. Luminance information is thought to be mediated via the non-opponent ganglion cells. Therefore, three main types of functionally different channels are distinguished:

- the R/G colour-opponent, which responds best to L-M stimuli (or vice versa)
- the B/Y colour-opponent, which responds best to S - (L+M) stimuli,
- and the non-opponent luminance channel, which has the best response to achromatic (L+M+S) stimuli.

2.1.3 Glaucomatous damage

The causes of glaucoma damage are still uncertain. Whether it is due to high IOP or poor blood perfusion to the optic nerve head (section 1.5) what is clear is that ganglion cells are damaged at early stages of the disease and that this results in functional defects.

Therefore, an important question is whether there is a specific type of ganglion cell relatively more vulnerable to the glaucomatous insult, which could reveal early abnormal physiological responses.

2.1.3.1 Preferential damage and reduced redundancy theories

There is histological evidence of preferential damage to large optic nerve fibres in human and experimental glaucoma, which has provided the enthusiasm for developing new psychophysical tests aimed at detecting Magnocellular dysfunction. However, these results have been challenged (section 1.5.4). Although several studies addressing visual functions subserved primarily by the Magno-pathway (e.g. motion, flicker frequency sensitivity, etc) have shown to be abnormal in glaucoma suspects, studies aimed to isolate P- cell function (e.g. chromatic discrimination, B/Y perimetry) have also demonstrated deficits in early glaucoma. Thus, size-dependent vulnerability cannot be sustained as the only basis for damage in glaucoma.

An alternative hypothesis considers that glaucoma affects a wider range of retinal cells. It suggests that isolating specific sub-populations of ganglion cells (regardless of fibre size), by evaluating specific functions, removes the redundancy given when non-selective tests are applied. Thus, by activating a single neural system there will be a better chance to detect the early onset of disease.

2.1.3.2 Functional defects

Many studies have proved a reduction in several aspects of visual perception in glaucoma (spatial and temporal contrast sensitivity, motion sensitivity, colour vision). However, not all these studies are relevant in terms of psychophysical channels. Some were undertaken long before the idea of parallel channelling in the visual system had emerged. Nevertheless, the results obtained still provided useful information about the types of visual processing information that are impaired in glaucoma.

2.1.3.3 Colour vision testing in glaucoma

The application of conventional colour vision tests in the diagnosis of glaucoma is limited. Standard clinical tests only assess foveal performance, whereas early glaucomatous damage may occur in peripheral parts of the visual field. In addition, the use of protan, deutan and tritan confusion pairs might be improper. These are appropriate to reveal congenital colour vision defects, which are generally due to

selective loss or abnormality of the visual pigment of the cones. Instead, glaucomatous colour vision deficiencies are due to damage along the axons of the affected ganglion cells. Thus, testing in 2nd stage cardinal directions is more appropriate (e.g. R/G and BY mechanisms) (section 1.7.3.1). Finally, early glaucomatous colour vision deficiencies are expected to be small deviations from normal colour vision, leading to small trichromatic anomalies, which can easily be missed with standard clinical tests.

The introduction of computerised high-resolution colour monitors, like the one used in our experiments, has made it possible to provide a more detailed evaluation of the deficient chromatic mechanisms. The chromatic discrimination ability can be quantified directly and the parameters of the stimulus can be selected as to size and shape, location on the screen, duration, chromaticity, etc.

2.2 Objectives of the study

The broad aims of the studies described in this thesis were twofold. First, to determine the chromatic discrimination ability in a group of subjects suffering from different stages of POAG (including suspects). Secondly, to determine the relative increase of chromatic and achromatic thresholds in a group of older normals and POAG subjects. This will provide the opportunity to investigate whether POAG affects selectively one of the parallel pathways in humans. Measurements were taken using a computerised colour display able to generate the stimuli on a background of luminance contrast noise which ensures effective masking of luminance contrast signals.

The study of the characterisation of chromatic discrimination ability in POAG subjects has been the starting point of the research reported in this thesis (Chapter 4). The analysis centres on the foveal and eccentric measurement of colour discrimination along 12 axes evenly spaced in CIE *xy* chromatic space and the fitting of CD ellipses to the mean data for the groups. This technique allowed the identification of certain chromatic discrimination loss patterns and offered a qualitative impression of its characteristics at different stages of the disease. The relative loss of chromatic discrimination along the R/G and B/Y colour opponent channels is also determined, by comparing the thresholds obtained for the B/Y chromatic mechanism with those obtained for the R/G chromatic mechanism in POAG, suspects and normal subjects

groups. Finally, a discriminant analysis is applied to all the chromatic discrimination sensitivity measurements generated from the study, in order to determine the parameter or combination of parameters that offers the best validity as a method for early detection of POAG.

Chapters 5 and 6 report on studies that focus on the evaluation of comparable chromatic and achromatic tests in the same group of subjects. The idea that the functioning of channels can be assessed selectively plays a central role in these chapters. Motion colour contrast thresholds embedded in dynamic noise, which ensures isolation of the colour opponent channels (R/G and B/Y mechanisms) were measured and compared to luminance contrast thresholds, embedded in static noise (aimed to isolate the first order, band pass motion detection mechanism) in different groups of subjects. This approach would demonstrate the relative loss of chromatic (R/G and B/Y) and achromatic sensitivities along these channels.

A group of POAG subjects was recruited to investigate whether glaucomatous damage selectively affects one of the visual processing mechanisms (chapter 5). Motion discrimination colour contrast (R/G and B/Y) and luminance contrast thresholds for foveal and eccentric areas (7 deg) were measured in a group of POAG subjects and compared to a similar-age control group. The relative loss was also analysed with reference to different stages of visual field loss. In addition, the relation between achromatic and chromatic visual loss was compared to global and localised indices of light sensitivity loss measured with a standard automated perimeter.

A group of healthy older subjects was also recruited (chapter 6) to establish whether ageing affects selectively one of the parallel pathways by comparing them to a group of younger normal subjects. As a consequence we were able to quantify the relative threshold increase in B/Y, R/G and achromatic sensitivities. In addition, the change in chromatic and achromatic sensitivities as a function of age and the effects of retinal eccentricity were studied.

2.3 Logistics

Patients for the study were recruited mainly from the Glaucoma Clinic of the Western Eye Hospital (St. Mary's Hospital, London) and the Fight for Sight Optometry Clinic

(Department of Optometry and Visual Science, City University). Most of the older control group subjects were recruited through an advert placed in a local newspaper, but a few subjects and the group of younger controls were staff or students at City University. Ethical approval was provided by the City University and St Mary's Hospital Ethical Committees. Subject recruitment followed the tenets of the Declaration of Helsinki.

All subjects who participated in the study were provided with a general outline of the proposed investigation. Informed written consent was obtained from all subjects after the nature of the procedure was fully explained.

All subjects were required to attend one appointment following recruitment. The visit lasted around 2 hours depending on the subject. During this time a full eye examination, including refraction, automated visual field assessment, cataract evaluation with LOCS III (The Lens Opacities Classification System III, Chylack *et al.* (1993)), fundus examination, monocular colour vision test and psychophysical testing were carried out.

3 Experimental methods

3.1 Summary

The CAD test (Colour Assessment and Diagnosis test) is a psychophysical, computerised test which has been developed at City University AVRC (Applied Vision Research Centre) (Barbur *et al.*, 1994; Barbur *et al.*, 1993; Birch *et al.*, 1992). This test allows measurement of chromatic thresholds, by means of a technique based on the use of spatio-temporal background perturbation methods that mask possible artefactual luminance signals that could arise from individual differences and/or the small but systematic variations in spectral luminous efficiency with age (Kraedel & Moreland, 1991; Werner *et al.*, 1990).

The equipment used in this study is described in this chapter. Sections 3.2 to 3.5 give general background information on the equipment common to the test. Section 3.6 provides details of the spatio-temporal and chromatic characteristics of the visual stimuli used. Subjects' recruitment details and inclusion criteria are given in section 3.7.

3.2 Random luminance modulation (RLM)

Background adaptation techniques have often been used to isolate activities of certain visual mechanisms. The isolation of spatio-temporal mechanisms involved the use of chromatic backgrounds. Similarly, Ishihara plates and other similar techniques employ spatially random luminance contrast variation to isolate the use of chromatic signals. Static and dynamic background perturbation techniques have also been used to isolate visual mechanisms involved in motion perception (Barbur *et al.*, 1980. *Biol. Cybern.* 37,77-92).

Barbur *et al.* (Barbur *et al.*, 1993; Birch *et al.*, 1992; Barbur *et al.*, 1994) extended the use of such techniques by introducing temporally modulated noise, which generates more effective masking of transient mechanisms that are sensitive to luminance contrast. This new technique employs a matrix of spatially discrete elements (square checks), which vary randomly in luminance in space and time, but their mean luminance is equal to that of the uniform background field. During the brief time in which the pattern is shown the individual elements scintillate as they take up different luminance values.

The amplitude of the RLM is selected and specified as a percentage of the background luminance (i.e., $\pm 16\%$), and determines the level of luminance masking achieved. In other words, the luminance of each check varies randomly in luminance every 50 to 80 ms within a range specified as a % of background luminance. For example, 12% luminance contrast noise for a background luminance of 28 cd/m² means that the luminance of each check will change randomly from 24.6 to 31.4 cd/m².

The effect of dynamic noise is to force the subject to use chromatic signals. When chromatic dynamic signals are not available as in or above threshold, the subject is unable to see the stimulus.

Results obtained in normal trichromats show that the presence of randomly varying, luminance contrast modulation does not affect thresholds for detection of chromatic signals (Barbur *et al.*, 1994).

3.3 Description of equipment

All stimuli presented during the experiments were generated on a 21" high resolution colour monitor operating at a frame rate of 75 Hz. The display was driven by an ELSA Gloria graphics card providing 1024 levels per gun with a resolution of 1280 x 1024 pixels. This was in addition to the standard SVGA adapter used by the experimenter to select stimulus parameters and monitor the experiment.

The system was re-calibrated periodically during the course of the experiments. Luminance was measured for each level for the three guns using a LMT 1003

photometer. A 45 minute warm-up period was always allowed before any experimental measurements were undertaken.

The stimulus parameters, previously specified for each experiment, were retrieved from a file at the beginning of each experiment. These parameters included stimulus size and shape, location on the screen, duration, chromaticity (using CIE (x,y) chromaticity co-ordinates), percentage of noise masking and luminance.

The versatility of the stimulus options made it possible to generate recipes for use at different retinal locations other than the fovea by means of maintaining the fixation at the centre of the screen and presenting the stimulus parafoveally. In these experiments the stimuli were presented foveally and at selected locations in the near periphery. Four possible eccentric locations, one in each quadrant of the visual field, were used.

The test pattern was essentially a square array of achromatic checks generated on a uniform background. The entire array is divided into smaller checks (Figure 3.1). A subset of these checks was the actual test stimulus, presented on this square array of achromatic checks, which ensured isoluminant conditions. This subset of checks was modulated in chromaticity (although it can also be modulated in luminance), whereas the rest of the checks were displayed as luminance contrast noise. The uniform background field chromaticity coordinates were chosen to correspond to the "white" reference used by MacAdam (1942) i.e. CIE (x,y) = (0.305, 0.323) or CIE (u' v') (0.1947, 0.4639). This background produced a uniform grey field of angular subtense 28°x23° and provided a steady state level of light adaptation.

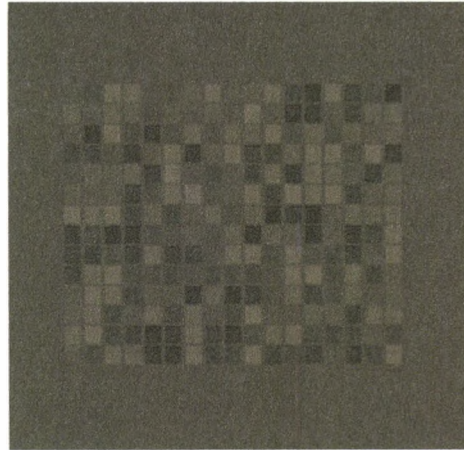


Figure 3.1: Square array of achromatic checks forming the stimulus template.

A response box is attached to the central processor unit (CPU) as an external button box, which the subject uses to provide a manual response for each presentation. In addition to the main response buttons (described in 3.6.2), this box has available two side buttons that could be pressed to repeat the same stimulus. So, the same pattern stimulus can be presented again in case the subject blinked or lapsed in concentration.

3.4 Experimental conditions

At the beginning of the test the subject was seated and the height of the chin rest and chair were adjusted so that the subject was comfortable throughout the experiment.

About 5 to 10 minutes were allowed for the subject to adapt to the uniform background before testing started, and this period was used to reiterate the instructions to the subject and present some examples of the stimuli. The subject was instructed to look at the fixation point and the test started with the first stimulus.

Subjects viewed the stimulus monocularly, wearing the appropriate spectacle correction when necessary. Each presentation was followed by a short beep, after which the subject was requested to respond to the previous stimulus by pressing the appropriate button on the response box.

In order to ensure reliable fixation, subjects were often monitored by means of a video system, in infra-red (IR) illumination. This system allowed compliance to be controlled, by encouraging the subject to maintain fixation especially for eccentric measurements and also assisted the subjective monitoring of pupil sizes.

To maintain consistency during the experiments and in order to minimise the effect of external variables, the following measures were taken. The walls and ceiling of the experimental room were painted matt black. The only illumination remaining during the experiments came from a Lambertian surface on the ceiling above the display monitor. This arrangement provided diffuse illumination, but contributed minimally to the luminance of the display ($< 0.2 \text{ cd/m}^2$). The subject's eyes were shielded from scattered light by a matt black horizontal housing, and the headrest and monitor units were covered with black velvet. In addition, subjects were encouraged to take breaks through the procedure to avoid fatigue.

3.5 Measurement procedure

Each measurement was obtained after a coarse and a fine run by means of interleaved staircases with variable step sizes. The "coarse" run provides a rapid way of obtaining an approximate threshold value and employed large size steps. The "fine" run takes the coarse threshold as the starting value and uses smaller size steps, thus providing a more refined threshold value. The starting chromaticity values for the coarse run were chosen to be well above the expected sensitivity, so the subject understood easily what he/she was required to detect. If the stimulus was detected, the chromaticity was reduced in discrete steps until it no longer could be detected. The chromaticity was then increased (using variable step sizes) until the stimulus was detected again producing the first reversal. The size of each chromaticity step was reduced at each reversal using an exponential function, allowing more precise refinement of the end point. The number of reversals and the initial and final step size were specified before the experiment began, together with the other stimulus parameters. The threshold was finally taken as the average of the last few reversals.

Subjects were tested foveally and at one eccentric location at about 7 deg from fixation. The eccentric measurement was taken in one of the four visual field quadrants, chosen

randomly for normal subjects. For glaucoma subjects the selection of the quadrant was randomised as well, among those quadrants that provided a loss of sensitivity of not greater than 10 dB, as shown in the pattern deviation print out of the Humphrey visual field probability plot. Preliminary testing revealed that measuring an eccentric location with greater sensitivity losses was confusing and stressful for the glaucoma subject. This is likely to be related to the large local fluctuations in sensitivity inherent to glaucoma.

The extent of colour modulation was limited by the phosphors of the monitor and is dependent on the background luminance used in the experiment.

Figure 3.2 shows the CIE (x,y) Chromaticity Diagram with the phosphor limits at the maximum available modulation used for the motion discrimination direction experiment with the CAD test at a 12 cd/m² luminance background field.

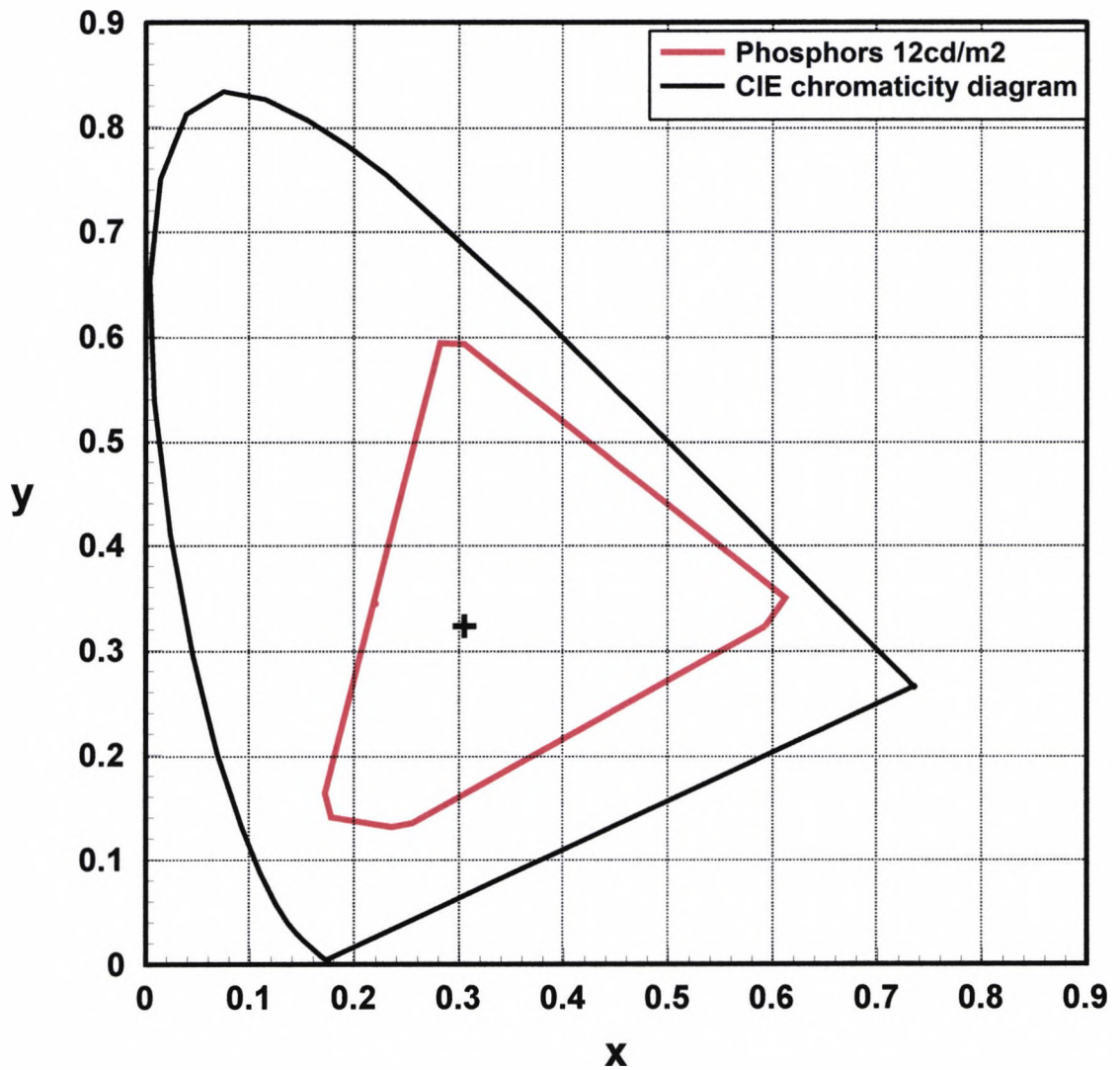


Figure 3.2: CIE (x,y) chromaticity diagram showing the phosphor limits used for the motion discrimination direction experiment with the CAD test (Colour Assessment and Diagnosis Test) for a 12 cd/m² luminance background field.

3.6 Visual Stimuli

3.6.1 Measurement of Chromatic Discrimination Ellipses

An early version of the CAD test was used to measure full chromatic discrimination ellipses along 12 directions in the chromaticity diagram (i.e. 0, 30, 60, 90, 120, 150, 180, 210, 240, 270, 300, 330 deg), for normal and glaucomatous subjects. The chromatic displacement (CD) threshold was defined to be a displacement from the background chromaticity at equiluminance towards a specified location on the spectrum locus.

CD ellipses were obtained in all subjects at the fovea and at one eccentric location (7 deg) for each subject, using an ascending staircase method of threshold measurement along 12 randomly interleaved directions. For each direction, the separation between the background target and target chromaticities was initially large, and decreased after each correct response for that direction and increased after each incorrect response. The test was terminated after 6 reversals on each of the 12 individual staircases. The threshold was finally taken as the average of the last 4 reversals of the fine run. The step size was computed in units of the CIE *xy* chromaticity space.

The background luminance was 28 cd/m². All experiments were carried out at a distance of 0.75 m, at which distance the monitor subtended a visual angle of 27° x 22°.

The noise stimulus was a square of 15x15 achromatic checks generated in the centre of the uniform grey background, which used a 14x14 pixel check size. The entire array subtended a square area of 5°. The test stimulus was a square subset of 9x9 checks, embedded in the array of achromatic checks and modulated in chromaticity. It subtended a visual angle of 3°. The rest of the checks were displayed as luminance contrast noise. The amplitude of the luminance noise used was ±30%.

All subjects were tested foveally and at one eccentric location at approximately 7° from fixation. Foveal measurements were obtained by placing the fixation point in the centre of the screen, where the stimulus was also presented. Eccentric measurements were obtained by displacing the fixation point from the centre of the stimulus 7.2° horizontally

be sufficient to achieve our purpose, therefore the use of temporal modulation was eschewed in this experiment.

Each stimulus was presented for 1s after a short time delay following the subject's response to the previous stimulus. The luminance contrast (LC) noise was present throughout the stimulus presentation. The chromatic test was generated for 500 ms following 500 ms of LC noise. The subjects were requested to press one of two buttons to indicate presence or absence of a chromatic square block in the centre of the "array of greyish patches".

The average total time required to obtain chromatic thresholds for 12 directions (one chromatic discrimination ellipse), was about 15-20 min in elderly subjects (age-matched control group).

3.6.2 Measurement of Luminance or Chromatic Motion Discrimination Direction

To avoid some of the problems encountered in the first study, a more advanced version of the CAD test, which isolates the use of either colour or luminance sensitive mechanisms was developed. We measured motion direction discrimination thresholds for both luminance and colour contrast defined signals at 3 levels of contrast noise (12, 24 and 48%). The original simple staircase method used previously with the earlier version was changed to a four-alternative forced choice procedure in which the chance probability of guessing the direction of motion was 1/16. The test was terminated after 8 reversals. The threshold was finally taken as the average of the last 6 reversals of the fine run.

Colour contrast (CC) thresholds were measured along 2 directions in colour space - 74.5° and 169°, which correspond approximately to Tritan and Protan colour confusion lines. The deutan confusion line (144.5°) was also considered but eventually rejected since preliminary testing provided very similar information to the results obtained along the Protan colour confusion line. Luminance contrast thresholds were also measured by modulating the test stimulus in mean luminance. Both luminance contrast (LC) and colour contrast (CC) thresholds were measured foveally and at 7 deg eccentricity.

Luminance contrast ($\delta L/L_{\text{bkg}}$) can be defined unambiguously, in the case of achromatic stimuli, when the relative spectral composition of the stimulus matches that of the background. Thus, the definition of luminance contrast is independent of the spectral responsivity of the photoreceptor, therefore an achromatic stimulus generates the same contrast in each photoreceptor class. Colour contrast, on the other hand, is more difficult to quantify since a coloured stimulus produces different contrasts in each class of cone photoreceptor. As one moves away from the “white” point along a line of constant hue in the CIE - (x,y) chromaticity chart, the saturation of stimulus increases and the cone contrasts generated increase linearly with chromatic displacement distance, without changing their relation proportion (Barbur *et al.*, 2005). The chromatic displacement distance measured in this way is therefore a good parameter to quantify the strength of the colour signal generated. However, this measure cannot be compared directly to luminance contrast.

The use of an achromatic moving target masked by static LC noise allowed the isolation of the first order, band-pass motion detection mechanism (magno-cellular pathway). The isolation of the chromatic system (possibly the parvo-cellular pathway) was accomplished by using colour-defined motion buried in dynamic LC noise. The use of dynamic noise masks the detection of luminance contrast defined motion, as can be seen in Figure 3.4. LC thresholds increase in a linear fashion with the increase of temporally modulated noise. In contrast, LC thresholds are not affected by the increase of static noise. In other words, using these conditions we can be sure that if there is any residual LC component in the isoluminant target it will not be detected by the subject since it is masked by the dynamic noise.

The luminance of the uniform background field was 12 cd/m^2 . All experiments were carried out at a distance of 0.70 m. The monitor display area subtended $28^\circ \times 23^\circ$ of visual angle at the chosen viewing distance.

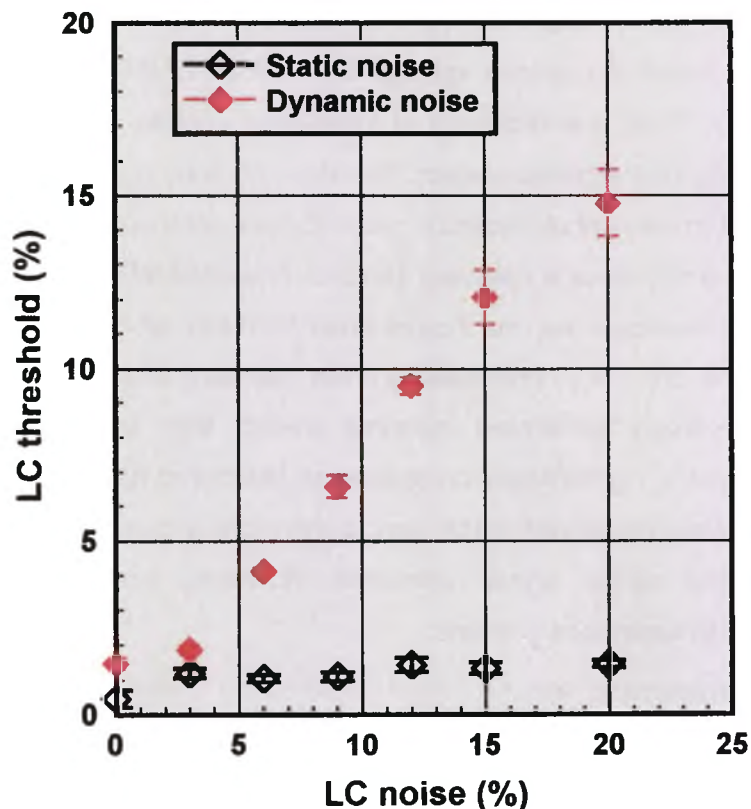


Figure 3.4: Effect of dynamic noise on the detection of luminance contrast defined motion. Mean luminance contrast thresholds for static and temporally modulated noise. Bars indicate 1 SE of the mean.

Foveal measurements were obtained by fixating a small cross that was presented continuously in the centre of the stimulus array in the middle of the screen (Figure 3.5). In order to investigate the effects of eccentricity four equidistant eccentric positions were used, which allowed investigation of one of the 4 visual field quadrants. These eccentric positions were achieved by changing co-ordinates of the stimulus (3.2° , 5.6°) horizontally and vertically from the centre of the screen. The fixation target remained in the centre of the screen and the subject was requested to fixate there.

The noise stimulus was a square of 14×14 achromatic checks. The eccentric stimulus was almost twice the size of the foveal stimulus in order to compensate for the loss of chromatic sensitivity in the periphery. The foveal stimulus used a 10×10 pixel check size, whereas the eccentric one was 21×21 pixels. The entire array subtended a square

area of approximately 4° and 7° for the foveal and eccentric measurements respectively. The centre of the eccentric stimulus was presented at an eccentricity of approximately 7 deg from fixation (Figure 3.6).

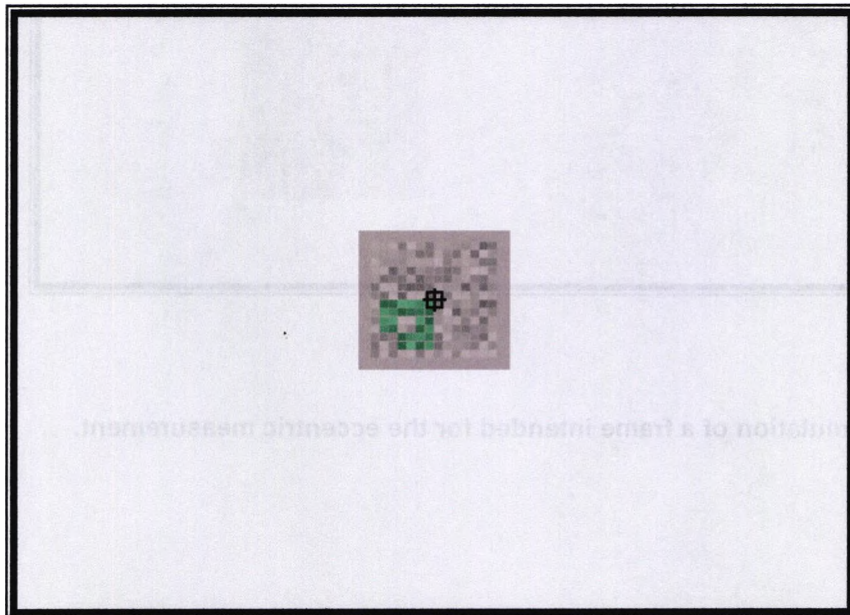


Figure 3.5: Simulation of a frame intended for foveal measurement.

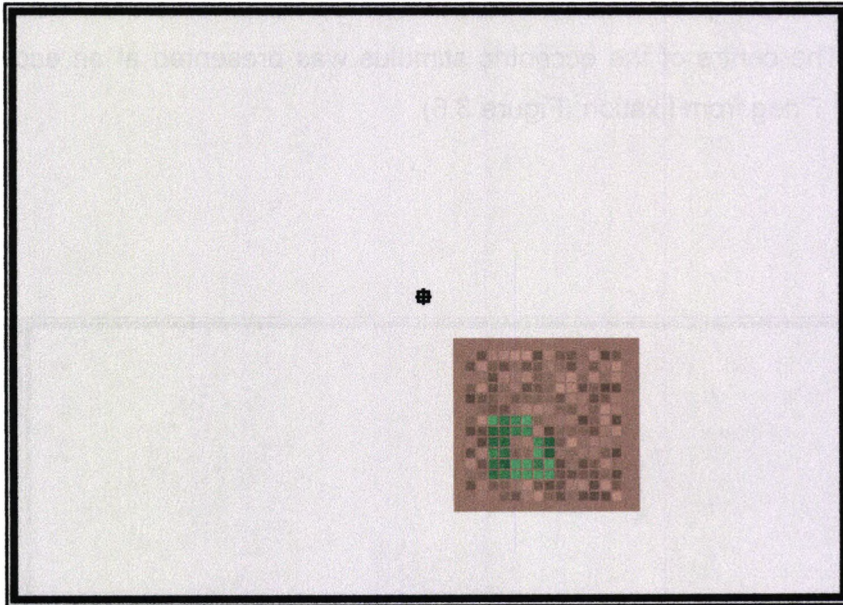


Figure 3.6: Simulation of a frame intended for the eccentric measurement.

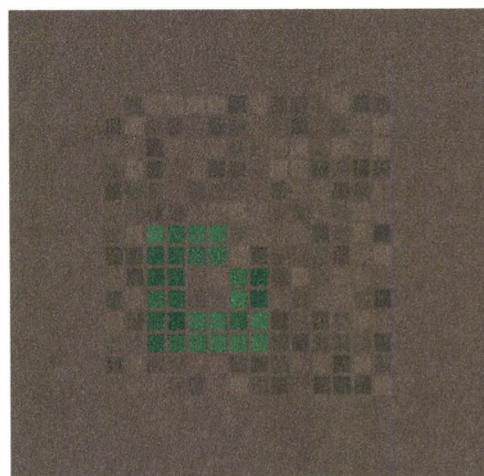


Figure 3.7: An example of a frame of the stimulus used to measure motion direction discrimination thresholds for colour contrast defined signals.

A subset of these checks formed the actual test stimulus, which had the shape of a square "annulus" with a corner missing (Figure 3.7 and Figure 3.8) This pattern moved across the noise background in 4 directions, from one corner to another. This moving subset of checks subtended 1.5° at the foveal presentation and 3.1° at the eccentric one.

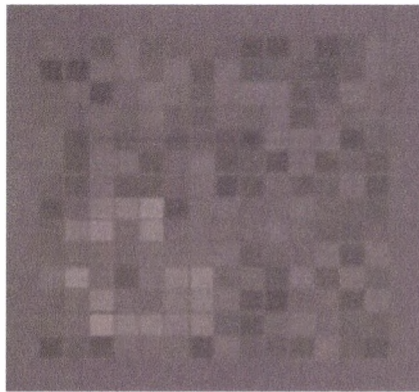


Figure 3.8: An example of a frame of the stimulus used to measure motion direction discrimination thresholds for luminance contrast defined signals.

The response box, in this case, had four main buttons arranged on the corners of a square and therefore related to four possible, diagonal directions of motion: from bottom right to top left, from bottom left to top right or their opposite directions (top right to bottom left and top left to bottom right). The subject had to make a manual response by pressing one of the 4 buttons to indicate the direction of the moving stimulus. So, if the stimulus moved diagonally towards the top left corner, then the subject was expected to indicate this by pressing the top left corner button (Figure 3.9). If the subject was unable to discern the target at all, he or she should press any button, hence making a totally random guess.

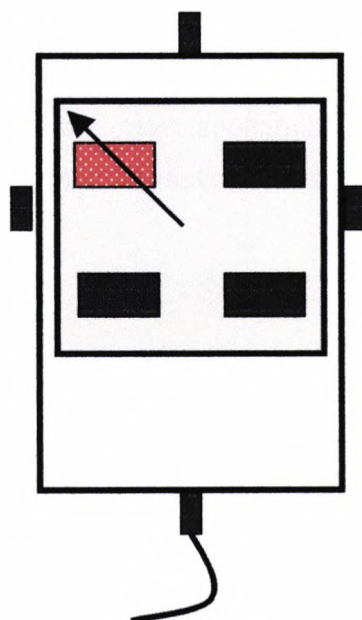


Figure 3.9: Schematic drawing of the response button box

Each presentation lasted for 1.23 s during which noise was present. The actual chromatic moving stimulus pattern was generated for 650 ms following a 240 ms period of noise and after this there was a short time delay that followed the subject's response to the previous stimulus.

3.7 Subjects

3.7.1 Assessment and diagnosis

All subjects underwent a full eye examination, including refraction, automated visual field assessment, cataract evaluation with LOCS III (The Lens Opacities Classification System III, Chylack *et al.* (1993)), fundus examination and monocular colour vision test with the Farnsworth-Munsell 100 Hue test. Severity of visual field damage was assessed with the AGIS (Advanced Glaucoma Intervention Study) scoring method

(Gaasterland *et al.*, 1994). Refer to section 2.3 in Research outline chapter for details of recruitment of subjects.

Some of the subjects participated in both experiments, which were separated by between 1 and 1.5 years. In these cases, subjects were re-examined to ensure they continued to fulfil the inclusion criteria.

One eye of each subject was selected at random for the study, when both eyes met the inclusion criteria.

Details on the number of subjects, average age of the group and clinical information of the participants in each study are provided in each results chapter under the heading "Subjects and method".

Normal (physiologic) pupil size was used for all subjects since we were interested in examining the characteristics of ageing under standard conditions.

3.7.2 Primary open angle glaucoma (POAG) subjects

The inclusion criteria for POAG subjects were defined as having glaucomatous optic neuropathy, glaucomatous visual field defects, with open anterior chamber angles and visual acuity equal to or better than 6/9. Patients under pilocarpine treatment were excluded. No attempt was made to select patients that belonged to a specific type of open angle (i.e. high tension, low tension). No other ocular or systemic relevant diseases were allowed. Congenital colour vision defects were also excluded.

3.7.3 Subjects at risk of developing POAG

A group of subjects who were considered at risk of developing POAG was also recruited to participate in one of the studies. These subjects usually had either IOPs consistently higher than 22 mm Hg or optic discs considered suspicious or a strong family history of glaucoma or all of these, but no clear visual field loss.

3.7.4 Control group

A younger normal group and an older group of similar age to the POAG subjects acted as control subjects. The inclusion criteria for control subjects were defined as having VA (visual acuity) of 6/9 or better; IOP < 21 mmHg; normal optic nerve head appearance; no visual field defect shown with HFA (24-2); minimal lenticular changes (none greater than NII, NCII, CII or PII by LOCS III, as in Chylack *et al.* (1993). No family history of glaucoma, diabetes mellitus and / or ocular or systemic relevant diseases were accepted. No systemic medication known to influence visual field or optic nerve was allowed. Congenital colour vision defects were also excluded.

4 Characterisation of chromatic sensitivity in POAG

4.1 Introduction

It is widely accepted that chromatic sensitivity is diminished in glaucoma. Some reports however do indicate a relatively more pronounced reduction along the tritan axis, presumably corresponding to the S-cone system (Feliuss *et al.*, 1995b; Yu *et al.*, 1991). This would be in accordance with results from B/Y perimetry (Johnson *et al.*, 1993a; Sample *et al.*, 1993).

Chromatic sensitivity can be assessed by measuring chromatic threshold ellipses. MacAdam (1942) measured chromatic discrimination thresholds for several directions of modulation in the CIE (x,y) Chromaticity Diagram from estimates of standard deviation associated with successive colour matches. The spatial extent of the isochromatic regions is determined by measuring colour detection thresholds along the colour confusion lines in CD experiments (Wright, 1952).

This form of colour vision assessment has its origins in the 19th century. The tradition of characterising colour deficiency by the extent of the colour-blind region of a chromaticity diagram first emerged in France. Chibret (1887) introduced the chromatophotometer as a device for establishing the subject's threshold along any axis of colour space. However, it was Bruno Kolbe of St Petersburg who first graphically represented thresholds in a quantitative colour diagram, thus providing, in effect, discrimination ellipses for R/G and B/Y forms of colour deficiency (Kolbe, 1881).

4.2 Aims of the study

The aim of this study is to assess and characterise the colour discrimination loss associated with the progression of the disease. In addition, the best combination of CD sensitivity parameters that would classify the largest percentage of subjects correctly will be investigated. This knowledge could assist in the early diagnosis of glaucoma.

4.3 Subjects and method

4.3.1 Subjects

Twenty POAG subjects participated in this study. The average age for the sample was 68.4 years (SD=6.8 years). Table 4.1 summarises the clinical details of the glaucomatous eyes.

A group of twenty-eight normal subjects of similar age served as a control group. Average age for the sample was 65.6 years (SD=7.1 years).

We also recruited a group of subjects who were considered at risk of developing POAG. Ten eyes of ten subjects, having an average age of 63.1 years (SD=9.3 years) were examined. These subjects had no clear glaucomatous visual field loss, but had one or more of the following characteristics: IOPs consistently higher than 22 mm Hg, family history of glaucoma (first degree relative), and suspicious optic nerve head. Clinical details of the subjects at risk of developing POAG are summarised in Table 4.2. Logistics of the subject's recruitment and details of the inclusion criteria can be found in sections 2.3 and 3.7, respectively.

POAG subjects	Gender & age (yr)	VA	Diagnosed (yrs ago)	Family History	C/D ratio	AGIS score*	VF defect at location tested (dB)			
							Pattern deviation plot		Total deviation plot	
							Fovea	7 deg	Fovea	7 deg
JD	♀ 70	6/9 ⁻²	8	-ve	0.8	19	5	3	-18	-16
DB	♂ 65	6/6 ⁻³	6	+ve	0.9	16	1.25	-9.5	-1.25	-12.5
PO	♂ 70	6/6	5	-ve	0.8	10	-3.5	-10	-7.25	-5.75
RH	♂ 68	6/6	3	unknown	0.85	11	-1.5	-1.5	-5.5	-5.5
EB	♂ 79	6/6 ⁻⁴	5	-ve	?	7	-1.75	-1	-4.5	-3.25
AK	♀ 60	6/6	1	+ve	0.7	6	-0.5	-4.5	-1.25	-5
PB	♀ 70	6/6	1	+ve	0.8	5	-0.25	-2.25	-2	-6
WH	♂ 75	6/9 ⁺²	2	Unknown	0.9	5	-3.25	-4.5	-6.25	-6.25
ZK	♂ 65	6/6	2	+ve	0.6/0.7	5	-1.75	-3.75	-2.75	-5.25
RS	♂ 72	6/9	1	-ve	0.8	5	0.5	-7.5	-1.5	-9.5
LC	♀ 55	6/9	20	+ve	0.8	5	-3.25	-5.75	-4.75	-7.75
SP	♂ 81	6/9 ⁻²	20	unknown	0.8	4	-1.75	-0.75	-2.75	-1.5
IH	♂ 55	6/5	3	+ve	0.8	4	1	-0.25	-0.25	-1.75
HF	♂ 74	6/9	9	-ve	0.9	7	-0.25	-5.5	-2	-7.25
RSh	♂ 64	6/5	7	+ve	0.8	4	-1.5	-0.25	-1.25	0

EC	♂ 72	6/9 ⁺²	4	Unknown	0.8	3	-2.5	-1.25	1.25	2.5
PR	♂ 74	6/6-	3	unknown	0.7	2	-1.5	-5.5	-0.5	-4.5
VF	♀ 65	6/6	18	-ve	0.85	2	0	1.75	-3.25	-5.25
CC	♂ 67	6/6 ⁻²	2	-ve	0.7/0.8	2	0.25	-3.25	0.75	-3
TH	♀ 67	6/6	1	-ve	0.3	2	0.75	-1.5	-0.5	-3

Table 4.1: Summary of clinical characteristics of the twenty POAG eyes. *AGIS score for severity of visual field loss (section 3.7.1)

POAG suspects	Gender & age (yr)	VA	Diagnosed (yrs ago)	Family History	IOP (at time of diagnosis)	C/D ratio	AGIS score*	VF defect at location tested (dB)			
								Pattern deviation plot		Total deviation plot	
								Fovea	7 deg	Fovea	7 deg
EP	♀ 73	6/9 ⁺²	8	+ve	24	0.4	1	-2.5	-3.75	-0.5	-3
RM	♀ 65	6/5	1	unknown	27	0.6	1	-2.75	-2.25	2.75	0.25
RP	♂ 63	6/6	1	+ve	22	0.3	1	-1	-1.25	0	-0.25
GM	♂ 69	6/6	5	+ve	14	0.8	0	-2.5	-3	2	0
EB2	♀ 63	6/6 ⁻²	9	+ve	23	0.45	0	-0.5	-2	-1.25	-3
RM2	♂ 77	6/5 ⁻²	10	-ve	25	?	0	-1	-2.25	0.5	1
MK	♂ 61	6/9 ⁺²	1	-ve	28	?	0	-0.25	-1	0.5	1.5
MS	♀ 45	6/6 ⁺²	2	-ve	24	?	0	-1.5	-1.5	2.5	1.5
BG	♂ 52	6/5	3	-ve	25	0.5	0	-1.5	-2.5	1.25	0.5
RB	♂ 63	6/6 ⁺²	1	-ve	28	?	0	-0.25	-2.25	1.25	-0.5

Table 4.2: Details of clinical characteristics of eyes at risk of developing POAG. *AGIS score for severity of visual field loss (section 3.7.1)

4.3.2 Methods

To determine the subjects' chromatic sensitivity, we measured chromatic discrimination (CD) ellipses. These consist of the threshold to detect a colour change for 12 directions evenly spaced in chromaticity space, and they were measured for normal and glaucomatous subjects as described in section 3.6.1. Measurements were performed with the stimulus centred at the fovea or 7 deg from fixation. The eccentric measurement was taken in either the superior nasal, superior temporal, inferior nasal or inferior temporal quadrant, chosen randomly for the control group. For POAG subjects the selection of the quadrant for the eccentric measurement was randomised among those that provided a loss of sensitivity of not greater than 10 dB, as explained in section 3.5.

The achromatic background was chosen to have a chromaticity of $x = 0.305$, $y = 0.323$, the chromaticity of MacAdam white (MacAdam, 1942). The results were expressed in units of the CIE (1931) x , y diagram and an ellipse was then fitted to the (x, y) -coordinates, using a direct least-square fitting algorithm (minimising the sum of squares of the log distances) (Fitzgibbon *et al.*, 1999). These results were also transformed into units of the CIE u' , v' diagram, since this is a more uniform colour diagram, but we found that this transformation reported similar information and therefore the former units were used for simplicity.

Several aspects of the fitted ellipses were studied. The orientation of the best-fitting ellipse, which is taken as the clockwise angle from the major axis of the ellipse to the horizontal, and the elongation of the ellipse, which is the ratio of the major (M) to the minor (m) axis length, were used to show the effect of glaucoma on chromatic sensitivity. In addition we estimated the colour-blind area of the chromaticity diagram by calculating the area of the fitted ellipse as;

Area of ellipse= $M*m*\pi$, where

M : major semi-axis of the ellipse

m : minor semi-axis of the ellipse

All areas were expressed in square CIE xy space multiplied by 10^3 .

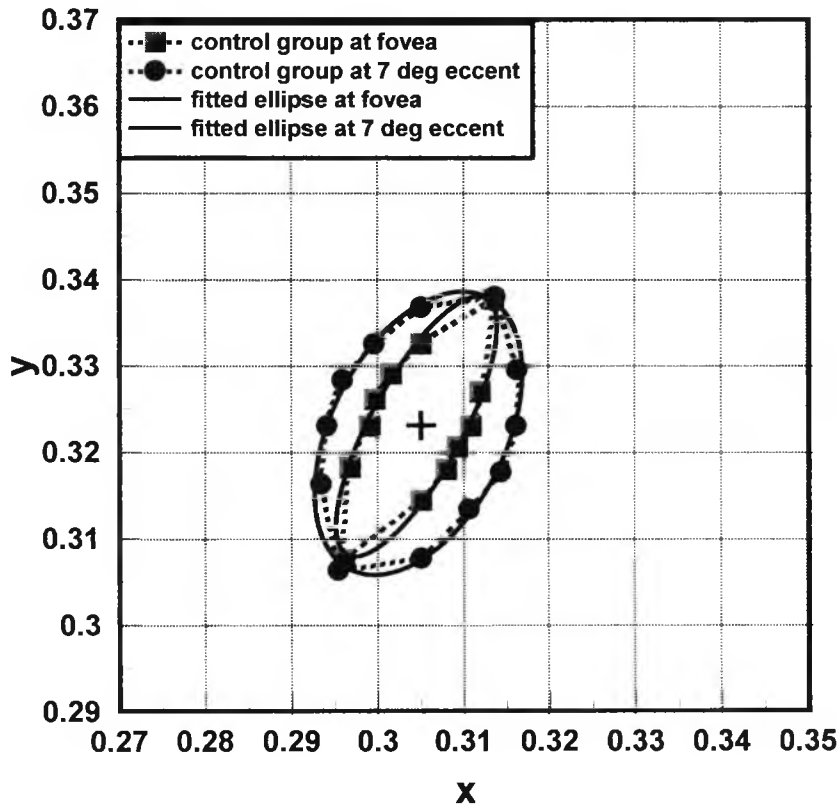


Figure 4.1: Ellipses fitted to the average chromatic discrimination thresholds, measured in the control group, along 12 directions in chromatic space. Measurements for fovea and 7 deg eccentricity are shown.

4.4.1.2 POAG group

The ellipse fitted to the average foveal CD thresholds for the POAG group (Figure 4.2) was oriented at 59.7 deg and the elongation was 3.27. This represents a relative, very small threshold increase (sensitivity reduction) along the major axis of the ellipse, compared to the corresponding foveal ellipse for the control group. The mean ellipse area, in square CIE xy units multiplied by 10^3 , was 0.863, approximately 3 times the size of the control group area (0.285), which implies a non-selective reduction of sensitivity. Therefore, a considerable non-selective reduction together with a marginal selective reduction, along B/Y colour confusion axis, of foveal chromatic sensitivity is

4.4 Results

4.4.1 Chromatic discrimination ellipses

The chromatic discrimination (CD) ellipses, for each group, were obtained by averaging the thresholds taken for each subject along each of the 12 directions of measurement and fitting an ellipse to these data. Figure 4.1, Figure 4.2 and Figure 4.3 show the fitted ellipses to the averaged data for the control, POAG and At risk groups, with the stimulus centred at the fovea and at 7 deg from fixation. The units of the two axes represent distances in x, y space. Table 4.3 shows a summary of the characteristics and sizes of the CD fitted ellipses for each of the groups tested. Individual data for each POAG and At risk subject can be seen in Table 4.9 and Table 4.10.

4.4.1.1 Control group

The foveal ellipse was oriented at 61.3 deg. This is close to the tritan colour confusion line, which in x, y chromaticity space corresponds to 67.3 deg (calculated from dichromatic copunctual points, $x=0.171, y=0$). The elongation of the fitted ellipse was 3.15, which reflects the expected lower sensitivity along the B/Y colour confusion axis compared to the sensitivity along R/G axes. The ellipse fitted to the averaged data measured at 7 deg eccentricity was oriented at 63 deg and had an elongation of 1.73, which when compared to the foveal ellipse, reflects an enlargement of the minor axis. Thus, for normal control subjects, there is a reduction in sensitivity along the R/G colour confusion axis at 7 deg eccentricity, which generates a less elongated ellipse.

shown in the glaucoma group. For the ellipse fitted to the mean CD thresholds measured at 7 deg eccentricity, the angle of orientation was 59.0 deg and the elongation was 1.48, which compared to the control group implies a relative larger threshold increase along the minor axis of the ellipse in the POAG group. The mean ellipse area at 7 deg was 1.416 square CIE xy units, approximately 2.5 times the size of the control group area (0.563).

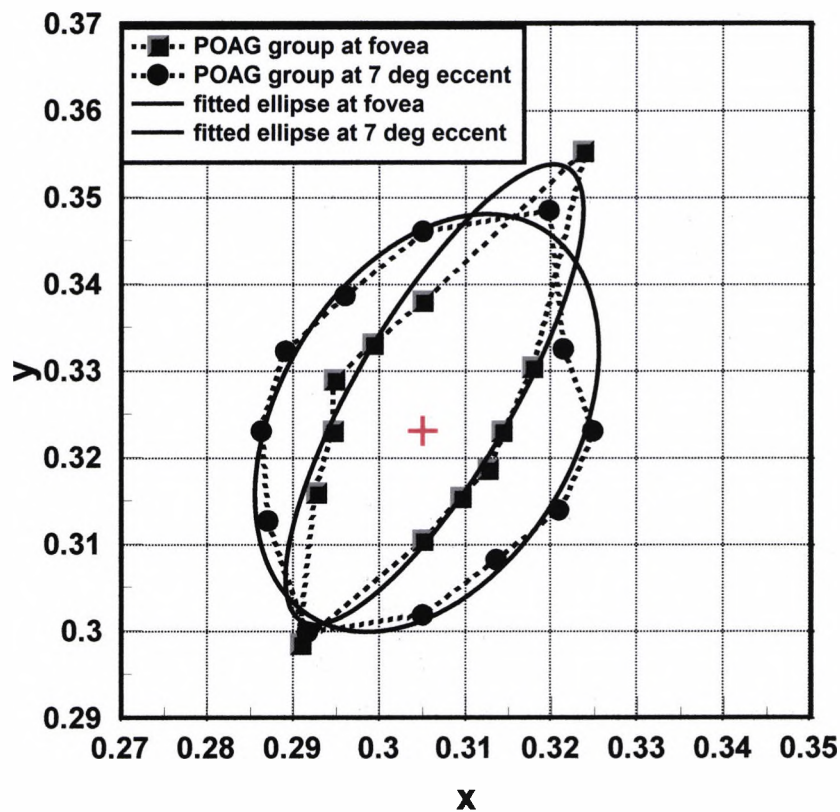


Figure 4.2: Ellipses fitted to the average chromatic discrimination thresholds, measured in the POAG group, along 12 directions in chromatic space. Measurements for fovea and 7 deg eccentricity are shown.

4.4.1.3 At risk group

The group at risk of developing glaucoma (Figure 4.3) presented a fitted foveal ellipse oriented at 63.3 deg with an elongation of 3.02 and an area 0.207 square CIE xy units. At 7 deg eccentricity the fitted ellipse was oriented at 60.8 deg with an elongation of 1.81. The mean area was 1.391, which implies an overall mean reduction in chromatic sensitivity of approximately two and a half times, for the eccentric measurement. However, there is a large variability in the size of the area between subjects, suggesting large differences in chromatic sensitivity at 7 deg, among subjects in this group (see Table 4.4).

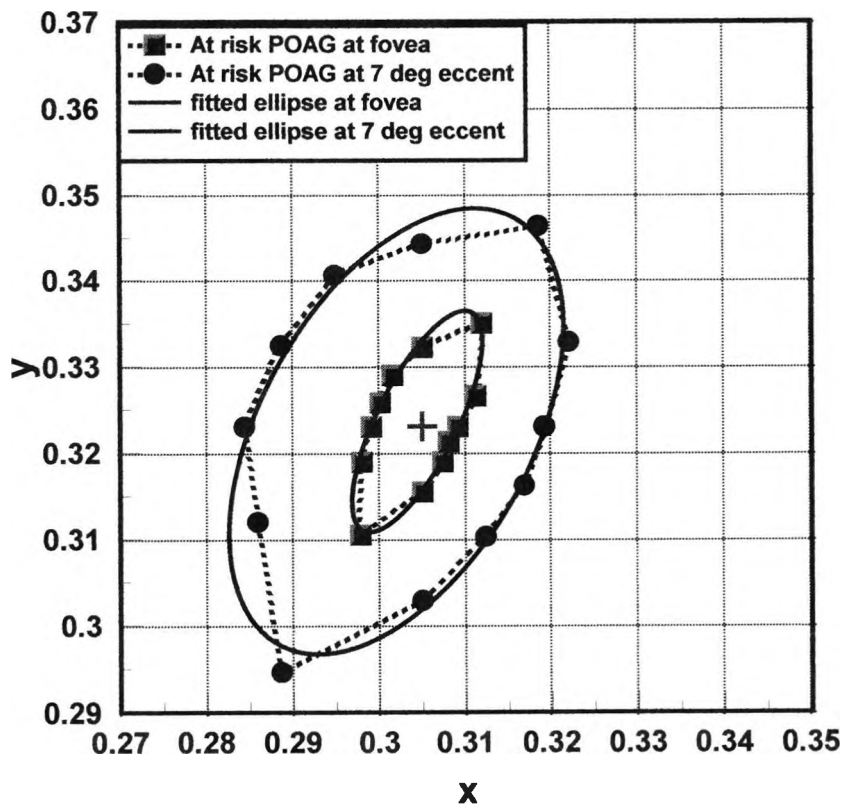


Figure 4.3: Ellipses fitted to the average chromatic discrimination thresholds, measured in the group at risk of developing glaucoma, along 12 directions in chromatic space. Measurements for foveal and 7 deg eccentricity are shown.

4.4.1.4 Comparison of CD ellipses for the three groups

The results in Table 4.3 correspond to the parameters of the ellipses fitted to the mean CD threshold values measured along 12 directions in chromatic space. Fitting ellipses to the average CD thresholds for each group of subjects is a visual representation of the CD ability and offers a useful qualitative impression of what the differences might be among the groups, but no statistical analysis can be obtained.

Group of subjects	Fovea			7 deg eccentricity		
	Area x10 ³ in xy units	Ellipse		Area x10 ³ in xy units	Ellipse	
		Elongation	Orientation		Elongation	Orientation
Control	0.285	3.15	61.3	0.563	1.73	63
POAG	0.863	3.27	59.7	1.416	1.48	59
at risk	0.207	3.02	63.3	1.391	1.81	60.8

Table 4.3: Summary of the parameters of the ellipses fitted to the average CD thresholds, along 12 directions in chromatic space, for each of the groups tested.

In order to apply a statistical analysis, which could prove significant differences between the groups, it is necessary to use the average of the parameters of the individual fitted ellipses (i.e. mean of individual areas, etc.). This approach yields to different mean values as it can be appreciated in Table 4.4.

Group	Control		Fovea		7 deg eccentricity	
			Mean	SD	Mean	SD
			Area	.244	.196	.553
		Elongation	4.12	1.84	2.40	.93
		Orientation (deg)	62	17	65	17
	POAG	Area	1.048	1.999	1.481	1.102
		Elongation	4.07	2.38	2.43	.84
		Orientation (deg)	68	31	74	37
	at risk	Area	.176	.156	1.754	1.956
		Elongation	3.72	1.35	2.23	.55
		Orientation (deg)	62	5	60	15

Table 4.4: Mean values and SD for the area, elongation and orientation of the fitted ellipses in each group tested.

Figure 4.4, Figure 4.5 and Figure 4.6 show the box-plots of the individual ellipses' parameters for each group.

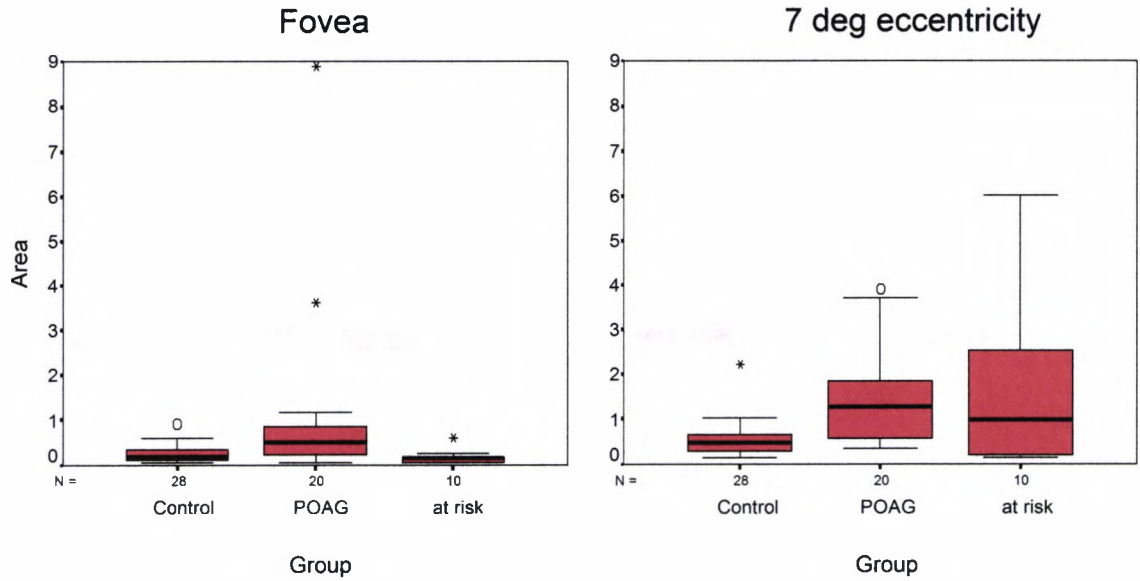


Figure 4.4: Box-and-whisker plots of the areas of the fitted ellipses, for foveal and 7 deg measurements, in each group tested.

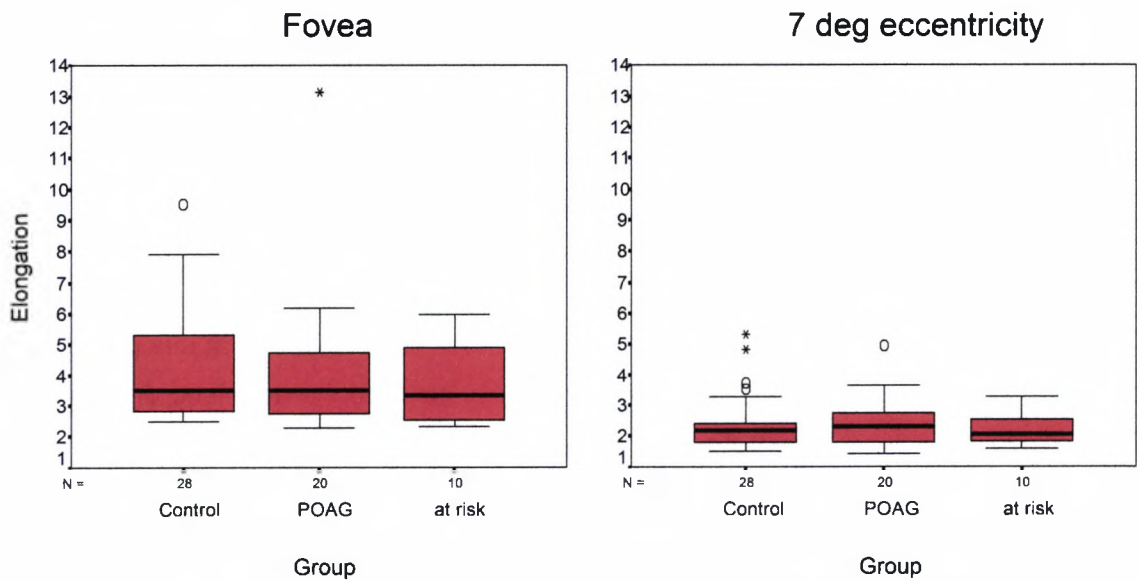


Figure 4.5: Box-and-whisker plots of the elongation of the fitted ellipses, for foveal and 7 deg measurements, in each group tested.

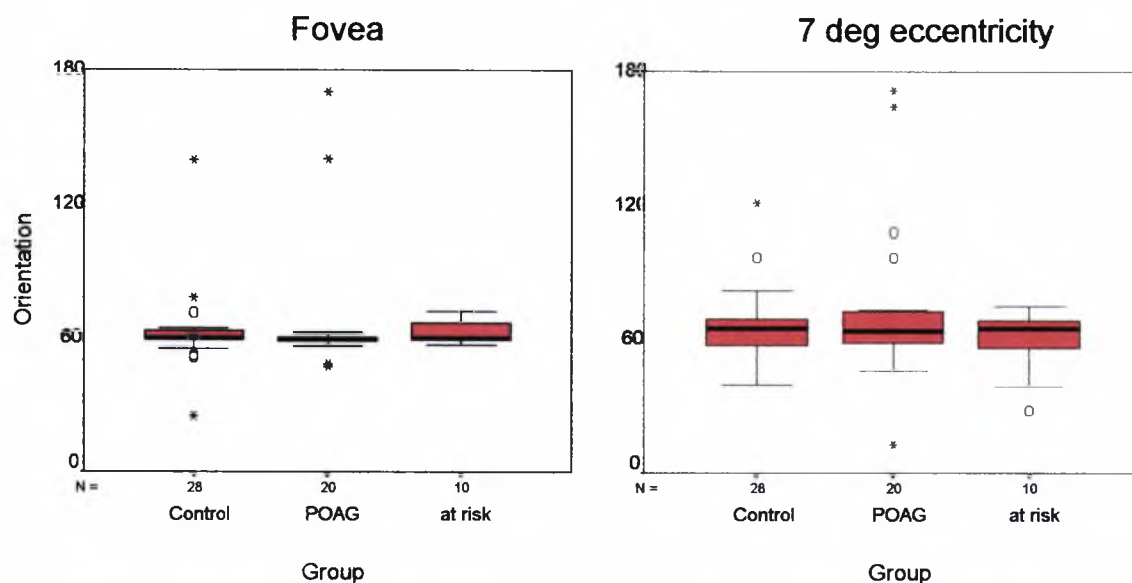


Figure 4.6: Box-and-whisker plots of the orientation (in deg) of the fitted ellipses, for foveal and 7 deg measurements, in each group tested.

The area data from the POAG group shows larger values at the fovea than both the control and At risk groups. At 7 deg both POAG and At risk groups show a large variability in the measurements (Figure 4.4). Some of these subjects lie within the normal range for the control group whereas others present with very large areas. This is particularly evident for the group at risk, which contains both very small and very large areas, at 7 deg. Interestingly, the data for foveal area in the group At risk lies within the normal range for the control group and the data are less variable.

The elongation of the fitted ellipses (Figure 4.5) does not suggest that this parameter would allow us to differentiate between groups or to find characteristic differences. Similarly, the angle of orientation of the ellipse (Figure 4.6) does not reveal clear differences between the groups. However, the orientation of the ellipses measured at 7 deg is more variable at the eccentric location for all groups, but in particular for the POAG group, which contains several extreme cases.

In order to obtain a normal distribution of variables and similar SDs, when comparing data among groups statistically, a logarithmic transformation was applied (Table 4.5). A

one-way ANOVA revealed significant differences between groups for the log area, both for foveal ($p < 0.001$) and 7 deg eccentricity ($p = 0.001$) locations tested. However, no significant difference was found between groups for the log elongation or the log orientation of the fitted ellipses at any of the locations tested.

Post Hoc tests (LSD) for the log area, measured at the fovea, revealed a significant difference between the control and the POAG groups ($p = 0.001$), and between the At risk and POAG groups ($p = 0.001$) but no significant difference was found between the control group and the At risk group ($p = 0.391$). For the eccentric location, post hoc tests (Tamhane, appropriate for unequal variances) for the log area revealed a significant difference between the control and the POAG group ($p < 0.001$). The At risk group was not significantly different from the control group ($p = 0.45$) nor was it significantly different from the POAG ($p = 0.926$) group, either.

It is not surprising to find significant differences between groups only for the area and not for elongation or orientation. Parameters such as elongation should be interpreted with caution in glaucoma. Some glaucoma cases present a totally distorted "ellipse", which might have a shape and angle of orientation completely different from that expected for a subject with normal chromatic sensitivity. The longest axis of the fitted ellipse might not fall close to the tritan colour confusion line. In such cases averaging individual elongation data without taking into account the angle of orientation would not only overestimate the elongation of the average ellipse but also present misleading information.

The elongation or ellipticity of a CD ellipse is usually regarded as an indication of the relative CD sensitivity along B/Y and R/G colour opponent channels. An elongated CD ellipse is usually interpreted as presenting reduced sensitivity along B/Y colour opponent axis relative to sensitivity along R/G. Therefore, it is more appropriate to analyse the relative loss of sensitivity for the groups using the thresholds obtained along the B/Y and R/G colour confusion axes, averaging them as a group and then comparing these with normal subjects (see section 4.4.3).

		Eccentricity				
		Fovea		7 deg eccentricity		
		Mean	SD	Mean	SD	
Group	Control	Log Area	-.740	.348	-.335	.255
		Log Elongation	.581	.166	.356	.139
		Log Orientation	1.781	.108	1.798	.104
POAG	Log Area	-.329	.509	.054	.334	
	Log Elongation	.566	.180	.365	.137	
	Log Orientation	1.806	.135	1.820	.226	
at risk	Log Area	-.869	.318	-.060	.586	
	Log Elongation	.545	.156	.337	.102	
	Log Orientation	1.794	.036	1.758	.136	

Table 4.5: Mean values and SD for Log of the area, elongation and orientation of the fitted ellipses in each group tested.

4.4.1.5 Characterisation of the CD loss (CD ellipses' changes) with progression of the disease

Differences in the extent and type of CD loss with severity of the disease have been suggested by other authors (Lachenmayr & Drance, 1992; Yamagami *et al.*, 1995; Greenstein *et al.*, 1996; Kalloniatis *et al.*, 1993; Pearson *et al.*, 2001). In an attempt to characterise the CD loss at different stages of the disease, the POAG group was divided into three sub-groups according to the AGIS score for severity of visual field loss (see Table 4.1 and Table 4.2). The Early damage group (N=8) contains cases with an AGIS score between 2 and 4, the Moderate damage group (N=8) contains cases with an AGIS score between 5 and 9, and the Advanced damage group (N=4) contains cases with AGIS scores of 10 and beyond.

CD ellipses were fitted, as explained earlier in section 4.4.1, to each of the POAG subgroups and the areas were calculated for the foveal and eccentric data (Figure 4.7, Figure 4.8 and Figure 4.9), in each subgroup. To provide a complete picture of the

progression of the CD loss with severity of the disease, the fitted ellipses for the group At risk (N=10, AGIS score 0-1) were also considered in this analysis (Figure 4.3).

Table 4.6 provides a summary of the parameters of the ellipses fitted to the average CD thresholds measured along 12 directions in chromatic space for the At risk, Early, Moderate and Advanced groups. The control group is also included to aid the comparison.

Group of subjects	Fovea			7 deg eccentricity		
	Area in units $\times 10^3$	Ellipse		Area in units $\times 10^3$	Ellipse	
		Elongation	Orientation		Elongation	Orientation
At risk AGIS=0-1	0.207	3.02	63.3°	1.391	1.81	60.8°
Early AGIS=2-4	0.493	3.22	59.5°	1.175	1.79	63.8°
Moderate AGIS=5-9	0.801	5.34	60.5°	1.361	1.7	57.2°
Advanced AGIS>9	2.054	1.89	55.1°	2.263	1.05	6.5°
Control	0.285	3.15	61.3°	0.563	1.73	63°

Table 4.6: Summary of the parameters of the fitted ellipses and mean areas for the At risk, Early, Moderate and Advanced glaucoma sub-groups.

An inspection of the characteristics of the fitted ellipses for all the glaucoma subgroups reveals the features of CD loss in different stages of severity of the disease.

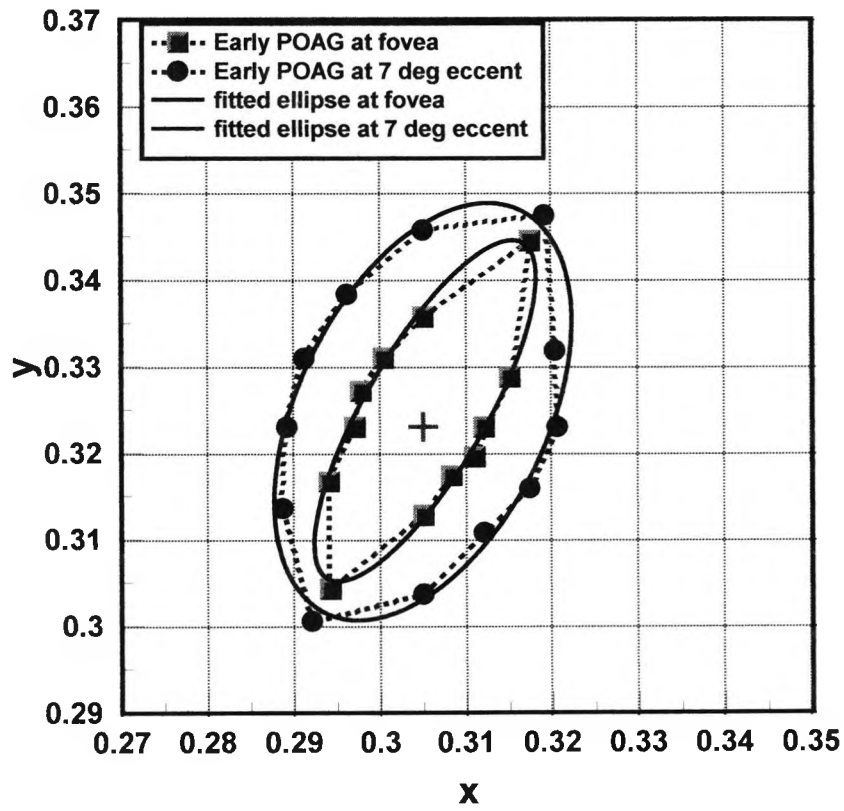


Figure 4.7: Ellipses fitted to the average CD thresholds, measured in the Early glaucoma group (AGIS=2-4). Measurements for foveal and 7 deg eccentricity are shown.

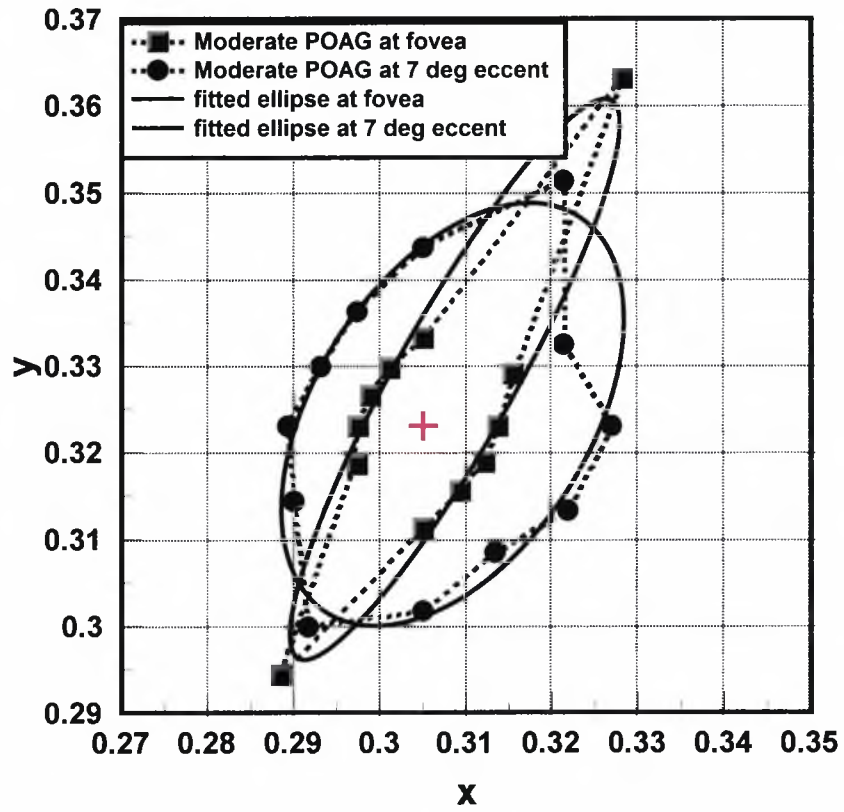


Figure 4.8: Ellipses fitted to the average CD thresholds, measured in the Moderate glaucoma group (AGIS=5-9). Measurements for foveal and 7 deg eccentricity are shown.

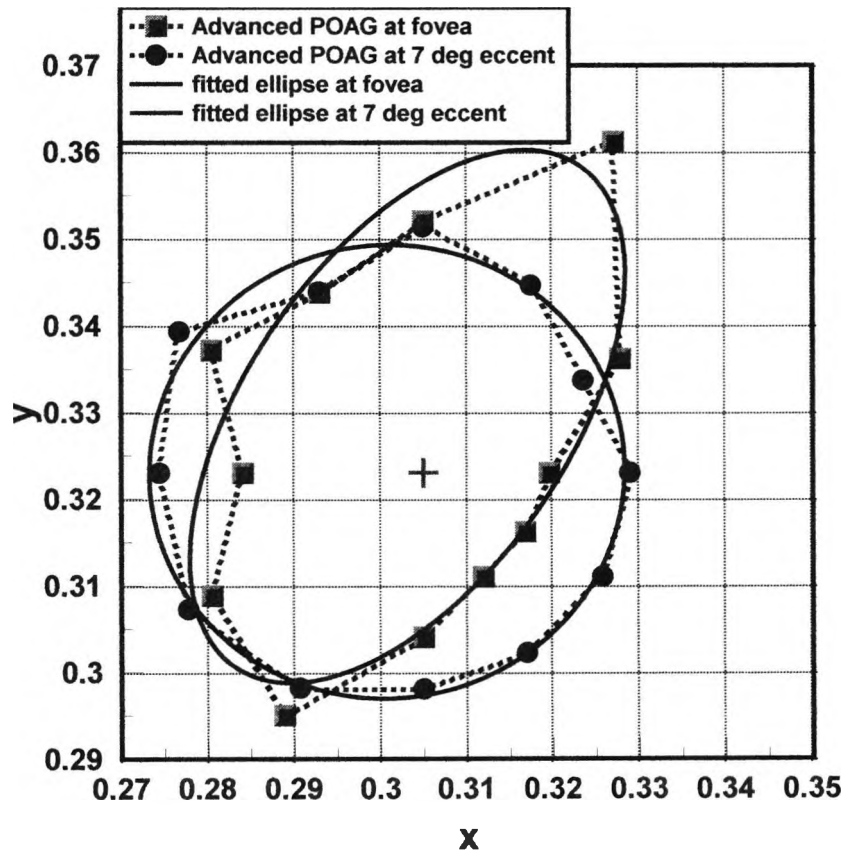


Figure 4.9: Ellipses fitted to the average CD thresholds, measured in the Advanced glaucoma group (AGIS>9). Measurements for foveal and 7 deg eccentricity are shown.

In the group At risk of developing glaucoma (Figure 4.3) we observe a tendency for a diffuse CD loss at the eccentric location (7 deg), shown as a fitted ellipse with a large area, which retains a similar elongation and angle of orientation as the control group. This could be regarded as the earliest sign of CD loss due to glaucoma. At this stage the foveal measurements are not affected.

In the Early glaucoma group (Figure 4.7) the foveal area now shows an enlargement (1.7x) compared with the control group, which is the first sign of foveal CD loss, whereas the area for the eccentric measurements does not suffer any further increase

at this stage beyond the increase observed in the At risk group. The elongation and orientation of this group's ellipses are still very similar to the control group. Therefore, the progression of the disease at this stage is beginning to affect the chromatic sensitivity of the fovea, in a non-selective way.

The most striking characteristic of the Moderate glaucoma group (Figure 4.8) is the large elongation of the foveal ellipse, which denotes a reduction of sensitivity (threshold increase) along the B/Y axis.

The Advanced group (Figure 4.9) shows very large areas, together with a reduction in elongation of both foveal and eccentric fitted ellipses, which suggests a substantial CD loss now affecting the rest of the chromatic directions measured. Interestingly, little further deterioration along the B/Y axis can be seen, which seems to have been preferentially affected, to its limit, in earlier stages of the disease. Thus, the chromatic sensitivity along the R/G axis is selectively affected at the Advanced stage.

Therefore, the natural history of CD loss with progression of the visual field loss could be summarised, according to our results, as follows:

Initially, there is an early diffuse, non-selective CD loss that affects eccentric locations (7 deg), which progresses and eventually affects also the foveal location. Next, a selective CD loss along the B/Y colour confusion axis affecting the foveal location is found when the disease has been established. As the disease progresses into the advanced stages, there is a final selective CD loss along the R/G colour confusion axis added to the previous loss, which affects both foveal and eccentric locations.

As explained in section 4.4.1.4, the CD fitted ellipses have allowed an inspection of the CD loss as the disease progresses. They provide us with an immediate, descriptive visual impression of the gradual development of chromatic sensitivity loss, which is apparent even in the limited sample studied. However, any statistical analysis can only be drawn from the average of the parameters of the individual fitted ellipses, as in Table 4.7.

		Fovea		7 deg eccentricity	
		Mean	SD	Mean	SD
Control	Area	.244	.196	.553	.403
	Elongation	4.12	1.84	2.40	.93
	Orientation (deg)	62	17	65	17
At risk	Area	.176	.156	1.754	1.956
	Elongation	3.72	1.35	2.23	.55
	Orientation (deg)	62	5	60	15
Early	Area	.476	.362	1.181	.809
	Elongation	3.34	.77	2.22	.42
	Orientation (deg)	59	2	63	7
Moderate	Area	.784	1.173	1.313	.892
	Elongation	5.21	3.44	2.87	1.04
	Orientation (deg)	73	39	80	41
Advanced	Area	2.720	4.123	2.418	1.679
	Elongation	3.26	1.14	2.00	.77
	Orientation (deg)	74	44	84	64

Table 4.7: Mean values and SD for the area, elongation and orientation of the fitted ellipses in each sub-group tested.

Figure 4.10, Figure 4.11 and Figure 4.12 show the box-plots of the individual ellipses' parameters for each sub-group.

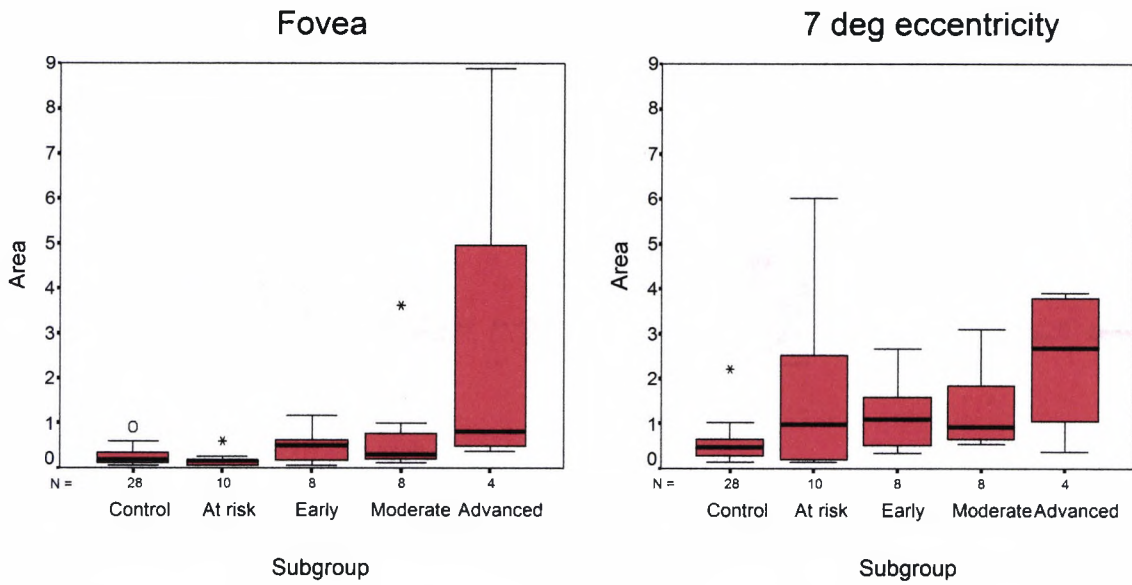


Figure 4.10: Box-and-whisker plots of the areas of the fitted ellipses, for foveal and 7 deg measurements, in each group tested.

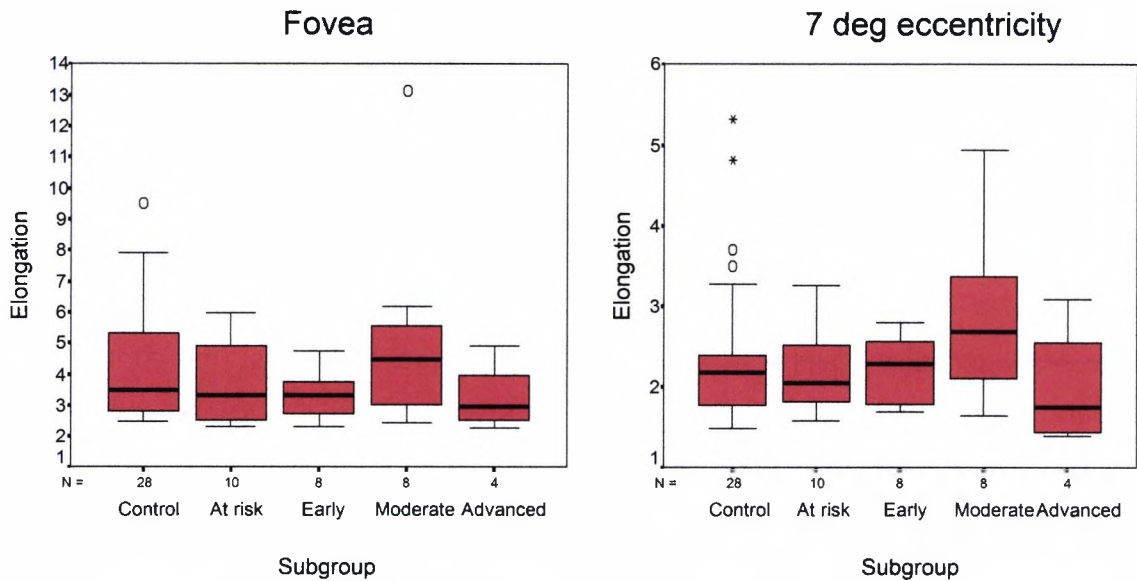


Figure 4.11: Box-and-whisker plots of the elongation of the fitted ellipses, for foveal and 7 deg measurements, in each group tested.

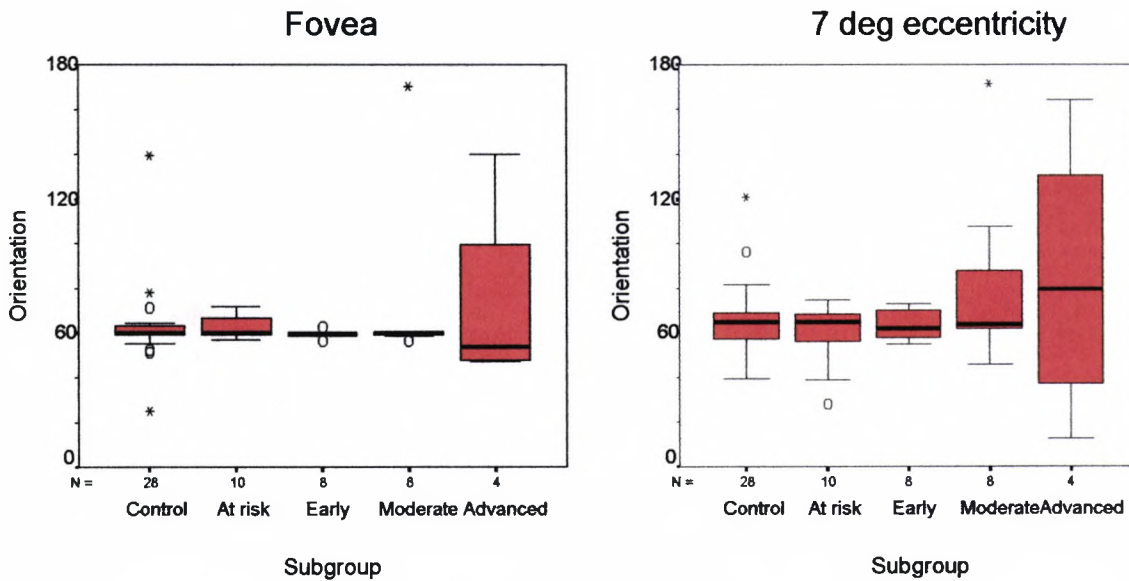


Figure 4.12: Box-and-whisker plots of the orientation of the fitted ellipses, for foveal and 7 deg measurements, in each group tested.

A one-way ANOVA applied to the log transformation of the variables tested (Table 4.8) showed significant differences between groups only for the area, both for foveal ($p=0.001$) and eccentric ($p=0.006$) locations.

Post Hoc tests (LSD) for the log area, measured at the fovea, showed significant differences between the Control and both Moderate ($p=0.03$) and Advanced ($p<0.001$) groups, and close to being significant compared to the Early damage group ($p=0.09$). At the eccentric location (Tamhane, appropriate for unequal variances), the control group was significantly different from the Moderate ($p=0.05$) group. No other statistically significant differences between the control and any of the other groups were found.

Elongation and orientation again did not show any significant differences among the groups. As explained in section 4.4.1.4, the elongation parameter is meaningful when the orientation of the ellipse is around “normal” values. However, in cases where the angle of orientation is far from that expected for the control group, it is advisable to

avoid drawing conclusions regarding the relative loss of CD, which is usually achieved by assessing the information given by the elongation.

		Fovea		7 deg eccentricity	
		Mean	SD	Mean	SD
Control	Log Area	-.740	.348	-.335	.255
	Log Elongation	.581	.166	.356	.139
	Log Orientation	1.781	.108	1.798	.104
At risk	Log Area	-.869	.318	-.060	.586
	Log Elongation	.545	.156	.337	.102
	Log Orientation	1.794	.036	1.758	.136
Early	Log Area	-.474	.436	-.026	.323
	Log Elongation	.514	.098	.339	.085
	Log Orientation	1.774	.013	1.799	.049
Moderate	Log Area	-.387	.483	.039	.276
	Log Elongation	.655	.235	.434	.150
	Log Orientation	1.831	.162	1.866	.181
Advanced	Log Area	.077	.606	.243	.469
	Log Elongation	.495	.141	.278	.156
	Log Orientation	1.821	.221	1.772	.482

Table 4.8: Mean values and SD for Log of the area, elongation and orientation of the fitted ellipses in each sub-group tested.

From the orientation plots (Figure 4.12) it is clear that the greatest variability is for measurements at 7 deg. Advanced cases are the most variable for both locations measured. In advanced disease the usual elliptical pattern of chromatic discrimination breaks down as the pattern becomes more circular due to loss along the R/G channel.

As a result the orientation of the “ellipse” becomes a less meaningful parameter. This has repercussions for the statistical analysis of differences in elongation.

4.4.2 Patterns of chromatic discrimination loss in glaucoma

We carried out a detailed inspection of the data obtained for each POAG and At risk subject. In particular, we were investigating the possible presence of specific characteristic patterns, which could identify certain stages of CD loss. To achieve this we considered the size and shape of the individual ellipses fitted to the data measured at the foveal and eccentric locations and, additionally, the eccentric to foveal area ratios were considered and compared individually to the control group data.

Individual ellipses' parameters as well as the individual stage of CD loss can be found in Table 4.9 and Table 4.10.

Stage 1: Some POAG cases (WH, ZK, PR) and several At risk subjects (RP, RM2, BG, MK) show no CD loss. The size and shape of the ellipses do not differ from the average ellipses in the control group. All cases in stage 1 have foveal and eccentric areas within 1 SD of the Control group. Figure 4.13 presents the raw data for subject PR, who demonstrates a characteristic stage 1 pattern of loss.

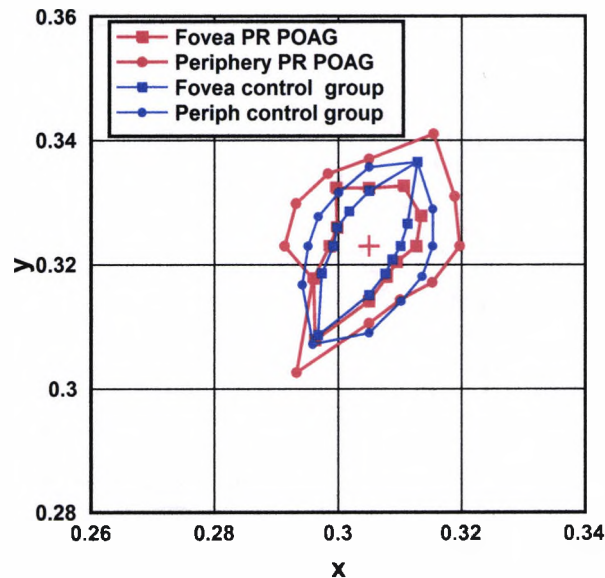


Figure 4.13: An example of a POAG subject (PR) classified in stage 1 of CD loss. Red shows foveal and eccentric measurements for this subject compared to the average measurements in the control group (blue). Notice the similarity of the size and shape of the measurements in the control group.

Stage 2: The earliest CD loss is commonly shown as an enlargement of the area measured at the eccentric location, relative to the foveal area for the same individual. The mean eccentric to foveal area ratio for the control group is 3.3.

All cases in stage 2 (AK, PB, IH, CC, EP, RM, GM, MS, RB) have foveal areas within 1 SD of the control group, but their eccentric to foveal area ratios are larger than 5.7, which is beyond 1 SD for the control group. Most of these cases belong to the At risk or Early groups. Figure 4.14 presents the raw data for subject RB, who demonstrates a characteristic stage 2 pattern of loss.

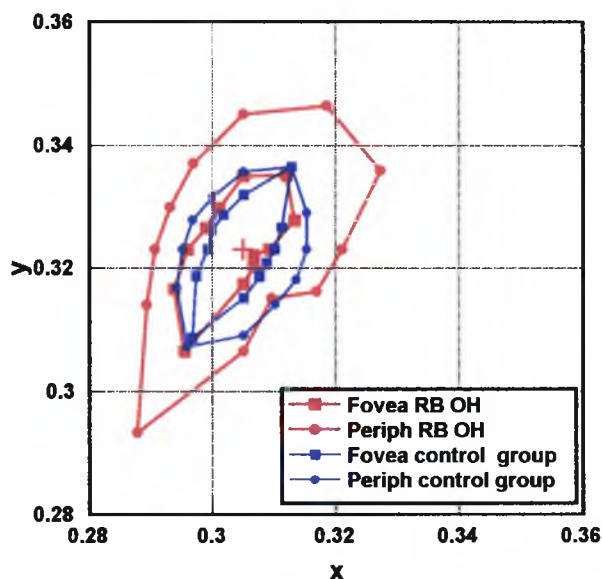


Figure 4.14: An example of an At risk subject (RB) classified in stage 2 of CD loss. Red shows foveal and eccentric measurements for this subject compared to the average measurements in the control group (blue). Notice the enlargement of the eccentric measurements compared to the control group.

The next sign of progression of CD loss is the enlargement of the foveal area. Foveal and eccentric areas, and the eccentric to foveal area ratio have been considered when classifying cases in stages 3 and 4.

Stage 3: All cases included (LC, VF, EB2) have foveal areas larger than normal (> 1SD for the control group) together with still considerably larger eccentric areas. The eccentric to foveal area ratios are still larger than 5.7. Figure 4.15 presents the raw data for subject VF, who demonstrates a characteristic stage 3 pattern of loss.

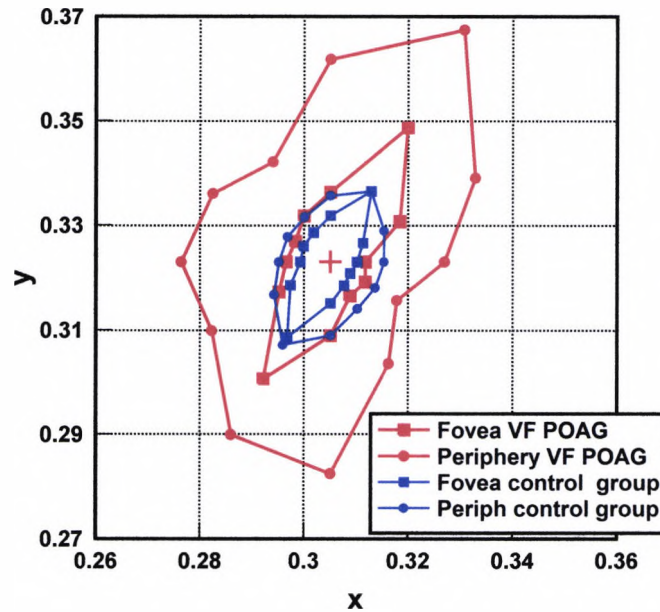


Figure 4.15: An example of a POAG subject (VF) classified in stage 3 of CD loss. Red shows foveal and eccentric measurements for this subject compared to the average measurements in the control group (blue). Notice the enlargement of the foveal and eccentric measurements compared to the control group.

Stage 4: Cases (PO, RH, SP, RSh, EC, TH) included here, like in stage 3, have foveal areas larger than normal. However, the eccentric to foveal area ratio is less than 5.7 due to the relative increase in size of the foveal area. Figure 4.16 presents the raw data for subject EC, who demonstrates a characteristic stage 4 pattern of loss.

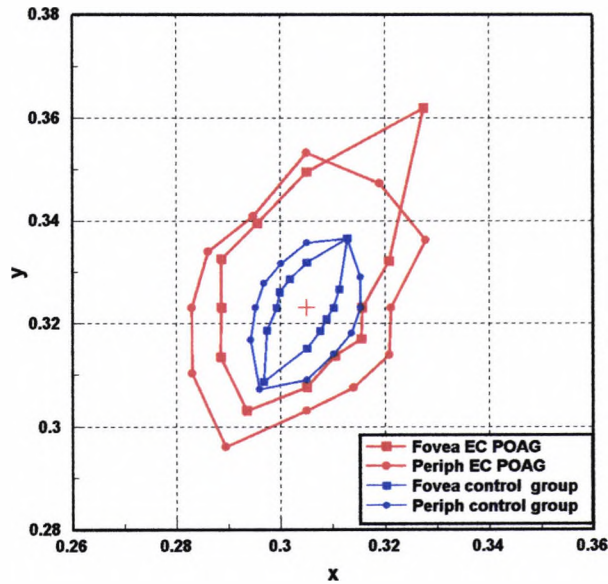


Figure 4.16: An example of a POAG subject (EC) classified in stage 4 of CD loss. Red shows foveal and eccentric measurements for this subject compared to the average measurements in the control group (blue). Both foveal and eccentric measurements are large compared to the control group. However, the eccentric to foveal area ratio is less than 5.7 due to the relative increase in size of the foveal area.

Stage 5: Some cases (EB, RS) show an elongated foveal ellipse (elongation > 6.00, which is beyond 1 SD for the control group), due to the threshold increase along the tritan colour confusion axis. This is usually accompanied by large foveal areas. Figure 4.17 presents the raw data for subject EB, who is an example of stage 5.

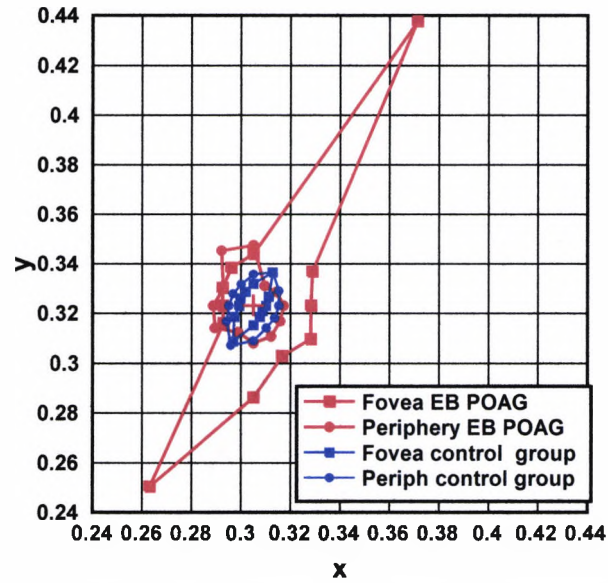


Figure 4.17: An example of a POAG subject (EB) classified in stage 5 of CD loss. Red shows foveal and eccentric measurements for this subject compared to the average measurements in the control group (blue). This case shows an elongated foveal ellipse compared to the control group.

Stage 6: At the most advanced stage of CD loss identified, both foveal and eccentric ellipses have massive areas. There is also a tendency for a reduction in the ellipses' elongation and for the orientation to vary because of the threshold increase along the R/G axis. Figure 4.18 presents the raw data for subject JD, who demonstrates a characteristic stage 6 pattern of loss.

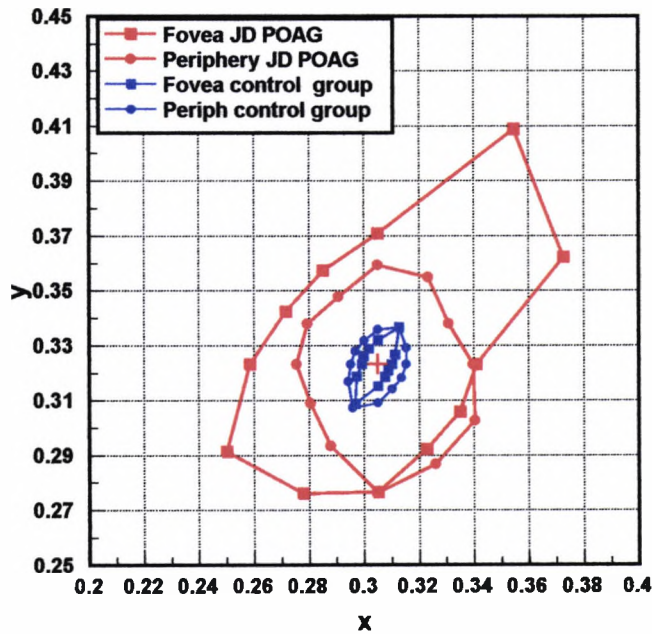


Figure 4.18: An example of a POAG subject (JD) classified in stage 6 of CD loss. Red shows foveal and eccentric measurements for this subject compared to the average measurements in the control group (blue). This case shows massive areas for both foveal and 7 deg measurements compared to the control group.

Thus, several patterns of CD loss in POAG have been identified and can be summarised as follows:

- Some POAG and At risk cases show no pattern of CD loss at any of the locations tested.
- A pattern of non-selective reduction in chromatic sensitivity at the eccentric location (7 deg). Usually affects early cases.
- A pattern of non-selective CD loss affecting both the foveal and the eccentric (7 deg) locations. Two patterns of loss were identified. Whilst some subjects still demonstrate a larger relative CD loss at the eccentric location, others demonstrate a relatively greater foveal CD loss.

- In the advanced stages of the disease POAG cases tend to show massive losses of CD affecting the foveal and / or the eccentric measurement at 7 deg.

Naturally, not all cases adhere rigorously to one of the above-mentioned patterns of CD loss. Although most subjects can be classified clearly as belonging to one stage, some cases may show characteristics of two non-consecutive stages (e.g. stages 3 and 5).

One case was not considered in the classification of patterns of CD loss. Subject HF had a relatively small foveal area, with a 2.5 elongation, but the angle of orientation was at 170 deg, far from the expected orientation of the tritan colour confusion axis.

Individual ellipses' cases can be viewed in Appendix 8.2. Note that the scales used for these plots of ellipses may vary from subject to subject.

Figure 4.19 shows the distribution of cases classified by the stages/ patterns of CD loss as a function of the AGIS score (severity of visual field loss). There is a significant association ($p < 0.01$) between the two variables (Spearman's $\rho = 0.58$) with $R^2 = 0.34$. Hence, the association between AGIS score and the stage of pattern of CD classification can explain 34% of the variability of the data. This R^2 is consistent with the clinical picture in which some cases show early signs of chromatic sensitivity loss and no visual field defect (e.g. cases in stages 2 or 3 of CD loss) while others show no CD loss but early to moderate visual field defects (e.g. some cases in stage 1 of CD loss).

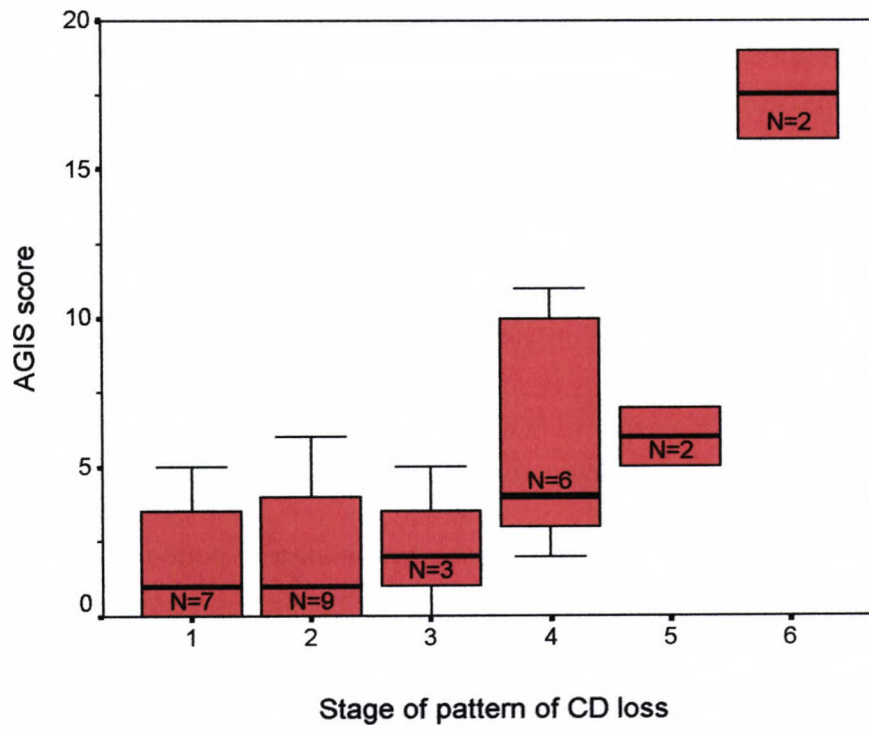


Figure 4.19: Distribution of CD loss stage with severity of VF damage as measured by the AGIS score in POAG and At risk subjects.

POAG Subjects	Sex & age (yrs)	F-M 100 hue TE Score	Fovea			7 deg eccentricity				Stage of CD loss
			Area $\pi \cdot M \cdot m$	(xy, Elongation	Orientation (deg)	Area $\pi \cdot M \cdot m$	(xy, Elongation	Orientation (deg)		
JD	♀ 70	156	8.892	2.27	48.5	3.897	1.50	96.5	6	
DB	♂ 65	236	1.016	2.81	140	3.692	3.09	164	6	
PO	♂ 70	96	0.588	3.06	59.5	1.702	1.40	12.5	4	
RH	♂ 68	68	0.477	4.90	47.5	0.383	2.00	62	4	
EB2	♂ 79	344	3.604	6.20	60.5	0.767	2.11	107.5	5	
AK	♀ 60	88	0.104	4.72	60	1.019	2.67	62	2	
PB	♀ 70	144	0.235	4.25	58.5	1.922	4.94	171.5	2	
WH	♂ 75	152	0.349	2.44	56.5	0.536	1.66	67.5	1	
ZK	♂ 65	20	0.179	4.94	60	0.552	3.62	60.5	1	
RS	♂ 72	184	0.993	13.12	60	1.783	3.13	64.5	5	
LC	♀ 55	124	0.539	3.52	60	3.096	2.69	62	3	
SP	♂ 81	424	0.538	3.44	59.5	0.356	2.80	71.5	4	
IH	♂ 55	116	0.063	4.75	59	0.399	2.52	57	2	
HF	♂ 74	108	0.273	2.49	170.5	0.832	2.11	45.5	?	
RSh	♂ 64	116	0.441	2.78	56.5	1.555	2.35	73	4	

EC	♂ 72	160	1.164	2.67	62.5	1.634	1.71	58.5	4
PR	♂ 74	36	0.233	2.34	59	0.681	1.86	58	1
VF	♀ 65	140	0.539	3.25	60.5	2.679	2.23	68.5	3
CC	♂ 67	24	0.100	3.81	58.5	0.612	1.70	54.5	2
TH	♀ 67	112	0.731	3.67	60	1.531	2.60	65	4

Table 4.9: Results for the POAG eyes.

POAG Suspects	Sex & age (yr)	F-M hue Score	Fovea			7 deg eccentricity			Stage of CD loss
			100 TE	Area $\pi \cdot M \cdot m$	(xy, Elongation	Orientation (deg)	Area $\pi \cdot M \cdot m$	(xy, Elongation	
EP	♀ 73	88	0.250	2.48	71.5	2.216	1.82	74.8	2
RM	♀ 65	100	0.064	5.22	57.3	3.957	2.52	63.2	2
RP	♂ 63	56	0.109	4.57	60	0.334	2.04	38.5	1
GM	♂ 69	164	0.134	5.98	61.5	2.546	1.75	66	2
EB	♀ 63	148	0.585	5.90	60.5	6.002	1.58	28	3
RM2	♂ 77	28	0.064	2.53	66.5	0.202	1.89	68.5	1
MS	♀ 45	32	0.047	3.05	59.5	0.827	3.26	71.5	2
BG	♂ 52	176	0.069	2.54	60.5	0.193	2.06	63	1
MK	♂ 61	160	0.166	3.62	60	0.156	2.97	66	1
RB	♂ 63	112	0.151	4.91	57	1.112	2.38	56	2

Table 4.10: Results for the eyes at risk of developing POAG

4.4.3 Chromatic sensitivity loss along R/G and B/Y colour opponent channels

In order to overcome the limitations encountered when comparing the ellipticity of the CD ellipses in at risk, POAG and control subjects and to minimise the error introduced by fitting ellipses to data that might not be of elliptical shape, we re-analysed the B/Y and R/G thresholds to investigate more specifically the relative loss of chromatic discrimination along two colour displacement directions in the CIE xy chromaticity diagram that maximise the activity of the B/Y and R/G chromaticity mechanisms.

Therefore, the mean of the thresholds along 60 and 240 deg directions and those along 150 and 330 deg directions, for each subject, were calculated. Our aim was to compare B/Y to R/G sensitivity by averaging the thresholds along these directions. Therefore, the mean of the subjects' thresholds for the 60 and 240 deg directions, which were the closest to the Tritan line, and the mean of the thresholds for the 150 and 330 deg directions, which lies in between the Protan and Deutan lines, were calculated for each individual. They will be referred to as B/Y and R/G thresholds from now on.

A logarithmic transformation was applied to the data in order to achieve a normal distribution and similar SD when comparing the means of the three groups. Figure 4.20 shows the mean of the log thresholds along 60 deg, 240 deg, 150 deg and 330 deg directions for each group. As can be appreciated there is no significant difference between 60 and 240 deg directions or between 150 and 330 deg directions, in any of the groups.

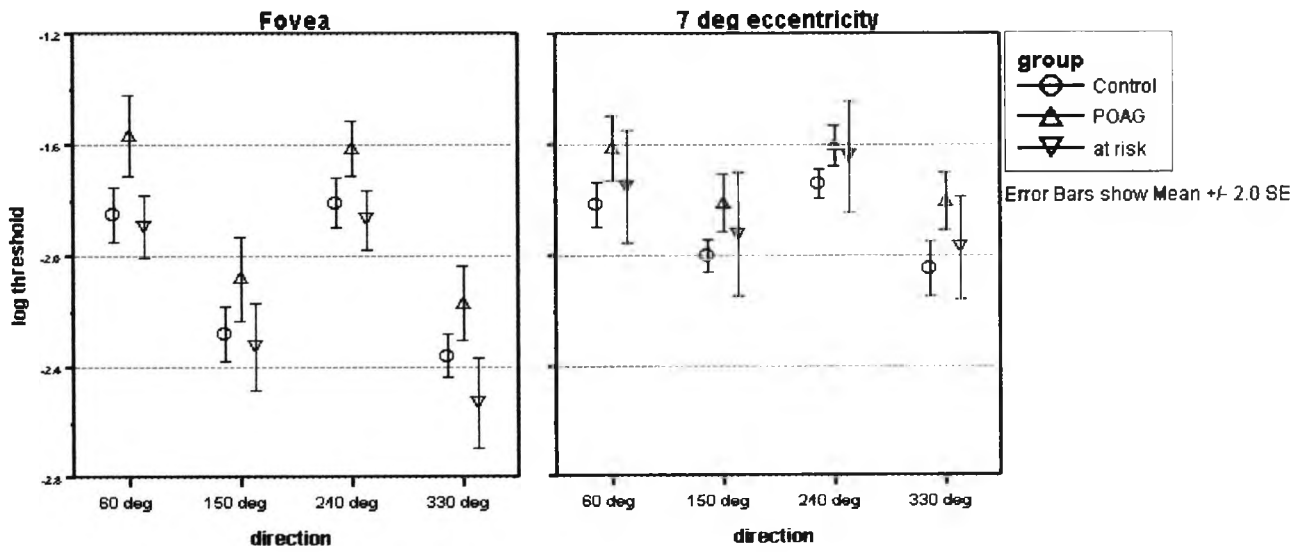


Figure 4.20: Mean log thresholds along the 60 deg and 240 deg directions and along the 150 deg and 330 deg direction for foveal and 7 deg eccentricity measurements in each group tested.

Figure 4.21 compares B/Y thresholds (average of the 60 - 240 deg colour confusion line) and R/G thresholds (average of the 150 - 330 deg colour confusion line) for each group. The mean B/Y and R/G log thresholds and SD for the control, POAG and At risk groups are shown in Table 4.11.

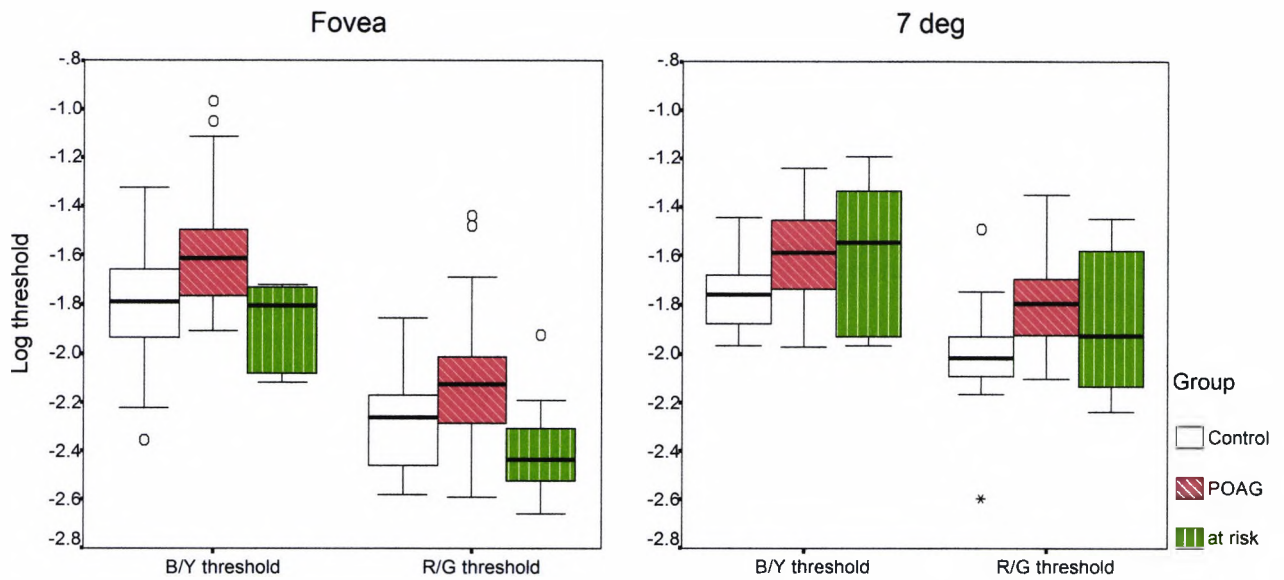


Figure 4.21: Box plots of the B/Y and R/G thresholds for foveal and 7 deg eccentricity measurements in each group tested.

			Fovea		7 deg eccentricity	
Log threshold	Group	Axis	Mean	Std Deviation	Mean	Std Deviation
			Control	B/Y	-1.817	.232
		R/G	-2.296	.185	-2.010	.182
	POAG	B/Y	-1.579	.271	-1.593	.197
		R/G	-2.109	.315	-1.787	.207
	at risk	B/Y	-1.875	.165	-1.610	.296
		R/G	-2.398	.218	-1.875	.291

Table 4.11: B/Y and R/G average log thresholds and SD for control, POAG and At risk groups at each location tested.

It is readily apparent from the inspection of Figure 4.20, Figure 4.21 and Table 4.11 that:

- As a general rule, B/Y discrimination was poorer than R/G discrimination, for both locations tested, in all groups.
- There is a clear difference in sensitivity between the POAG and control groups, particularly for measurements taken at the eccentric location.
- The group At risk cannot be differentiated from the control group at the foveal location, neither for the B/Y nor for R/G thresholds. At 7 deg the variability in the group At risk is large, suggesting considerable differences in sensitivity among the subjects in this group, both for B/Y and R/G thresholds.
- Large ranges of discrimination abilities are exhibited by different subjects. Some POAG subjects lie within the normal range for the control group, conversely some control subjects show large excursions in one or both colour confusion lines.

A one-way ANOVA, applied to compare the differences in group means for the log B/Y and R/G thresholds, revealed significant differences between groups for the B/Y log threshold, both for foveal ($p=0.001$) and 7 deg eccentricity ($p=0.009$) locations tested, as well as for the R/G log threshold, both for foveal ($p=0.005$) and 7 deg eccentricity ($p=0.003$) locations tested.

Post Hoc tests (LSD) for the B/Y log threshold at the fovea revealed a significant difference between the control and the POAG groups ($p=0.001$), however no significant difference was found between the control group and the group At risk ($p=0.508$). For the eccentric location, post hoc tests (Tamhane, appropriate for unequal variances) for the B/Y log threshold revealed a significant difference between the control and the POAG group ($p=0.008$). There was no significant difference between the control and At risk groups ($p=0.378$), nor between the POAG and the At risk group ($p=0.998$), which reflects the similarity between the POAG and the At risk groups.

Post Hoc tests (LSD) for the R/G log threshold at the fovea revealed a significant difference between the control and the POAG groups ($p=0.011$), however no significant difference was found between the control group and the group At risk ($p=0.262$). For

the eccentric location, post hoc tests (Tamhane, appropriate for unequal variances) for the R/G log threshold revealed a significant difference between the control and the POAG group ($p=0.001$). There was no significant difference between the control and At risk groups ($p=0.478$).

Table 4.12 and Table 4.13 show the differences between the group means, the significance and the 95% confidence interval for foveal and 7 deg measurements.

Multiple comparisons of R/G and B/Y chromatic sensitivity measured at the fovea

Dependent Variable: Log threshold
LSD

			Mean Differen	Std. Error	Sig.	95% Confidence Interval	
						Lower Bound	Upper Bound
B/Y threshold	Control	POAG	-.238*	6.93E-02	.001	-.377	-9.9E-02
		at risk	5.810E-02	8.73E-02	.508	-.117	.233
	POAG	Control	.238*	6.93E-02	.001	9.936E-02	.377
		at risk	.296*	9.17E-02	.002	.113	.480
	at risk	Control	-5.8E-02	8.73E-02	.508	-.233	.117
		POAG	-.296*	9.17E-02	.002	-.480	-.113
R/G threshold	Control	POAG	-.188*	7.10E-02	.011	-.330	-4.5E-02
		at risk	.101	8.93E-02	.262	-7.78E-02	.280
	POAG	Control	.188*	7.10E-02	.011	4.532E-02	.330
		at risk	.289*	9.39E-02	.003	.101	.477
	at risk	Control	-.101	8.93E-02	.262	-.280	7.8E-02
		POAG	-.289*	9.39E-02	.003	-.477	-.101

*. The mean difference is significant at the .05 level.

Table 4.12: Pairwise comparisons of R/G and B/Y sensitivity of the Control, POAG and At risk group means for LSD post hoc test, measured at the fovea.

Multiple comparisons of R/G and B/Y chromatic sensitivity measured at 7 deg eccentricity

Dependent Variable: Log threshold
Tamhane

			Mean Differen	Std. Error	Sig.	95% Confidence Interval	
						Lower Bound	Upper Bound
B/Y threshold	Control	POAG	-.170*	5.72E-02	.008	-.300	-3.918E-02
		at risk	-.153	7.19E-02	.378	-.428	.123
	POAG	Control	.170*	5.72E-02	.008	3.918E-02	.300
		at risk	1.702E-02	7.56E-02	.998	-.265	.300
	at risk	Control	.153	7.19E-02	.378	-.123	.428
		POAG	-1.702E-02	7.56E-02	.998	-.300	.265
R/G threshold	Control	POAG	-.223*	6.21E-02	.001	-.367	-7.929E-02
		at risk	-.135	7.81E-02	.478	-.409	.138
	POAG	Control	.223*	6.21E-02	.001	7.929E-02	.367
		at risk	8.830E-02	8.21E-02	.790	-.191	.368
	at risk	Control	.135	7.81E-02	.478	-.138	.409
		POAG	-8.830E-02	8.21E-02	.790	-.368	.191

*. The mean difference is significant at the .05 level.

Table 4.13: Pairwise comparisons of R/G and B/Y sensitivity of the Control, POAG and At risk group means for Tamhane post hoc test, measured at 7 deg eccentricity.

4.4.3.1 R/G and B/Y chromatic discrimination loss as a function of severity of the disease

The B/Y and R/G thresholds were also plotted for each of the POAG subgroups classified according to the severity of visual field damage (AGIS score).

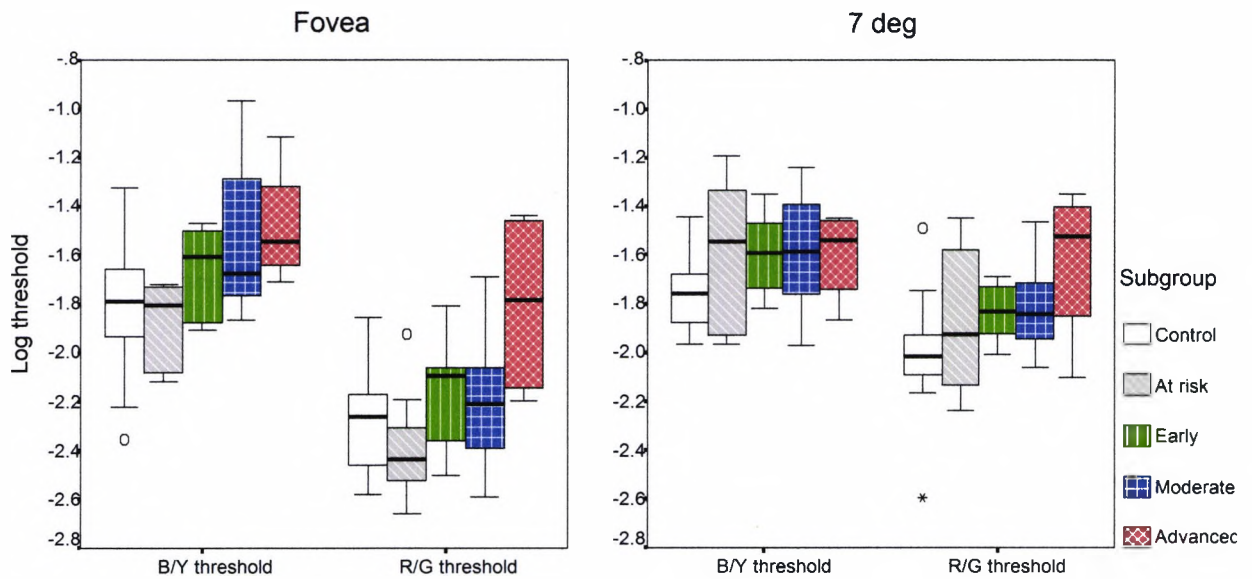


Figure 4.22: Box plots of the B/Y and R/G thresholds for foveal and 7 deg eccentricity measurements are shown for each POAG subgroup classified according to the severity of VF damage (AGIS score).

		Fovea		7 deg eccentricity		
Log threshold	Group	Axis	Mean	Std Deviation	Mean	Std Deviation
	Control		B/Y	-1.817	.232	-1.763
R/G			-2.296	.185	-2.010	.182
At risk		B/Y	-1.875	.165	-1.610	.296
		R/G	-2.398	.218	-1.875	.291
Early		B/Y	-1.669	.191	-1.597	.168
		R/G	-2.169	.231	-1.836	.119
Moderate		B/Y	-1.537	.342	-1.587	.247
		R/G	-2.201	.283	-1.818	.188
Advanced		B/Y	-1.481	.257	-1.601	.193
		R/G	-1.803	.399	-1.626	.335

Table 4.14: B/Y and R/G log thresholds mean and SD for control, and each of the POAG subgroups tested.

The function that best describes how the R/G and B/Y chromatic thresholds increase with the severity of visual field loss can be identified in Figure 4.23 and Figure 4.24. For foveal measurements, the increase for B/Y thresholds and R/G thresholds is well described by a linear function (Figure 4.23). The R/G thresholds display a greater increase and better correlation with progressive field loss than the B/Y thresholds. Thus approaching the values of B/Y thresholds for Moderate and Advanced glaucomatous damage cases.

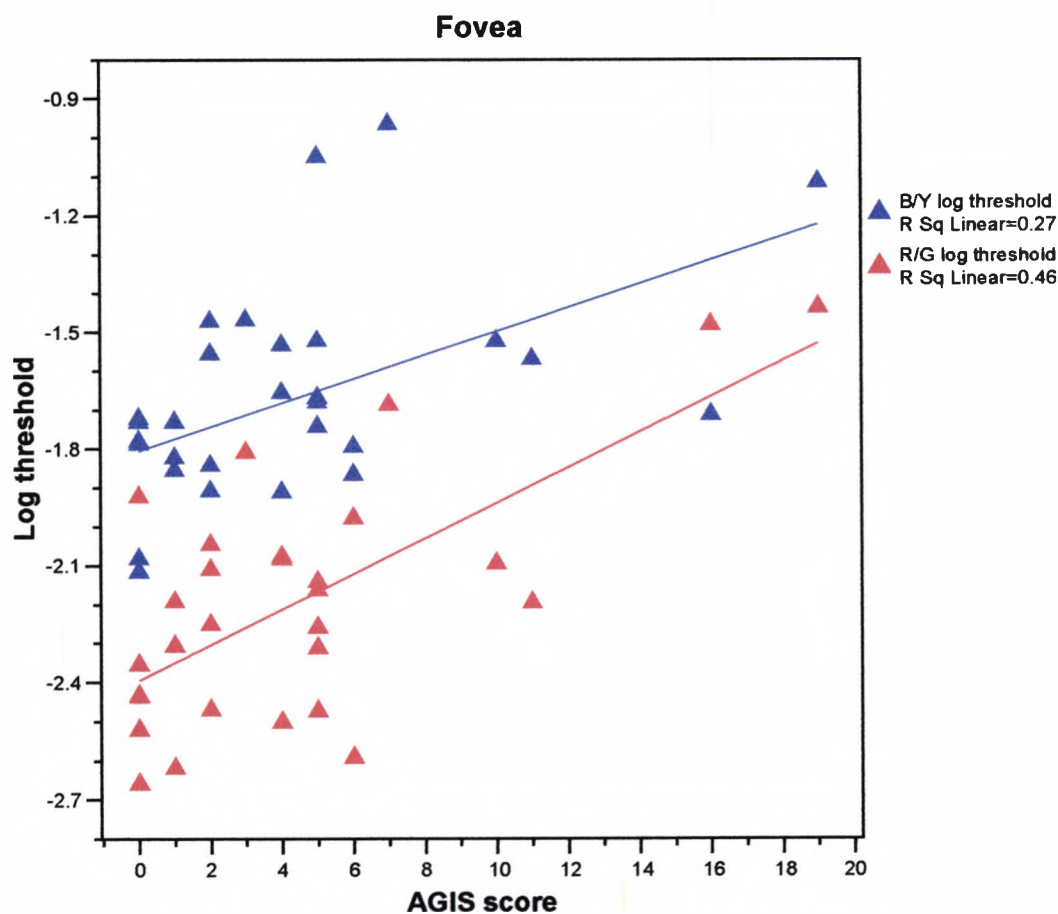


Figure 4.23: Comparison of foveal measurements of R/G and B/Y chromatic log threshold increases in the POAG and At risk subjects as a function of visual field loss (AGIS score). Linear functions are fitted to the data.

At 7 deg eccentricity, the R/G thresholds show a linear increase as a function of visual field damage (Figure 4.24). However, the B/Y thresholds show no increase with severity of the visual field loss, suggesting that all the B/Y CD loss has occurred in the early stages.

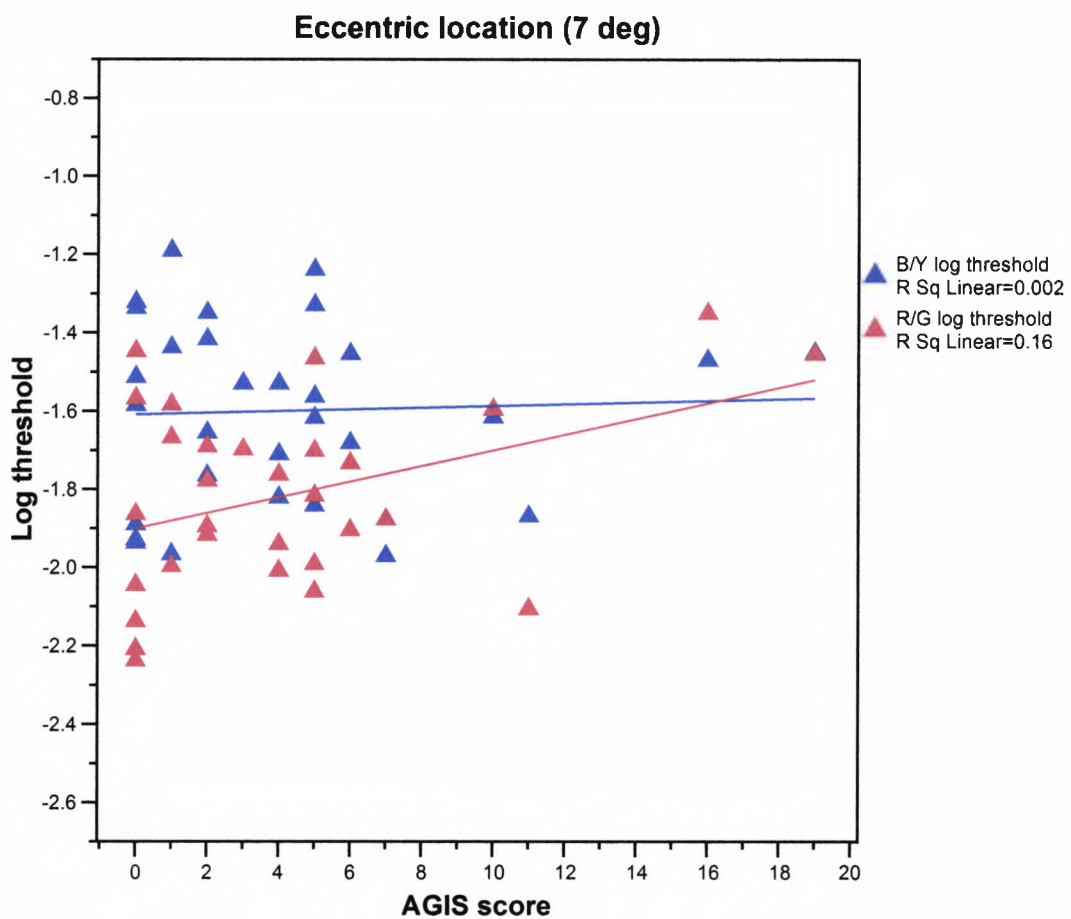


Figure 4.24: Comparison of 7 deg measurements of R/G and B/Y chromatic log thresholds increases in the POAG and At risk subjects as a function of visual field loss (AGIS score).

From Figure 4.22, Figure 4.23, Figure 4.24 and Table 4.14 we can appreciate:

- The CD threshold along the B/Y axis increases (sensitivity reduction) progressively with severity of the disease up to the Moderate stages of visual field loss, for measurements taken at the fovea, whereas eccentric measurements reach their maximum loss in the early stages of the disease and do not show much further deterioration.
- Although R/G thresholds, both for foveal and eccentric measurements, show an initial increase in the early stages of the disease it is in the advanced stages of the disease when they are most affected.
- The group At risk only shows a reduction in sensitivity, when compared with the control group, for eccentric (7 deg) measurements, both along B/Y and R/G colour confusion axes. It also shows one of the largest variabilities among the groups studied.

A one-way ANOVA applied to the log transformations of the B/Y and R/G thresholds showed significant differences between the groups for the B/Y log threshold, both for foveal ($p=0.004$) and 7 deg eccentricity ($p=0.05$) locations tested, as well as for the R/G log threshold, both for foveal ($p=0.001$) and 7 deg eccentricity ($p=0.006$) locations tested.

Post Hoc tests (LSD) for the B/Y log threshold at the fovea revealed a significant difference between control and Moderate groups ($p=0.005$) and between control and Advanced groups ($p=0.01$), however no significant difference was found between control and At risk groups ($p=0.508$) nor between control and Early damage groups ($p=0.508$). For the eccentric location, post hoc tests (Tamhane, appropriate for unequal variances) for the B/Y log threshold revealed no significant differences between any of the groups.

Post Hoc tests (LSD) for the R/G log threshold at the fovea revealed a significant difference only between control and Advanced groups ($p<0.001$), however no significant difference was found between control and any of the other glaucoma subgroups. For the eccentric location, post hoc tests (Tamhane, appropriate for unequal variances) for the R/G log threshold revealed no significant difference between any of the groups.

Table 4.15 and Table 4.16 show the differences between the group means, the significance and the 95% confidence intervals for foveal and 7 deg measurements.

Multiple comparisons of R/G and B/Y chromatic sensitivity measured at the fovea

Dependent Variable: Log threshold
LSD

			Mean Differen	Std. Error	Sig.	95% Confidence Interval	
						Lower Bound	Upper Bound
B/Y threshold	Control	At risk	5.810E-02	8.72E-02	.508	-.117	.233
		Early	-.148	9.49E-02	.125	-.338	4.24E-02
		Moderate	-.280*	9.49E-02	.005	-.470	-9.0E-02
		Advanced	-.336*	.126	.010	-.590	-8.2E-02
	At risk	Control	-5.810E-02	8.72E-02	.508	-.233	.117
		Early	-.206	.112	.072	-.431	1.91E-02
		Moderate	-.338*	.112	.004	-.563	-.113
		Advanced	-.394*	.140	.007	-.675	-.113
	Early	Control	.148	9.49E-02	.125	-4.24E-02	.338
		At risk	.206	.112	.072	-1.91E-02	.431
		Moderate	-.132	.118	.269	-.369	.105
		Advanced	-.188	.145	.200	-.479	.103
	Moderate	Control	.280*	9.49E-02	.005	6.974E-02	.470
		At risk	.338*	.112	.004	.113	.563
		Early	.132	.118	.269	-.105	.369
		Advanced	-5.575E-02	.145	.702	-.346	.235
	Advanced	Control	.336*	.126	.010	8.206E-02	.590
		At risk	.394*	.140	.007	.113	.675
		Early	.188	.145	.200	-.103	.479
		Moderate	5.575E-02	.145	.702	-.235	.346
R/G threshold	Control	At risk	.101	8.41E-02	.234	-6.74E-02	.270
		Early	-.127	9.15E-02	.171	-.310	5.65E-02
		Moderate	-9.503E-02	9.15E-02	.304	-.279	8.85E-02
		Advanced	-.494*	.122	.000	-.738	-.249
	At risk	Control	-.101	8.41E-02	.234	-.270	6.74E-02
		Early	-.228*	.108	.040	-.445	-1.1E-02
		Moderate	-.196	.108	.076	-.413	2.09E-02
		Advanced	-.595*	.135	.000	-.866	-.324
	Early	Control	.12699835	9.15E-02	.171	-5.65E-02	.3104804
		At risk	.22816459*	.1082385	.040	1.11E-02	.4452635
		Moderate	3.197E-02	.1140934	.780	-.1968737	.2608109
		Advanced	-.36674215*	.1397353	.011	-.6470156	-8.6E-02
	Moderate	Control	9.503E-02	9.15E-02	.304	-8.85E-02	.2785118
		At risk	.19619597	.1082385	.076	-2.09E-02	.4132948
		Early	-3.197E-02	.1140934	.780	-.2608109	.1968737
		Advanced	-.39871077*	.1397353	.006	-.6789842	-.118437
	Advanced	Control	.49374049*	.1219709	.000	24909778	.7383832
		At risk	.59490674*	.1349971	.000	32413687	.8656766
		Early	.36674215*	.1397353	.011	8.65E-02	.6470156
		Moderate	.39871077*	.1397353	.006	.11843733	.6789842

*. The mean difference is significant at the .05 level.

Table 4.15: Pairwise comparisons of R/G and B/Y sensitivity of the Control, At risk and POAG subgroups means for LSD post hoc test, measured at the fovea.

Multiple comparisons of R/G and B/Y chromatic sensitivity measured at 7 deg eccentricity

Dependent Variable: Log threshold
Tamhane

Axis	Mean	Std. Error	Sig.	95% Confidence Interval			
				Lower Bound	Upper Bound		
B/Y threshold	Control	At risk	-153	7.32E-02	.795	-495	190
		Early	-167	7.97E-02	.252	-399	6.55E-02
		Moderate	-177	7.97E-02	.603	-520	.167
		Advanced	-162	.106	.880	-.791	.466
	At risk	Control	.153	7.32E-02	.795	-.190	.495
		Early	-1.385E-02	9.43E-02	1.000	-.378	.350
		Moderate	-2.385E-02	9.43E-02	1.000	-.439	.391
		Advanced	-9.689E-03	.118	1.000	-.509	.489
	Early	Control	.167	7.97E-02	.252	-6.547E-02	.399
		At risk	1.385E-02	9.43E-02	1.000	-.350	.378
		Moderate	-9.998E-03	9.94E-02	1.000	-.369	.349
		Advanced	4.164E-03	.122	1.000	-.512	.520
	Moderate	Control	.177	7.97E-02	.603	-.167	.520
		At risk	2.385E-02	9.43E-02	1.000	-.391	.439
		Early	9.998E-03	9.94E-02	1.000	-.349	.369
		Advanced	1.416E-02	.122	1.000	-.489	.518
	Advanced	Control	.162	.106	.880	-.466	.791
		At risk	9.689E-03	.118	1.000	-.489	.509
		Early	-4.164E-03	.122	1.000	-.520	.512
		Moderate	-1.416E-02	.122	1.000	-.518	.489
R/G threshold	Control	At risk	-.135	7.74E-02	.886	-.473	.203
		Early	-.175*	8.42E-02	.050	-.349	-1.2E-04
		Moderate	-.192	8.42E-02	.232	-.452	6.80E-02
		Advanced	-.384	.112	.664	-1.538	.769
	At risk	Control	.135	7.74E-02	.886	-.203	.473
		Early	-3.946E-02	9.97E-02	1.000	-.382	.304
		Moderate	-5.669E-02	9.97E-02	1.000	-.426	.313
		Advanced	-.249	.124	.944	-1.165	.667
	Early	Control	.175*	8.42E-02	.050	1.201E-04	.349
		At risk	3.946E-02	9.97E-02	1.000	-.304	.382
		Moderate	-1.723E-02	.105	1.000	-.286	.252
		Advanced	-.210	.129	.973	-1.329	.909
	Moderate	Control	.192	8.42E-02	.232	-6.804E-02	.452
		At risk	5.669E-02	9.97E-02	1.000	-.313	.426
		Early	1.723E-02	.105	1.000	-.252	.286
		Advanced	-.192	.129	.986	-1.201	.816
	Advanced	Control	.384	.112	.664	-.769	1.538
		At risk	.249	.124	.944	-.667	1.165
		Early	.210	.129	.973	-.909	1.329
		Moderate	.192	.129	.986	-.816	1.201

*. The mean difference is significant at the .05 level.

Table 4.16: Pairwise comparisons of R/G and B/Y sensitivity of the Control, At risk and POAG subgroups means for Tamhane post hoc test, measured at 7 deg eccentricity.

4.4.3.2 Relative loss of chromatic discrimination in glaucoma

The relative loss of chromatic discrimination was also assessed by calculating individual log threshold differences from the control group mean, for B/Y and R/G thresholds. Figure 4.25 and Figure 4.26 show the differences for the B/Y log thresholds plotted against the R/G log thresholds, for foveal and 7 deg eccentricity, respectively. The units of the two axes are distances in x, y space. Each triangle represents the difference in log threshold for an individual POAG subject from the control mean. The X symbols represent differences in log threshold values for each At risk subject from the control mean. The mean threshold for the control group is represented by (0,0). The circles represent differences in log threshold values for each control subject compared to the mean log threshold value for control subjects.

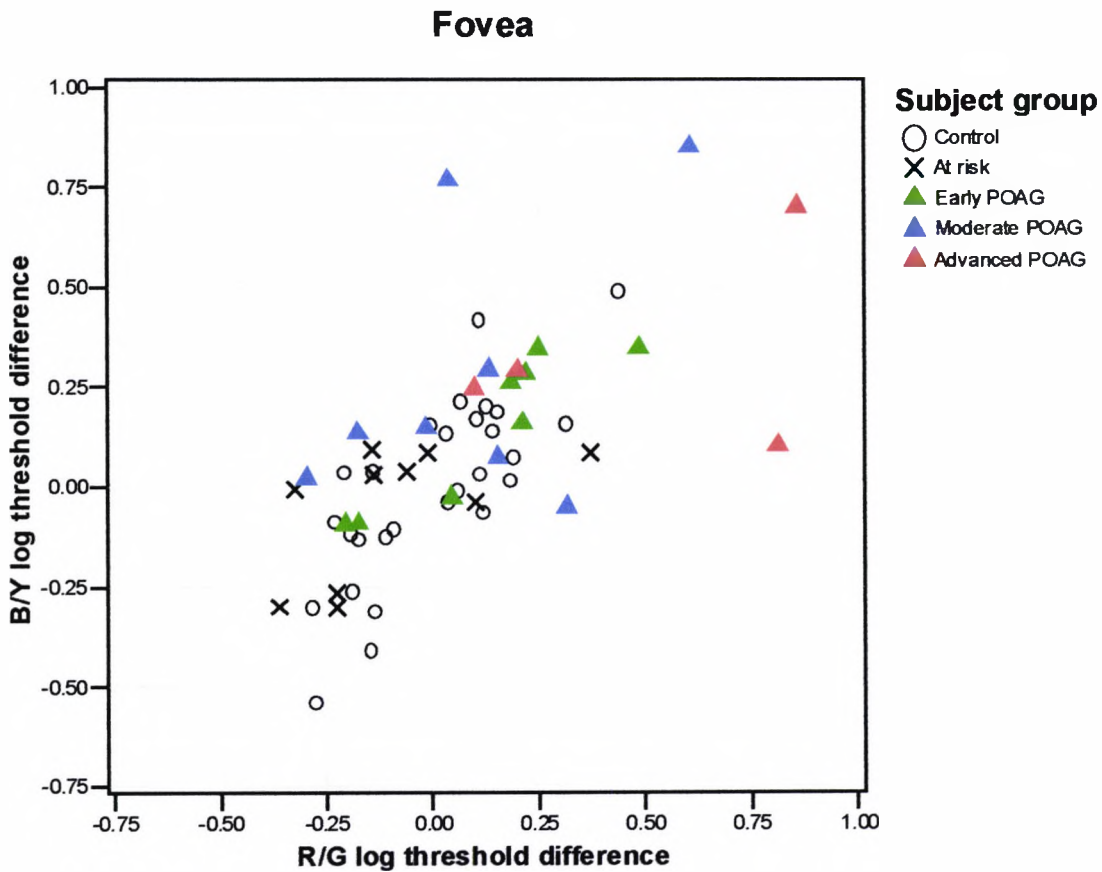


Figure 4.25: A comparison of threshold differences for B/Y with those for R/G sensitivities (log threshold units), for each individual subject. The triangles represent differences for individual POAG subjects, from the control mean. The X symbols represent differences for individual At risk subjects from the control mean. The circles represent differences for each control subject compared to the mean for control subjects (the point (0,0) represents the "mean control value"). POAG cases are classified according to the severity of glaucomatous damage.

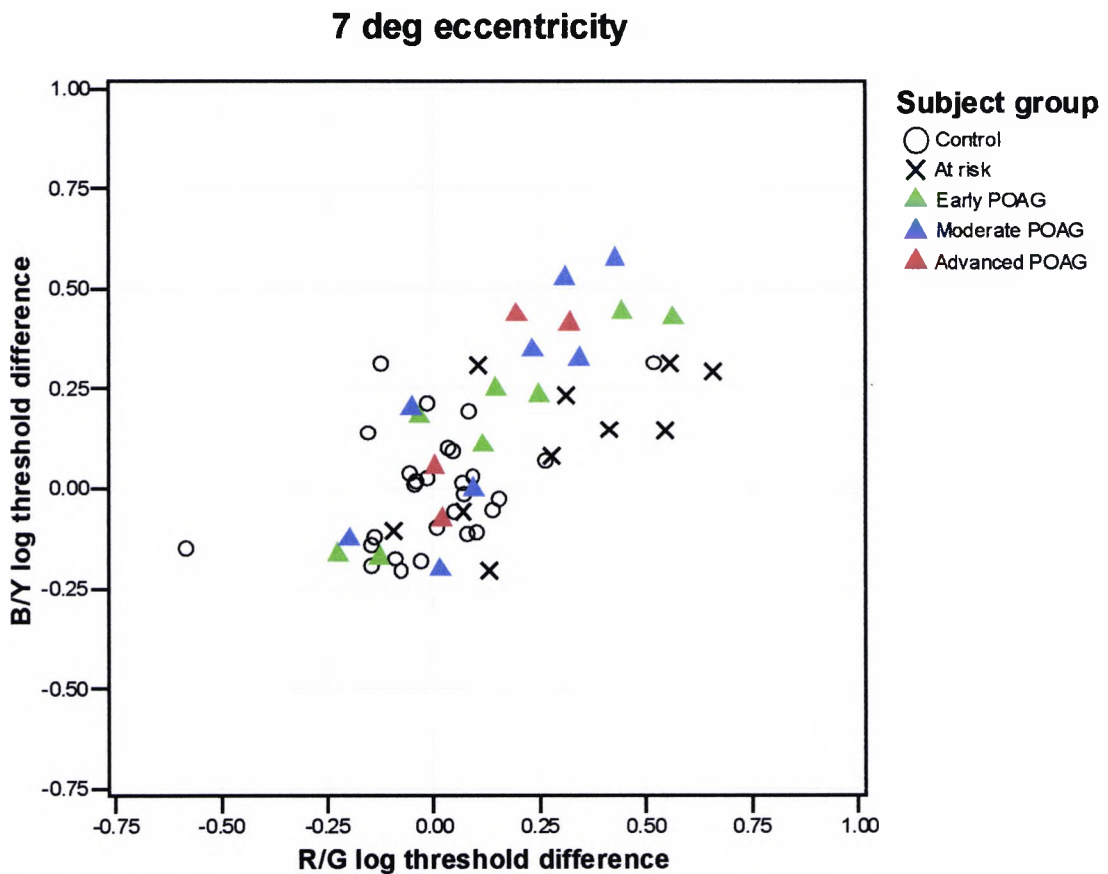


Figure 4.26: Threshold differences for B/Y sensitivity compared with those for R/G sensitivities (log threshold units), for each individual POAG, At risk and control subject. For details see caption to Figure 4.25.

In Figure 4.27 and Figure 4.28 only the mean regression line and confidence intervals for the control group have been plotted instead of the individual data. By comparing individual glaucoma subjects to this line we get an impression as to whether the relative loss of CD sensitivity is greater along the B/Y or R/G chromatic axis. The continuous lines along the x and y axes represent the upper limit for the reference range in the control group (+1.96 SD).

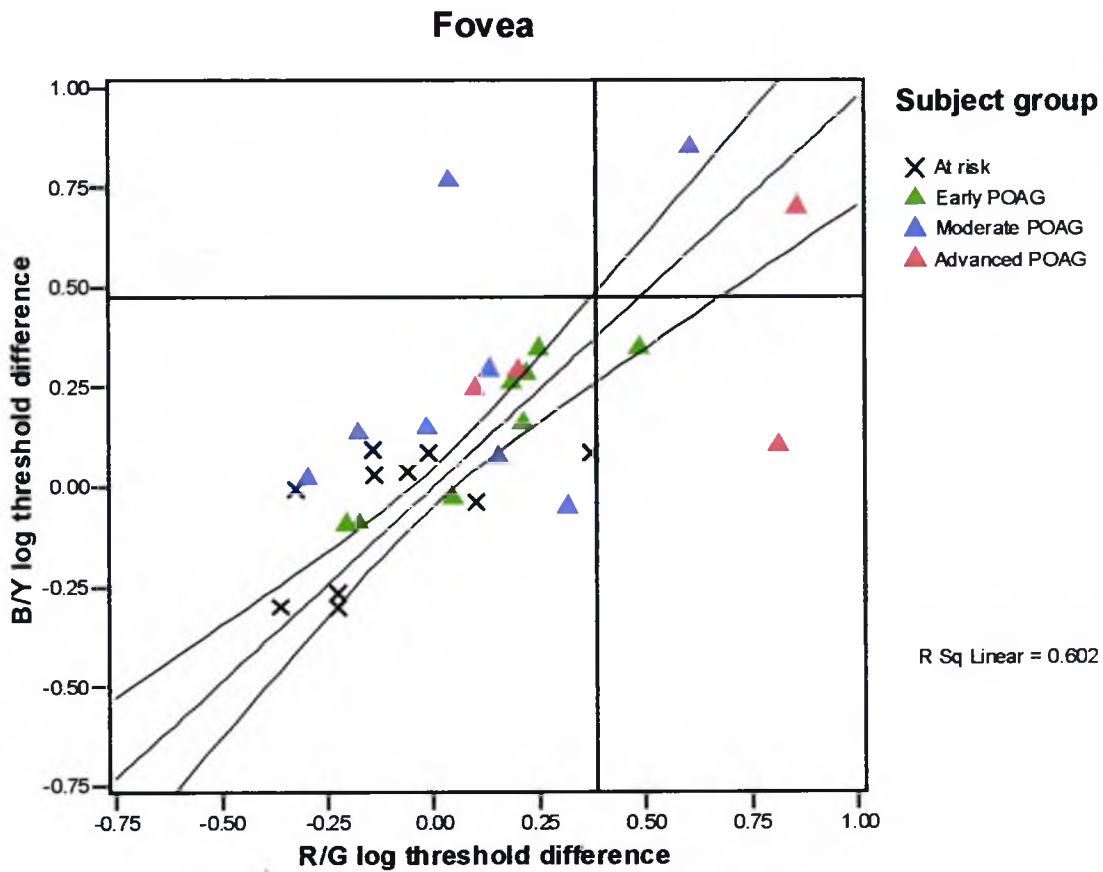


Figure 4.27: Same data as Figure 4.25 above. The mean regression line and the confidence intervals for the control group have been plotted instead of the individual data ($R^2=0.60$). Point (0,0) is the mean for the control group. Continuous lines along the x and y axes show the upper limit for the reference range in the control group.

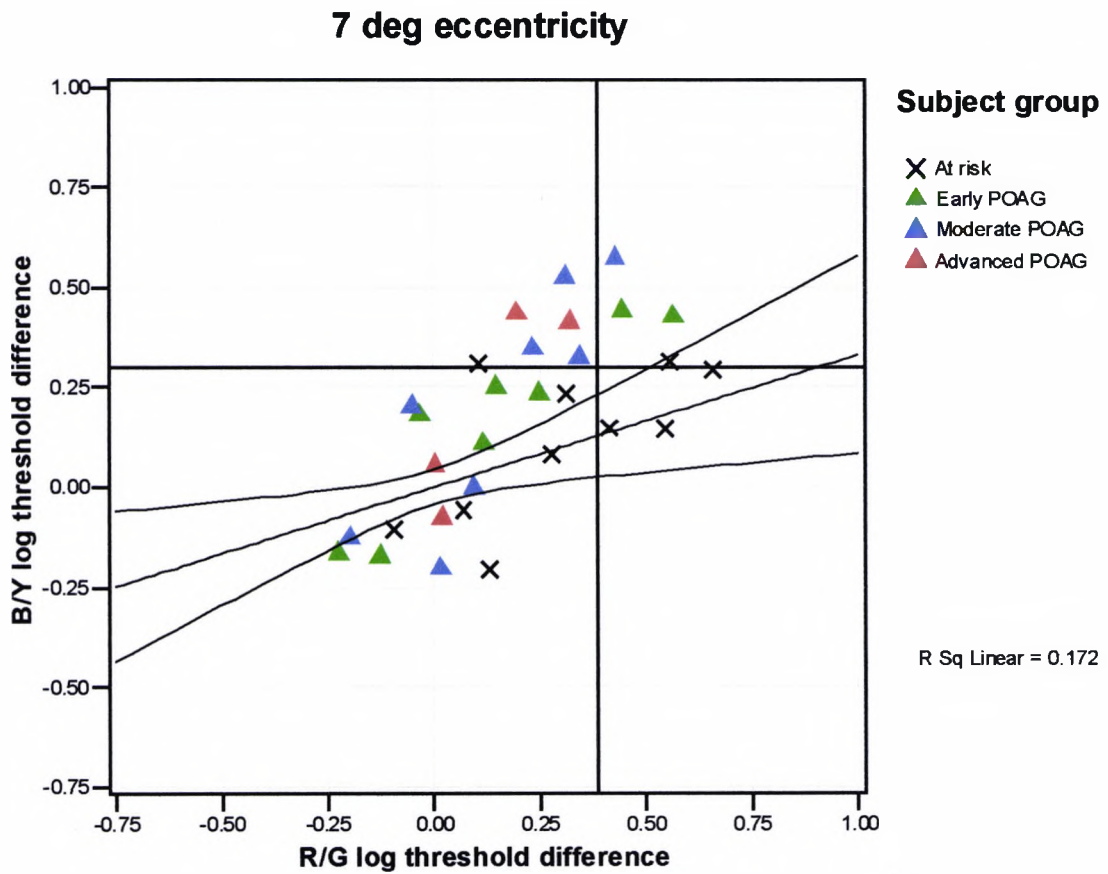


Figure 4.28: Same data as Figure 4.26 above. The mean regression line and the confidence intervals for the control group have been plotted instead of the individual data ($R^2=0.17$). Point (0,0) is the mean for the control group. Continuous lines along the x and y axes show the upper limit for the reference range in the control group.

From these graphs we can conclude that for foveal measurements:

- Most glaucomatous (except 5 subjects) and all At risk subjects lie within the normal reference range (2 SD) for the control group.
- 4 POAG cases are beyond the normal range for R/G log thresholds and 3 are beyond the normal range for B/Y log thresholds (2 of which are beyond both limits).

- More glaucoma and At risk subjects tend to show a larger relative B/Y loss. Although no definite pattern emerges from inspection of Figure 4.27, as to whether this tendency increases or decreases with severity, the POAG cases beyond the normal range are, with one exception, drawn from the Advanced or Moderate groups.

For 7 deg eccentric measurements:

- Three POAG and 4 At risk cases are beyond the normal range for R/G log thresholds, whereas 8 POAG and 3 At risk cases lie beyond the normal range for B/Y log thresholds (5 of these 11 cases are beyond both limits).
- Seventy percent of glaucoma cases and 50% of At risk are above the mean regression line for the control group, suggesting a larger B/Y CD loss.

4.4.4 Validation of the CD sensitivity measurements as a method for detecting glaucoma.

In order to determine the ability of CD sensitivity to classify correctly the subjects studied we performed a discriminant analysis. With this analysis it was established if there is either a combination or a subset of variables that classifies a large proportion of subjects into the correct group, so that there is a good chance of clasifying new subjects correctly.

Firstly, the discriminant analysis was used as an exploratory technique to study all variables, i.e.: all ellipse parameters (area, elongation and orientation) and CD thresholds along both chromatic axes (B/Y and R/G thresholds) for both locations measured. Following an examination of the results, all except the B/Y and R/G log threshold measurements at foveal and 7 deg eccentricity retinal locations were excluded. As expected, the inclusion of log elongation and log orientation did not improve the classification method, since as already discussed they fail to show significant group differences at any of the locations measured. Both log area parameters were also excluded since their inclusion merely supplied repeated information and did not provide any further improvement to the method. This is not

surprising since the area is calculated from the product of the ellipse's semi-axes (area of ellipse= $M*m*\pi$), which are directly related to the B/Y and R/G thresholds.

The best combination of variables that maximised the separation between groups was found by using 4 variables: B/Y log threshold for the fovea, B/Y log threshold for 7 deg, R/G log threshold for the fovea and R/G log threshold for 7 deg.

Discriminant analysis on the 3 groups (control, POAG and At risk subjects) yielded a model comprising 2 canonical variables (or discriminant functions), both significant ($p=0.001$ and $p=0.034$). The structure matrix (Table 4.17) identifies the variables that make significant contributions to the predictive process. B/Y thresholds measured at the fovea and R/G thresholds measured at 7 deg eccentricity showed the highest correlations in our model.

Structure Matrix

	Function	
	1	2
B/Y log thresh Fov	.833*	-.373
R/G log thresh 7 deg	.755*	.417
R/G log thresh Fov	.670*	-.494
B/Y log thresh 7 deg	.589*	.576

Pooled within-groups correlations between discriminating variables and standardized canonical discriminant functions
Variables ordered by absolute size of correlation within function.

*. Largest absolute correlation between each variable and any discriminant function

Table 4.17: Structure matrix table for control, At risk and POAG groups showing correlations between discriminating variables and discriminant functions

The "all-groups" scatter plot in Figure 4.29 shows the degree of success in minimising the overlap between the distributions of the linear function.

Canonical Discriminant Functions

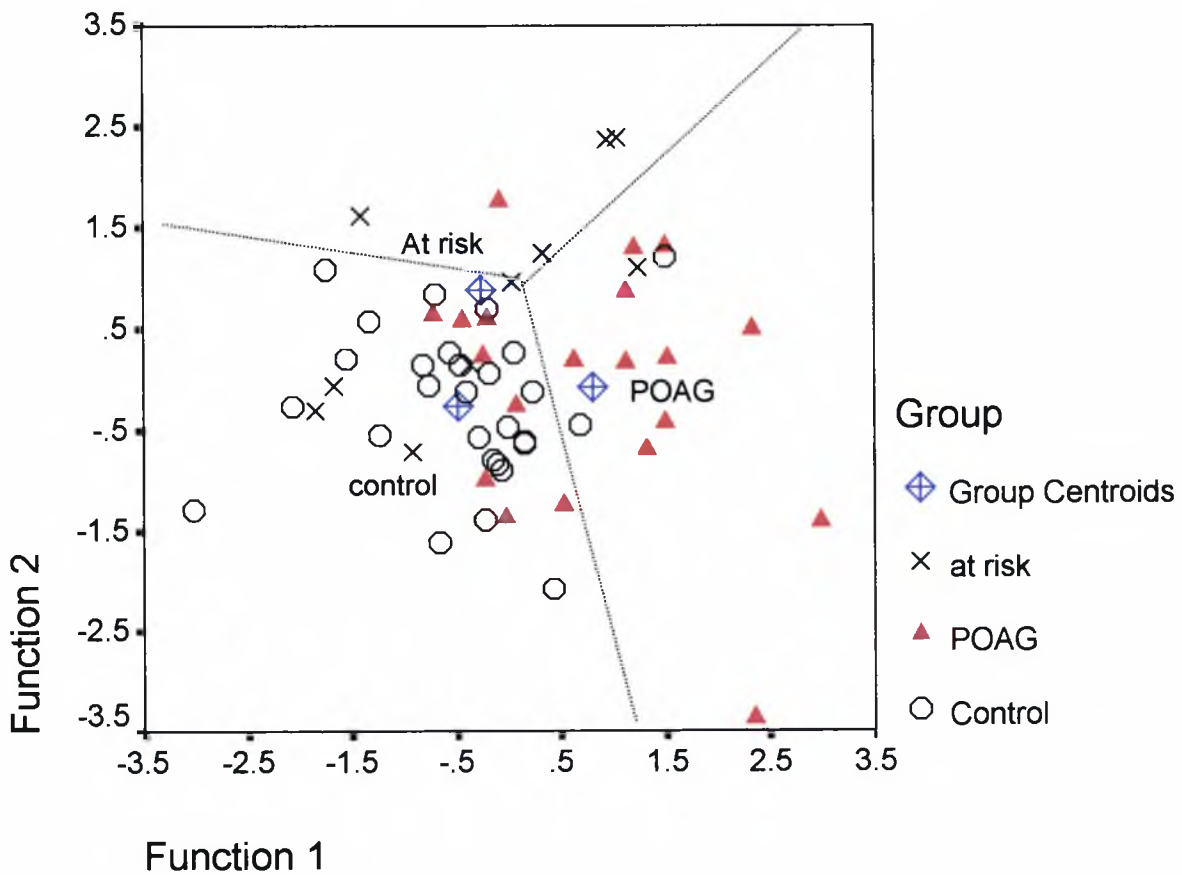


Figure 4.29: Plot of discriminant function 1 and 2 for the control, POAG and At risk groups.

Table 4.18 provides an indication of the success rate for predictions of membership (classification) of the grouping variable's categories. Of the 58 observations the model correctly predicted 26/28 (92.9%) of the normal control group, 11/20 (55%) of the

POAG group and 4/10 (40%) of the At risk group, which leads to an overall success rate of 70.7% of cases correctly classified.

Classification Results^a

		Group	Predicted Group Membership			Total
			Control	POAG	at risk	
Original	Count	Control	26	2	0	28
		POAG	8	11	1	20
		at risk	5	1	4	10
	%	Control	92.9	7.1	.0	100.0
		POAG	40.0	55.0	5.0	100.0
		at risk	50.0	10.0	40.0	100.0

a. 70.7% of original grouped cases correctly classified.

Table 4.18: Discriminant analysis classification results for control, POAG and At risk groups. The number and percentage of cases correctly classified and misclassified are displayed.

Discriminant analysis was also performed for the control and POAG groups only. We wanted to determine what the diagnosing success rate would be when excluding the At risk group. Inclusion of the at risk group will always reduce the success of the diagnosing method since it is likely that some of the subjects included in this group will never develop POAG, therefore they should actually belong to the control group. This time the model showed an overall success rate of 79.2% of cases correctly classified, basically due to an increase in the sensitivity (correctly identified POAG cases) and a reduction in the number of false negative cases (Table 4.19). In this case the variables that contributed most to the correct classification were the log R/G and B/Y thresholds measured at 7 deg eccentricity (Table 4.20).

Classification Results^a

		Group	Predicted Group Membership		Total
			Control	POAG	
Original	Count	Control	26	2	28
		POAG	8	12	20
	%	Control	92.9	7.1	100.0
		POAG	40.0	60.0	100.0

a. 79.2% of original grouped cases correctly classified.

Table 4.19: Discriminant analysis classification results for control and POAG groups. The number and percentage of cases correctly classified and misclassified are displayed.

Structure Matrix

	Function
	1
R/G log thresh 7 deg	.814
B/Y log thresh 7 deg	.707
B/Y log thresh Fov	.674
R/G log thresh Fov	.534

Pooled within-groups correlations between discriminating variables and standardized canonical discriminant functions
 Variables ordered by absolute size of correlation within function.

Table 4.20: Structure matrix table for control and POAG group showing correlations between discriminating variables and discriminant functions.

Finally, discriminant analysis was also performed for control and all POAG subgroups (including At risk cases). In this case the model showed a 63.8% of overall success in classifying subjects (Table 4.21). Although the specificity is very high for this model (96.4%), the sensitivity among the groups is not. Forty percent of the group At risk are correctly classified, 10% are classified in the Early group and 50% are classified as normal by the model. The Early damage group shows a 25% sensitivity, and yet 62.5% of them are false negative (i.e. placed by the model in the control group). The Moderate group has 25% of cases correctly classified and 37.5% of false negative cases. The

remaining misclassifications are spread evenly among the rest of the groups. Finally, the Advanced group has a 50% sensitivity, a 25% of false negative cases, with the rest classified as Moderate cases. The variables with the highest correlation were the log R/G and B/Y thresholds measured at the foveal location.

Classification Results ^a

		Predicted Group Membership					Total
		Control	At risk	Early	Moderate	Advanced	
Original	Count						
	Control	27	0	0	1	0	28
	At risk	5	4	1	0	0	10
	Early	5	0	2	0	1	8
	Moderate	3	1	1	2	1	8
	Advanced	1	0	0	1	2	4
%	Control	96.4	.0	.0	3.6	.0	100.0
	At risk	50.0	40.0	10.0	.0	.0	100.0
	Early	62.5	.0	25.0	.0	12.5	100.0
	Moderate	37.5	12.5	12.5	25.0	12.5	100.0
	Advanced	25.0	.0	.0	25.0	50.0	100.0

a. 63.8% of original grouped cases correctly classified.

Table 4.21: Discriminant analysis classification results for control, At risk and all POAG subgroups. The number and percentage of cases correctly classified and misclassified are displayed.

It is interesting to note that no matter how advanced the visual loss in the glaucoma groups there is always a percentage of cases considered normal by the model based on CD sensitivity. Misclassification within the groups could result from discrepancies in interpreting the severity and type of visual loss. The POAG subgroups have been classified according to severity of visual field loss, which is based on a different visual function compared to chromatic sensitivity, therefore they could very well disagree in their classification system. However, the large percentage of POAG cases classified by our model as falling within the limits for the control group indicates either the failure of the method to detect chromatic loss in the location tested or that the chromatic sensitivity function is within normal limits in those cases.

4.5 Summary of results

From the different chromatic sensitivity parameters used in the study, the B/Y and R/G thresholds together with the CD ellipse areas, measured at both eccentricities (fovea and 7 deg), have proven to be the most useful variables for demonstrating differences between the groups. All of these variables have shown significant differences between the control and the POAG groups, at both foveal and 7 deg eccentricity locations. However, no statistically significant differences were found between the control and At risk groups, for any of the variables. In particular, any significant differences that may have existed between groups for the eccentric location could not be demonstrated due to unequal variances between the groups.

A characterisation of CD loss with progression of glaucomatous damage has been established based on the average CD fitted ellipses and the average thresholds along the B/Y and R/G axes, for each glaucoma subgroup, and can be summarised as follows:

- The first sign of CD loss in glaucoma can be found at eccentric locations (7 deg). This will usually be an early diffuse CD loss accompanied by a certain degree of selective loss along the B/Y axis.
- As the disease develops foveal measurements are progressively affected by a diffuse CD loss. In addition, a selective CD loss along the B/Y colour confusion axis sometimes becomes apparent in the early stages of POAG, affecting the foveal location, reaching a maximum in established cases.
- In advanced stages, both foveal and eccentric locations show a selective CD loss along the R/G colour confusion axis.

In addition a thorough analysis of the CD ellipses obtained for each subject allowed the identification of characteristic patterns of CD loss that tend to recur in a number of glaucoma subjects. These patterns showed a moderate association with the AGIS score for severity of visual field loss. Some POAG subjects displayed normal chromatic sensitivity at the location tested and yet they presented other clear signs of glaucomatous damage. Conversely, some glaucoma suspects considered At risk of

developing the disease, but showing no clear signs of glaucomatous damage, already displayed a measurable chromatic discrimination loss.

The analysis of the relative loss of chromatic discrimination along the B/Y and R/G opponent channels suggests a marginal tendency for larger relative B/Y loss of chromatic discrimination in glaucoma, particularly for eccentric measurements (7 deg).

The B/Y and R/G log thresholds were identified as the most successful variables in classifying cases using discriminant analysis. The overall success rate in classifying POAG, At risk and control groups subjects correctly was around 71%. The analysis showed a good specificity (93%) but a mediocre sensitivity (55%).

4.6 Discussion

In this study we describe the characteristics of CD loss in glaucoma subjects based on the analysis of CD fitted ellipses and the thresholds measured along B/Y and R/G colour confusion axes, for two locations: the fovea and 7 deg eccentricity. CD ellipses were fitted to a group of POAG subjects and to a group of subjects at risk of developing the disease, in order to obtain the extent of the colour-blind region of a chromaticity diagram. This way of characterising the colour deficiency offered a graphical representation of the thresholds in a quantitative colour diagram.

We found a significant enlargement of the mean ellipse area in the POAG group, when comparing the CD ellipses' parameters to those of the control group. The mean foveal area increased to about 3 times the area of the control group, and the area measured at 7 deg increased to approximately 2.5 times the area of the control group. Since neither the elongation nor the orientation parameters offered assistance in differentiating between the control and glaucoma groups we conclude that, as a group, the POAG subjects showed a significant considerable non-selective reduction of chromatic sensitivity at both eccentricities measured.

On the other hand, the group At risk only showed an increase of the mean area (approx 2.5 times) for the eccentric location, with no changes in the elongation or the orientation. However, this non-selective reduction of chromatic sensitivity was not statistically significant, which may in part be due to a large variability in the At risk

group's data, which suggests large differences in the chromatic sensitivity of the subjects identified as at risk of developing glaucoma.

In contrast, Castelo-Branco *et al.* (2004) tested a group of glaucoma and OH patients along 8 confusion line vectors in colour space to fit discrimination ellipses. They found the mean ellipse axis length and the mean confusion vectors for protan, deutan and tritan significantly increased for both the glaucoma and the OH group. The tritan axis length showed a slight tendency for a steeper increase. The axis ratio showed a significant but modest increase only for the glaucoma group, suggesting that damage may be preferential to the B/Y axis but not at all specific. The angle of orientation of the CD ellipse, like in the present study, did not change significantly among groups.

From the parameters chosen for the analysis of the CD ellipses, the ellipse's area offered some useful information to discriminate among groups, but neither the elongation nor the orientation were helpful to prove significant differences among the groups. Fitting ellipses to our data is a useful method to illustrate the mean chromatic sensitivity of the groups as well as a consistent way of summarising the results for a large range of different chromatic discrimination abilities. However, this method has its limitations. It is not totally appropriate to fit ellipses in all cases, particularly to those subjects with more advanced glaucomatous damage. Some POAG subjects exhibited a totally distorted "ellipse". In such cases the accuracy of the fitted ellipse may be poor and parameters like the elongation or the orientation may become meaningless. Increased variability in the angle of orientation of the CD ellipses has also been reported in glaucoma but not in OH patients (Castelo-Branco *et al.*, 2004).

Therefore, to minimise the error introduced by fitting ellipses to data that might not be elliptical in shape and overcome the limitations found with parameters such as the elongation, the loss of chromatic sensitivity along the R/G and B/Y colour confusion axes was additionally investigated.

The large variability for measurements taken at the eccentric location in the group at risk was confirmed again for the thresholds along the R/G and B/Y colour confusion axes. Compared to the control group, the POAG group revealed significant differences for both the B/Y and R/G log thresholds, at both locations tested. As for the At risk group, despite showing large mean threshold increases along both the B/Y and R/G

colour confusion axes at the eccentric location, no statistically significant differences were achieved. The fovea showed no elevation of the mean B/Y or R/G thresholds.

The inability to show significant differences between the control and At risk groups at the eccentric location may be the result of increased intra- and inter-subject variability in threshold estimation with patients at risk of developing glaucoma or may simply indicate that the chromatic sensitivity is not significantly affected in this group.

Other studies have previously shown large variability in the responses of POAG suspects. Falcao-Reis *et al.* (1991) assessed macular colour contrast sensitivity in ocular hypertensive and POAG eyes. They divided the OH group into high, medium and low risk patients. Significant reductions in sensitivity along the 3 colour confusion axes were demonstrated in POAG subjects. However, the OH group only demonstrated significant threshold elevations ($>2SD$ mean of control group) along the tritan axis in one third of the cases. The distribution of results for tritan thresholds in the low and medium risk OH groups almost overlapped entirely the control group's distribution. They argued that these cases may represent the fraction of OH with abnormal colour vision prone to develop visual field defects. In a similar study, Yu *et al.* (1991) measured extrafoveal colour contrast thresholds along colour confusion axes for a 12 deg ring. The test was applied to OH and POAG patients. All POAG had thresholds $> 2 SD$ above the normal mean. Most OH or those with clinical signs indicating a low or medium risk of conversion to glaucoma had thresholds under the upper limit of normal. High-risk patients fell into 2 groups, one with lower values, which approximated to normal; the other had elevated thresholds more than 3 SD above the normal mean.

Studies on visual field sensitivity have also described an overall increase in variance for the threshold determinations or alternatively a diffuse loss of sensitivity to occur at an early stage of POAG, before distinct local loss is present (Anctil & Anderson, 1984).

We also found, in the present study, a great disparity in the chromatic sensitivities of some of the At risk subjects at 7 deg eccentricity. Some subjects displayed very large values (i.e. large areas, large B/Y and/or R/G thresholds) whilst others fell within the normal range for the control group. When statistically comparing the group At risk to the POAG group no significant differences were found, either. This variability found in the group At risk may be reflecting the early signs of pathological changes that occur to

surviving dysfunctional cells. Logically, these fluctuating responses would be expected to be detected earlier from eccentric areas where chromatic mechanisms have a lower rate of redundancy. In contrast, foveal data, in the group at risk, laid within the normal range for the control group, and its variability also fell within the normal limits for the control group.

Therefore, it is likely that our small group of subjects at risk of developing POAG contains some "normal" healthy subjects in addition to some subjects at the sub-clinical stage of the disease who showed the first signs of chromatic sensitivity loss at the paracentral location (7 deg).

In addition, the changes in chromatic loss were analysed as a function of severity of glaucomatous damage. The POAG group was subdivided, according to the severity of visual field damage into Early, Moderate and Advanced damage subgroups and together with the At risk group were compared to the control group. The progression of chromatic sensitivity loss has been described by means of the average CD ellipses fitted to each glaucomatous subgroup, as well as by the decline in chromatic sensitivity along the B/Y and R/G colour confusion axes with progression of glaucomatous damage. Both approaches lead to similar conclusions:

There is an initial diffuse CD loss accompanied by a certain degree of selective loss along the B/Y axis, which affects paracentral areas (7 deg).

As the disease develops foveal measurements are progressively affected by a diffuse CD loss. In addition, a selective CD loss along the B/Y colour confusion axis sometimes becomes apparent in the early stages of POAG, affecting the foveal location, reaching a maximum in established cases

In the advanced stages of the disease, a selective CD loss along the R/G colour confusion axis is added to the previous loss, affecting both foveal and eccentric locations.

The relative R/G and B/Y CD loss in glaucomatous damage was also investigated. It is difficult to determine whether, as a whole, the glaucoma group shows larger relative losses for one or the other chromatic mechanism. A trend for a marginally larger relative B/Y loss is observed in Figure 4.27 and Figure 4.28, which display the

comparison of threshold differences for B/Y to those for R/G sensitivities, for each individual subject. Evidence in our data reveals that the relative loss of chromatic sensitivity may depend on the severity of the glaucomatous damage incurred (Figure 4.23 and Figure 4.24). Hence, it might be more appropriate to describe the relative loss of chromatic sensitivity as a function of the visual field damage.

In general, thresholds for the B/Y mechanism show a larger relative increase at the earlier stages of the disease, whereas the relative loss is larger for the R/G chromatic mechanism at more advanced stages of the disease (Figure 4.23 and Figure 4.24). More specifically, there is a larger B/Y relative loss found at the fovea, for the Early and Moderate glaucomatous damage groups, which is neutralised when the disease is established, by the R/G loss. At moderate/ advanced stages the relative rate of loss becomes larger for the R/G thresholds. For eccentric measurements, the initial larger B/Y relative loss found in the At risk group is soon matched and surpassed by a larger R/G relative loss as the disease progresses (around Early stages), since there is, mainly, no further deterioration of the B/Y sensitivity.

This could in part be an explanation for the lack of consistency in the literature about the relative loss of chromatic sensitivity in glaucoma. Many studies suggest a greater relative B/Y loss of chromatic sensitivity (Johnson *et al.*, 1993a; Sample *et al.*, 1993; Felius *et al.*, 1995b), whereas some argue that a similar relative loss along the B/Y and R/G colour confusion axes can be expected (Greenstein *et al.*, 1996; Pearson *et al.*, 2001) or even a greater R/G relative loss (Alvarez *et al.*, 1997). Here, we present some evidence suggesting that the relative chromatic loss will depend on the severity of glaucomatous damage of the eyes affected, among other factors.

The early relative greater B/Y deficit finding in paracentral areas is in agreement with reports suggesting that suspects show an early loss of short wavelength sensitivity (SWS) in perimetry (Heron *et al.*, 1988; Johnson *et al.*, 1993a; Sample *et al.*, 1993) and early CD loss along the tritan axis (Adams *et al.*, 1982; Drance *et al.*, 1981; Gunduz *et al.*, 1988; Yu *et al.*, 1991). Furthermore, at the eccentric location we find no further deterioration of the B/Y sensitivity beyond the loss found at early stages, which adds support to reports on blue/yellow perimetry suggesting this to be more sensitive to glaucomatous damage than conventional perimetry in early stages of the disease, but not more sensitive than conventional perimetry in manifest stages of glaucoma (Wild *et*

al., 1995); (Hart, Jr. *et al.*, 1990). In fact, the B/Y threshold shows no correlation with the global index of visual field loss, at 7 deg eccentricity. For foveal measurements, both B/Y and R/G thresholds are better correlated with the global index of field loss, however the R/G thresholds show a higher correlation ($R^2=0.47$) than the B/Y thresholds ($R^2=0.31$).

Lack of correlation between the B/Y threshold and mean deviation loss (MD) in the visual field has recently been reported by Castelo-Branco *et al.* (2004) in spite of a significant B/Y loss of sensitivity in a glaucoma group. In contrast, sensitivity losses along protan and deutan colour confusion lines were found to be significantly good predictors of perimetric damage. This is also in agreement with findings by Fristrom (2002) that development of glaucoma may actually be better predicted by change over time in colour contrast in the protan axis.

This suggests that loss of B/Y sensitivity, although one of the first signs and a measure of significant glaucomatous damage it is not a clinically useful parameter of progression of field loss. It also implies that these two functions are not related. AGIS score is a global measure of the light sensitivity function in the visual field, which unselectively targets the sensitivity of all mechanisms using a small size stimulus. In contrast, the B/Y thresholds were designed to isolate the sensitivity of the B/Y mechanism.

Our results also show a greater R/G relative loss from moderate stages of glaucoma, earlier than previously suggested according to the idea that significant damage to the R/G chromatic mechanism is only associated with advanced glaucoma (Kalloniatis *et al.*, 1993; Pearson *et al.*, 2001).

Classifying all our subjects according to the severity of visual field loss has allowed predicting the evolution of CD loss in glaucoma with progression of the disease. Nonetheless, this approach is dependent on the classification given by the light sensitivity function and, as mentioned, does not necessarily share the same visual pathway as the chromatic mechanisms. Hence, we also investigated the existence of specific recurring patterns of CD loss, hoping they could identify characteristic stages of glaucomatous damage. This was based on the inspection of individual CD ellipses and the relative foveal to eccentric pattern of CD loss. The stages in the patterns of CD loss identified were:

Stage 1: No CD loss at any of the locations tested.

Stage 2: A non-selective reduction in chromatic sensitivity at the eccentric location (7 deg).

Stage 3 and 4: A non-selective reduction in chromatic sensitivity affecting the fovea, accompanied by a reduction of CD loss at 7 deg. At this stage the relative involvement of the eccentric to foveal CD loss (ratio) is related to the severity of damage. Relatively larger foveal CD loss usually indicates greater glaucomatous damage.

Stage 5: A large selective foveal CD loss along the tritan colour confusion axis. This pattern usually coexists with increasing CD loss at the eccentric location.

Stage 6: A large selective CD loss along the R/G colour confusion axis, affecting the foveal and / or the eccentric measurement at 7 deg. Usually coexists with massive CD losses.

Once the stages of the pattern of chromatic discrimination loss were identified they were correlated with the severity of visual field loss (AGIS score) (Figure 4.19). Although a significant association was shown ($R^2=0.34$), there were a number of eyes (15%) with glaucomatous field defects that showed no abnormality in chromatic discrimination (e.g. some cases in stage 1 of CD loss). These are false negative cases according to this classification. Other patients showed early signs of chromatic sensitivity loss and no visual field defect (e.g. cases in stages 2 or 3 of CD loss).

This lack of clear-cut relationship between chromatic discrimination and severity of visual field loss has previously been mentioned in the literature (Drance & Lakowski, 1983). In a longitudinal study with ocular hypertensive eyes, which had been assessed with the F-M 100 hue and the Pickford-Nicholson anomaloscope, Drance *et al* (1981) found that one third of the eyes developed a visual field loss after 5 years. Of those, a 20-25% had originally shown chromatic scores within normal ranges, thus these turned out to be false negative cases according to the colour vision tests used. The rest of eyes (75-80%) had originally displayed poor scores on the colour vision tests mentioned. Although the study did not control for factors such as age, cataracts or visual acuity and did not establish what was considered as a visual field defect, it

nevertheless provides good available data regarding the predictive ability of clinical colour vision tests.

Differences in the pathologic mechanisms mediating the visual loss have been suggested as being responsible for the absence of chromatic sensitivity loss in some glaucoma patients (Yamagami *et al.*, 1995; Yamazaki *et al.*, 1989; Lachenmayr & Drance, 1992).

In the present study, when all the CD sensitivity parameters used were pulled together and discriminant analysis was applied to determine the ability of the method to correctly classify glaucoma subjects, we found the B/Y and R/G log thresholds to be the most successful predicting variables. The overall success rate in classifying POAG, At risk and control group's subjects correctly was around 71%. This is a reasonable success rate, with a good specificity (93%) but a modest sensitivity (55%), which improves slightly (60%) when the group At risk is excluded. Previous studies on chromatic sensitivity in glaucoma have also reported modest sensitivities. Lakowski and Drance (1979) also reported on the sensitivity of the F-M 100 hue test to predict POAG. They found that 34, 54 and 74% of the patients with mild, medium and severe visual field defects, respectively, were detected by the F-M 100 hue test.

However, moderate levels of sensitivity in detecting eyes with glaucomatous optic neuropathy are not restricted to chromatic sensitivity techniques. Sample *et al.* (2000) compared four perimetric techniques in order to determine the percentage of eyes with glaucomatous optic neuropathy that showed abnormality in each test and assess the agreement among them. They used standard perimetry (SAP), blue-on-yellow perimetry (SWAP), frequency-doubling perimetry (FDT) and a motion-automated technique (MAP), based on a RD kinematogram. A total of 46% of glaucomatous eyes were identified with SAP, 61% with SWAP, 70% with FDT, and 52% with MAP. Additionally, they reported that a high percentage of POAG eyes only showed abnormal results in one test. They concluded that not all eyes are affected in the same way by glaucomatous neuropathy and that a combination of these tests would improve detection of functional loss. In fact, this is in agreement with a more general concept that different procedures should enhance the clinical management in glaucoma (Harwerth *et al.*, 2002).

The results in this study have implications for the selection of the testing conditions to optimise the clinical management of early versus advanced glaucoma subjects. However, chromatic discrimination loss due to glaucomatous damage is proven far from being homogeneous in all eyes. Multiple mechanisms of damage have been described in POAG (section 1.5), which may affect visual function in different ways. Some eyes show early signs of chromatic discrimination loss whereas some may not develop CD loss until more advanced stages of the disease.

5 Chromatic and achromatic loss of sensitivity in POAG

5.1 Introduction

Over the past decade efforts have been invested to determine whether there are visual functional channels that are relatively more susceptible to glaucomatous damage. Many studies have reported losses with short-wavelength stimuli and motion luminance contrast stimuli (Johnson *et al.*, 1993a; Johnson *et al.*, 1993b; Moss *et al.*, 1995; Sample *et al.*, 1994; Tyler, 1981; Wild *et al.*, 1995). These losses would be consistent with the preferential damage theory or even the reduced redundancy theory (section 1.5.4). However, a number of studies have subsequently reported early losses with R/G stimuli (Alvarez *et al.*, 1997; Felius *et al.*, 1995b; Greenstein *et al.*, 1996; Kalloniatis *et al.*, 1993). Therefore, it is unclear whether early deficiencies occur preferentially in one or another channel, arising from specific cell classes being more susceptible to damage.

Most of these studies comparing visual losses associated with the three psychophysical mechanisms were aimed at early detection of glaucoma. However, few studies have placed an emphasis on comparing the effects of different stages of severity of glaucoma on visual losses of the two colour-opponent and luminance mechanisms (Greenstein *et al.*, 1993; Greenstein *et al.*, 1996; Pearson *et al.*, 2001).

In this study the sensitivities of the two colour-opponent and the luminance channels were evaluated in a group of POAG and age-matched normal subjects. Motion discrimination targets designed to isolate the responses of the R/G, the B/Y and the achromatic mechanisms were used in order to secure psychophysical evidence for or against preferential damage to the visual channels. If early preferential damage indeed occurs to one channel, the development of psychophysical tests that generate specific

stimulation of that channel could be used in clinical practice or as a screening technique.

5.2 Aim

The purpose of this study is to test the hypothesis that glaucoma leads to selective deficits in parallel pathways. The term selective implies that the pathways are differentially affected by the disease process. In order to investigate selective damage chromatic (R/G and B/Y) and achromatic sensitivity losses in POAG, for foveal and eccentric areas (7 deg), were compared. We also aim to compare the pattern of achromatic and chromatic visual loss with different stages of visual field loss.

5.3 Subjects and method

5.3.1 Subjects

Thirteen POAG subjects participated in this study. The average age for the sample was 70.3 years (SD=6.5 years). Table 5.1 summarises the clinical details of the glaucomatous eyes. Results were compared with those of seventeen control subjects of similar age. These were the same subjects that acted as the older group in chapter 6. The average age for this sample was 67.9 years (SD=6.0 years). A 2 Sample t-test on the age means confirmed no statistically significant difference ($p=0.33$) between the POAG and control group's mean ages. For full details on logistics of subjects' recruitment and inclusion criteria refer to sections 2.3 and 3.7.

The severity of the visual field damage was assessed with the AGIS (Advanced Glaucoma Intervention Study) scoring method (Gaasterland *et al.*, 1994), which is shown in Table 5.1. As in chapter 4, the POAG group was divided into three sub-groups according to the AGIS score for severity of visual field loss. The Early damage group (N=3) contains cases with an AGIS score between 1 and 4, the Moderate damage group (N=6) contains cases with an AGIS score between 5 and 9 and the Advanced damage group (N=4) contains cases with AGIS score 10 and beyond.

POAG subj	Gender age (yr)	& VA	Diagnosed (yrs ago)	Family History	C/D ratio	MD	AGIS score*	VF defect at location tested (dB)			
								Pattern deviation plot		Total deviation plot	
								Fovea	7 deg	Fovea	7 deg
JD	♀73	6/9 ⁻²	11	-ve	0.8	-17.3	14	-5.5	1	-10	-3.5
DBR	♂65	6/6 ⁻³	9	+ve	0.9	-16.5	13	-0.25	-4.5	-3.25	-7.5
DB	♂69	6/5	9	+ve	0.8	-12.4	9	-7.5	0.5	-8.25	0.25
RH	♂70	6/6	6	unknown	0.85	-12.2	11	-0.75	-1.5	-5.5	-5.5
EB	♀69	6/9 ⁻¹	8	+ve	0.8	-11	9	-9.25	-1.75	-7.5	0
AK	♀60	6/6	3	+ve	0.7	-2.3	3	-0.5	-1.5	0.5	-0.5
PF	♂72	6/9	10	-ve	0.8	-6.1	8	0.5	-4.25	-1	-5.5
WH	♂78	6/9 ⁺²	4	unknown	0.9+	-6.5	5	-2.25	-5	-6.75	-9.75
ZK	♂67	6/6	4	+ve	0.65	-8.4	5	-1.75	-3.75	-2.75	-5.25
GT	♂76	6/6	8	+ve	0.5	-12.1	13	-7	-7	-7	-7
SP	♂83	6/9	22	unknown	0.8	-3.8	5	-1.75	-3.75	-2.75	-4.5
IH	♂58	6/5	5	+ve	0.8	-1.7	1	-1	-2.5	-0.75	-2.5
VF	♀68	6/9	21	-ve	0.85	-3.2	1	-0.25	-1.5	-2	-3

Table 5.1: Summary of clinical characteristics of the thirteen POAG eyes. *AGIS score for severity of visual field loss (see section 3.7.1).

5.3.2 Methods

Motion direction discrimination thresholds were measured using the CAD test, as described in section 3.6.2, both for luminance and colour contrast motion defined signals, at three levels of background masking noise (12, 24 and 48%). Colour contrast (CC) thresholds were measured along 2 directions in colour space, 74.5° for B/Y discrimination and 169° for R/G discrimination. Luminance contrast thresholds were also measured by modulating the test stimulus in luminance. Subjects were tested at one position centred on fixation (fovea) and one eccentric location centred 7 deg from fixation. The eccentric measurement was taken in either the superior nasal, superior temporal, inferior nasal or inferior temporal quadrant, chosen randomly for the control group. For POAG subjects the selection of the quadrant was randomised among those that provided a loss of sensitivity at the eccentric location, of not greater than 10 dB, as explained in section 3.5.

Changes in the strength of either colour or luminance contrast signals needed for threshold detection of the moving stimulus can be compared directly when the thresholds are plotted on a log scale and the changes are therefore expressed in log units. Since the principal aim of this study was to compare changes in colour and luminance contrast sensitivity as a function of glaucomatous damage, we have chosen to quantify all changes in log units.

5.4 Results

In order to obtain a normal distribution and similar SDs when comparing data between groups, a logarithmic transformation was applied. An analysis of variance (UNIANOVA) revealed that log contrast thresholds were significantly affected by the following variables: group (i.e. glaucomatous damage) ($F= 131.4, p<0.001$), type of stimulus (i.e. Achromatic, R/G and B/Y) ($F= 117.7, p<0.001$), and the eccentricity of the location tested ($F= 110.3, p<0.001$). Also, the interactions between the type of stimulus and group ($F= 8.4, p=0.001$), the type of stimulus and location tested ($F= 19.9, p<0.001$)

and the type of stimulus and background noise level ($F= 2.4$, $p=0.045$) were significant. These effects will be studied in depth in the following sections.

5.4.1 Effect of background noise level

The interaction between the stimulus type and the percentage of background LC noise used was investigated. The aim was to determine whether the noise level used had a differential effect depending on the type of stimulus or on the sensitivity of the glaucoma subjects.

Figure 5.1 shows the average chromatic (R/G and B/Y) and achromatic log thresholds for control and POAG subjects, as a function of background noise. Data points represent the mean and 2 SE for each level of LC noise (12, 24 and 48%) used in the masking background, both for foveal and 7 deg eccentricity locations.

A one-way ANOVA, performed separately for each type of stimulus (i.e. Achromatic, R/G and B/Y), for all subjects taken together, showed that noise had a significant effect on the log thresholds for the achromatic stimulus ($F= 8.9$, $p<0.001$), but not for the R/G or B/Y ($F= 0.76$, $p=0.47$ and $F= 1.02$, $p=0.36$, respectively) stimuli thresholds. Post-hoc tests (LSD) showed a significant difference ($p<0.001$) between 12 and 48% luminance contrast noise levels. In other words, the achromatic thresholds had a tendency to increase with increasing background noise in which the target was embedded. This effect was not present when measuring colour contrast thresholds with the target embedded in dynamic noise. Since the achromatic target is presented embedded in static LC noise, this effect can be expected and explained as a consequence of subjects' small eye movements during testing, which can produce the effect of inducing some dynamic noise to their target. The effect of dynamic noise on the detection of LC defined motion has been illustrated in Figure 3.4.

The effect of noise on the log thresholds obtained for the control and POAG groups was not statistically significantly different for any of the stimuli tested. In other words, the analysis of variance did not identify a significant interaction between background noise and group (group by background noise interaction: Achromatic, $F= 0.41$, $p=0.66$; R/G, $F= 0.063$, $p=0.93$; B/Y, $F= 0.062$, $p=0.94$).

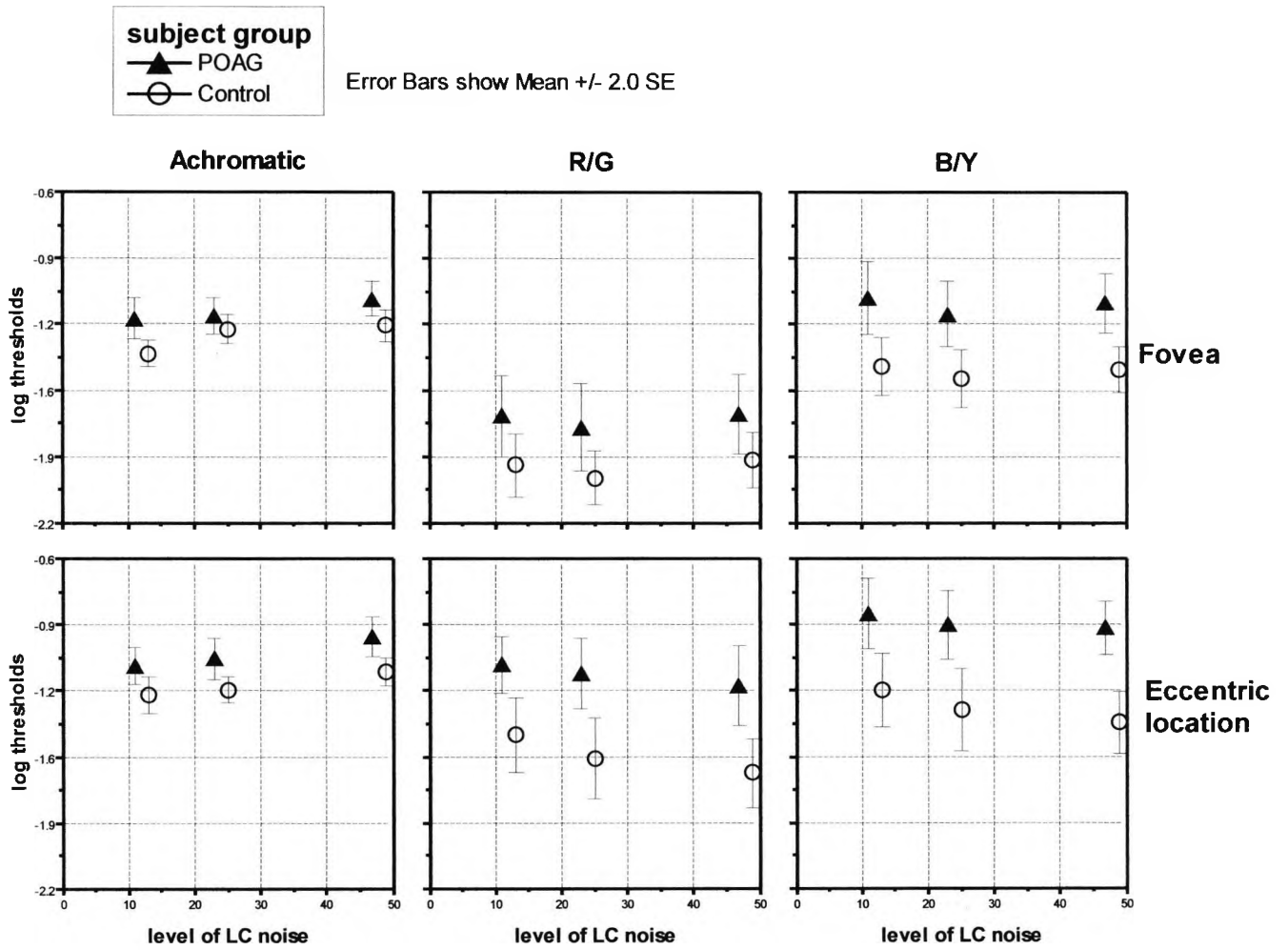


Figure 5.1: Mean chromatic (R/G and B/Y) and achromatic motion discrimination thresholds (log units) of the control and POAG observers, as a function of the three levels of background LC noise (12, 24 and 48%) at foveal and 7 deg eccentricity locations. Bars indicate 2 SE of the mean.

5.4.2 Effect of glaucoma on chromatic and achromatic sensitivity

Table 5.2 summarises the mean and SD of the contrast motion discrimination thresholds (log units) data for achromatic and both chromatic (R/G and B/Y) stimuli in the control and the POAG group. To facilitate comparisons the three noise levels were averaged, for each individual, based on the finding that the background noise level had no statistically significant differential effect on the sensitivity of the groups.

Box-plots in Figure 5.2 provide a visual comparison of the distribution of the log thresholds for the chromatic and achromatic sensitivities in the POAG and control group.

An independent samples-t test (Table 5.3) showed that the mean threshold differences between the POAG and the control groups were statistically significant, both at the fovea and at the eccentric location. The chromatic (B/Y and R/G) and achromatic log threshold increments in the POAG compared to the control group are shown by the mean differences of the groups in Table 5.3. For achromatic mean thresholds the increase was approximately 1.3 and 1.4 times, for fovea and 7 deg eccentricity, respectively. For chromatic mean thresholds along the R/G colour confusion axis the increase was approximately 1.7 and 2.4 times and for thresholds along the B/Y colour confusion axis the increase was approximately 2.1 and 2.6 times, for fovea and 7 deg eccentricity, respectively. This implies that the greatest threshold increase is found along the B/Y colour confusion axis.

log thresholds

location tested	stimulus	subject group					
		Control			POAG		
		N	Mean	SD	N	Mean	SD
Fovea	Achromatic	17	-1.287	.119	13	-1.171	.152
	R/G	17	-1.926	.280	13	-1.691	.349
	B/Y	17	-1.459	.259	13	-1.141	.284
Eccentric location	Achromatic	17	-1.204	.135	13	-1.056	.168
	R/G	17	-1.528	.351	13	-1.149	.277
	B/Y	17	-1.305	.354	13	-.897	.263

Table 5.2: The mean log thresholds, for the three levels of noise used, for achromatic and chromatic (R/G and B/Y) conditions for the control and the glaucoma (POAG) groups, at both locations tested.

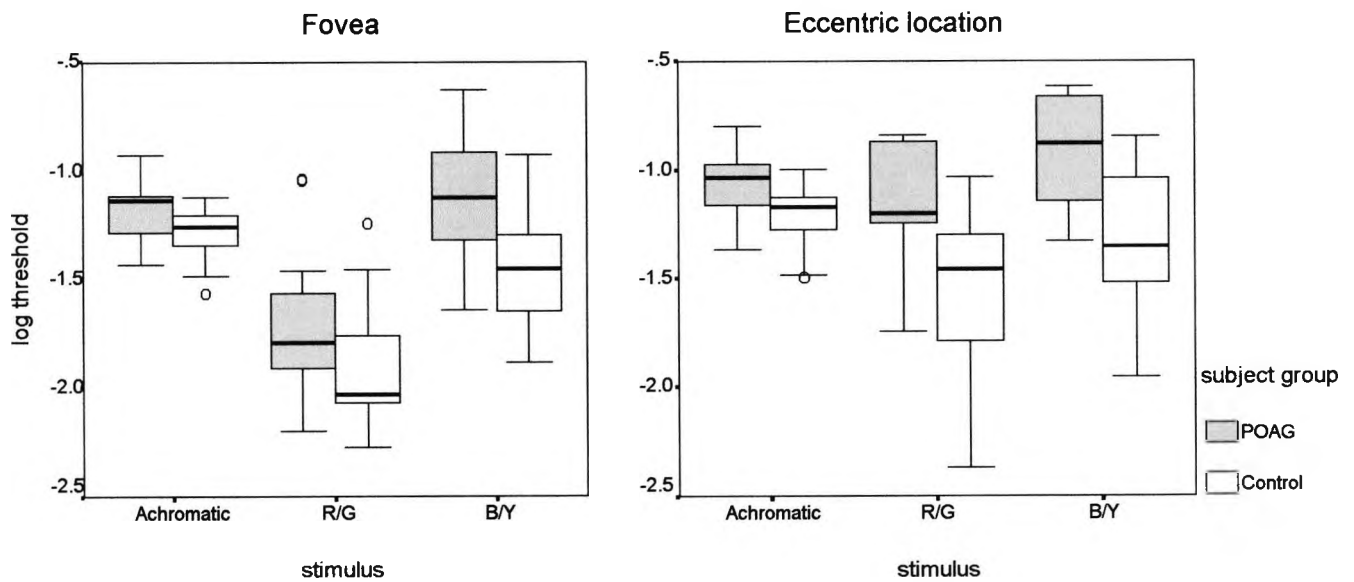


Figure 5.2: Box-plots of the log thresholds for chromatic (R/G and B/Y) and achromatic sensitivity allow a comparison of the POAG (N=13) and control (N=17) groups. The box contains the middle 50% of the cases.

Independent Samples Test

log thresholds

location tested			Levene's Test for Equality of Variances		t-test for Equality of Means						
			F	Sig.	t	df	Sig. (2-tailed)	Mean Differ	Std. Error Differ	95% Confidence Interval of the Difference	
										Lower	Upper
stimulus											
Fovea	Achromatic	Equal variances assumed	1.145	.294	-2.351	28	.026	-.116	4.938E-02	-.217	-1.493E-02
		Equal variances not assumed			-2.273	22.174	.033	-.116	5.107E-02	-.222	-1.022E-02
	R/G	Equal variances assumed	.698	.411	-2.046	28	.050	-.235	.115	-.470	3.081E-04
		Equal variances not assumed			-1.986	22.629	.059	-.235	.118	-.480	1.005E-02
	B/Y	Equal variances assumed	.145	.706	-3.205	28	.003	-.318	9.934E-02	-.522	-.115
		Equal variances not assumed			-3.164	24.634	.004	-.318	.101	-.526	-.111
Eccentric location	Achromatic	Equal variances assumed	.893	.353	-2.693	28	.012	-.149	5.524E-02	-.262	-3.560E-02
		Equal variances not assumed			-2.613	22.603	.016	-.149	5.693E-02	-.267	-3.089E-02
	R/G	Equal variances assumed	.579	.453	-3.208	28	.003	-.380	.118	-.622	-.137
		Equal variances not assumed			-3.313	27.953	.003	-.380	.115	-.615	-.145
	B/Y	Equal variances assumed	2.651	.115	-3.484	28	.002	-.408	.117	-.648	-.168
		Equal variances not assumed			-3.626	27.990	.001	-.408	.113	-.638	-.177

Table 5.3: Achromatic, B/Y and R/G mean log threshold differences between POAG and control groups for the foveal and eccentric locations tested.

5.4.2.1 Relative loss of sensitivity with glaucoma

We have investigated, so far, whether the motion discrimination thresholds for the chromatic (R/G and B/Y) and achromatic conditions were differentially affected by glaucoma. A greater increase in thresholds with glaucomatous damage for chromatic compared to achromatic sensitivities is apparent from Figure 5.1 and Figure 5.2.

The relative loss of B/Y versus R/G chromatic sensitivity can be inferred by comparing the mean differences between the control and POAG groups in Table 5.3. These suggest that the relative threshold increase in the POAG group is greatest along the B/Y colour confusion axis. However, for the R/G and B/Y mean differences for the groups, although these are greater for B/Y, the 95% confidence intervals of the differences overlap substantially. This is particularly so for the eccentric location, where the data exhibit a larger variability.

Therefore, to thoroughly study the differential effect of glaucomatous damage on chromatic and achromatic thresholds the individual threshold difference (log units) from the control observers' mean was calculated for each sensitivity. Figure 5.3 plots the differences for each POAG and control subject from the mean of the control group. Log threshold differences along the R/G colour confusion axis are compared to those along B/Y axis. The triangles represent the difference for an individual POAG subject from the control mean. The (0,0) represents the average control value. The circles represent differences for each control observer compared to the mean value for the control group. The solid line is the best-fit regression line for the control group. The dotted lines correspond to the reference range for the control group (+1.96 SD).

Although there are similar increases along R/G and B/Y axes and a considerable overlapping of the two samples, more POAG subjects present with a greater increase along the B/Y colour confusion axis (Figure 5.3). This is shown by cases above the best-fit linear regression line and confidence intervals for the control group, which indicates slightly larger differences along this axis. Points beyond the continuous lines along the x and y axes represent eyes outside the normal reference range (1.96 SD) for the control group. For foveal measurements 4 POAG subjects fall beyond the B/Y thresholds reference range, 2 of which are moderate cases and 2 advanced cases. The 2 advanced cases are also beyond the R/G reference range.

For 7 deg eccentricity measurements nine of the 13 POAG subjects fall above the linear regression line, which represents a tendency for greater B/Y loss (69% of the total). However, the thresholds of some POAG subjects could not be measured since they were larger than the largest possible colour signals we could generate on the visual display (Figure 3.2 shows phosphor limits at the maximum available modulation). This only occurred for chromatic thresholds measured at the eccentric location for 4 subjects in R/G sensitivity (JD, GT, DBR, RH) and for 5 subjects (JD, GT, DBR, RH, EB) in B/Y sensitivity. Under these circumstances, the threshold was taken to be the maximum contrast available. These cases can be seen in Figure 5.3 and the following graphs (Figure 5.4 and Figure 5.5) as reaching a ceiling measurement. In the eccentric location graph in Figure 5.3, four POAG subjects (3 advanced and 1 moderate cases) fall on, approximately, the same point for B/Y and R/G differences, due to the limitation of the display. This makes it more difficult to quantify the relative increase at this eccentricity.

Similar summaries were obtained for comparisons between the B/Y and the achromatic sensitivities (Figure 5.4) and between R/G and achromatic sensitivities (Figure 5.5).

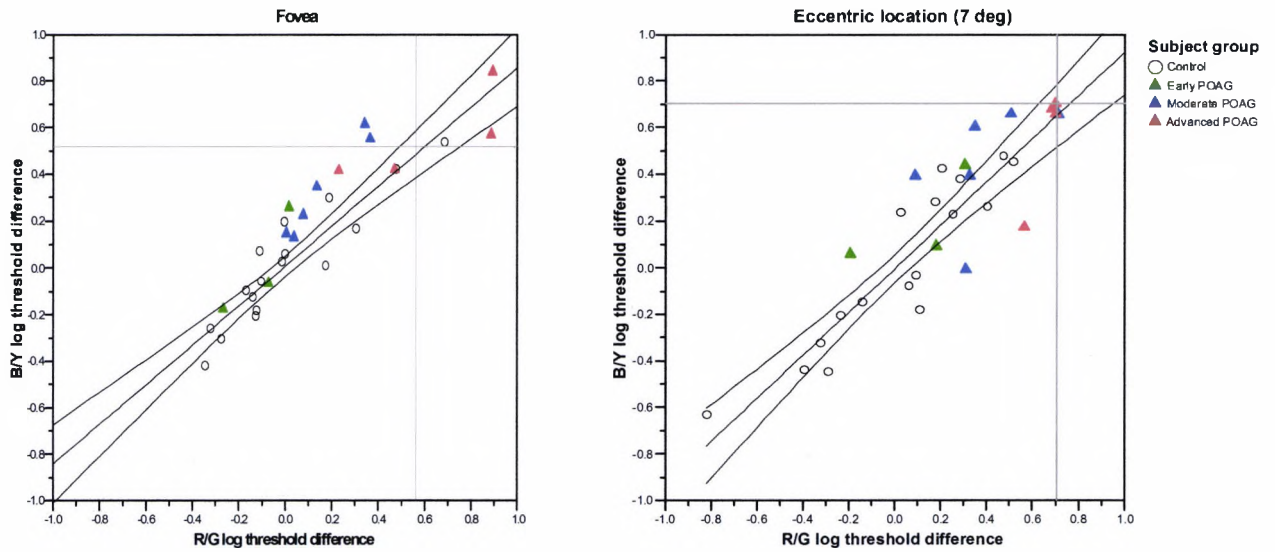


Figure 5.3: A comparison of the threshold differences (log units) for B/Y to those for R/G sensitivity for each individual subject. The triangles represent the difference for each POAG subject from the control group mean. The colour code represents the severity of visual field loss (AGIS score sub-classification section 5.3.1) for each POAG subject. The circles represent differences for individual control observers compared to the mean value for control observers (the point (0,0) represents the mean control value). The mean regression line and the confidence intervals for the control group have been plotted ($R^2=0.85$ and $R^2=0.85$, for foveal and 7 deg data, respectively). Continuous lines along the x and y axes show the upper limit for the reference range in the control group (+1.96 SD).

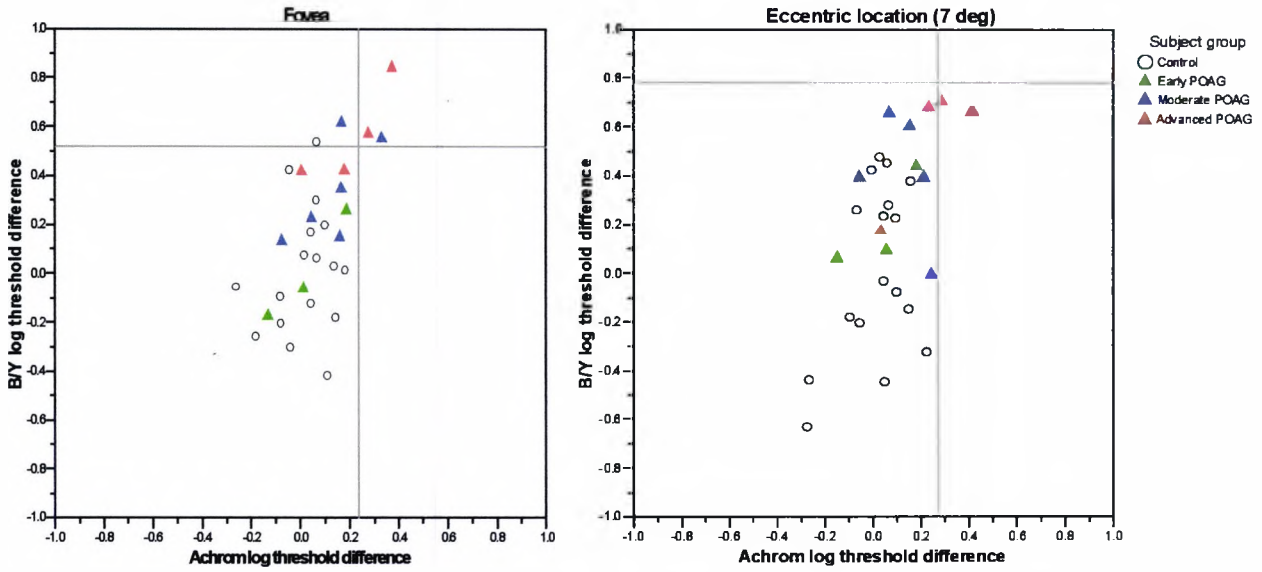


Figure 5.4: Threshold differences for B/Y sensitivity plotted against those for achromatic sensitivity (log units), for each individual POAG and control subject. For details see caption to figure 5.3.

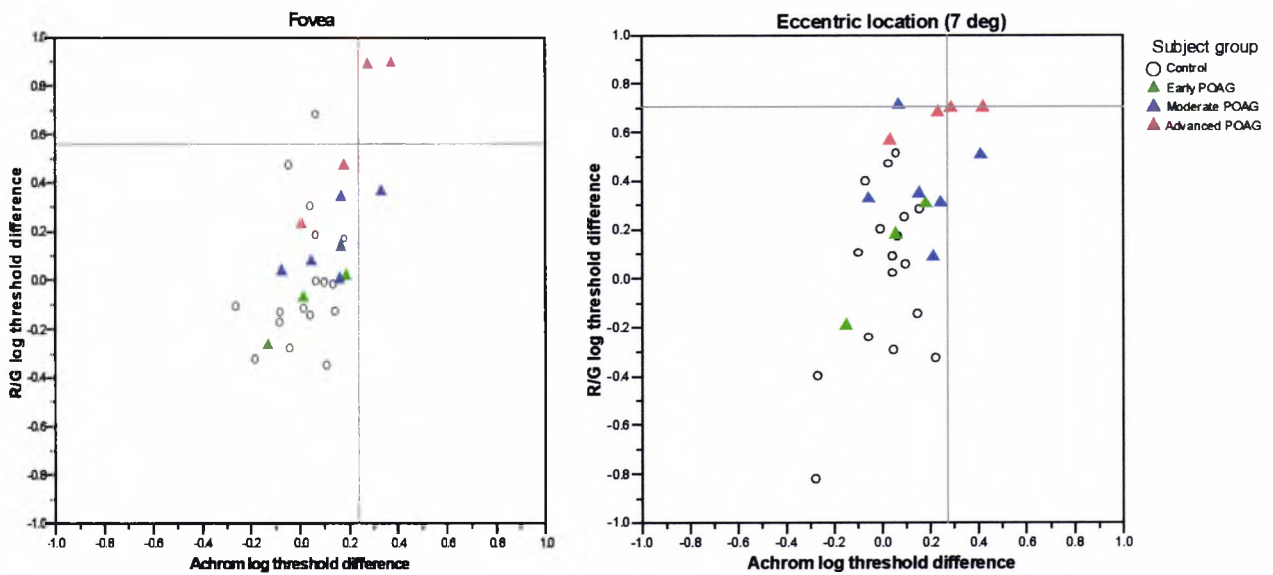


Figure 5.5: Threshold differences for R/G sensitivity compared to those for achromatic sensitivity (log units), for each individual POAG and control subject. For details see caption to Figure 5.3.

The relative increases in thresholds are greater along each of the chromatic mechanisms (R/G and B/Y) compared to the achromatic system. In both cases the eccentric location shows the largest differences in sensitivity between the glaucoma and the control groups. These differences at the eccentric location were likely to be even greater if the thresholds of the subjects mentioned above had not been limited by the phosphors of the display.

5.4.2.2 Loss of chromatic and achromatic sensitivity and its relation to severity of visual field loss

The relationships between the chromatic and achromatic motion discrimination thresholds and visual field loss were also studied. The increase in log threshold values was compared, for each POAG subject, to their level of visual field loss. The AGIS score (Gaasterland *et al.*, 1994) (see Table 5.1 and section 3.7.1) was used as a global measure of severity of visual field loss and the loss of light sensitivity (in dB) at the locus tested, as a localised measure of visual field loss. Both the foveal and the 7 deg stimulus locations overlapped four individual test points in the Humphrey Field Analyzer 24-2 static threshold visual field test (Figure 5.6). Therefore, the average of these four points given by the total deviation probability plots was taken as the measure of localised loss of light sensitivity.

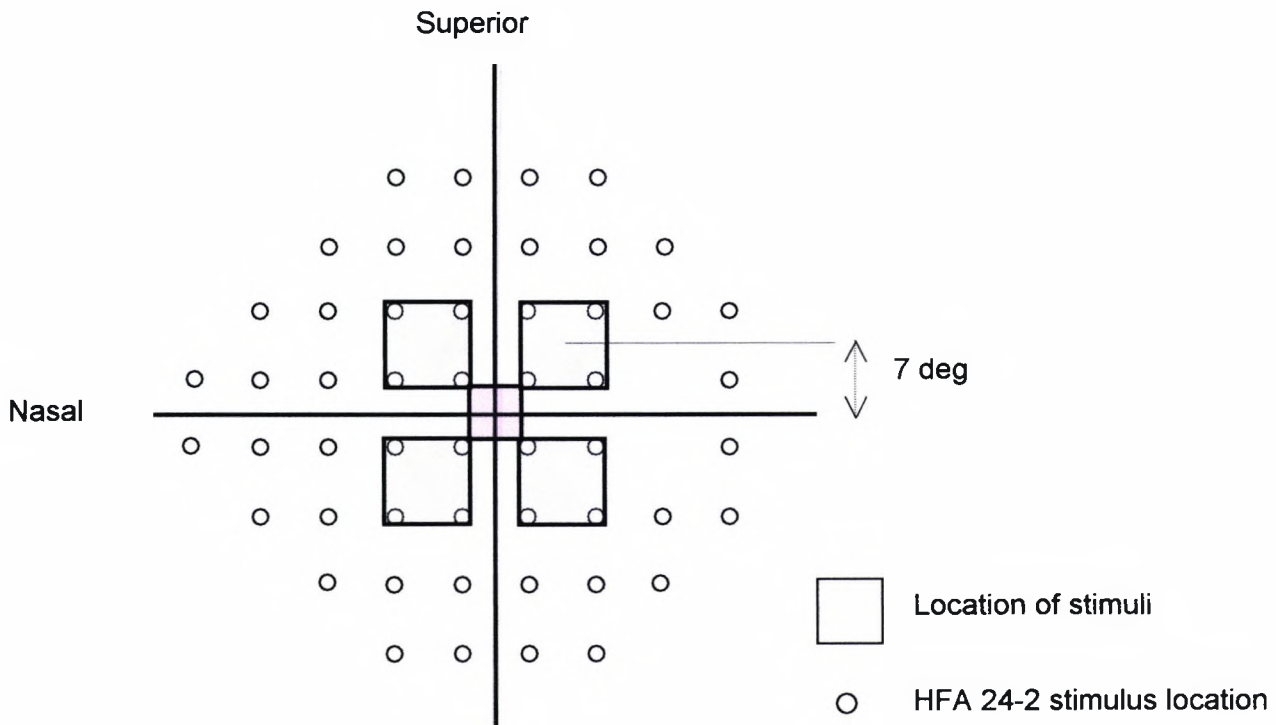


Figure 5.6: Foveal and 7 deg eccentricity stimulus locations. The stimulus presentation at the fovea and at one of the four possible eccentric (sup temporal, sup nasal, inf temporal and inf nasal) measurements is shown overlapping the distribution of locations on the 24-2 Humphrey visual field program to demonstrate the area coverage in the visual field. The light sensitivity loss (dB) for the foveal and 7 deg locations was the average of the four corresponding HFA stimuli locations in the total deviation probability plot.

Figure 5.7 shows the increase in B/Y, R/G and luminance contrast log thresholds at the foveal and eccentric locations as a function of the AGIS score for visual field loss.

It is clear from these graphs that both chromatic thresholds are better able to discriminate between different levels of severity of visual field loss (AGIS score) in POAG subjects than the achromatic thresholds. The Spearman's rank correlation coefficients for each of the conditions tested are shown in Table 5.4. These positive correlations indicate that motion discrimination thresholds increased with increasing

severity of the visual field loss in all conditions tested. The achromatic thresholds showed very low correlations, which were not significant. The R/G chromatic mechanism showed the largest correlations, which were significant at the 5% level. In contrast, the B/Y chromatic mechanism only showed a significant correlation for the foveal location ($p=0.012$). It is possible that had we been able to fully measure the large threshold values in the POAG subjects who reached the phosphor limits of the monitor, the eccentric location would also have shown a significant correlation.

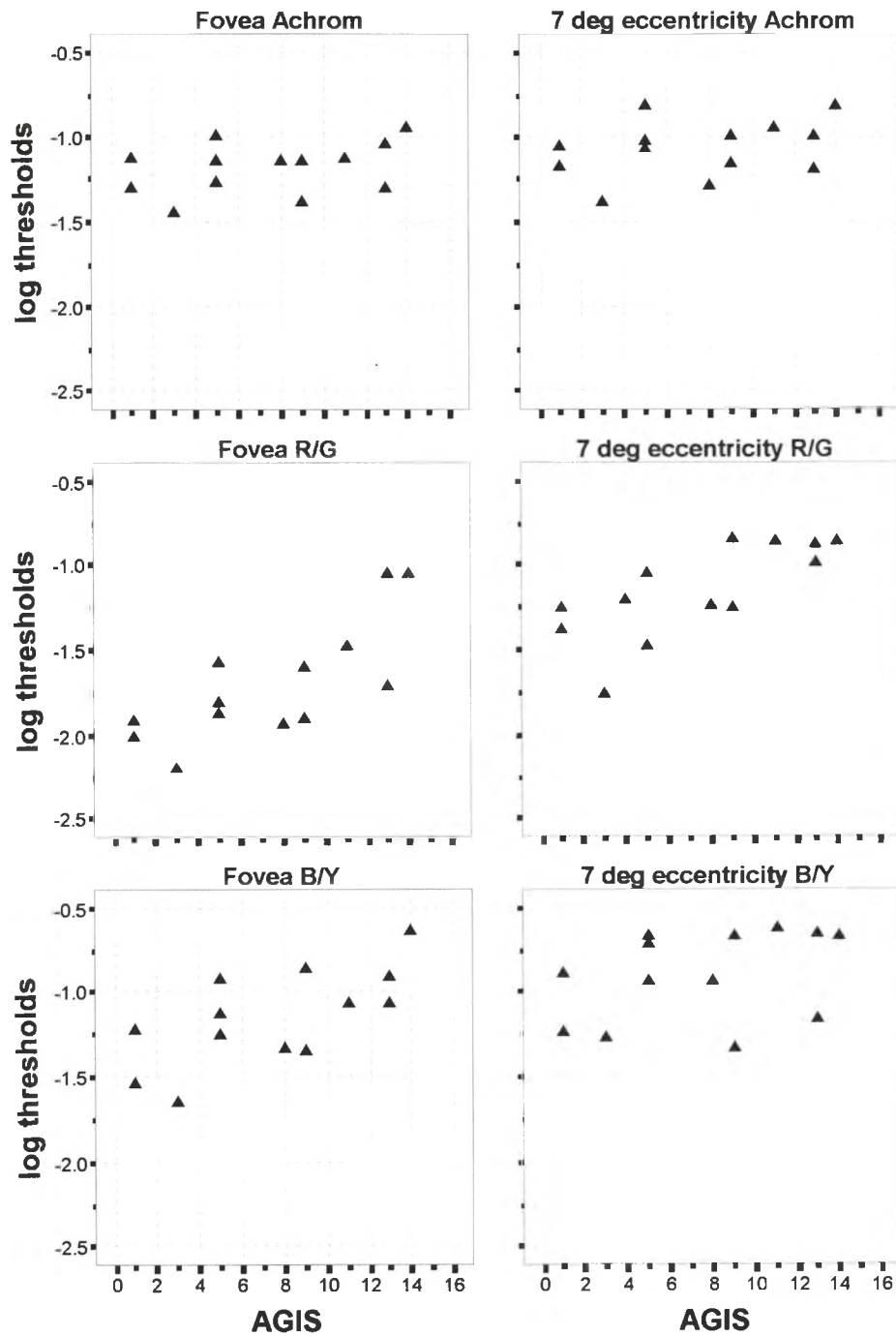


Figure 5.7: Achromatic and chromatic (R/G and B/Y) contrast log thresholds plotted as a function of severity of visual field loss (AGIS score) for the POAG subjects.

It is also interesting to identify the function that best describes how the R/G and B/Y chromatic thresholds increase with the severity of visual field loss. For foveal measurements, B/Y thresholds increase in a fairly linear manner, whereas the R/G threshold increase is best described by a quadratic function (Figure 5.8). The R/G thresholds show an accelerated increase in the moderate and advanced stages of the visual field loss, thus approaching the values of B/Y thresholds.

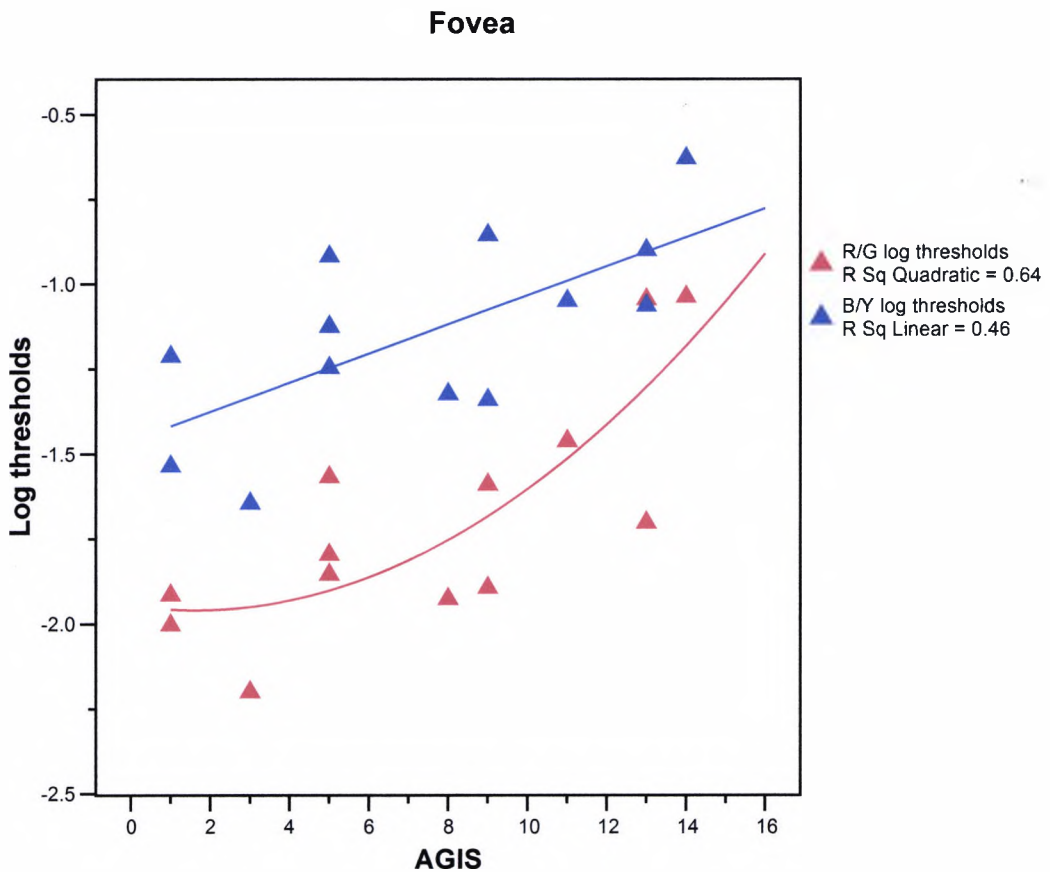


Figure 5.8: Comparison of foveal measurements of R/G and B/Y chromatic log threshold increases in the POAG subjects as a function of visual field loss (AGIS score). A quadratic function gave a statistically significant fit with the R/G threshold data, whereas the B/Y thresholds are equally well described by a linear function. This highlights the differential effect of the severity of the disease on B/Y and R/G thresholds.

For eccentric measurements at 7 deg, for both R/G and B/Y thresholds the increase in log threshold is linear (Figure 5.9). The R/G thresholds show a more pronounced increase as a function of increased visual field damage than the B/Y thresholds, which exhibit larger variability. However, this observation should be treated with caution due to the difficulties of obtaining actual thresholds at the eccentric location in 5 of these cases.

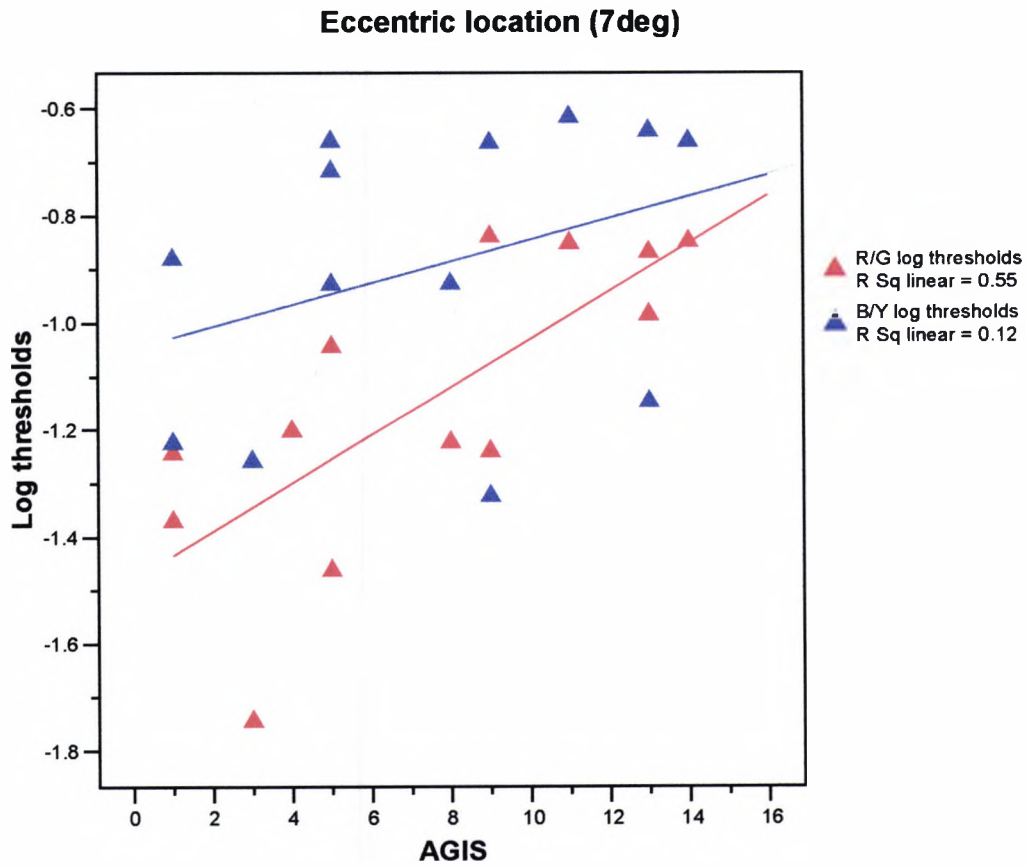


Figure 5.9: Comparison of 7 deg measurements of R/G and B/Y chromatic log threshold increases in the POAG subjects as a function of visual field loss (AGIS score).

Figure 5.10 shows the increase in B/Y, R/G and luminance contrast log thresholds at the foveal and eccentric locations as a function of the loss of light sensitivity (in dB) at the locus tested, obtained from the total deviation probability plot. As is clearly shown from the graphs and from the correlation coefficients in Table 5.4, the achromatic thresholds showed a poor correlation, with the localised measure of visual field loss, as had been the case with the AGIS score (global measure of visual field loss). For the chromatic thresholds measured at the foveal location there were moderate correlations that were significant at the 5% level. The chromatic thresholds measured at the eccentric location showed low correlations with the loss of light sensitivity measured at the eccentric locus tested. The R/G threshold correlation was particularly low, in contrast with the correlations obtained for the AGIS score. It is impossible to know how much higher the correlations measured at the eccentric location would have been if full measurement had been achieved for all POAG cases.

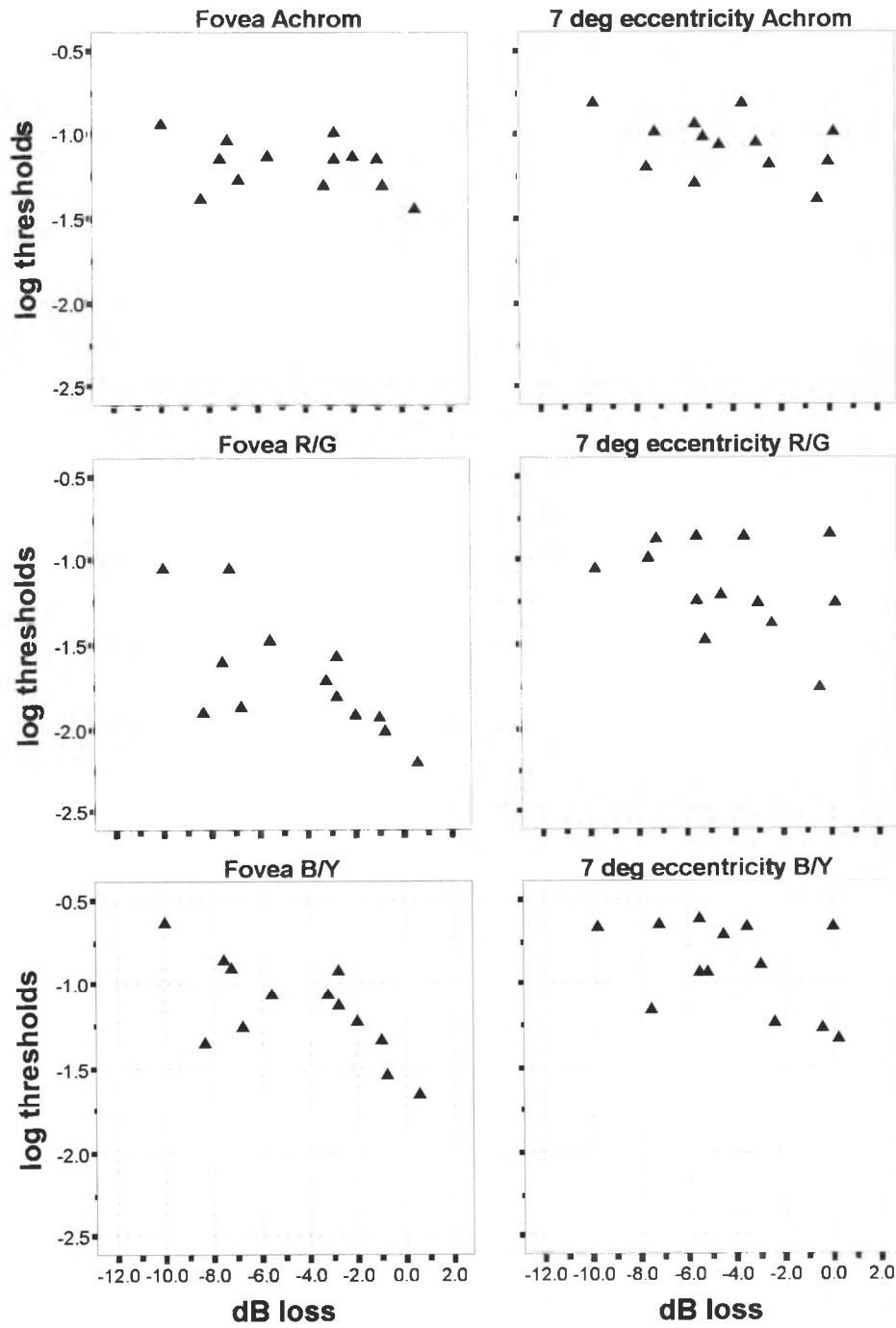


Figure 5.10: Increase in achromatic and chromatic (R/G and B/Y) contrast log threshold as a function of the loss of light sensitivity (in dB) at the locus tested given by the HFA total probability plot for the POAG subjects.

			Fovea		
			Achrom	R/G	B/Y
Spearman's rho	AGIS score	Correlation Coefficient	0.30	0.77	0.67
		Sig. (2-tailed)	0.32	0.002	0.012
		N	13	13	13
	light sensitivity loss (dB)	Correlation Coefficient	-0.35	-0.73	-0.65
		Sig. (2-tailed)	0.242	0.005	0.017
		N	13	13	13
			Eccentric location (7 deg)		
			Achrom	R/G	B/Y
Spearman's rho	AGIS score	Correlation Coefficient	0.183	0.77	0.42
		Sig. (2-tailed)	0.183	0.002	0.157
		N	13	13	13
	light sensitivity loss (dB)	Correlation Coefficient	-0.19	-0.27	-0.52
		Sig. (2-tailed)	0.523	0.368	0.069
		N	13	13	13

Table 5.4: Spearman's rho correlation coefficients for the rank correlation between chromatic (R/G and B/Y) and achromatic log thresholds, and AGIS score and loss of light sensitivity at the locus tested.

5.5 Summary of main results

1. Both chromatic (R/G and B/Y) and achromatic thresholds are significantly increased (representing drop of sensitivity) in glaucoma subjects compared to the control group, for the fovea and the 7 deg eccentricity locations tested.
2. The relative threshold increase in the POAG group is greater for the chromatic thresholds. On average, the increase in chromatic thresholds was more than 1.5 times the increase suffered by the achromatic mechanism (1.3 and 1.7 times greater along the R/G colour confusion axis and 1.6 and 1.9 times greater along B/Y the colour confusion axis than corresponding achromatic thresholds, for foveal and eccentric locations, respectively).
3. Although the thresholds measured along the B/Y mechanism show a slight tendency to be greater than the thresholds measured along the R/G axis at the foveal location, the eccentric location shows similar differences between the groups for B/Y and R/G thresholds and increased variability.
4. The severity of visual field loss measured with the global (AGIS score) and localised indices (loss of light sensitivity) correlated better with the colour discrimination thresholds than with the achromatic. The AGIS score showed, to some extent, better correlations than those for loss of light sensitivity, which indicates that a good proportion of the variance in the chromatic sensitivity is accounted for by the global index of visual field loss, particularly for the R/G thresholds.
5. The R/G and B/Y chromatic thresholds show differences in the fashion of increase as a function of the severity of visual field loss, according to the AGIS score. At both locations, measurements along the R/G colour confusion axis show a faster rate of increase with severity of loss. In the case of the foveal location this is an accelerated increase that affects mostly moderate and advanced cases. Therefore, although in early glaucoma subjects the greatest loss is usually for the B/Y sensitivity, this difference tends to be reduced substantially in moderate and advanced cases.

5.6 Discussion

In this study investigating the effects of glaucoma on the sensitivities of the colour-opponent and luminance systems we aimed to determine if POAG resulted in selective deficits in parallel pathways. Our results indicate that the relative loss of chromatic and achromatic sensitivity, measured both at the fovea and 7 deg locations, was greater for the chromatic mechanisms. When comparing the relative loss along R/G and B/Y colour opponent channels we found the greater sensitivity losses to be along the B/Y colour confusion axis. However, comparable sensitivity losses occurred along the R/G colour confusion axis, this was particularly so for measurements at 7 deg eccentricity.

These findings are consistent with results reported in a number of previous studies that have also aimed to selectively stimulate the colour-opponent and luminance contrast mechanisms, separately, on the same subject, which, in turn, allows a direct assessment of the relative loss of chromatic (R/G and B/Y) and achromatic sensitivities.

For instance, Pearson *et al.* (2001) used a 3° stimulus to selectively mediate detection by the R/G, blue-on chromatic mechanisms and the high-frequency flicker achromatic mechanism and tested perimetrically abnormal regions at eccentric locations (12 - 20 deg). They found larger chromatic losses in a greater number of POAG subjects of which, red and blue contrast sensitivity defects were similar in magnitude.

Greenstein *et al.* (1996) measured foveal discrimination thresholds along the RG and B/Y colour axes and along an achromatic luminance axis in POAG and suspects. As in the present study they found an increase in chromatic and achromatic thresholds when compared to a control group. As in their preliminary study (Greenstein *et al.*, 1993), they found that the greatest relative sensitivity loss was for the S-cone system. However, since this sensitivity loss was accompanied by significant reductions of R/G sensitivity, they concluded that the loss was not selective for the B/Y channel.

Felius *et al.* (1995b) measured the heterochromatic flicker photometric match, based on the peripheral colour contrast test developed by Yu *et al.* (1991), using a 12° ring. They tested early glaucoma patients and also reported a uniform threshold elevation

for luminance and colour-opponent mechanisms. However, the B/Y mechanism showed a small but significant preference for elevation compared to those of the R/G and luminance mechanisms.

Similarly, Kelly *et al.* (1996) measured foveal isoluminant colour and luminance thresholds in POAG and found that both colour and luminance thresholds were increased. Relative to the control subjects, the patients with glaucoma showed a non-selective defect in both colour and luminance sensitivity for red-green stimuli ($P < .05$), but a selective colour defect for yellow-blue stimuli ($P < .01$).

Alvarez *et al.* (1997) also measured foveal colour mixture thresholds for early glaucomatous damage eyes, following Grigsby's technique (Grigsby *et al.*, 1991), which is based on fitting an ellipse (length chromatic, width achromatic) to each subject's data. The ratio showed more or less diffuse or selective loss for B/Y and R/G versus achromatic sensitivity, however B/Y and R/G sensitivities were not compared. Two patterns of loss were identified: non-selective loss (similar ratio chromatic/achromatic to controls) and selective loss (greater than normal ratio) with chromatic thresholds significantly increased. R/G sensitivity selective losses were represented by 6 cases out of 11 (5 cases of non-selective loss). For B/Y sensitivity, they found 5 cases of selective and 7 of non-selective loss. They concluded that R/G chromatic sensitivity was significantly more affected than achromatic sensitivity.

Recently, Beirne *et al.* (2003) measured peripheral (13 deg) resolution acuity using achromatic and blue-cone isolating gratings in eyes with early to moderate glaucoma. Although significantly lower mean chromatic and achromatic acuity resolutions were found in the glaucoma group compared to normal subjects, no selective loss of mean SWS acuity was shown. However, a lower than normal chromatic/achromatic resolution ratio at certain locations, in some individuals with early glaucoma, was reported.

Not only psychophysical, but also a number of electrophysiological studies have aimed at selectively stimulating parallel pathways and comparing the relative loss of chromatic (R/G and B/Y mechanisms) and luminance channels. Many of them have substantiated similar findings, i.e. that chromatic responses have shown to be more sensitive to glaucoma damage than are responses to achromatic patterns.

Horn *et al.* (2000) found the chromatic VEP peak time responses to be significantly increased and more affected than the VEP peak time responses to achromatic pattern reversal stimulation, compared to a control group. Particularly, the peak time of the B/Y VEP showed the highest sensitivity in separating normal from POAG subjects and the highest correlation coefficients with visual field defects.

Porciatti *et al.* (1997) measured the PERG and the VEPs for red-green gratings of pure colour contrast, as well as yellow-black gratings of pure luminance contrast. As compared with controls, POAG patients' responses to luminance stimuli were little affected, whereas those to chromatic stimuli were both reduced in amplitude and delayed.

Greenstein *et al.* (1998) obtained sweep VEPs to isolated-check stimuli that were modulated sinusoidally in either isoluminant colour contrast or in positive and negative luminance contrast. Response functions obtained from POAG patients and suspects showed the VEP for POAG subjects to be significantly reduced for colour contrast and luminance contrast conditions, whereas VEP responses for suspects were significantly reduced only for the 15-Hz positive LC condition.

It is clear that most of these studies, including the present one, agree in that the chromatic mechanisms are more affected than the achromatic by glaucoma damage. However, the conclusions of these research studies about the relative loss of R/G and B/Y sensitivity are not unanimous. This is not surprising since these studies, which in many cases show small relative differences, are subject to methodological differences and subjective interpretation of results. Changes in the relative level of R/G and B/Y involvement as a function of the type of glaucoma (Greenstein *et al.*, 1996; Lachenmayr & Drance, 1992; Yamagami *et al.*, 1995; Yamazaki *et al.*, 1989), or as a function of the severity of glaucomatous damage (Pearson *et al.*, 2001) have also been described.

In an attempt to investigate the latter issue we analysed the loss of chromatic sensitivity as a function of severity of visual field loss and found that the B/Y and R/G thresholds were differentially affected. In general, the increment of chromatic thresholds was greater for POAG subjects showing greater severity of visual field loss. Conversely, the achromatic thresholds revealed a non-significant low positive correlation with severity of visual field loss (Figure 5.7). The increase in R/G thresholds, as a function of severity of visual field loss given by the global index (AGIS score), was

more pronounced than the B/Y increase, for both locations (fovea and 7 deg eccentricity) tested. This is in disagreement with Greenstein *et al.* (1996) who found that POAG subjects showed no difference in the pattern of sensitivity loss along the achromatic, R/G and B/Y colour opponent mechanisms with increasing severity of the disease.

In terms of location, it is interesting to note that the rate of foveal R/G threshold increase accelerates with increasing visual field loss, therefore affecting predominantly the Moderate and Advanced cases (Figure 5.8). This suggests that, for foveal measurements, in Moderate and Advanced glaucoma patients the R/G chromatic mechanism is selectively affected. In contrast, the B/Y threshold increase followed a roughly linear function, with a greater B/Y relative loss in early glaucoma subjects.

For measurements taken at 7 deg eccentricity, both R/G and B/Y mechanisms showed a linear increase, with greater B/Y relative loss of sensitivity in glaucoma subjects with early visual field loss and R/G thresholds increasing and catching up in early and moderate stages of visual field loss (Figure 5.9). However, full threshold measurements could not be attained in five of the glaucoma subjects, at this eccentricity. Consequently, this conclusion should be treated with caution. Although the mean B/Y threshold increase in the POAG group, compared to the control group, was greater than the R/G threshold increase, data collected at this eccentricity showed large variability, which decreases precision and therefore a clear relative difference could not be demonstrated. Factors other than those related to psychophysical methodology have recently been described as responsible for the large variability associated with glaucomatous sensitivity loss. The fluctuating responses of dysfunctional glaucomatous ganglion cells (Morgan, 2002) and the decreased probability summation among independent detection mechanisms affected with different degrees of damage (Harwerth *et al.*, 2002) are examples of factors that increase the variance in sensitivity.

These findings substantiate the results found in chapter 4. Again R/G thresholds were better correlated and increased more rapidly with the global index of field loss than the B/Y thresholds and a greater R/G relative loss was found at earlier stages of glaucomatous damage than other studies had suggested (Kalloniatis *et al.*, 1993; Pearson *et al.*, 2001).

Evidence for selective nerve fibre losses in glaucoma comes from histologic studies of retinal ganglion cells in experimentally induced (Glovinsky *et al.*, 1991) and human chronic glaucoma (Quigley *et al.*, 1988). These results have been interpreted as providing evidence for selective loss of large ganglion cells (preferential damage hypothesis), which implies a selective damage to the magnocellular pathway.

The differential sensitivity of chromatic and achromatic tests found in our results contradicts the hypothesis that in glaucoma there is selective damage to the magnocellular pathway and suggests that there is considerable damage to the B/Y mechanism, which is mediated by the small bistratified ganglion cells (Dacey & Lee, 1994; Martin *et al.*, 1997) and to the R/G mechanism, which is mediated by the midget cells (Dacey, 2000; Lee *et al.*, 1990). The pattern of loss obtained showed that defects with the achromatic stimulus (which should be mediated by the magnocellular pathway) were less important than those obtained with the B/Y or even the R/G chromatic stimulus.

Glaucoma studies investigating the relative changes in cell morphology (Morgan, 2002) and the alterations in metabolic activity of neurons in the laminae of the LGN (Crawford *et al.*, 2000) suggest no differential effect on ganglion cell types. In contrast, results at a higher level of visual processing (V1) suggest that glaucoma has a differential effect with more significant metabolic changes at anatomic sites innervated by P-cell (layer 4C β) versus M-cell (layer 4C α) inputs (Crawford *et al.*, 2001).

Alternatively the reduced redundancy hypothesis, based on properties of the ganglion cell mosaic, proposes that using methods able to stimulate individual ganglion cell mosaics will be more sensitive to damage than using "unselective" tests stimulating several mosaics, since "holes" in different mosaics may not overlap (Johnson, 1995). Several studies have demonstrated better and earlier detection of glaucomatous damage with methods able to isolate specific neuronal populations (Alvarez *et al.*, 1997; Harwerth *et al.*, 1999b; Johnson *et al.*, 1993a; Sample *et al.*, 2000). This hypothesis is based on the well-established psychophysical principle of probability summation, which follows the assumption that when several mechanisms can detect a stimulus, the stimulus will be detected as any one of the detection mechanisms responds.

Indeed, our results suggest that this hypothesis can account partly for the relative B/Y and R/G threshold increase at the foveal and eccentric location. As the disease worsens, the number of viable retinal ganglion cells decreases. The loss of a number of mechanisms from a large population (midget ganglion cells mediating the R/G mechanism) will be less affected than the loss of the same number of mechanisms from a smaller population (small bistratified ganglion cells mediating the B/Y mechanism). Potentially, the same insult to B/Y and R/G chromatic mechanisms would increase thresholds early in the B/Y mechanism, whereas the R/G mechanism would not show reduced sensitivity until the damage was wide spread. However, for the same reason, the achromatic (first order motion) threshold increase would be expected to be larger according to the reduced probability summation hypothesis.

It is often assumed that the relative loss of the various channels at the anatomical level will be directly reflected in the relative loss of psychophysical sensitivity. However, psychophysical data on spatial properties of chromatic and achromatic pathways are consistent with the idea that some cortical neurons mediating chromatic thresholds display a larger spatial summation than do cortical neurons mediating achromatic thresholds (Humanski & Wilson, 1993; Sekiguchi *et al.*, 1993). In addition, unpublished data from our laboratories suggest that the size of the stimulus we employ is closer to the limit of the area summation of the B/Y mechanism than to the R/G limit, suggesting a smaller area summation for the R/G mechanism.

Thus, if achromatic and chromatic (B/Y and R/G) mechanisms had a differential spatial summation, glaucomatous ganglion cell loss would be expected to have a differential influence on the sensitivity of B/Y, R/G and achromatic stimuli. An unselective damage to individual ganglion cells would result in a greater threshold increase for those mechanisms with larger spatial summation (i.e. B/Y mechanism). In this case each cortical neuron integrates signals from a larger number of ganglion cells, thus resulting in a population of neurons all with similarly reduced sensitivity. On the other hand, the same damage would result in a smaller relative increase for those mechanisms with smaller spatial summation (i.e. luminance mechanism), since each cortical neuron, in this case, receives excitatory input from a small number of ganglion cells. Therefore, some would show reduced sensitivity but some would show normal sensitivity.

The small achromatic threshold elevation found, in the present study, versus the larger chromatic losses is consistent with this idea. B/Y thresholds increased early in the glaucomatous damage process after the loss of a small number of ganglion cells. As the severity of damage increased, the R/G mechanism was progressively affected. Meanwhile, the achromatic thresholds resisted better.

In conclusion, when we compared the motion discrimination thresholds obtained for those stimulus conditions which reduced the functional overlap between psychophysical parallel pathways (luminance, R/G and B/Y colour-opponent mechanisms) we found evidence for larger chromatic deficits for the group of patients with POAG. However, motion discrimination thresholds were significantly increased for both chromatic and luminance contrast conditions, which reflects a certain degree of damage to all detection mechanisms. Other studies comparing a wide range of tests (psychophysical and electrophysical and electrophysiological measures) have found that most parameters reflected some degree of glaucomatous loss and that a variety of tests designed to isolate either M- or P- pathways indicate abnormalities even in early cases (Graham *et al.*, 1996; Johnson, 2001; Ruben *et al.*, 1994; Sample *et al.*, 2000). The differential sensitivity found, in this study, between chromatic and achromatic mechanisms can be explained by spatial summation properties of cortical neurones and probability summation among the neural detectors.

6 Chromatic and achromatic loss of sensitivity in ageing

6.1 Introduction

The knowledge of how sensitivity changes as a function of age is a valuable tool. Firstly, it allows us to determine whether an individual's visual function is above or below the average for an age-matched control, which in turn assists in distinguishing between healthy subjects and those with disease affecting the visual system. This is crucial when the disease tends to be more frequent with advancing age. Secondly, it provides the basis on which to assess the differential effect of ageing on different visual mechanisms.

A number of psychophysical studies have reported changes in the visual system as a function of the normal ageing process. Among the visual functions that exhibit age-related changes are: differential light sensitivity (Spry & Johnson, 2001), dark adaptation (Jackson *et al.*, 1999), colour discrimination (Knoblauch *et al.*, 1987; Knoblauch *et al.*, 2001; Lakowski, 1974), motion sensitivity (Wojciechowski *et al.*, 1995) and spatial resolution (Hennelly *et al.*, 1998; Artal *et al.*, 1993). However, there is some controversy about the magnitude of these effects, about the specific function (linear versus non-linear) describing sensitivity loss and about the relative roles of optical (Burton *et al.*, 1993) and neural factors (Spear, 1993).

Some studies on visual ageing have investigated whether there is a selective deterioration of the luminance or the colour opponent mechanisms (the magnocellular or the parvocellular pathways) in older age groups (Fiorentini *et al.*, 1996; Johnson & Marshall, 1995; Spear, 1993). The results of these studies do not show full agreement on this matter.

Measuring motion colour contrast thresholds embedded in dynamic noise, which ensures isolation of the chromatic pathway (Barbur *et al.*, 1994) and comparing them to motion LC thresholds, embedded in static noise, which isolates first order, band pass motion detection mechanisms (Barbur, 2004) provides the opportunity to investigate whether ageing affects selectively either the chromatic or the achromatic neural pathways, in humans.

6.2 Aim

The main aim of this study is to investigate how the processing of colour and luminance contrast signals deteriorates with age, and to quantify their relative loss of sensitivity.

6.3 Subjects and methods

6.3.1 Subjects

Thirty visually normal observers took part in this study. These subjects were selected to form two distinct groups. The “older” group sample had seventeen subjects with an average age of 67.9 years (SD=6.0 years) and the “younger” group had an average age of 31 years (SD=8.6 years). Logistics of the subjects’ recruitment and details of the inclusion criteria can be found in sections 2.3 and 3.7, respectively.

6.3.2 Methods

Motion direction discrimination thresholds were measured using the CAD test (Colour Assessment and Diagnosis), as described in section 3.6.2, both for luminance and colour contrast defined motion signals at 3 levels of background masking noise (12, 24 and 48%). Colour contrast (CC) thresholds were measured along 2 directions in colour space, 74.5° and 169°, which favour selectively the B/Y and the R/G chromatic mechanisms. Luminance contrast (LC) thresholds were measured by defining the test stimulus in luminance contrast. Subjects were tested at one position centred on fixation

(fovea) and at one eccentric location, at 7 deg from fixation. The eccentric measurement was taken in one of the four visual field quadrants, superior nasal, superior temporal, inferior nasal or inferior temporal. The older group had only one of these four eccentric locations measured, which was chosen randomly. The younger group had all four eccentric locations measured, since they were better able to cope with the longer duration of this extended test.

As discussed in chapter 5, in order to compare directly changes in colour and luminance contrast sensitivity as a function of age and stimulus location in the visual field, we have chosen to quantify all changes in log units.

6.4 Results

In order to obtain a normal distribution and similar SDs, when comparing data among groups, a logarithmic transformation was applied. An analysis of variance (UNIANOVA) revealed that log contrast thresholds were significantly affected by the following variables: age group ($F= 449.2$, $p<0.001$), type of stimulus ($F= 449.7$, $p<0.001$), and the eccentricity of the location tested ($F= 141.2$, $p<0.001$). Also, the interactions between the type of stimulus and age group ($F= 34.2$, $p<0.001$), the type of stimulus and location tested ($F= 19.3$, $p<0.001$) and the type of stimulus and background noise level ($F= 5.35$, $p<0.001$) were significant. These effects will be examined in depth in the following sections.

6.4.1 Effect of background noise level

The interaction between the stimulus and the background LC noise level used was investigated to determine whether the noise level used as background (i.e. 12, 24, 48%) had a differential effect on the type of stimulus or on the sensitivity of the age group. Figure 6.1 shows the averaged results of the older and younger observers, as a function of background noise level, for the fovea and the eccentric locations tested. In the younger group the eccentric location represents an average of the four quadrant measurements.

A one-way ANOVA, performed separately for each type of stimulus (i.e. achromatic, R/G and B/Y), for all subjects taken together, showed that noise had a significant effect on the thresholds for the achromatic stimulus ($F= 30.6$, $p<0.001$), but not for the R/G or B/Y stimuli thresholds. Post-hoc tests (LSD) showed a significant difference ($p<0.001$) between 12 and 48% luminance contrast noise levels for the achromatic stimulus. As discussed in section 5.4.1 this is most likely to be a consequence of the subjects' small eye movements during testing with the achromatic target embedded in static noise, which produces the effect of inducing some dynamic noise to the target. The effect of dynamic noise on the detection of LC defined motion has been illustrated in Figure 3.4.

The effect of noise on the log thresholds obtained for the younger and older groups was not statistically significantly different for any of the stimuli tested, in other words the analysis of variance did not identify a significant interaction between background noise and age group (age group by background noise interaction: Achromatic, $F= 1.44$, $p=0.24$; R/G, $F= 1.81$, $p=0.16$; B/Y, $F= 0.477$, $p=0.62$).

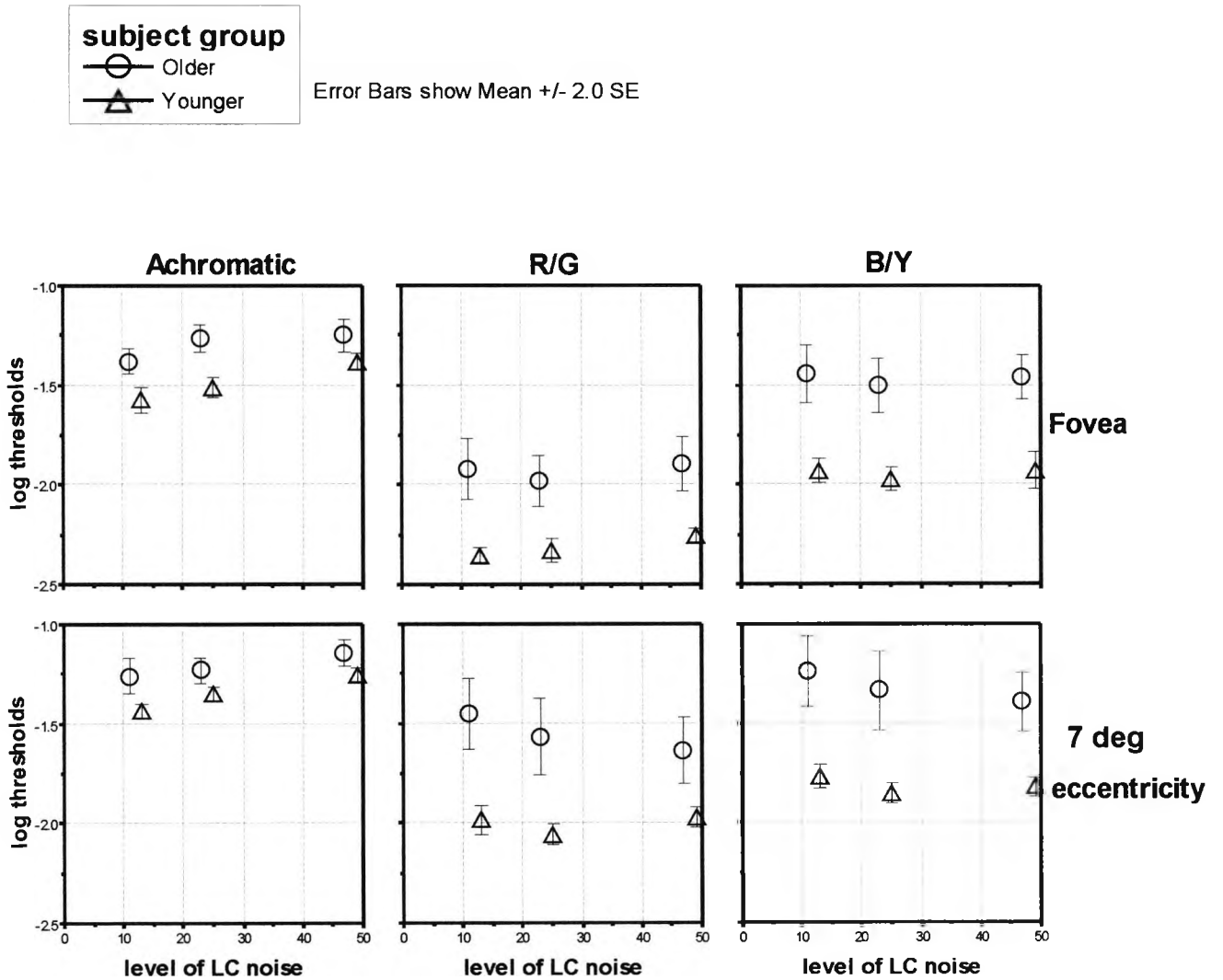


Figure 6.1: Mean log thresholds of the older and younger normal subjects for chromatic (R/G and B/Y) and achromatic sensitivity, as a function of the three LC background noise levels (12, 24 and 48%) used, at each location. Bars indicate 2 SE of the mean.

6.4.2 Relative loss of sensitivity with age.

Table 6.1 summarises the average and SD of the log contrast motion discrimination threshold data for both the achromatic and the colour defined stimuli in each group. To facilitate comparisons thresholds measured for the three noise levels were averaged for each individual. This is justified since the background noise level had no statistically significant effect on threshold discrimination in either age group. In the case of the younger group, the four quadrant eccentric measurements were also averaged, for each individual. The differential effect on regional sensitivity will be considered in section 6.4.4.

The box-plots in Figure 6.2 show the distribution of the log thresholds for achromatic and chromatic sensitivity in the older and younger group. A significant difference in motion direction discrimination thresholds between the older and younger groups was detected when log thresholds for the foveal and eccentric locations were tested for chromatic and achromatic sensitivity. An independent samples t-test (Table 6.2) showed that the mean threshold differences between the older and the younger group are highly statistically significant, both at the fovea and at the eccentric location. Tests that do not assume equal variances were used for both chromatic stimuli (Levene's test, $p < 0.05$).

		Fovea			
		Older		Younger	
log thresholds		Mean	SD	Mean	SD
stimulus	Achrom	-1.299	.158	-1.490	.123
	R/G	-1.933	.283	-2.313	.091
	B/Y	-1.468	.267	-1.943	.132

		Eccentric location			
		Older		Younger	
log thresholds		Mean	SD	Mean	SD
stimulus	Achrom	-1.215	.158	-1.347	.134
	R/G	-1.553	.373	-2.005	.216
	B/Y	-1.323	.364	-1.814	.202

Table 6.1: The mean and SD for the log thresholds for young and old normal groups are shown for achromatic and chromatic (R/G and B/Y colour confusion axes) conditions, at both locations tested.

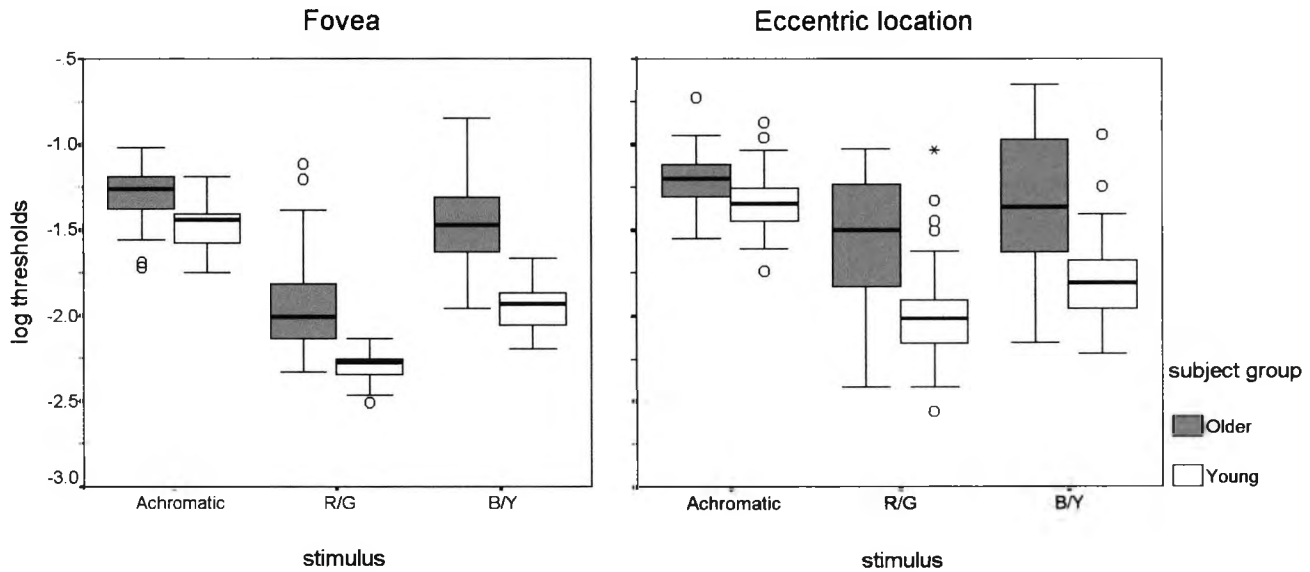


Figure 6.2: Box-plots of the log thresholds for chromatic (R/G and B/Y) and achromatic sensitivity allow a comparison of the younger (N=13) and older (N=17) groups. The box contains the middle 50% of the cases.

The chromatic (B/Y and R/G) and achromatic log threshold increments in the older compared to the younger group are shown by the mean differences of the groups in Table 6.2. For the achromatic thresholds the increase was approximately 1.5 and 1.3 times, for fovea and 7 deg eccentricity, respectively. For the chromatic thresholds along the R/G colour confusion axis the increase was approximately 2.4 and 2.8 times and for thresholds along the B/Y colour confusion axis the increase was approximately 3 and 3.1 times, for fovea and 7 deg eccentricity, respectively. Although this implies that the greatest threshold increase is found along the B/Y colour confusion axis (both for foveal and 7 deg measurements), given that the 95% confidence interval of the difference of means overlap, the slightly larger age-related loss for B/Y chromatic stimuli is not clinically significant.

Independent Samples Test

Log thresholds

			Levene's Test for Equality of Variances		t-test for Equality of Means						
			F	Sig.	t	df	Sig. (2-tailed)	Mean Difference	Std. Error Difference	95% Confidence Interval of the Difference	
stimulus	location tested								Lower	Upper	
Achrom	Fovea	Equal variances assumed	1.573	.213	-6.238	88	.000	-.191	3.066E-02	-.252	-.130
		Equal variances not assumed			-6.447	87.960	.000	-.191	2.967E-02	-.250	-.132
	Eccentric location	Equal variances assumed	1.644	.201	-5.687	181	.000	-.132	2.325E-02	-.178	-8.6E-02
		Equal variances not assumed			-5.289	79.346	.000	-.132	2.500E-02	-.182	-8.2E-02
R/G	Fovea	Equal variances assumed	24.175	.000	-8.050	88	.000	-.380	4.717E-02	-.473	-.286
		Equal variances not assumed			-8.985	62.879	.000	-.380	4.225E-02	-.464	-.295
	Eccentric location	Equal variances assumed	32.150	.000	-10.659	205	.000	-.452	4.242E-02	-.536	-.369
		Equal variances not assumed			-8.216	61.287	.000	-.452	5.504E-02	-.562	-.342
B/Y	Fovea	Equal variances assumed	14.746	.000	-10.164	88	.000	-.475	4.669E-02	-.567	-.382
		Equal variances not assumed			-11.031	76.845	.000	-.475	4.303E-02	-.560	-.389
	Eccentric location	Equal variances assumed	50.319	.000	-12.122	205	.000	-.491	4.051E-02	-.571	-.411
		Equal variances not assumed			-9.177	60.306	.000	-.491	5.351E-02	-.598	-.384

Table 6.2: Independent samples t-test for Achromatic, B/Y and R/G log thresholds between older and younger group for both foveal and eccentric locations tested.

Figure 6.3 plots the differences for each subject with respect to the mean of the younger group. Log threshold differences along the R/G colour confusion axis are compared to those along B/Y axis. The circles represent the differences for an individual older subject from the younger mean. The (0,0) represents the average younger value. The triangles represent differences for each younger observer compared to the mean value for younger observers. The solid line is the best fit regression line for the younger group. The dotted lines correspond to the reference range for the younger group (+1.96 SD).

In general, older subjects with increased threshold differences along the R/G axis have similar increases along the B/Y axis, for the foveal measurements. This represents a non-selective loss of chromatic sensitivity. All cases beyond the limits of the normal reference range (1.96 SD) for R/G thresholds differences (14) are also beyond the normal reference range for B/Y thresholds differences (82.4%). However, there is a slight tendency for larger B/Y differences, which can be noticed as more of the older subjects fall above the fitted regression line (9 out of 17, which represents 52.9% of the total). In this sense, a tendency for the difference in B/Y threshold to reach a peak plateau compared with the R/G difference, which takes a more gradual route to the maximum difference was found. Two older subjects show equal B/Y and R/G threshold increases (11.7%) and 3 fall below the fitted regression line (17.6%), which represents a relative R/G threshold increase. Finally, 3 older subjects fall within the younger group range (17.6%).

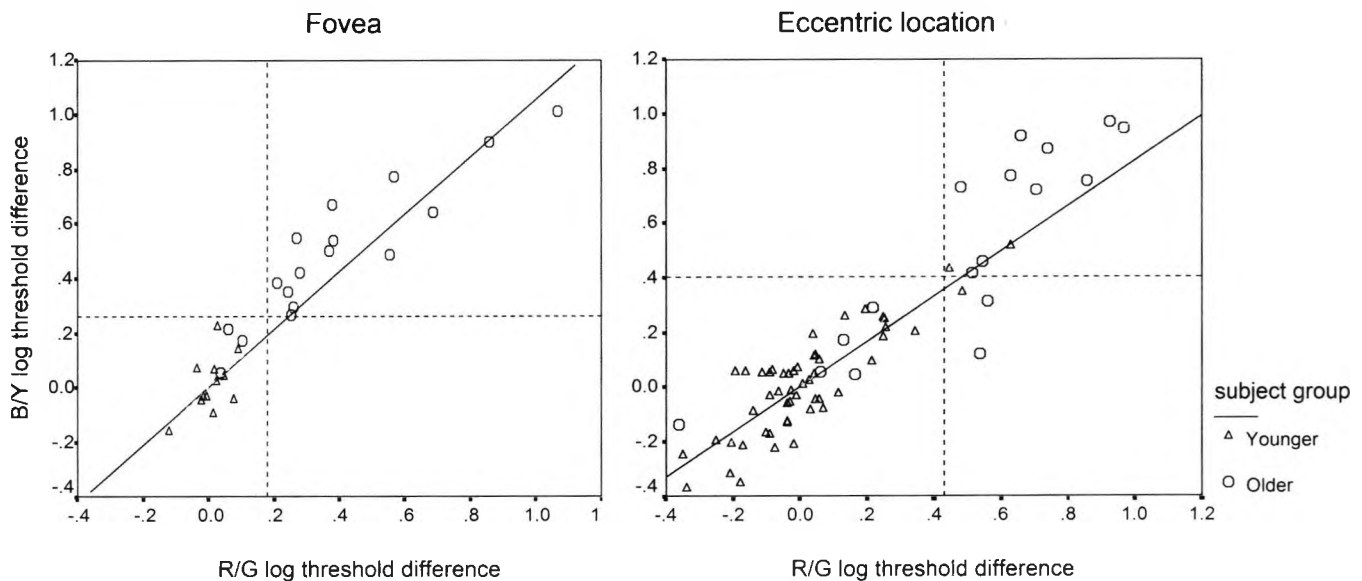


Figure 6.3: A comparison of threshold differences for R/G sensitivity to those for B/Y sensitivity (log units), for each subject. The circles represent the differences in log threshold units for each old observer from the young mean log threshold value. The triangles represent differences in log threshold values for each young observer compared to the mean log threshold value for young observers. Point (0,0) represents the mean young value. The solid line corresponds to the linear regression for the younger group ($R^2=0.31$ and $R^2=0.72$, for foveal and 7 deg data, respectively). The dotted lines correspond to the reference range for the younger group (+1.96 SD).

Similarly, at 7 deg eccentricity there is a tendency for non-selective loss. Ten of the 17 older subjects fall beyond both limits of the normal reference range (58.8%), and most of these display a tendency for relative B/Y threshold increase (8 out of 17, which represents 47%). However, 2 older subjects fall beyond the normal range for R/G thresholds, but within the normal range for B/Y thresholds (11.8%), which indicates a selective R/G threshold increase. Finally, 5 older subjects fall within the younger group range (29.4%). Although there is a tendency for larger B/Y differences, in some cases (more older subjects fall above the fitted regression line), the variability of the data is large (SE of the mean difference in the older group is three times that of the younger

group) and therefore as a group the older subjects exhibit a non-selective loss of R/G and B/Y sensitivity, at 7 deg eccentricity.

Similar graphs are presented for comparisons between the B/Y and the achromatic sensitivities (Figure 6.4) and between R/G and achromatic sensitivities (Figure 6.5). A clear tendency for selective B/Y or R/G loss can be observed when these log threshold differences are compared to achromatic ones, both for foveal and eccentric locations.

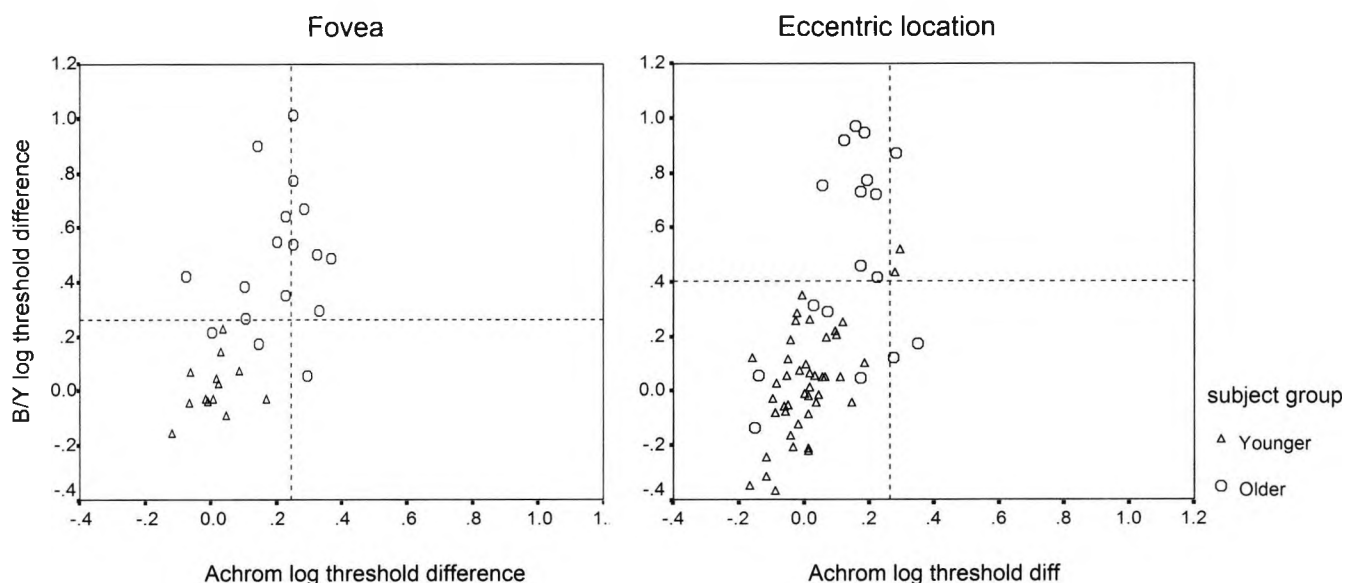


Figure 6.4: Threshold differences for B/Y sensitivity compared to those for achromatic sensitivity (log units), for each individual subject. For details see caption to Figure 6.3.

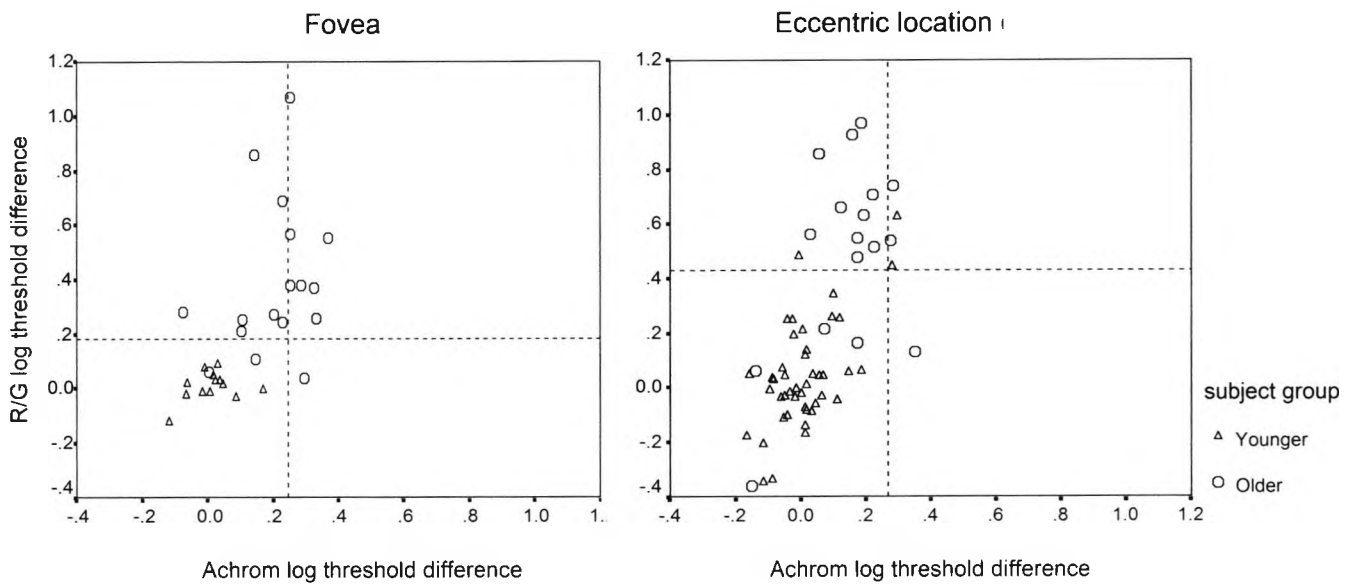


Figure 6.5: Threshold differences for R/G sensitivity compared to those for achromatic sensitivity (log units), for each individual subject. For details see caption to Figure 6.3.

Log threshold differences for the older group along the B/Y axis are significantly positively correlated with differences along the R/G axis (Pearson's correlation coefficient: 0.92 and 0.88 for fovea and 7 deg, respectively). This is not the case for differences along either of the chromatic systems (B/Y and R/G axes) compared to the achromatic (Table 6.3).

Therefore, a clear relative loss of chromatic versus achromatic sensitivity is found. This suggests that ageing has a greater effect on chromatic rather than achromatic motion discrimination thresholds.

Pearson Correlations for the older group

		location tested					
		Fovea			Eccentric location		
		Achrom log thresh difference	R/G log thresh difference	B/Y log thresh difference	Achrom log thresh difference	R/G log thresh difference	B/Y log thresh difference
Achrom log thresh difference	Pearson Correlation	1.000	.253	.191	1.000	.476	.373
	Sig. (2-tailed)		.326	.463		.053	.140
	N	17	17	17	17	17	17
R/G log thresh difference	Pearson Correlation	.253	1.000	.922**	.476	1.000	.877**
	Sig. (2-tailed)	.326		.000	.053		.000
	N	17	17	17	17	17	17
B/Y log thresh difference	Pearson Correlation	.191	.922**	1.000	.373	.877**	1.000
	Sig. (2-tailed)	.463	.000		.140	.000	
	N	17	17	17	17	17	17

** Correlation is significant at the 0.01 level (2-tailed).

Table 6.3: Pearson's correlation coefficients for the achromatic and chromatic (R/G and B/Y) log threshold differences in the older group.

6.4.3 Effect of age across the span of life

A cross-sectional investigation of all subjects (N=30) was conducted in order to study in depth the effects of ageing. Although our primary aim was the recruitment of two different age groups (i.e. older and younger), in order to compare these, we also wished to offer a more descriptive analysis on how chromatic and achromatic sensitivities change as a function of age. Therefore, the age distribution shown in the following scatter-plot graphs, has a gap between the ages of 45 and 56 years.

Figure 6.6, Figure 6.7 and Figure 6.8 show the scatter plots of the motion direction discrimination log thresholds measured for achromatic and chromatic (along the R/G and B/Y colour confusion axes) sensitivities, as a function of age. The data were fitted with a least squares linear regression model. The coefficients of determination (R^2) and the increase (slope) in average threshold with age (log units/ decade) for the linear regression model are summarised in Table 6.4.

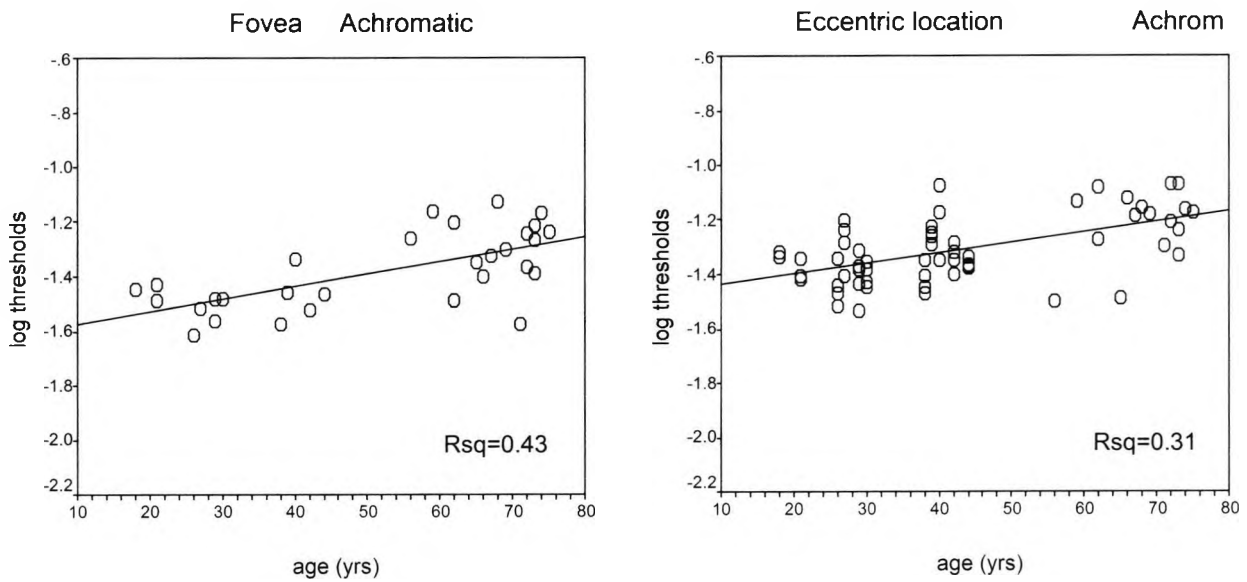


Figure 6.6: Distribution of achromatic log thresholds as a function of age. Each point represents data from a single observer. At the eccentric location each young subject displays 4 measurements, one for each quadrant. The solid line is the best fitting regression line for the data.

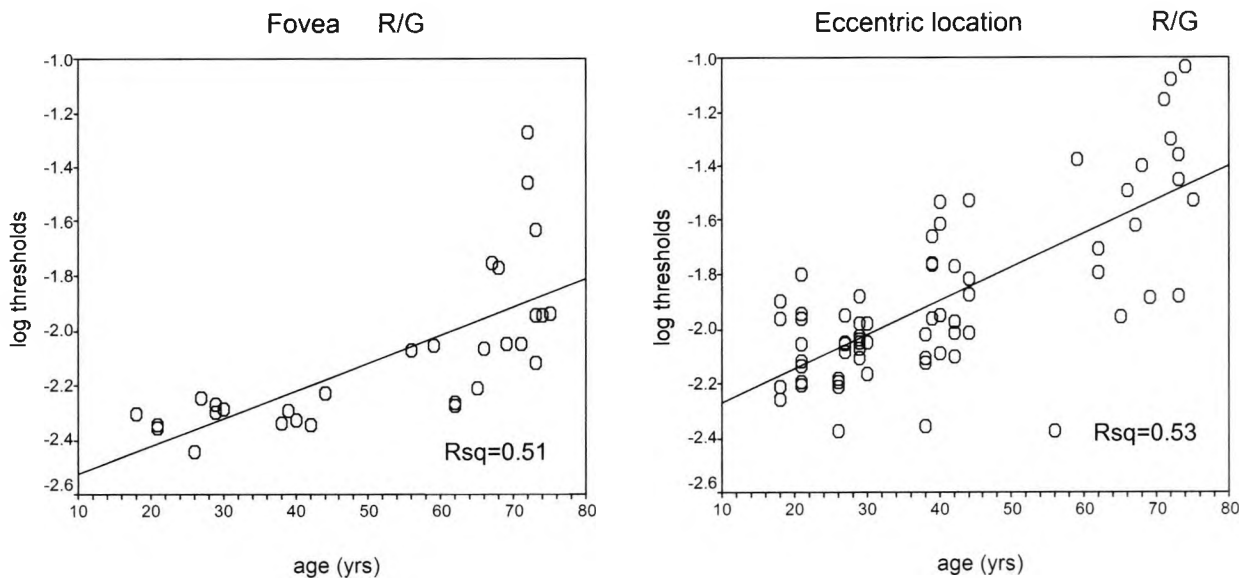


Figure 6.7: Distribution of R/G chromatic log thresholds as a function of age. For details see caption to Figure 6.6.

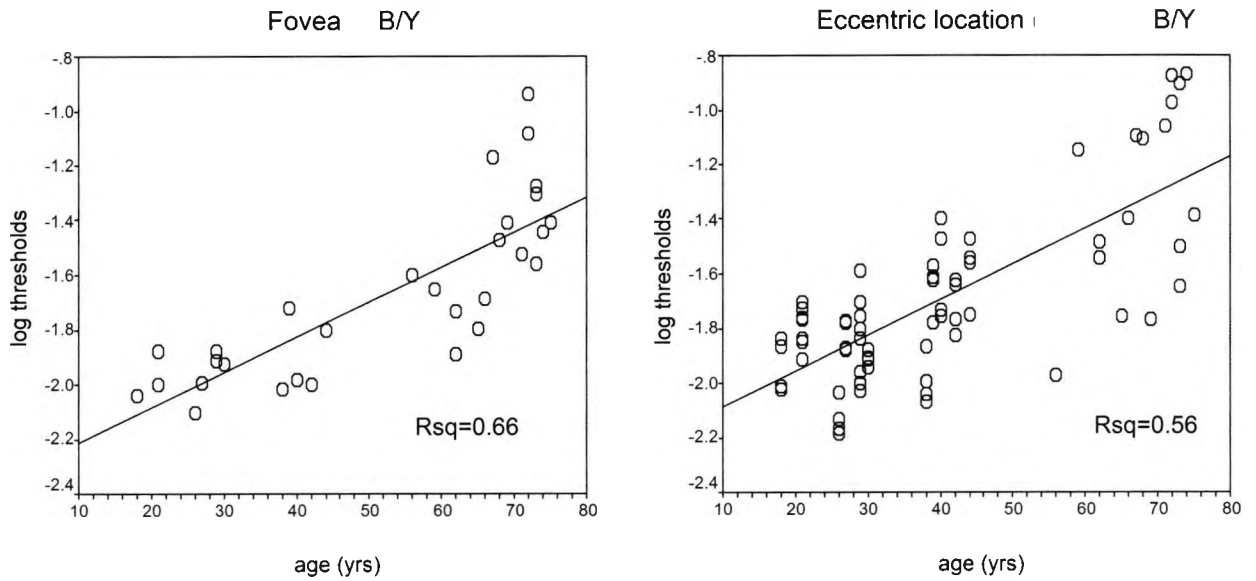


Figure 6.8: Distribution of B/Y chromatic log thresholds as a function of age. For details see caption to Figure 6.6.

Stimulus	Location	Coefficient of determination (R^2)	Mean increase in threshold (log units /decade)
Achromatic	Fovea	0.43	5×10^{-2}
	Eccentric loc (7 deg)	0.31	4×10^{-2}
R/G	Fovea	0.51	10×10^{-2}
	Eccentric loc (7 deg)	0.53	12×10^{-2}
B/Y	Fovea	0.66	13×10^{-2}
	Eccentric loc (7 deg)	0.56	13×10^{-2}

Table 6.4: Coefficients of determination (R^2) and increase in mean log threshold (reduction in sensitivity) for the linear regression model fitted to the data, for each condition tested.

An inspection of the former graphs suggests that data for both chromatic sensitivities could benefit from fitting a non-linear model. For descriptive purposes a quadratic function fitted the chromatic data well. The data for achromatic sensitivity appeared sufficiently well described by the linear model and no statistically significant improvement was found with the quadratic model ($R^2 = 0.44$ and 0.31 for foveal and eccentric data, respectively).

A quadratic model without the linear term was fitted to the chromatic data, which was not significantly different from a full quadratic model. This model will be used due to its simplicity. Equation 1 describes these functions:

$$\text{Equation 1: } \log_{10}(T) = aA^2 + c$$

where T is the threshold chromatic discrimination, A the age in years and a and c are fitted parameters. The values of the slopes and coefficient of determination for the quadratic fit are given in Table 6.5. Figure 6.9 and Figure 6.10 provide the scatter plots and fits for the quadratic model.

Stimulus	Location	$a \cdot 10^4$	c	R^2
R/G	Fovea	1.1	-2.4	0.55
	Eccentric location (7 deg)	1.3	-2.2	0.55
B/Y	Fovea	1.4	-2.1	0.70
	Eccentric location (7 deg)	1.4	-2.0	0.58

Table 6.5: Summary of parameter fits for quadratic function fitted to the chromatic measurements.

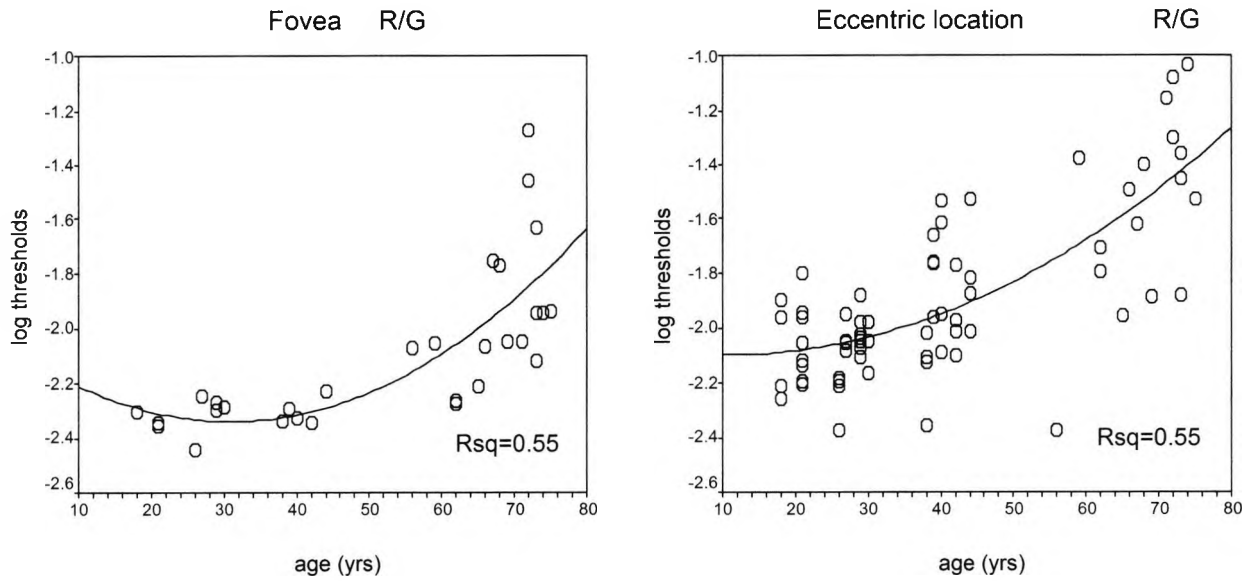


Figure 6.9: Distribution of R/G chromatic motion discrimination log thresholds as a function of age. At the eccentric location each young subject displays 4 measurements, one for each quadrant. The solid line is the best fit for the quadratic model (Equation 1).

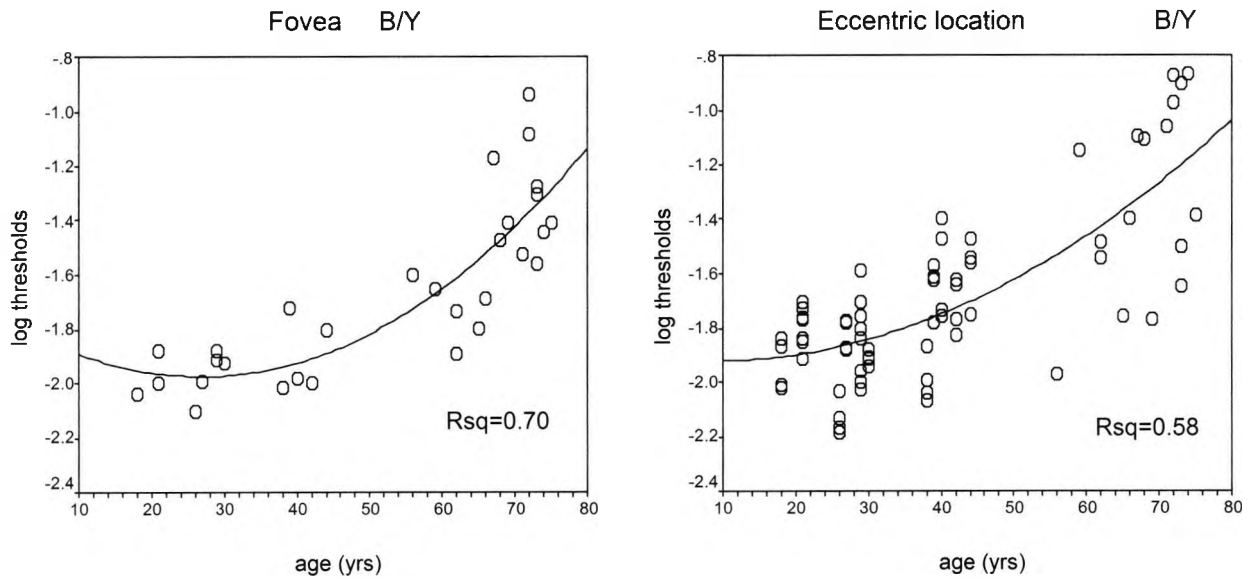


Figure 6.10: Distribution of B/Y chromatic motion discrimination log thresholds as a function of age. For details see caption to Figure 6.9.

The scatter plots show that this sample varies between subjects. However, a decline can be noticed for the older subjects when compared to the younger group. For the achromatic sensitivity the increase in motion discrimination threshold with age is similar for foveal and 7 deg eccentricity measurements, revealing a mild linear reduction of sensitivity of 5 and 4×10^{-2} log threshold units/ decade of age, respectively. However, the coefficient of determination ($R^2=0.43$ and 0.31 , respectively) for this linear fit showed that a considerable amount of the variability within the threshold data remained unaccounted for by age. The chromatic results show a much greater increase in motion discrimination threshold with age.

The chromatic thresholds measured at the fovea show a moderate relationship with age. They increase with increasing age in an accelerated fashion, particularly for individuals over their mid-fifties. The quadratic term (A^2) from Equation 1 explains a significant part of the threshold variability. The chromatic thresholds (R/G and B/Y) measured at the eccentric location also increase proportionally with age.

The rate of increase for log chromatic thresholds is proportional to a factor with each doubling of age. Thresholds measured at the fovea increase with a rate of 1.1 and 1.4 for measurements along R/G and B/Y axes, respectively and thresholds at 7 deg increased with a rate of 1.3 and 1.4 , for R/G and B/Y axes, respectively, for each doubling of age (Table 6.5). This suggests that the B/Y mechanism ages at the same speed for foveal and parafoveal eccentricities, whereas the R/G mechanism ages slightly faster at eccentric locations.

Although, B/Y thresholds increase slightly more rapidly than R/G thresholds as the age (A) increases (in older ages), at both locations tested, the rate of change is not significantly different. However, it is worth mentioning that the coefficients of determination for B/Y thresholds ($R^2=0.70$ and 0.58 for foveal and 7 deg, respectively) are larger than for R/G thresholds ($R^2=0.55$ and 0.55 for foveal and 7 deg, respectively), which indicates that a higher proportion of variation in the B/Y threshold data is accounted for by the fitted curve.

6.4.4 Effect of age on regional sensitivity

The interaction between the type of stimulus and the eccentricity of the location tested was investigated. A one-way ANOVA was used to analyse differential regional sensitivity for each of the stimulus conditions tested. Firstly, this was carried out within the younger group to establish the pattern of regional sensitivity in normal young subjects. Secondly, an analysis within the older group was performed to show how the effect of ageing changes the pattern of regional sensitivity. Finally, the differential effect of ageing on regional sensitivity was also studied by examining the data for differences between young and elderly subjects for the visual mechanisms studied. Post-Hoc tests for multiple comparisons were applied (LSD test was used unless the error variances were unequal across the groups, in which case the Tamhane test was used) in the following analysis.

Table 6.6 summarises the average and SD of the motion discrimination chromatic and achromatic thresholds (log units) for younger and older groups, measured at the fovea and four eccentric locations (i.e. inferior nasal, inferior temporal, superior nasal and superior temporal). Figure 6.11 shows older and younger groups' means and 2 SE for motion discrimination log thresholds of chromatic (R/G and B/Y) and achromatic sensitivities, measured for the fovea and four eccentric locations. These graphs allow the assessment of the relative reduction in regional sensitivity in the older group.

6.4.4.1 Regional sensitivity in younger subjects

Achromatic: the fovea was significantly more sensitive than all the eccentric locations tested ($p < 0.001$). No significant differences were found between the four eccentric locations, i.e. inferior nasal (IN), inferior temporal (IT), superior nasal (SN), and superior temporal (ST).

R/G (Tamhane test): The fovea was significantly more sensitive than all the eccentric locations tested ($p < 0.001$). The inferior temporal location was found to be more sensitive than both the superior locations (ST and SN) ($p < 0.001$), but there was no significant difference between the two inferior (IN, IT) or two superior (SN, ST) quadrants.

B/Y: The fovea was significantly more sensitive than both superior locations (ST, SN) ($p < 0.001$), but not significantly more sensitive than the inferior (IT, IN) locations. A significant difference is shown between ST and both inferior locations (IT and IN) ($p < 0.05$), which are more sensitive, but no significant difference was found between the two inferior (IN, IT) or the two superior (SN, ST) quadrants.

Therefore, regional sensitivity for the young healthy subjects in this sample shows the following pattern:

Achromatic motion discrimination sensitivity is significantly better at the foveal location than at any of the 7 deg eccentric locations, and none of the four eccentric locations (SN, ST, IN, IT) show a significant difference in sensitivity. R/G motion discrimination sensitivity is again significantly better at the foveal location than at any of the 7 deg eccentric locations. However, the inferior temporal (IT) is the most sensitive of the eccentric locations (significantly more sensitive than either of the superior locations). B/Y motion discrimination sensitivity at the fovea is significantly better than both superior locations, but shows no significant difference compared with the inferior locations. Both inferior locations (IT, IN) show significantly better sensitivity than the superior temporal (ST) does. None of the sensitivities tested show any significant difference between nasal and temporal quadrants for a given superior or inferior hemifield.

log thresholds

stimulus	location tested	subject group							
		Older				Younger			
		N	Mean	Std. Deviation	Std. Error Mean	N	Mean	Std. Deviation	Std. Error Mean
Achrom	Fovea	51	-1.299	.158	2.E-02	39	-1.490	.123	2.E-02
	Inferior Nasal	12	-1.185	.123	4.E-02	30	-1.363	.117	2.E-02
	Inferior Temporal	9	-1.136	.185	6.E-02	30	-1.359	.121	2.E-02
	Superior Nasal	12	-1.302	.150	4.E-02	33	-1.330	.157	3.E-02
	Superior Temporal	18	-1.216	.154	4.E-02	39	-1.341	.138	2.E-02
R/G	Fovea	51	-1.933	.283	4.E-02	39	-2.313	9.09E-02	1.E-02
	Inferior Nasal	12	-1.523	.213	6.E-02	39	-2.047	.154	2.E-02
	Inferior Temporal	9	-1.657	.297	1.E-01	39	-2.092	.149	2.E-02
	Superior Nasal	12	-1.627	.508	.15	39	-1.946	.259	4.E-02
	Superior Temporal	18	-1.472	.393	9.E-02	39	-1.935	.242	4.E-02
B/Y	Fovea	51	-1.468	.267	4.E-02	39	-1.943	.132	2.E-02
	Inferior Nasal	12	-1.369	.243	7.E-02	39	-1.876	.190	3.E-02
	Inferior Temporal	9	-1.387	.341	.11	39	-1.866	.161	3.E-02
	Superior Nasal	12	-1.258	.448	.13	39	-1.775	.216	3.E-02
	Superior Temporal	18	-1.303	.401	9.E-02	39	-1.738	.207	3.E-02

Table 6.6: Average and SD for motion discrimination of chromatic (R/G and B/Y) and achromatic log thresholds measured for younger and older subjects at the fovea and all eccentric locations.

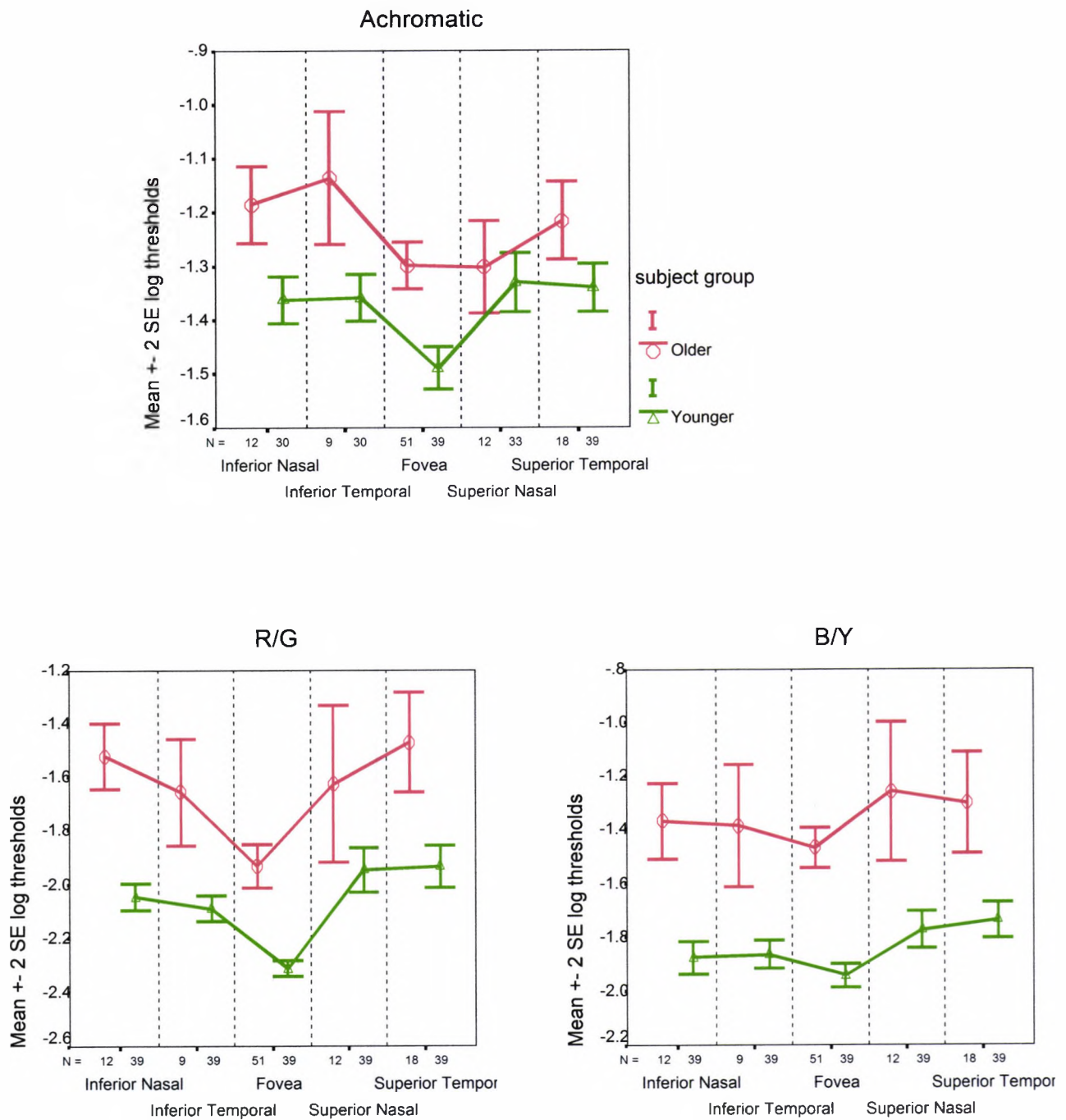


Figure 6.11: Average and ± 2 SE for motion discrimination log thresholds of chromatic (R/G and B/Y) and achromatic sensitivities, measured for the fovea and four eccentric locations, in younger and older subjects.

6.4.4.2 Regional sensitivity in older subjects

Achromatic: The fovea was significantly more sensitive than both inferior (IN, IT) locations ($p < 0.05$), but was no longer significantly more sensitive than both superior locations. A significant difference is found between SN and IT ($p < 0.05$), but no significant difference was found between the two inferior (IN, IT) or the two superior (SN, ST) quadrants.

R/G (Tamhane test): The fovea was significantly more sensitive than the IN and ST locations ($p < 0.001$). No significant difference was found between the thresholds at the eccentric locations.

B/Y (Tamhane test): No significant difference was found between any locations.

The change in the pattern of regional sensitivity due to the effects of ageing is shown in Figure 6.11 and can be summarised as follows:

Achromatic motion discrimination sensitivity for the foveal location was no longer significantly better than both superior locations (SN, ST), but still better than both inferior locations. The superior nasal location now shows better sensitivity than the inferior locations. R/G motion discrimination sensitivity for the foveal location is now only better than for IN and ST locations. B/Y motion discrimination sensitivity at the fovea and inferior locations was no longer more sensitive than superior locations.

Another characteristic of the older subjects' sensitivity is the larger variability of the data, particularly the superior locations, for both chromatic sensitivities (Table 6.6). It is possible that the high intersubject variability of the older group relative to the threshold change is responsible for the absence of statistically significant differences.

6.4.4.3 Differential effect of ageing on regional sensitivity

The ageing effect on location sensitivity differences was also studied by examining the data for differences between young and elderly subjects (independent samples t-test in Table 6.7). A summary of these age-related threshold increments at the fovea and at the different quadrant locations is shown in Figure 6.12. Most locations show a statistically significant difference with age at the $p < 0.001$ level, for the conditions

tested. However, the superior nasal location shows no significant difference for the achromatic ($p=0.6$) nor for the R/G ($p=0.06$) stimuli, which implies that, except for B/Y sensitivity, this location seems to be less affected by the ageing process. The largest ageing effects are shown for both chromatic (R/G and B/Y) sensitivities at the inferior nasal locations and also for B/Y chromatic sensitivity at the fovea and superior nasal

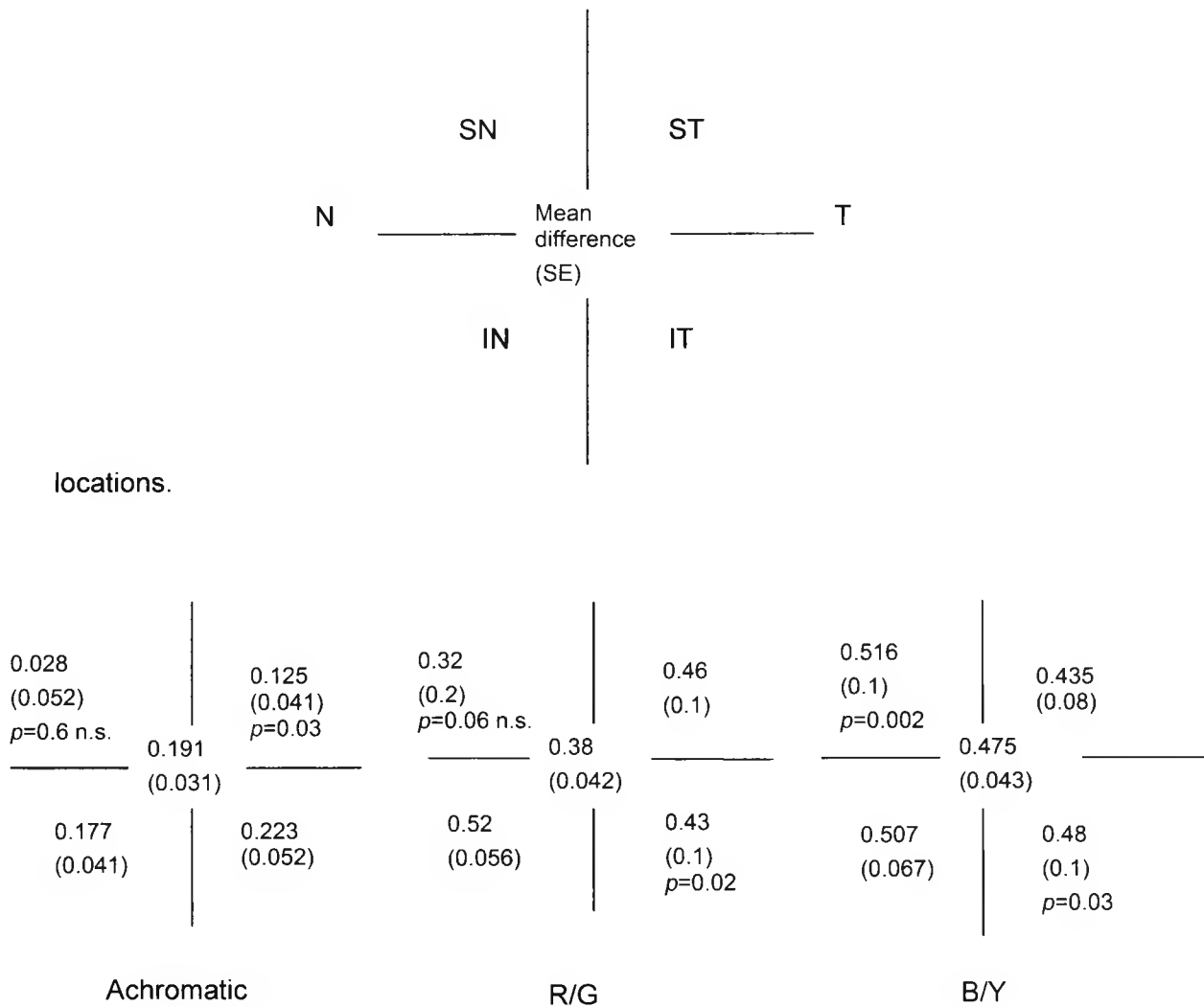


Figure 6.12: Effect of age on regional sensitivity. Mean threshold differences (in log units), between older and younger groups, for the fovea and each of the four eccentric locations tested, for chromatic (R/G and B/Y) and achromatic stimuli. All differences are statistically significant at the $p < 0.001$ level, apart from those marked (n.s.= not significant).

Independent Samples Test

log thresholds

location tested		stimulus																										
		Achrom										R/G								B/Y								
		Levene's Test for Equality of Variances		t-test for Equality of Means								Levene's Test for Equality of Variances		t-test for Equality of Means						Levene's Test for Equality of Variances		t-test for Equality of Means						
		F	Sig.	t	df	Sig. (2-tailed)	Mean Differ	Std. Error Differ	95% Confidence Interval of the Difference		F	Sig.	t	df	Sig. (2-tailed)	Mean Differ	Std. Error Differ	95% Confidence Interval of the Difference		F	Sig.	t	df	Sig. (2-tailed)	Mean Differ	Std. Error Differ	95% Confidence Interval of the Difference	
							Lower	Upper									Lower	Upper								Lower	Upper	
Fovea	Equal variances assumed	1.57	.213	6.24	88	.000	.191	3.1E-02	.130	.252	24.2	.000	8.05	88	.000	.380	4.7E-02	.286	.473	14.7	.000	10.2	88	.000	.475	4.7E-02	.382	.567
	Equal variances not assumed			6.45	88.0	.000	.191	3.0E-02	.132	.250			8.99	62.9	.000	.380	4.2E-02	.295	.464			11.0	76.8	.000	.475	4.3E-02	.389	.560
Inferior Nasal	Equal variances assumed	422	.520	4.36	40	.000	.177	4.1E-02	9.5E-02	.260	1.36	.250	9.38	49	.000	.525	5.6E-02	.413	.637	464	.499	7.58	49	.000	.507	6.7E-02	.373	.642
	Equal variances not assumed			4.26	19.4	.000	.177	4.2E-02	9.0E-02	.264			7.91	14.7	.000	.525	6.6E-02	.383	.667			6.64	15.4	.000	.507	7.6E-02	.345	.670
Inferior Temporal	Equal variances assumed	2.02	.163	4.26	37	.000	.223	5.2E-02	.117	.328	10.8	.002	6.42	46	.000	.435	6.8E-02	.299	.571	12.7	.001	6.36	46	.000	.479	7.5E-02	.328	.631
	Equal variances not assumed			3.39	10.1	.007	.223	6.6E-02	7.6E-02	.369			4.28	8.947	.002	.435	.1	.205	.665			4.11	8.836	.003	.479	.1	.215	.744
Superior Nasal	Equal variances assumed	.003	.958	539	43	.593	.028	5.2E-02	-8.E-02	.133	15.5	.000	2.91	49	.005	.319	.1	9.9E-02	.539	12.0	.001	5.49	49	.000	.516	9.4E-02	.327	.706
	Equal variances not assumed			.551	20.4	.588	.028	5.1E-02	-8.E-02	.134			2.09	12.8	.057	.319	.2	-1.E-02	.649			3.86	12.6	.002	.516	.1	.226	.807
Superior Temporal	Equal variances assumed	.897	.348	3.07	55	.003	.125	4.1E-02	4.3E-02	.206	10.3	.002	5.47	55	.000	.463	8.5E-02	.293	.633	23.1	.000	5.42	55	.000	.435	8.0E-02	.274	.596
	Equal variances not assumed			2.94	30.1	.006	.125	4.2E-02	3.8E-02	.211			4.61	23.1	.000	.463	.1	.255	.671			4.35	21.3	.000	.435	.1	.227	.643

Table 6.7: Independent samples t-test for chromatic (R/G and B/Y) and achromatic mean log threshold differences between older and younger groups, measured at the fovea and four eccentric locations.

The significant differences found in regional sensitivity, for chromatic or achromatic stimuli within the younger group, were always found between the superior and inferior hemifields, with no significant difference found between nasal and temporal quadrants for a given superior or inferior hemifield. Therefore, nasal and temporal values were averaged to provide a measure of superior and inferior hemifield sensitivity. A summary of the mean log threshold differences with age, obtained with an independent sample t-test (Table 6.9), for the fovea and the superior and inferior locations, is provided in Table 6.8. For all stimulus conditions the largest loss of sensitivity was in the inferior hemifield. The B/Y stimulus was systematically the most affected by age for all locations.

Location	Stimulus	Mean log threshold difference (p value)	SE
Fovea	Achrom	0.191 ($p < 0.001$)	0.031
	R/G	0.38 ($p < 0.001$)	0.042
	B/Y	0.475 ($p < 0.001$)	0.043
Superior	Achrom	0.086 ($p = 0.009$)	0.032
	R/G	0.407 ($p < 0.001$)	0.085
	B/Y	0.471 ($p < 0.001$)	0.079
Inferior	Achrom	0.196 ($p < 0.001$)	0.032
	R/G	0.49 ($p < 0.001$)	0.058
	B/Y	0.495 ($p < 0.001$)	0.064

Table 6.8: Effect of age on regional sensitivity. Mean log thresholds differences, between the older and younger groups, for the fovea, and the superior and inferior eccentric locations tested, for chromatic (R/G and B/Y) and achromatic conditions.

Independent Samples Test

log thresholds

stimulus	location tested		Levene's Test for Equality of Variances		t-test for Equality of Means						
			F	Sig.	t	df	Sig. (2-tailed)	Mean Differ	Std. Error Differ	95% Confidence Interval of the Difference	
										Lower	Upper
Achrom	Fovea	Equal variances assumed	1.57	213	6.24	88	.000	.191	.031	.130	.252
		Equal variances not assumed			6.45	87.96	.000	.191	.030	.132	.250
	Inferior	Equal variances assumed	.156	694	6.09	79	.000	.196	.032	.132	.261
		Equal variances not assumed			5.41	29.07	.000	.196	.036	.122	.271
	Superior	Equal variances assumed	1.11	294	2.65	100	.009	.086	.032	.021	.150
		Equal variances not assumed			2.58	51.34	.013	.086	.033	.019	.152
R/G	Fovea	Equal variances assumed	24.2	.000	8.05	88	.000	.380	.047	.286	.473
		Equal variances not assumed			8.99	62.88	.000	.380	.042	.295	.464
	Inferior	Equal variances assumed	15.1	.000	11.2	97	.000	.490	.044	.403	.577
		Equal variances not assumed			8.41	23.98	.000	.490	.058	.369	.610
	Superior	Equal variances assumed	22.0	.000	6.04	106	.000	.407	.067	.273	.540
		Equal variances not assumed			4.77	36.35	.000	.407	.085	.234	.580
B/Y	Fovea	Equal variances assumed	14.7	.000	10.2	88	.000	.475	.047	.382	.567
		Equal variances not assumed			11.0	76.84	.000	.475	.043	.389	.560
	Inferior	Equal variances assumed	7.82	.006	10.0	97	.000	.495	.049	.396	.593
		Equal variances not assumed			7.67	24.31	.000	.495	.064	.362	.628
	Superior	Equal variances assumed	38.1	.000	7.80	106	.000	.471	.060	.352	.591
		Equal variances not assumed			5.96	34.97	.000	.471	.079	.311	.632

Table 6.9: Independent samples t-test for mean log threshold differences with age, for achromatic, B/Y and R/G sensitivities measured at the fovea and the superior and inferior locations.

6.5 Summary of results

1. In general the older group exhibits poorer sensitivity and greater intersubject variability.
2. Both chromatic (B/Y and R/G) and achromatic thresholds were higher in the older group. The differences were statistically significant for foveal as well as for 7 deg measurements. For achromatic mean thresholds the increase was approximately 1.5 and 1.3 times, for fovea and 7 deg eccentricity, respectively. For chromatic mean thresholds along the R/G colour confusion axis the increase was approximately 2.4 and 2.8 times and for thresholds along the B/Y colour confusion axis the increase was approximately 3 and 3.1 times, for fovea and 7 deg eccentricity, respectively.
3. The greater relative loss was found to be for the chromatic sensitivity. On average, R/G thresholds were 1.6 and 2.2 times greater and B/Y thresholds were 2 and 2.4 times greater than corresponding achromatic thresholds, for foveal and eccentric locations, respectively.
4. The relative loss of chromatic sensitivity in the older group is mostly non-selective for both foveal and 7 deg eccentricity locations. However, a tendency for larger relative B/Y loss exists in some individual older subjects, particularly at the fovea. The 7 deg eccentricity measurements show a typically large variability in the data.
5. Achromatic thresholds increase in a mild linear fashion with age, for both foveal and eccentric (7 deg) measurements (5 and 4 log units/ decade, respectively).
6. Chromatic thresholds (R/G and B/Y) show a greater increase with age. They are better described by a quadratic function, which indicates an accelerated threshold increase with increasing age. For foveal measurements this increase is proportional to a factor of 1.1 to 1.4 (R/G and B/Y respectively), with each doubling of age. For eccentric measurements this increase is proportional to a factor of 1.3 and 1.4 (R/G and B/Y respectively), with each doubling of age.

7. Although, B/Y thresholds increase marginally more rapidly with age than R/G thresholds, at both locations tested, the rate of change is not significantly different.
8. The largest effect of ageing was found in the inferior hemifield, particularly the inferior nasal quadrant, for both chromatic (R/G and B/Y) sensitivities. Sensitivity along the B/Y colour confusion axis was the most affected.

6.6 Discussion

The human visual system undergoes a number of physiological changes due to the ageing process. Dysfunction or loss of neural elements in the primary visual pathways (Jonas *et al.*, 1990), reduced vascular supply to the retina and higher visual areas (Weale, 1986), and deterioration of the optical quality of the ocular media (Guirao *et al.*, 1999) have all been described. As a consequence, several visual functions are significantly affected by age-related changes.

Reduction in chromatic sensitivity with ageing has been reported in a number of previous studies. Studies using the Farnsworth-Munsell 100 Hue Test have shown how the Total Error Score worsens with age (Kinnear & Sahraie, 2002; Verriest, 1963) and have suggested a tendency for increased diffuse loss accompanied by moderate tritan-like (B/Y) defects (Pinckers, 1980; Knoblauch *et al.*, 1987).

Current evidence from human and monkey experiments supports the view that sensitivity to colour contrast is sub-served by the P-pathway, while luminance contrast motion sensitivity is transferred via the Magno-cellular channel (Merigan *et al.*, 1991; Merigan & Maunsell, 1993). In the last decade, some studies on visual ageing have tried to discern whether there is a selective deterioration of one of the main neural pathways (luminance or colour opponent mechanisms) in older age groups. The stimuli chosen in our experiment were selected to enhance the selective contribution of different neuronal populations to the loss of contrast sensitivity with age. Our aim was to establish whether the luminance or the chromatic channels are more affected by the ageing process and whether chromatic discrimination mediated by the B/Y colour mechanism is more affected than the R/G mechanism.

In the present study we observed a significant increase in thresholds in the older group relative to the younger group both for luminance and colour defined signals. However, the relative loss of sensitivity due to the ageing effect was larger for the chromatic stimuli. Chromatic thresholds modulated along the R/G and the B/Y axes, measured at the fovea, increased 2.4 and 3 times, respectively. This represents a marked increase compared with that observed in the luminance channel (1.5 times). For measurements taken at 7 deg eccentricity, the increase for R/G and B/Y chromatic thresholds in the older group was more than double (2.8 and 3.1 times, respectively) whilst the luminance contrast thresholds increased 1.3 times.

Other studies on age-related sensitivity loss for opponent mechanisms have demonstrated greater vulnerability of the S- wavelength-sensitive pathway (Haegerstrom-Portnoy, 1988; Johnson & Marshall, 1995). However, a larger relative increase for chromatic thresholds compared to achromatic is not a universal finding. Steen *et al.* (1994) measured luminance and colour contrast sensitivity with isoluminant colour gratings modulated either along the R/G or B/Y axis for young and elderly subjects. These measurements were taken with and without glare in order to determine the effect of disability glare. Without glare the only significant ageing effect was found for the B/Y gratings, but not for R/G or LC modulated gratings. Both groups were most affected by glare on the R/G gratings. In contrast, other studies have found an unspecific decline of the response to luminance and colour contrast. For instance, Fiorentini *et al.* (1996) measured the detection and discrimination of motion direction for luminance and colour contrast gratings in a group of young and old subjects (modulated along the R/G axis). They observed a significant age-related increase in both luminance contrast (0.2 log units) and R/G colour contrast (0.27 log units). Although they found a larger age-related loss for R/G gratings, the difference compared with the luminance contrast loss was not considered statistically significant. Likewise, Kelly *et al.* (1996) found a non-selective decrease in both colour and luminance sensitivity with age when measuring foveal thresholds.

In contrast to our results, neither of these studies showed significant differences between the age-related change for luminance and for R/G colour contrast thresholds, regardless of whether the increase in thresholds was significant with age or not. Among other reasons this could be due to the nature of the stimuli used. In both of the aforementioned studies the stimuli consisted of horizontal sinusoidal gratings of spatial

frequency 1 cpd and of a larger size than the stimulus used in the foveal conditions of the present study.

6.6.1 Rate of chromatic and achromatic sensitivity loss with ageing

A cross-sectional examination of the younger and older group's data revealed a mild, linear increase in the motion discrimination achromatic thresholds with age, which were similar for the foveal and the eccentric (7 deg) measurements (5 and 4×10^{-2} log threshold units/ decade of age, respectively). In contrast, the chromatic thresholds showed a much greater increase.

For chromatic thresholds these increases were well described by quadratic models showing a small age-related threshold increment during the first 5 - 6 decades of life and were followed by a rapid increase in later life. Based on the equations of the fitted quadratic regressions (Equation 1), the rate of ageing in our sample, for foveal measurements, indicates that they increased by a factor of 1.1 and 1.4 with each doubling of age, along R/G and B/Y axes, respectively. For eccentric measurements, the rate of ageing increased by a factor of 1.3 and 1.4 with each doubling of age (R/G and B/Y, respectively). This means that the rate of ageing for B/Y chromatic sensitivity is equally fast for foveal and 7 deg eccentricity locations, whereas the R/G sensitivity ages faster for the eccentric location and to a similar rate compared to the eccentric B/Y sensitivity.

Although thresholds for the B/Y colour opponent system were found to increase marginally more rapidly than the R/G thresholds with ageing, there were no significant differences between the rate of ageing for R/G and B/Y mechanisms.

Our chromatic foveal results are close in agreement with those of Knoblauch *et al.* (2001). They used a modification of Barbur's technique (Barbur *et al.*, 1993; Barbur *et al.*, 1994) to study the variation of chromatic sensitivity during life. The chromatic detection thresholds tested (along tritan, deutan and protan directions) were found to vary similarly, through life. Although thresholds along the tritan direction (B/Y axis) "aged" slightly less rapidly than those along the R/G axis, the rate of increase of the mean tritan thresholds did not differ significantly from the rate of increase for the mean R/G thresholds. The curves describing the chromatic threshold change, as a function of age, showed two phases of variation of chromatic sensitivity. During development,

thresholds decreased with each doubling of age by nearly a factor of 2, until adolescence. Thereafter, in the ageing phase, thresholds increased by a factor of 1.4 - 2 with each doubling of age. Although the study by Knoblauch *et al.* (2001) had particular emphasis on the recruitment of very young subjects and young and middle aged adults and did not recruit as many old-age subjects as the present study, there is still a substantial agreement on the rate of age-related change and the relative loss of R/G versus B/Y chromatic sensitivity, which highlights the relevance of similar methodological approaches when comparing results.

A non-linear increase with age has been reported in other visual functions, such as visual field (Spry & Johnson, 2001), and contrast sensitivity (Owsley *et al.*, 1983). In addition, spectrally selective nonlinear changes in the crystalline lens transmission, absorption, autofluorescence (Pokorny J *et al.*, 1987), and the light scattering characteristics of the eye (Hennelly *et al.*, 1998) have also been described.

Zlatkova *et al.* (2003) measured peripheral (13 deg) resolution using achromatic and blue-cone isolating gratings, in order to determine how performance changed with age. They found that resolution was higher for achromatic compared to B/Y gratings and performance was flat for both until the fifth decade. After this, performance declined for both at a rate of approximately 14%/decade with no significant difference between the two rates of decline. The differences observed in the relative rate of B/Y versus achromatic sensitivity loss compared to our results could be attributed to differences in the experimental technique, in particular, the use of an achromatic stimulus which isolates the first order motion mechanism (Barbur, 2004).

Sample and Weinreb (1992) found the normal age-related increases in mean log threshold for the overall B-on-Y visual field to be 0.10 log units per decade, in a group of 88 normal subjects ranging in age from 19 to 78 yrs. This is not far from our findings, which reveal an increase of 0.13 log units/decade in mean log threshold when fitting the linear regression model to the B/Y data, measured at foveal and eccentric locations.

6.6.2 Regional sensitivity

In younger subjects, the foveal location was significantly more sensitive for achromatic and R/G stimuli than the eccentric (7 deg) locations. For B/Y stimuli, the fovea and the

inferior hemifield showed no significant difference and were significantly more sensitive than the superior hemifield. In fact, the inferior hemifield was found to be significantly more sensitive than the superior hemifield for both (R/G and B/Y) chromatic motion sensitivities. Therefore, the analysis by quadrant suggests that there is a difference in chromatic sensitivity across the horizontal midline, in the younger group. This is in agreement with earlier previous findings on functional specialisation and cell distribution (Previc, 1990), as well as the suggestion of Bilodeau and Faubert (1997) that the lower visual field specialises for colour motion information.

The higher motion discrimination sensitivity in the inferior hemifield compared to the superior has been related to the anatomical characteristics of the optic nerve and retina (Jonas J.B. & Nauman G.O.H., 1993):

- (1) the diameter of the retinal artery and vein are wider in the inferior temporal arcade.
- (2) visibility of the retinal nerve fibre bundles is often better detectable in the inferior temporal region than in the superior.
- (3) location of the foveola is 0.53 mm inferior to the optic disc centre, which makes the neuroretinal rim above the horizontal raphe significantly larger than it is below.

This difference across the horizontal midline tends to fade away in the older group. As a consequence of the reduction of the asymmetry with age, the largest age-related local increases in chromatic thresholds occur for R/G and B/Y sensitivities in the inferior quadrants. However, the age-related increases given at each of the four quadrant locations tested showed no significant differences, for any of the chromatic mechanisms. In fact, one of the characteristics of the older group is the higher variability of the data, which tends to wash away differences in sensitivity between different locations. Overall, the B/Y mechanism showed the largest threshold differences for all locations.

This suggests that in older normal subjects, sensitivity to moving chromatic and achromatic stimuli is poorer than in younger subjects, with the largest difference in the lower visual hemifield.

In conclusion, the present findings show a greater effect of ageing on the visual responses to colour defined stimuli, which deteriorates from the sixth decade onwards

in an accelerated, but similar fashion for both the R/G and B/Y mechanisms. The stimulus and experimental conditions were expected to favour differentially the contribution of the luminance or chromatic channels. Therefore, the differential effect of ageing in the various stimulus conditions tested suggests that the sensitivity of the chromatic pathway is more affected by the ageing process.

Since pupil size was not standardised, it is possible that senile miosis may have lowered retinal illumination in some subjects and contributed to a larger B/Y defect. Some studies have described that B/Y defects can be induced by a reduction in mean luminance (Knoblauch *et al.*, 1987; Werner *et al.*, 1990) due to changes in the ocular media. However, attempts to simulate the optics of the elderly eye in young subjects, in terms of reduction of pupil size, increased absorption of the media and increased light scatter, have suggested that in many instances they produce no significant change in sensitivity in the younger subjects (Whitaker & Elliott, 1992; Elliott *et al.*, 1990). Therefore, decreased neural function in the afferent visual pathway should be considered as an important contributor to loss of sensitivity with ageing.

The size and motion characteristics of the retinal image of our stimuli were designed to be little affected by the optical degradation produced by the elderly eye. Although these factors cannot be ruled out completely, it is unlikely that they have contributed to the differential age-related sensitivity loss between hemifields.

The present study provides information on the expected variation in normal threshold values through life for chromatic and achromatic sensitivity measured at foveal and parafoveal locations. From the results of this chapter it is apparent that the neural pathways mediating the detection of luminance and colour-defined signals, at different eccentricities, may be affected differently by the ageing process. In order to establish the limits of normal visual performance the effects of ageing have to be taken into account. Indeed, this age variation may be different for the luminance and chromatic mechanisms. Such data are needed in order to establish whether small changes in such thresholds represent significant changes in early stages of disease or the normal fluctuations expected for that age group.

7 Summary of results and conclusions

The incentive of much of the research reported in this thesis has been the urge to resolve the frequently pursued questions:

- “Is the chromatic relative loss greater for the B/Y or the R/G colour opponent channels as a result of glaucomatous damage?”
- “Does this relative loss change along the different stages of severity of the disease or with retinal eccentricity?”
- “Is the sensitivity loss for colour greater than the sensitivity loss for luminance contrast mechanisms?”

In addition, we also aimed to establish the relative loss of chromatic and achromatic sensitivity loss as a result of the ageing process.

The identification of parallel channels serving the processing of visual information has resulted in the tendency to study visual functioning separately with respect to these channels. This is usually achieved by selective pre-adaptation of the other channels, or using stimuli that are silent for the other channels. In the present study we used a strategy that allowed for comparable and simultaneous testing of chromatic and achromatic mechanisms in the same group of subjects.

The assessment of selective loss of visual sensitivity can improve earlier recognition of damage. Even if certain classes of ganglion cells are not relatively more susceptible to damage than others, it may still be worthwhile to assess the functioning of some channel selectively. As pointed out in section 5.6, a homogeneous loss of cells need not imply that the sensitivity of all channels decreases equally. A different spatial summation in cortical neurones may cause a different relative amount of sensitivity loss.

Motion discrimination targets designed to isolate the luminance and the R/G and B/Y colour opponent mechanisms were used to find evidence of preferential damage to one of the visual functional channels. Findings in patients with POAG, subjects at risk of developing POAG and normal subjects of similar and younger age were compared. The extent of sensitivity loss with ageing and glaucomatous damage (chapter 6 and 5) for both colour and luminance contrast processing was determined. The characterisation of chromatic sensitivity loss in POAG subjects by determining the pattern of total sensitivity loss at different stages of the disease and at different retinal eccentricities was also investigated.

A summary of the results is given here, together with an attempt to integrate the findings from the various chapters.

7.1 Summary of results

In chapter 4 a thorough investigation of the chromatic sensitivity loss associated with glaucomatous damage was addressed. Colour contrast discrimination thresholds were measured for twelve directions in colour space, which allowed the fitting of full ellipses to each set of data (a group of POAG subjects, a group At risk of developing POAG and a control group). This provided a characterisation of the total loss in chromatic sensitivity in glaucoma subjects.

When examined as a group, POAG subjects showed a significant non-selective reduction of chromatic sensitivity at both eccentricities measured. The group At risk also showed large mean differences when compared with the control group, but only for the eccentric location. However, these differences did not reach statistical significance. Half of the subjects at risk showed large values for the area of the CD ellipse and for the B/Y and R/G thresholds at the eccentric location, which suggests large interindividual variations in the At risk group. This was interpreted to be an early sign of functional loss in those subjects.

The analysis of chromatic sensitivity loss in relation to the severity of the visual field loss revealed that the earliest signs of damage were found at the paracentral location (7 deg), causing a non-selective CD loss associated with a characteristic increase in variance. As glaucomatous damage advances the foveal location is also progressively

affected with a greater B/Y relative loss, which is neutralised by the R/G loss when the disease is established. For moderate and advanced stages of the disease, the relative loss becomes greater for the R/G thresholds at both foveal and 7 deg.

A number of recurrent patterns of chromatic discrimination loss were identified and although a significant correlation between them and the severity of visual field loss was found, some individual discrepancies occurred. The test showed an overall success rate of 71% in identifying cases correctly when using the B/Y and R/G thresholds variables.

Given the controversy on preferential damage to large ganglion cells in glaucoma, in chapter 5 the more general question was addressed, whether a preferential sensitivity loss of chromatic versus achromatic processing mechanisms can be identified due to glaucomatous damage and what is the extent of any preferential sensitivity loss. Consequently, motion direction discrimination targets designed to isolate the colour opponent and the luminance mechanisms were used to find evidence of preferential damage to one or the other of the visual functional mechanisms.

Although both mechanisms were significantly affected by glaucomatous damage, the chromatic thresholds had a greater relative increase. On average, chromatic thresholds suffered more than 1.5 times the increase observed by the achromatic mechanism. A slightly greater B/Y relative loss of chromatic sensitivity due to glaucomatous damage was found at the foveal location, but similar differences between the groups and increased variability, for R/G and B/Y thresholds, were found at 7 deg eccentricity.

The R/G and B/Y chromatic thresholds showed differences in the pattern of increase as a function of the severity of visual field loss. At both locations, measurements for the R/G mechanism showed a faster rate of increase and a better correlation with severity of field loss than the B/Y thresholds. In the case of the foveal location this was an accelerated increase that affected moderate and advanced cases mostly. Therefore, although in early glaucoma subjects the greatest loss was usually for the B/Y sensitivity, this difference tended to be reduced and surpassed in moderate and advanced cases.

The increase in achromatic thresholds with severity of visual field loss, on the other hand, revealed a non-significant low positive correlation. This small threshold elevation

found versus the larger chromatic losses can be explained by different spatial summation properties of the chromatic and achromatic cortical neurones.

In conclusion, we found evidence for larger chromatic deficits in POAG, which contradicts the hypothesis that in glaucoma there is preferential damage to the magnocellular pathway. However, motion discrimination thresholds were significantly increased for both chromatic and luminance contrast conditions, which reflects a certain degree of damage to all detection mechanisms. The differential sensitivity found, in this study, between chromatic and achromatic mechanisms can be explained by spatial summation properties of cortical neurones and probability summation among the neural detectors

Having found a preferential sensitivity loss of chromatic mechanisms above luminance mechanisms under motion direction discrimination conditions, for POAG subjects, in chapter 6 the same questions were addressed to find out the differential effect of ageing on colour and luminance visual mechanisms. Contrast thresholds for direction discrimination of motion were measured in a group of younger and older normal subjects. The relative loss of chromatic and achromatic sensitivity was established by comparing both groups.

Although the ageing process affected significantly both mechanisms, the greatest effect was found for the visual responses to colour defined patterns. Chromatic threshold increases were on average nearly twice the increase suffered by the achromatic mechanism for foveal thresholds and more than twice for thresholds at 7 deg eccentricity.

As a function of age, there was a fundamental difference between the rate of increase in chromatic and achromatic thresholds. Whereas the achromatic thresholds increased at a slow linear pace throughout life (4 and 5 log units/ decade, for foveal and 7 deg eccentricity), the chromatic thresholds (along R/G and B/Y mechanisms) increased in an accelerated fashion from the 5th-6th decade onwards. Foveal thresholds increased by a factor of 1.1 and 1.4 and eccentric thresholds by a factor of 1.3 and 1.4 with each doubling of age, for R/G and B/Y, respectively.

In spite of the slightly faster increase along the B/Y colour opponent system (particularly for foveal thresholds), there were no significant differences between the

rate of ageing for R/G and B/Y mechanisms. Therefore, the relative age-related loss of R/G and B/Y sensitivity is mostly non-selective at both locations tested.

The effects of ageing and retinal eccentricity were also examined. First, the regional sensitivity of a young normal group was established and it was determined that the inferior hemifield is more sensitive than the superior for chromatic motion sensitivity. However, this specialisation of the lower hemifield disappears with the ageing process, since the largest age-related loss of chromatic sensitivity occurs in the lower hemifield. Overall, the B/Y mechanism showed the largest threshold differences for all locations.

7.2 Overview and conclusions

When examined together, the results obtained in Chapters 4 to 6 lead to a number of general conclusions. The following conclusions may be the most important:

1. Glaucomatous damage leads to greater chromatic functional defects.
2. The relative B/Y versus R/G chromatic loss in POAG depends on the severity of glaucomatous damage.
3. Chromatic discrimination loss due to glaucomatous damage is not homogeneous (it is not affected equally for comparable levels of visual field loss).
4. The first signs of chromatic discrimination loss in the patients at risk of suffering POAG appear in the paracentral locations (7 deg) and are characterised by a non-selective loss of chromatic sensitivity and an increased intra- and inter-subject variability.
5. The ageing process has a greater relative effect on the chromatic mechanisms compared to the luminance mechanism.
6. There were no significant differences between the rate of ageing for R/G and B/Y mechanisms.

Conclusion 1 highlights the greater relative functional loss of chromatic sensitivity found in POAG subjects. This loss is also accompanied by a significant smaller relative loss of achromatic sensitivity, which demonstrates a certain degree of damage to all mechanisms. The occurrence of sensitivity loss in several channels suggests non-selective loss in various classes of cells. However, relative loss of the various channels at the anatomical level need not be the same as the relative loss of corresponding psychophysical sensitivity, as pointed out in section 5.6. The differential sensitivity found between chromatic and achromatic mechanisms, as well as the relative B/Y versus R/G chromatic loss (conclusion 2) in POAG, can be explained by the differential spatial summation properties of the B/Y, R/G and achromatic mechanisms and by different redundancy among these mechanisms.

The relative greater loss of B/Y sensitivity at earlier stages of POAG versus greater loss of R/G chromatic sensitivity at more advanced stages of the disease (conclusion 2) has implications for the selection of testing conditions to optimise the clinical management of early versus advanced glaucoma subjects. This conclusion together with conclusions 3 and 4 may also help explain the current controversy in the literature regarding the relative loss of chromatic sensitivity (R/G versus B/Y) in glaucoma. Different degrees of damage in the subjects studied, the fact that not all eyes are affected equally by glaucomatous damage, increased characteristic variability found in early stages of the disease at the eccentric location together with different methodological approaches may all have an impact on the relative loss of R/G versus B/Y chromatic sensitivity.

The ageing process has also shown a greater effect on the visual responses to colour defined stimuli (conclusion 5). Both, the R/G and B/Y chromatic thresholds increased in an accelerated fashion from the 5th-6th decade, unlike the achromatic thresholds, which increased in a mild linear fashion. Although the B/Y thresholds increased marginally more rapidly (and correlated better) with age than the R/G thresholds, the rate of change was not significantly different (conclusion 6). It is interesting to note that the ageing process correlates better with loss of B/Y sensitivity, particularly at the fovea, whereas glaucomatous damage assessed by the visual field loss correlates better with the loss of R/G sensitivity. The largest effect of ageing was found in the inferior hemifield, which incidentally was the most sensitive location for chromatic motion sensitivity in the younger group.

In conclusion, the results from this thesis suggest glaucoma damage and ageing to have a relatively larger effect on the chromatic sensitivity accompanied by a significant loss of sensitivity on the achromatic mechanism.

7.3 Perspective

The CAD test is an example of how one can make use of calibrated visual displays and visual psychophysical methods to enhance assessment of early functional visual damage and monitor the progression of vision-related diseases. The stimulus and experimental conditions used in this study were designed to isolate the contribution of the luminance and chromatic (R/G and B/Y) mechanisms.

Although the finding of greater relative functional loss in the chromatic mechanisms for the ageing process and even greater for the glaucomatous damage is encouraging and suggests that earlier detection of functional loss can be achieved by testing the R/G and B/Y colour mechanisms, the large inter-subject variability and the lack of a clear selectivity for one of the chromatic mechanisms (B/Y and R/G) limit the usefulness of such measurements.

The finding that the relative functional loss in chromatic sensitivity depends on the severity of damage offers a number of possibilities. Selection of testing conditions should be modified according to the severity of damage to optimise the clinical management of early versus advanced glaucoma subjects.

8 Appendices

8.1 Appendix of supporting publications.

8.1.1 Peer-reviewed published papers.

Pacheco-Cutillas, M., Edgar, D. F., & Sahraie, A. (1999). Acquired colour vision defects in glaucoma -their detection and clinical significance. *Br J Ophthalmol* **83**, 1396-1402.

8.1.2 Conference abstracts

Pacheco-Cutillas, M., Sahraie, A., Edgar, D. F., Barbur, J. L., & Bentley, C. R. (1998). Assessment of chromatic discrimination loss in glaucoma. *Ophthalmic Physiol.Opt.* **18**, 381.

Pacheco-Cutillas, M., Barbur, J. L., & Edgar, D. F. Chromatic discrimination performance in POAG. American Academy of Optometry. Sydney, Australia (1998).

Pacheco-Cutillas, M. Patterns of chromatic discrimination loss in POAG compared to a control group. American Academy of Optometry. Madrid, Spain (2000).

Pacheco-Cutillas, M., Barbur, J. L., & Edgar, D. F. (2001). Comparison of chromatic and achromatic loss of sensitivity in ageing and glaucoma. European Association for Vision and Eye Research (EVER). Alicante, Spain. *Ophthalmic Res* **33**, 11-204.

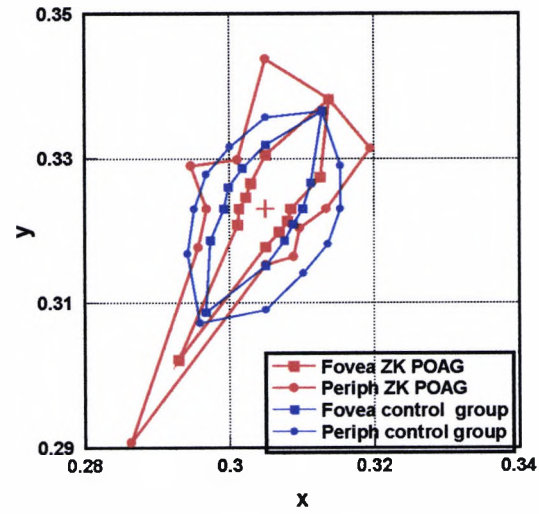
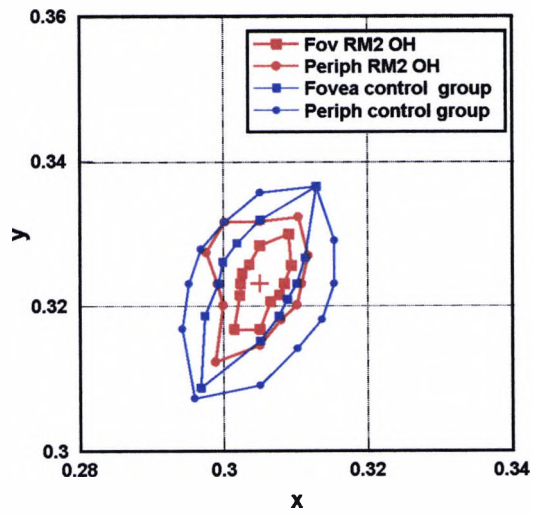
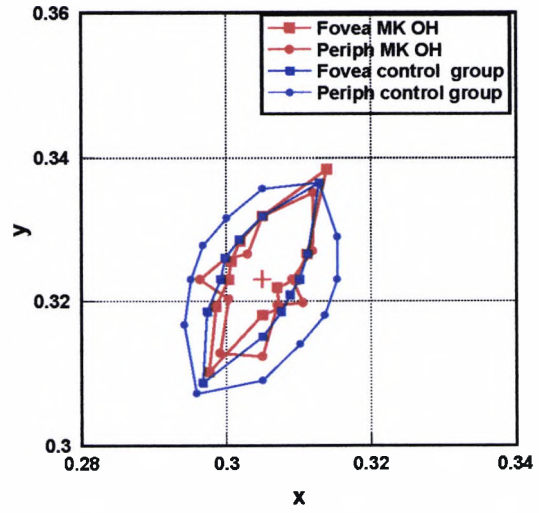
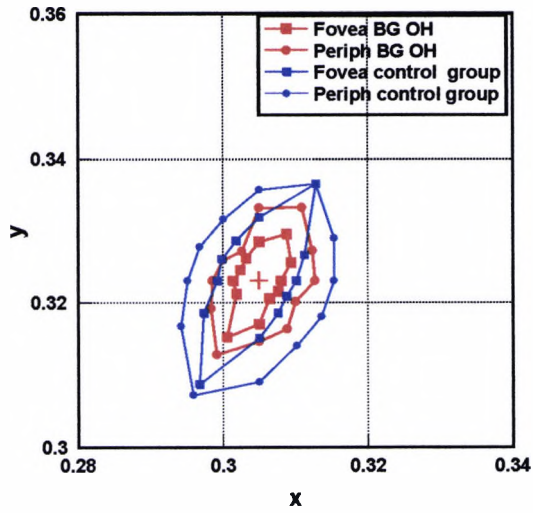
Pacheco-Cutillas, M., Barbur, J. L., & Edgar, D. F. (2002). Characterisation of chromatic and luminance contrast sensitivity loss in glaucoma. European Association for Vision and Eye Research (EVER). Alicante, Spain. *Ophthalmic Res* **34**, 10-210.

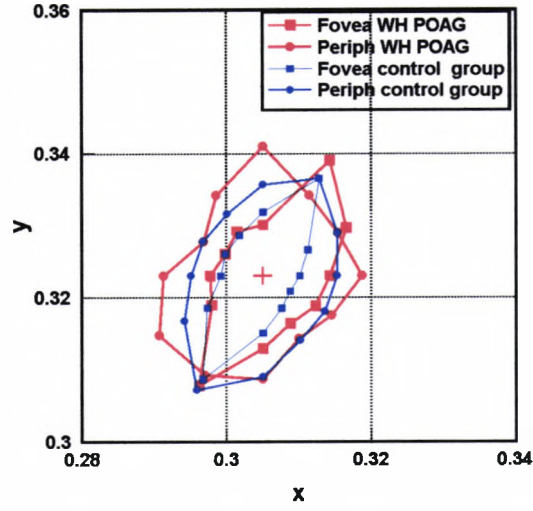
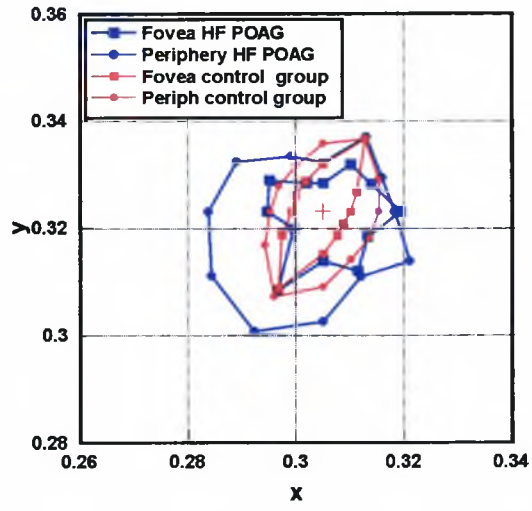
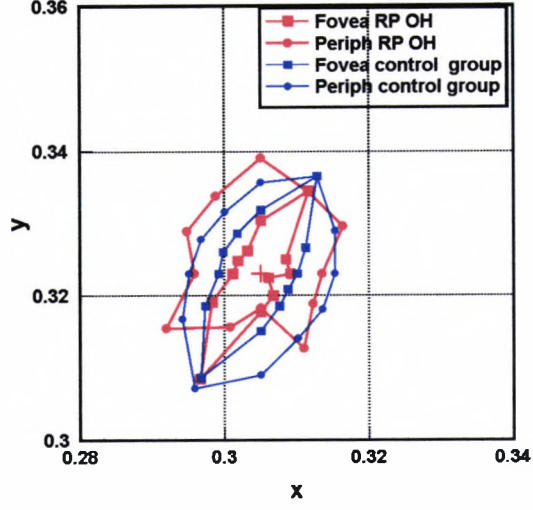
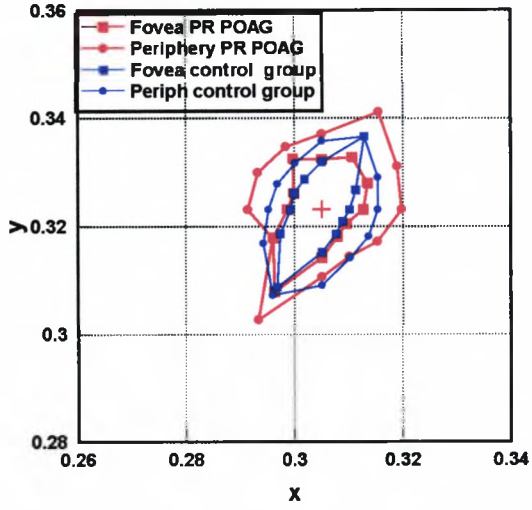
Pacheco-Cutillas, M., Edgar, D. F., & Barbur, J. L. (2002). Chromatic and achromatic loss of sensitivity in glaucoma. *Ophthalmic Physiol.Opt.* **22**, 54.

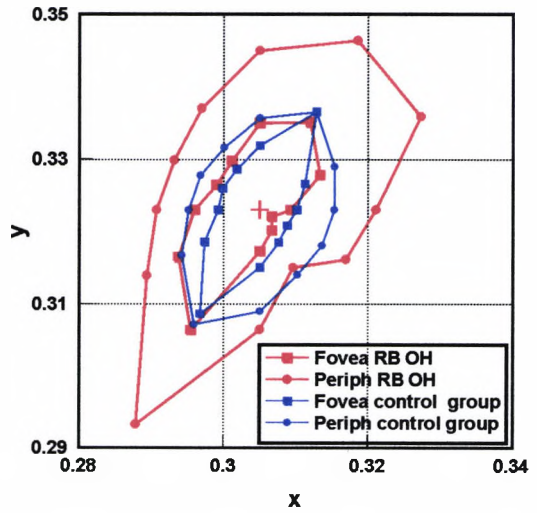
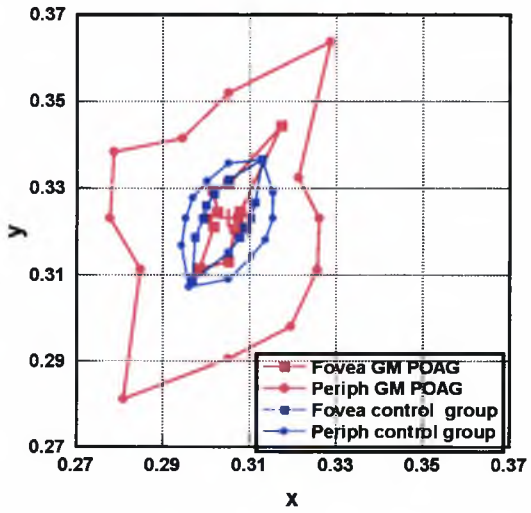
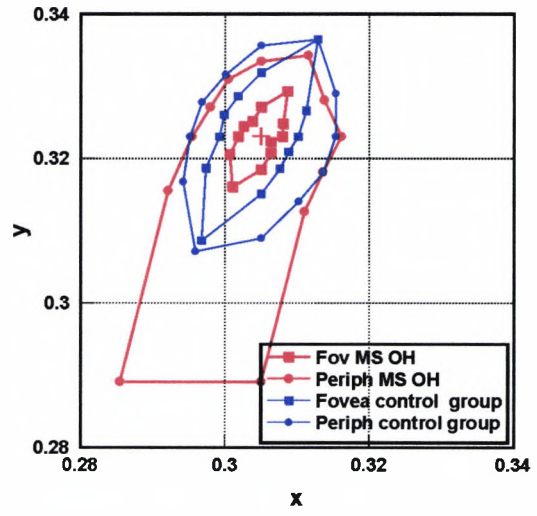
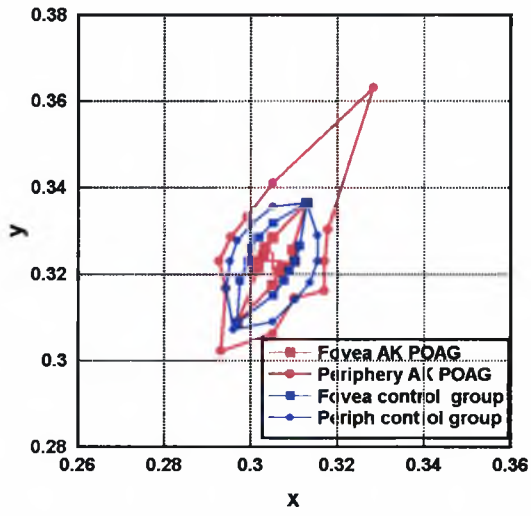
8.1.3 Other publications.

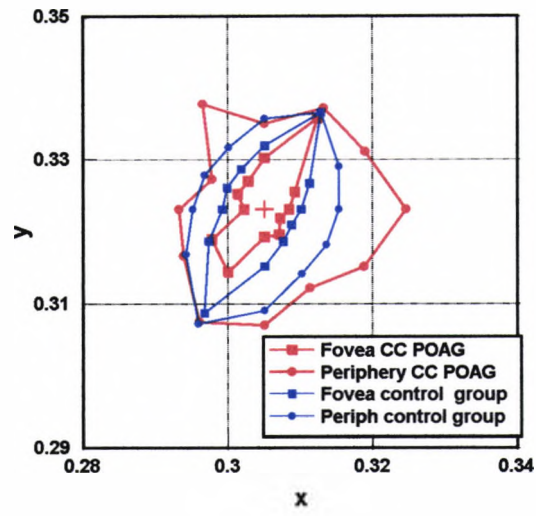
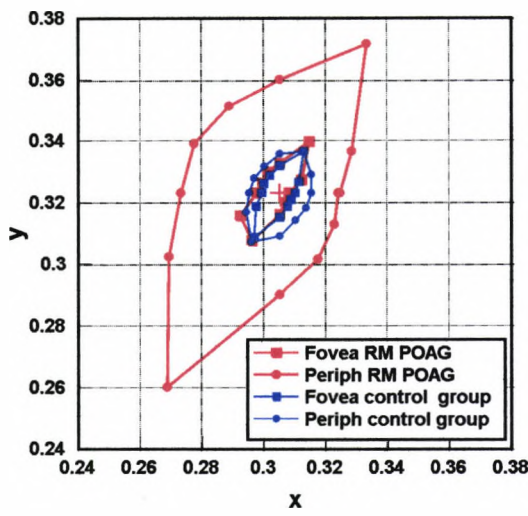
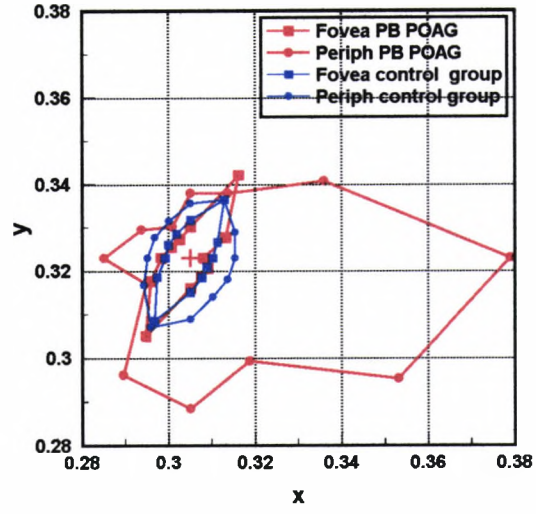
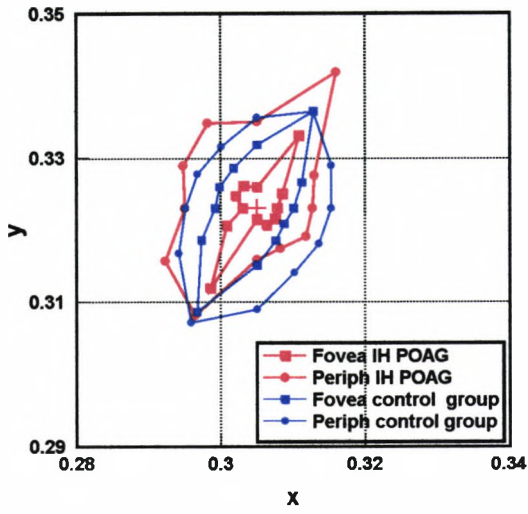
Pacheco-Cutillas, M. (1998). Los defectos de la visión del color en Glaucoma. *Archivos Optometricos* **2**, 107-126.

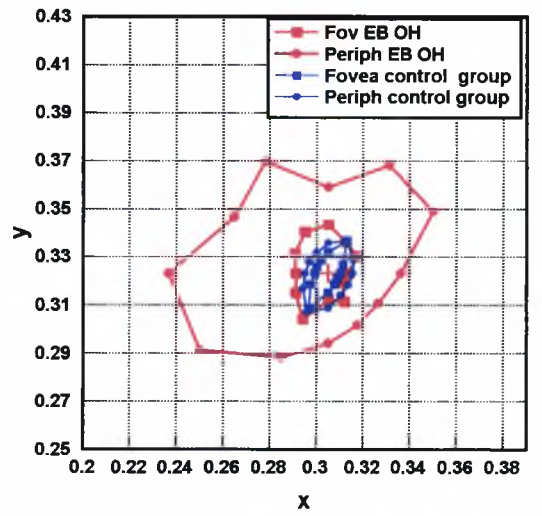
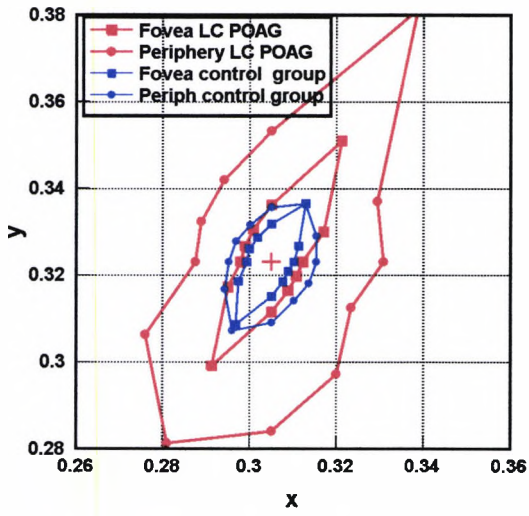
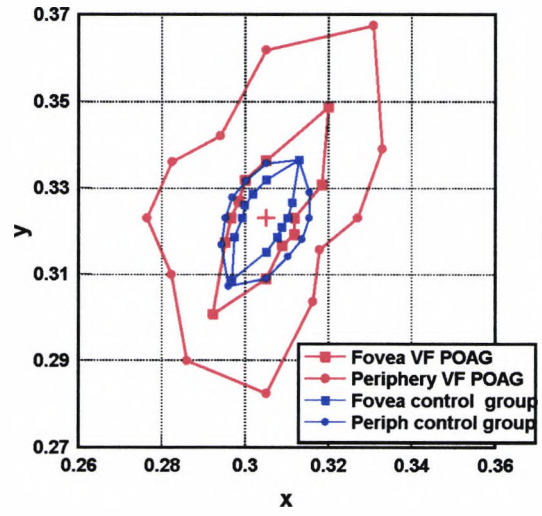
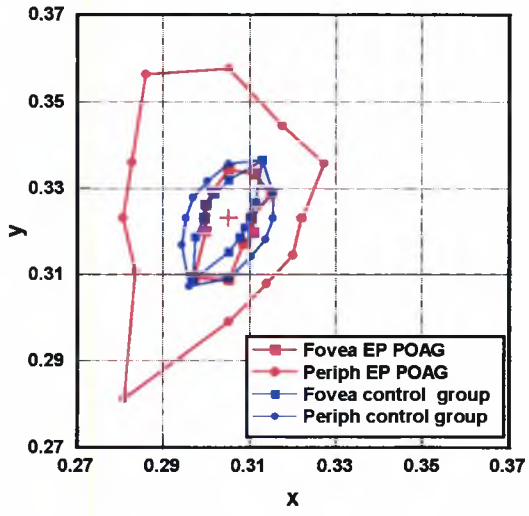
8.2 Individual CD ellipses' cases

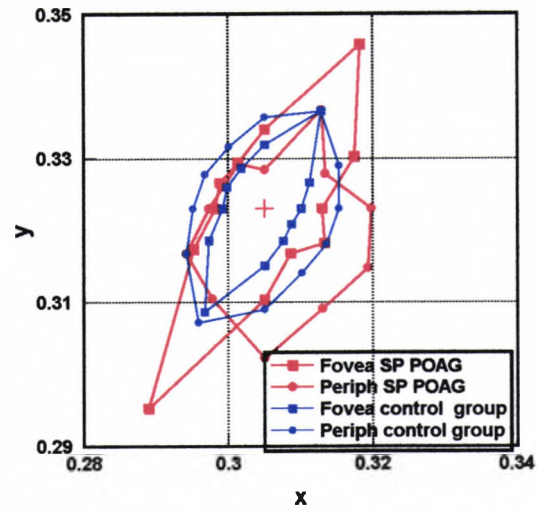
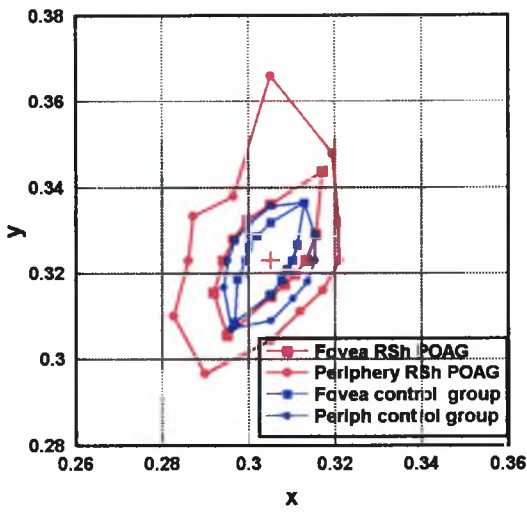
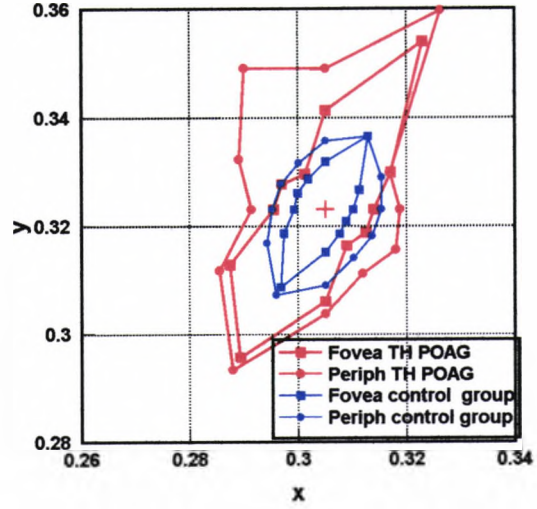
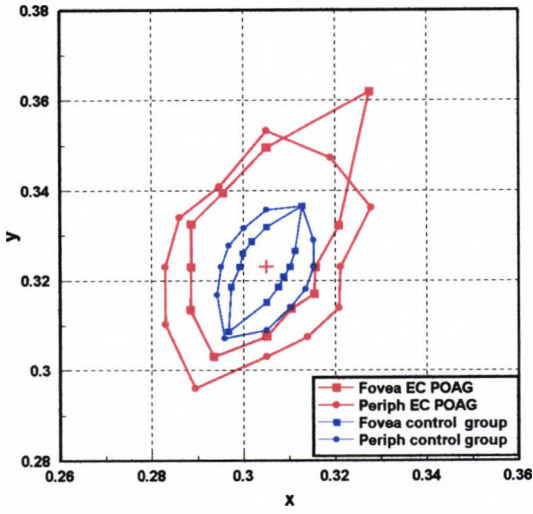


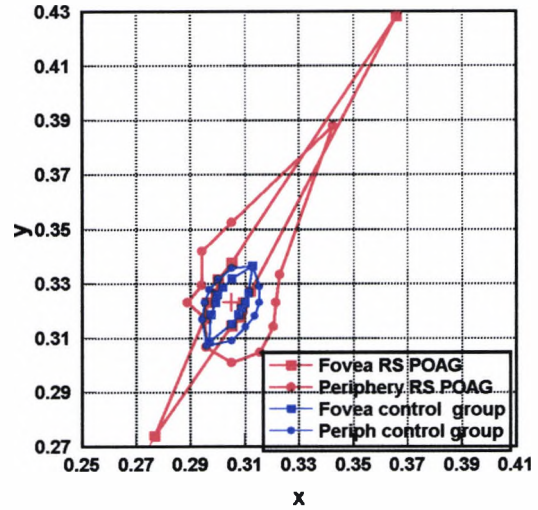
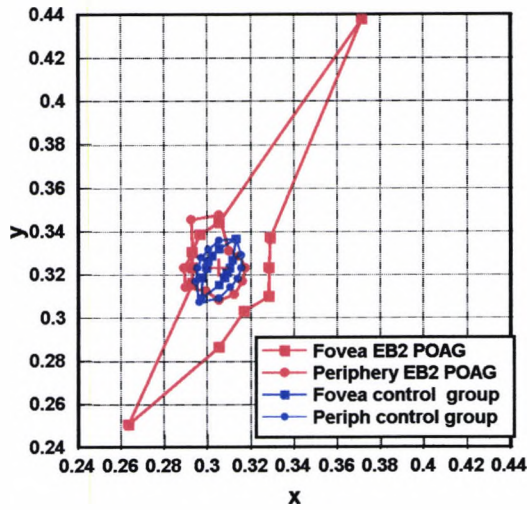
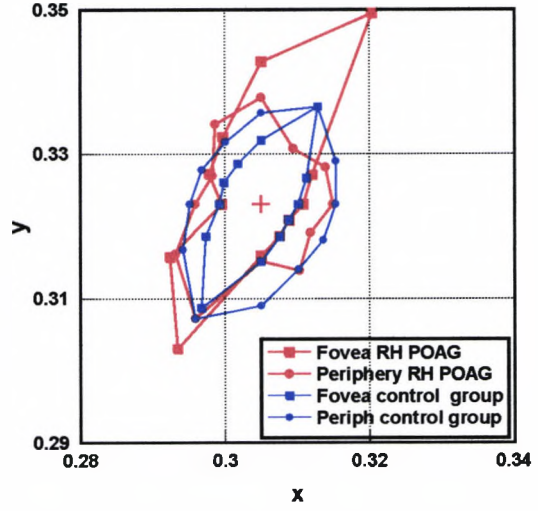
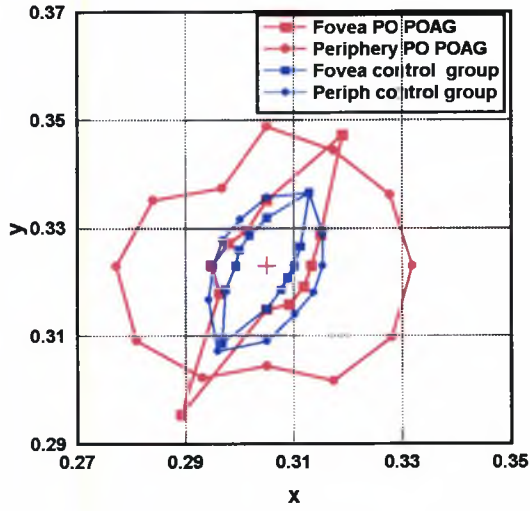












9 Reference list

- Adams, A. J., Rodic, R., Husted, R., & Stamper, R. (1982). Spectral sensitivity and color discrimination changes in glaucoma and glaucoma-suspect patients. *Investigative Ophthalmology Visual Science* **23**, 516-524.
- Airaksinen, P. J. (1989). Retinal Nerve Fiber Layer and Neuroretinal Rim Changes in Ocular Hypertension and Early Glaucoma (Summary). *Surv.Ophthalmol.* **33**, 413-414.
- Alvarez, S. L., Pierce, G. E., Vingrys, A. J., Benes, S. C., Weber, P. A., & KingSmith, P. E. (1997). Comparison of red-green, blue-yellow and achromatic losses in glaucoma. *Vision Research* **37**, 2295-2301.
- Ancil, J. L. & Anderson, D. R. (1984). Early foveal involvement and generalized depression of the visual field in glaucoma. *Arch.Ophthalmol.* **102**, 363-370.
- Anderson, D. R. (1987). *Perimetry, With and Without Automation*, 2nd ed. C.V. Mosby, Co., St. Louis.
- Arden, G., Gunduz, K., & Perry, S. (1988). Color vision testing with a computer graphics system: preliminary results. *Doc.Ophthalmol.* **69**, 167-174.
- Arden, G. B. & Jacobson, J. J. (1978). A simple grating test for contrast sensitivity: preliminary results indicate value in screening for glaucoma. *Invest.Ophthalmol Vis.Sci.* **17**, 23-32.
- Artal, P., Ferro, M., Miranda, I., & Navarro, R. (1993). Effects of aging in retinal image quality. *J Opt.Soc.Am.A.* **10**, 1656-1662.
- Atkin, A., Bodis-Wollner, I., Wolkstein, M., Moss, A., & Podos, S. M. (1978). Abnormalities of central contrast sensitivity in glaucoma. *Am J Ophth* 201-211.
- Austin, D. J. (1974). Acquired color vision defects in patients suffering from chronic simple glaucoma. *Trans Ophthalmol.Soc.of the UK.* **94**, 880-883.
- Baker, G. (2000). Visual pathways. Part II. *Optometry Today* **10th March**, 37-41.
- Barbur, J. L. (2004). 'Double-blindsight' revealed through the processing of color and luminance contrast defined motion signals. *Prog.Brain Res.* **144**, 243-259.
- Barbur, J. L., Birch, J., & Harlow, J. (1993). Colour vision testing using spatiotemporal luminance masking: psychophysical and pupillometric methods. In *Colour Vision Deficiencies XI*, ed. Drum, B., pp. 417-426. Kluwer Academic Publishers, Netherlands.
- Barbur, J. L., Harlow, A. J., & Plant, G. T. (1994). Insights into the different exploits of colour in the visual cortex. *Proc.R.Soc.Lond.B.Biol.Sci.* **258**, 327-334.

Barbur, J. L., Harlow, J. A., & Rodriguez-Carmona, M. A new Colour Assessment and Diagnosis (CAD) test for measuring changes in chromatic sensitivity (in preparation). 2005.

Barton, J. J., Rizzo, M., Nawrot, M., & Simpson, T. (1996). Optical blur and the perception of global coherent motion in random dot cinematograms. *Vision Res.* **36**, 3051-3059.

Beirne, R. O., Logan, J. F., Zlatkova, M. B., Jackson, A. J., Rankin, S. J., Demirel, S., & Anderson, R. S. (2003). Peripheral resolution for achromatic and SWS gratings in early to moderate glaucoma and the implications for selective ganglion cell density loss. *Invest Ophthalmol Vis. Sci.* **44**, 4780-4786.

Bill, A. (1993). Vascular physiology of the optic nerve. In *The optic nerve in glaucoma*, eds. Varma, R. & Spaeth, G. L., pp. 37-50. Lippincott Co., Philadelphia.

Bilodeau, L. & Faubert, J. (1997). Isoluminance and chromatic motion perception throughout the visual field. *Vision Res.* **37**, 2073-2081.

Birch, J. (1991). Colour Vision Tests: General Classification. In *Inherited and Acquired Colour Vision Deficiencies*, ed. Foster, D. H., pp. 215-234. MacMillan Press.

Birch, J. (1993). Acquired colour vision defects. In *Diagnosis of Defective Colour Vision*, ed. Butterworth-Heinemann, pp. 140-167. Oxford University Press.

Birch, J., Barbur, J. L., & Harlow, A. J. (1992). New method based on random luminance masking for measuring isochromatic zones using high resolution colour displays. *Ophthalmic Physiol. Opt.* **12**, 133-136.

Bodis-Wollner, I. & Brannan, J. R. (1994). Assessment of current visual psycho-physical testing methods with special reference to primary open angle glaucomatous disease (POAGD). *Neuro-ophthalmology* **14**, 61-71.

Bowmaker, J. K. & Dartnall, H. J. (1980). Visual pigments of rods and cones in a human retina. *J Physiol.* **298**, 501-511.

Breton, M. E. & Krupin, T. (1987). Age covariance between 100-hue color scores and quantitative perimetry in primary open angle glaucoma. *Archives Of Ophthalmology* **105**, 642-645.

Brody, H. (1955). Organization of the cerebral cortex. III. A study of aging in the human cerebral cortex. *J Comp Neurol.* **102**, 511-516.

Bron, A. J. & Caird, F. I. (1997). Loss of vision in the ageing eye. Research into Ageing Workshop, London, 10 May 1995. *Age Ageing* **26**, 159-162.

Brubaker, R. F. (1996). Delayed functional loss in glaucoma. LII Edward Jackson Memorial Lecture. *Am. J Ophthalmol* **121**, 473-483.

- Bruce, V. & Green, P. R. (1990). *Visual perception, physiology, psychology and ecology*, 2nd ed. Erlbaum, Hove.
- Bullimore, M. A., Wood, J. M., & Swenson, K. (1993). Motion perception in glaucoma. *Invest. Ophthalmol Vis. Sci.* **34**, 3526-3533.
- Burton, K. B., Owsley, C., & Sloane, M. E. (1993). Aging and neural spatial contrast sensitivity: photopic vision. *Vision Res.* **33**, 939-946.
- Calkins, D. J., Schein, S. J., Tsukamoto, Y., & Sterling, P. (1995). Ganglion cell circuits in primate fovea. In *Colour Vision Deficiencies XII*, ed. Drum, B., pp. 267-274. Kluwer Academic Publishers, Dordrecht.
- Calkins, D. J. & Sterling, P. (1996). Absence of spectrally specific lateral inputs to mid-ganglion cells in primate retina. *Nature* **381**, 613-615.
- Calkins, D. J., Tsukamoto, Y., & Sterling, P. (1998a). Microcircuitry and mosaic of a blue-yellow ganglion cell in the primate retina. *J Neurosci.* **18**, 3373-3385.
- Calkins, D. J., Tsukamoto, Y., & Sterling, P. (1998b). Microcircuitry and mosaic of a blue-yellow ganglion cell in the primate retina. *J Neurosci.* **18**, 3373-3385.
- Caprioli, J., Sears, M., & Miller, J. M. (1987). Patterns of early visual field loss in open-angle glaucoma. *Am J Ophthalmol* **103**, 512-517.
- Cartwright, M. J. & Anderson, D. R. (1988). Correlation of asymmetric damage with asymmetric intraocular pressure in normal-tension glaucoma (low-tension glaucoma). *Arch. Ophthalmol* **106**, 898-900.
- Casson, E. J., Johnson, C. A., & Shapiro, L. R. (1993). Longitudinal comparison of temporal-modulation perimetry with white-on-white and blue-on-yellow perimetry in ocular hypertension and early glaucoma. *J Opt. Soc. Am. A* **10**, 1792-1806.
- Castelo-Branco, M., Faria, P., Forjaz, V., Kozak, L. R., & Azevedo, H. (2004). Simultaneous comparison of relative damage to chromatic pathways in ocular hypertension and glaucoma: correlation with clinical measures. *Invest Ophthalmol Vis. Sci.* **45**, 499-505.
- Chibret, J. B. P. L. (1887). Contribution a l'etude du sens chromatique au moyen du chromatophotometre de Colardeau. Izarn et Dr. Chibret. *Revue Generale d'Ophthalmologie* **29**, 49-59.
- Chylack, L. T., Wolfe, J. K., Singer, D. M., Leske, M. C., Bullimore, M. A., Bailey, I. L., Friend, J., McCarthy, D., & Wu, S. (1993). The Lens Opacities Classification System III. *Arch. Ophthalmol.* **111**, 831-836.
- Cicerone, C. M. & Nerger, J. L. (1989). The relative numbers of long-wavelength-sensitive to middle-wavelength-sensitive cones in the human fovea centralis. *Vision Res.* **29**, 115-128.

Cleland, B. G., Dubin, M. W., & Levick, W. R. (1971). Sustained and transient neurones in the cat's retina and lateral geniculate nucleus. *J Physiol.* **217**, 473-496.

Coffey, M., Reidy, A., Wormald, R., Xian, W. X., Wright, L., & Courtney, P. (1993). Prevalence of glaucoma in the west of Ireland. *Br.J Ophthalmol* **77**, 17-21.

Cohen, A. I. (1992). The retina. In *Adler's physiology of the eye: clinical application*, ed. Hart W.M.Jr, pp. 579-615. Mosby, St. Louis, Missouri.

Crawford, M. L., Harwerth, R. S., Smith, E. L., III, Mills, S., & Ewing, B. (2001). Experimental glaucoma in primates: changes in cytochrome oxidase blobs in V1 cortex. *Invest Ophthalmol. Vis. Sci.* **42**, 358-364.

Crawford, M. L., Harwerth, R. S., Smith, E. L., Shen, F., & Carter-Dawson, L. (2000). Glaucoma in primates: cytochrome oxidase reactivity in parvo- and magnocellular pathways. *Invest. Ophthalmol Vis. Sci.* *2000.Jun.*; **41**(7.):1791.-802. **41**, 1791-1802.

Curcio, C. A., Allen, K. A., Sloan, K. R., Lerea, C. L., Hurley, J. B., Klock, I. B., & Milam, A. H. (1991). Distribution and morphology of human cone photoreceptors stained with anti-blue opsin. *J Comp. Neurol.* **312**, 610-624.

Curcio, C. A., Sloan, K. R., Kalina, R. E., & Hendrickson, A. E. (1990). Human photoreceptor topography. *J Comp. Neurol.* **292**, 497-523.

Dacey, D. M. (1996). Circuitry for color coding in the primate retina. *Proc. Natl. Acad. Sci. U. S. A.* **93**, 582-588.

Dacey, D. M. (1999). Primate retina: cell types, circuits and color opponency. *Prog. Retin. Eye Res.* **18**, 737-763.

Dacey, D. M. (2000). Parallel pathways for spectral coding in primate retina. *Annu. Rev. Neurosci.* *2000.*; **23**(4.):743.-75. **23**, 743-775.

Dacey, D. M. & Lee, B. B. (1994). The "blue on" opponent pathway in primate retina originates from a distinct bistratified ganglion type. *Nature* **367**, 731-735.

Dandona, L., Quigley, H. A., Brown, A. E., & Enger, C. (1990). Quantitative regional structure of the normal human lamina cribrosa. A racial comparison. *Arch. Ophthalmol* **108**, 393-398.

De Monasterio, F. M. (1978). Properties of concentrically organized X and Y ganglion cells of macaque retina. *J Neurophysiol.* **41**, 1394-1417.

De Monasterio, F. M. & Gouras, P. (1975). Functional properties of ganglion cells of the rhesus monkey retina. *J Physiol.* **251**, 167-195.

De Monasterio, F. M., McCrane, E. P., Newlander, J. K., & Schein, S. J. (1985). Density profile of blue-sensitive cones along the horizontal meridian of macaque retina. *Invest. Ophthalmol Vis. Sci.* **26**, 289-302.

- Derrington, A. M., Krauskopf, J., & Lennie, P. (1984). Chromatic mechanisms in lateral geniculate nucleus of macaque. *J Physiol.* **357**, 241-265.
- Derrington, A. M. & Lennie, P. (1984). Spatial and temporal contrast sensitivities of neurones in lateral geniculate nucleus of macaque. *J Physiol.* **357**, 219-240.
- Desimone, R. & Schein, S. J. (1987). Visual properties of neurons in area V4 of the macaque: sensitivity to stimulus form. *J Neurophysiol.* **57**, 835-868.
- Devos, M., Devos, H., Spileers, W., & Arden, G. B. (1995). Quadrant analysis of peripheral color contrast thresholds can be of significant value in the interpretation of minor visual- field alterations in glaucoma suspects. *Eye* **9**, 751-756.
- Dielemans, I., Vingerling, J. R., Wolfs, R. C., Hofman, A., Grobbee, D. E., & de Jong, P. T. (1994). The prevalence of primary open-angle glaucoma in a population-based study in The Netherlands. The Rotterdam Study. *Ophthalmology.* **101**, 1851-1855.
- Dowling, J. E. (1987). *The retina: an approachable part of the brain*. Belknap Press of Harvard University Press.
- Dowling, J. E. (1990). Functional and pharmacological organization of the retina: dopamine, interplexiform cells, and neuromodulation. In *Vision and the brain*, ed. Cohen, B. B.-W. I., pp. 1-18. Raven Press Ltd, New York.
- Drance, S. M. (1985). The early structural and functional disturbances of chronic open-angle glaucoma. *Ophthalmology* **92**, 853-857.
- Drance, S. M. (1989). Glaucomatous visual field defects. In *The Glaucomas*, eds. Rich, R., Shields, M. B., & Krupin, T., pp. 393-402. CV Mosby, St. Louis, MO, USA.
- Drance, S. M. (1992). Bowman Lecture. Glaucoma -changing concepts. *Eye* **6 (Pt 4)**, 337-345.
- Drance, S. M. (1997). Glaucoma: a look beyond intraocular pressure. *Am.J Ophthalmol* **123**, 817-819.
- Drance, S. M., Douglas, G. R., Airaksinen, P. J., Schulzer, M., & Hitchings, R. A. (1987). Diffuse visual field loss in chronic open-angle and low-tension glaucoma. *Am.J Ophthalmol* **104**, 577-580.
- Drance, S. M. & Lakowski, R. (1983). Colour vision in glaucoma. In *Glaucoma update*, eds. Krieglstein, GK. & Leydecker, W., pp. 117-121. Springer-Verlag, Berlin.
- Drance, S. M., Lakowski, R., Schulzer, M., & Douglas, G. R. (1981). Acquired color vision changes in glaucoma. Use of 100-hue test and Pickford anomaloscope as predictors of glaucomatous field change. *Arch.Ophthalmol.* **99**, 829-831.
- Elliott, D., Whitaker, D., & MacVeigh, D. (1990). Neural contribution to spatiotemporal contrast sensitivity decline in healthy ageing eyes. *Vision Res* **30**, 541-547.

Falcao-Reis, F., O'Donoghue, E., Buceti, R., Hitchings, R. A., & Arden, G. B. (1990). Peripheral contrast sensitivity in glaucoma and ocular hypertension. *Br.J.Ophthalmol.* **74**, 712-716.

Falcao-Reis, F. M., O'sullivan, F., Spileers, W., Hogg, C., & Arden, G. B. (1991). Macular color contrast sensitivity in ocular hypertension and glaucoma - evidence for 2 types of defect. *British Journal Of Ophthalmology* **75**, 598-602.

Fallowfield, L. & Krauskopf, J. (1984). Selective loss of chromatic sensitivity in demyelinating disease. *Investigative Ophthalmology Visual Science* **25**, 771-773.

Farber, D. B., Flannery, J. G., Lolley, R. N., & Bok, D. (1985). Distribution patterns of photoreceptors, protein, and cyclic nucleotides in the human retina. *Invest. Ophthalmol Vis. Sci.* **26**, 1558-1568.

Farnsworth, D. The Farnsworth-Munsell 100 hue and dichotomous tests for color vision. *J.Opt.Soc.Am.* **33**, 568-578. 1943.

Farnsworth, D. The Farnsworth dichotomous test for color blindness-Panel D-15. Psychological Corporation. 1947. New York.

Felius, J., de Jong, L. A., van den Berg, T. J., & Greve, E. L. (1995a). Functional characteristics of blue-on-yellow perimetric thresholds in glaucoma. *Investigative Ophthalmology & Visual Science* **36**, 1665-1674.

Felius, J., Vandenberg, T. J. T. P., & Spekrijse, H. (1995b). Peripheral cone contrast sensitivity in glaucoma. *Vision Research* **35**, 1791-1797.

Fiorentini, A., Porciatti, V., Morrone, M. C., & Burr, D. C. (1996). Visual ageing: unspecific decline of the responses to luminance and colour. *Vision Res.* **36**, 3557-3566.

Fitzgibbon, A., Pilu, M., & Fisher, R. B. Direct Least Square Fitting of Ellipses. *IEEE Transactions on Pattern Analysis and Machine Intelligence* **21**[5], 476-480. 1999.

Fitzke, F. W. (1988). Clinical psychophysics. *Eye*. **2 Suppl**, S233-S241.

Fitzke, F. W., Poinosawmy, D., Nagasubramanian, S., & Hitchings, R. A. Peripheral displacement thresholds in glaucoma and ocular hypertension. Heijl, A. *Perimetry Update*[Proceedings of the VIIIth International Perimetric Society Meeting], 399-405. 1989. Amsterdam, Berkeley, Milano, Kugler & Ghedini Publications.

Flammer, J. (2001). *Glaucoma: a guide for patients; an introduction for care-providers; a reference for quick information.*, 1st ed. Hans Huber, Bern.

Flammer, J. & Drance, S. M. (1984). Correlation between color vision scores and quantitative perimetry in suspected glaucoma. *Arch.Ophthalmol.* **102**, 38-39.

Flammer, J., Haefliger, I. O., Orgul, S., & Resink, T. (1999). Vascular dysregulation: a principal risk factor for glaucomatous damage? *J Glaucoma.* **8**, 212-219.

- Fletcher, R. J. A modified D-15 test. *Mod.Probl.Ophthalmol.* 11, 22-24. 1972.
- Francois, J. & Verriest, G. (1959). Les dyschromatopsies acquises dans les glaucome primaire. *Ann. Oculistique* **192**, 191-199.
- Fristrom, B. (1997). Peripheral colour contrast thresholds in ocular hypertension and glaucoma. *Acta Ophthalmol.Scand.* **75**, 376-382.
- Fristrom, B. (2002). Colour contrast sensitivity in ocular hypertension. A five-year prospective study. *Acta Ophthalmol Scand.* **80**, 155-162.
- Gaasterland, D. E., Ederer, F., Sullivan, E. K., Caprioli, J., & Cyrlin, M. N. (1994). Advanced Glaucoma Intervention Study. 2. Visual field test scoring and reliability. *Ophthalmology.* **101**, 1445-1455.
- Gherghel, D., Orgul, S., Gugleta, K., & Flammer, J. (2001). Retrobulbar blood flow in glaucoma patients with nocturnal over-dipping in systemic blood pressure. *Am.J Ophthalmol* 2001.Nov.;132.(5):641.-7. **132**, 641-647.
- Giaschi, D. E., Trope, G. E., Kothe, A. C., & Hong, X. H. (1996). Loss of sensitivity to motion-defined form in patients with primary open-angle glaucoma and ocular hypertension. *J.Opt.Soc.Am.A.* **13**, 707-715.
- Glovinsky, Y., Quigley, H. A., & Dunkelberger, G. R. (1991). Retinal Ganglion Cell Loss is Size Dependent in Experimental Glaucoma. *Investigative Ophthalmology & Visual Science* **32**, 484-491.
- Gouras, P. (1969). Antidromic responses of orthodromically identified ganglion cells in monkey retina. *J Physiol.* **204**, 407-419.
- Gouras, P. & Link, K. (1966). Rod and cone interaction in dark-adapted monkey ganglion cells. *J Physiol.* **184**, 499-510.
- Graham, S. L., Drance, S. M., Chauhan, B. C., Swindale, N. V., Hnik, P., Mikelberg, F. S., & Douglas, G. R. (1996). Comparison of psychophysical and electrophysiological testing in early glaucoma. *Invest.Ophthalmol Vis.Sci.* **37**, 2651-2662.
- Greenstein, V. C., Halevy, D., Zaidi, Q., Koenig, K. L., & Ritch, R. H. (1996). Chromatic and luminance systems deficits in glaucoma. *Vision Research* **36**, 621-629.
- Greenstein, V. C., Seliger, S., Zemon, V., & Ritch, R. (1998). Visual evoked potential assessment of the effects of glaucoma on visual subsystems. *Vision Res.* **38**, 1901-1911.
- Greenstein, V. C., Shapiro, A., Hood, D. C., & Zaidi, Q. (1993). Chromatic and luminance sensitivity in diabetes and glaucoma. *J.Optical Society Am A-Optics &* **10**, 1785-1791.
- Grigsby, S. S., Vingrys, A. J., Benes, S. C., & King-Smith, P. E. (1991). Correlation of chromatic, spatial, and temporal sensitivity in optic nerve disease. *Investigative Ophthalmology Visual Science* **32**, 3252-3262.

- Grutzner, P. (1972). Acquired color vision defects. In *Handbook of sensory Physiology*, eds. Jameson, D. & Hurvich, L. M., pp. 643-659. Springer Verlag, Berlin.
- Guirao, A., Gonzalez, C., Redondo, M., Geraghty, E., Norrby, S., & Artal, P. (1999). Average optical performance of the human eye as a function of age in a normal population. *Invest. Ophthalmol Vis. Sci.* **40**, 203-213.
- Gunduz, K., Arden, G. B., Perry, S., Weinstein, G. W., & Hitchings, R. A. (1988). Color vision defects in ocular hypertension and glaucoma. Quantification with a computer-driven color television system. *Arch. Ophthalmol.* **106**, 929-935.
- Haegerstrom-Portnoy, G. (1988). Short-wavelength-sensitive-cone sensitivity loss with aging: a protective role for macular pigment? *J Opt. Soc. Am. A* **5**, 2140-2144.
- Hamill, T. R., Post, R. B., Johnson, C. A., & Keltner, J. L. (1984). Correlation of color vision deficits and observable changes in the optic disc in a population of ocular hypertensives. *Arch. Ophthalmol.* **102**, 1637-1639.
- Hart, W. M., Jr. (1987). Acquired dyschromatopsias. *Surv. Ophthalmol.* **32**, 10-31.
- Hart, W. M., Jr., Hartz, R. K., Hagen, R. W., & Clark, K. W. (1984). Color contrast perimetry. *Investigative Ophthalmology Visual Science* **25**, 400-413.
- Hart, W. M., Jr., Silverman, S. E., Trick, G. L., Neshler, R., & GORDON, M. O. (1990). Glaucomatous visual field damage. Luminance and color-contrast sensitivities. *Investigative Ophthalmology Visual Science* **31**, 359-367.
- Hartwick, A. T. (2001). Beyond intraocular pressure: neuroprotective strategies for future glaucoma therapy. *Optom. Vis. Sci.* **78**, 85-94.
- Harwerth, R. S., Carter-Dawson, L., Shen, F., Smith, E. L., III, & Crawford, M. L. (1999a). Ganglion cell losses underlying visual field defects from experimental glaucoma. *Invest Ophthalmol Vis. Sci.* **40**, 2242-2250.
- Harwerth, R. S., Crawford, M. L., Frishman, L. J., Viswanathan, S., Smith, E. L., & Carter-Dawson, L. (2002). Visual field defects and neural losses from experimental glaucoma. *Prog. Retin. Eye Res.* **21**, 91-125.
- Harwerth, R. S., Smith, E. L., & Chandler, M. (1999b). Progressive visual field defects from experimental glaucoma: measurements with white and colored stimuli. *Optom. Vis. Sci.* **76**, 558-570.
- Heijl, A. (1985). Computerised perimetry. *Trans. Ophthalmol Soc. U.K.* **104 (Pt 1)**, 76-87.
- Hendry, S. H. & Yoshioka, T. (1994). A neurochemically distinct third channel in the macaque dorsal lateral geniculate nucleus. *Science* **264**, 575-577.

- Hennelly, M. L., Barbur, J. L., Edgar, D. F., & Woodward, E. G. (1998). The effect of age on the light scattering characteristics of the eye. *Ophthalmic Physiol.Opt.* **18**, 197-203.
- Hermes, D., Roth, A., & Borot, N. (1989). The two Equation Method II. Results in Retinal and Optic Nerve Disorders. In *Colour Vision Deficiencies IX.*, eds. B.Drum & G.Verriest, pp. 417-426. Kluwer Academic Publishers, Netherlands.
- Heron, G., Adams, A. J., & Husted, R. (1988). Central visual fields for short wavelength sensitive pathways in glaucoma and ocular hypertension. *Investigative Ophthalmology & Visual Science* **29**, 64-72.
- Heron, G., Erskine, N. A., Farquharson, E., Moore, A. T., & White, H. (1994). Color-vision screening in glaucoma - the tritan album and other simple tests. *Ophthalmic And Physiological Optics* **14**, 233-238.
- Hoffmann, A. & Menozzi, M. (1998). [Computer-based determination of red/green color vision defects]. *Biomed.Tech.(Berl)* **43**, 124-132.
- Holopigian, K., Seiple, W., Mayron, C., Koty, R., & Lorenzo, M. (1990). Electrophysiological and psychophysical flicker sensitivity in patients with primary open-angle glaucoma and ocular hypertension. *Invest Ophthalmol Vis.Sci.* **31**, 1863-1868.
- Horn, F. K., Bergua, A., Junemann, A., & Korth, M. (2000). Visual evoked potentials under luminance contrast and color contrast stimulation in glaucoma diagnosis. *J.Glaucoma.* **9**, 428-437.
- Horton, J. C. (1984). Cytochrome oxidase patches: a new cytoarchitectonic feature of monkey visual cortex. *Philos.Trans.R.Soc.Lond.B.Biol.Sci.* **304**, 199-253.
- Horton, J. C. (1992). The central visual pathways. In *Adler's physiology of the eye: clinical applicaltion*, ed. Hart W.M.Jr, Mosby, St. Louis, Missouri.
- Horton, J. C. & Hubel, D. H. (1981). Regular patchy distribution of cytochrome oxidase staining in primary visual cortex of macaque monkey. *Nature* **292**, 762-764.
- Hubel David H. (1998). *Eye, brain and vision* Scientific American Library.
- Hubel, D. H. & Wiesel, T. N. (1962). Receptive fields, binocular interaction and functional architecture in the cat's visual cortex. *J Physiol.* **160**, 160.
- Hubel, D. H. & Wiesel, T. N. (1968). Receptive fields and functional architecture of monkey striate cortex. *J Physiol.* **195**, 215-243.
- Hubel, D. H. & Wiesel, T. N. (1972). Laminar and columnar distribution of geniculo-cortical fibers in the macaque monkey. *J Comp.Neurol.* **146**, 421-450.
- Hubel, D. H., Wiesel, T. N., & Stryker, M. P. (1978). Anatomical demonstration of orientation columns in macaque monkey. *J Comp.Neurol.* **177**, 361-380.

Humanski, R. A. & Wilson, H. R. (1993). Spatial-frequency adaptation: evidence for a multiple-channel model of short-wavelength-sensitive-cone spatial vision. *Vision Res.* **33**, 665-675.

Ing, E. B., Parker, J. A., & Emerton, L. A. (1994). Computerized colour vision testing. *Can.J.Ophthalmol.* **29**, 125-128.

Jackson, G. R., Owsley, C., & McGwin, G. J. (1999). Aging and dark adaptation. *Vision Res* **39**, 3975-3982.

Johnson, C. A. (1995). The Glenn A. Fry Award Lecture. Early losses of visual function in glaucoma. *Optom. Vis. Sci.* **72**, 359-370.

Johnson, C. A. (1996). Standardizing the measurement of visual fields for clinical research: Guidelines from the Eye Care Technology Forum. *Ophthalmology* **103**, 186-189.

Johnson, C. A. (2001). Psychophysical measurement of glaucomatous damage. *Surv.Ophthalmol* **45**, 313-318.

Johnson, C. A., Adams, A. J., Casson, E. J., & Brandt, J. D. (1993a). Blue-on-yellow perimetry can predict the development of glaucomatous visual-field loss. *Archives Of Ophthalmology* **111**, 645-650.

Johnson, C. A., Adams, A. J., Casson, E. J., & Brandt, J. D. (1993b). Progression of early glaucomatous visual-field loss as detected by blue-on-yellow and standard white-on-white automated perimetry. *Archives Of Ophthalmology* **111**, 651-656.

Johnson, C. A. & Marshall, D. J. (1995). Aging effects for opponent mechanisms in the central visual field. *Optom. Vis. Sci.* **72**, 75-82.

Johnson, C. A. & Samuels, S. J. (1997). Screening for glaucomatous visual field loss with frequency-doubling perimetry. *Invest.Ophthalmol Vis.Sci.* **38**, 413-425.

Jonas J.B. & Nauman G.O.H. (1993). The optic nerve: Its embryology, Histology, and Morphology. In *The optic nerve in glaucoma*, eds. Varma, R. & Spaeth, G. L., pp. 3-26. Lippincott Co., Philadelphia.

Jonas, J. B. (1990). *Biomorphometrie des nervus optikus* Enke-Verlag, Stuttgart.

Jonas, J. B., Budde, W. M., & Panda-Jonas, S. (1999). Ophthalmoscopic evaluation of the optic nerve head. *Surv.Ophthalmol* **43**, 293-320.

Jonas, J. B., Gusek, G. C., & Naumann, G. O. (1988). Optic disc, cup and neuroretinal rim size, configuration and correlations in normal eyes. *Invest.Ophthalmol Vis.Sci.* **29**, 1151-1158.

Jonas, J. B., Muller-Bergh, J. A., Schlotzer-Schrehardt, U. M., & Naumann, G. O. (1990). Histomorphometry of the human optic nerve. *Invest.Ophthalmol Vis.Sci.* **31**, 736-744.

- Kaiser, P. K., Lee, B. B., Martin, P. R., & Valberg, A. (1990). The physiological basis of the minimally distinct border demonstrated in the ganglion cells of the macaque retina. *J Physiol.* **422**, 153-183.
- Kalloniatis, M., Harwerth, R. S., Smith, E. L., & Desantis, L. (1993). Color-vision anomalies following experimental glaucoma in monkeys. *Ophthalmic And Physiological Optics* **13**, 56-67.
- Kalmus, H., Luke, I., & Seeburgh, D. (1974). Impairment of colour vision in patients with ocular hypertension and glaucoma. *British Journal Of Ophthalmology* **58**, 922-926.
- Kaplan, E. & Shapley, R. M. (1986). The primate retina contains two types of ganglion cells, with high and low contrast sensitivity. *Proc.Natl.Acad.Sci.U.S.A.* **83**, 2755-2757.
- Katz, J., Gilbert, D., Quigley, H. A., & Sommer, A. (1997). Estimating progression of visual field loss in glaucoma. *Ophthalmology* **104**, 1017-1025.
- Kaushik, S., Pandav, S. S., & Ram, J. (2003). Neuroprotection in glaucoma. *J Postgrad.Med.* **49**, 90-95.
- Kelly, J. P., Fourman, S. M., & Jindra, L. F. (1996). Foveal color and luminance sensitivity losses in glaucoma. *Ophthalmic Surgery And Lasers* **27**, 179-187.
- Kerrigan-Baumrind, L. A., Quigley, H. A., Pease, M. E., Kerrigan, D. F., & Mitchell, R. S. (2000). Number of ganglion cells in glaucoma eyes compared with threshold visual field tests in the same persons. *Investigative Ophthalmology & Visual Science* **41**, 741-748.
- KingSmith, P. E. (1991). Psychophysical methods for the investigation of Acquired Colour Vision Deficiencies. In *Inherited and Acquired Colour Vision Deficiencies*, ed. Foster, D. H., pp. 38-55. MacMillan Press.
- KingSmith, P. E., Chioran, G. M., Sellers, K. L., & Alvarez, S. L. (1983). Normal and deficient colour discrimination analysed by colour television. In *Colour vision: Physiology and Psychophysics*, eds. Molon, J. D. & Sharpe, L. T., pp. 167-172. Academic Press, London.
- Kinnear, P. R. (1970). Proposals for scoring and assessing the 100-Hue test. *Vision Res.* **10**, 423-433.
- Kinnear, P. R. & Sahraie, A. (2002). New Farnsworth-Munsell 100 hue test norms of normal observers for each year of age 5-22 and for age decades 30-70. *Br.J Ophthalmol* **86**, 1408-1411.
- Klein, B. E., Klein, R., Sponsel, W. E., Franke, T., Cantor, L. B., Martone, J., & Menage, M. J. (1992). Prevalence of glaucoma. The Beaver Dam Eye Study. *Ophthalmology* **99**, 1499-1504.
- Knoblauch, K., Sundera F., Kusuda M, Hynes R, Podgor M, & Higgins KE (1987). Age and illuminance effects in the Farnsworth-Munsell 100-hue test. *Applied Optics* **26**, 1441-1448.
- Knoblauch, K., Vital-Durand, F., & Barbur, J. L. (2001). Variation of chromatic sensitivity across the life span. *Vision Res.* **41**, 23-36.

- Kolb, H. (1991). The neural organization of the human retina. In *Principles of Retinal Cell Biology. Principles and Practice of Clinical Electrophysiology of Vision.*, ed. Heckenlively, J. A. G. B., pp. 25-52. Mosby, Chicago.
- Kolb, H., Goede, P., & Roberts, S. (1997). Uniqueness of the S-cone pedicle in the human retina and consequences for colour processing. *J. Comp. Neurol.* **386**, 443-460.
- Kolbe, B. Geometrische Darstellung der Farbenblindheit. Buchdruckerei der Kaiserlichen Akademie der Wissenschaften . 1881. St Petersburg.
- Köllner, H. Ihre Klinische Bedeutung und ihre Diagnose. Die Störungen des Farbensinnes. 1912. Berlin, Karger.
- Krastel, H. & Moreland, J. D. (1991). Colour Vision Deficiencies in Ophthalmic Diseases. In *Inherited and Acquired Colour Vision Deficiencies*, ed. Foster, D. H., pp. 115-172. MacMillan Press.
- Krauskopf, J., Williams, D. R., & Heeley, D. W. (1982). Cardinal directions of color space. *Vision Res* **22**, 1123-1131.
- Kremers, J., Scholl, H. P., Knau, H., Berendschot, T. T., Usui, T., & Sharpe, L. T. (2000). L/M cone ratios in human trichromats assessed by psychophysics, electroretinography, and retinal densitometry. *J. Opt. Soc. Am. A. Opt. Image. Sci. Vis.* 2000. Mar.; **17**(3):517.-26. **17**, 517-526.
- Lachenmayr, B. J. (1994). The role of temporal threshold criteria in psychophysical testing in glaucoma. *Curr. Opin. Ophthalmol.* **5**, 58-63.
- Lachenmayr, B. J., Airaksinen, P. J., Drance, S. M., & Wijsman, K. (1991). Correlation of retinal nerve-fiber-layer loss, changes at the optic nerve head and various psychophysical criteria in glaucoma. *Graefes Arch. Clin. Exp. Ophthalmol* **229**, 133-138.
- Lachenmayr, B. J. & Drance, S. M. (1992). Central function and visual field damage in glaucoma. *Int. Ophthalmol.* **16**, 203-209.
- Lakowski, R. (1974). Effects of age on the 100-hue scores of red-green deficient subjects. *Mod. Probl. Ophthalmol.* **13**, 124-129.
- Lakowski, R., Bryett, J., & Drance, S. M. (1972). A study of colour vision in ocular hypertensives. *Canad. J. Ophthal.* **7**, 86-95.
- Lakowski, R. & Drance, S. M. (1979). Acquired dyschromatopsias. The earliest functional losses in glaucoma. *Doc Ophthal. Proc. S* **19**, 159-165.
- Laties, A. M. & Enoch, J. M. (1971). An analysis of retinal receptor orientation. I. Angular relationship of neighboring photoreceptors. *Invest. Ophthalmol* **10**, 69-77.
- Lee, B. B. (1996). Receptive Field Structure in the Primate Retina. Minireview. *Vision Res.* **36**, 631-644.

- Lee, B. B., Martin, P. R., & Valberg, A. (1988). The physiological basis of heterochromatic flicker photometry demonstrated in the ganglion cells of the macaque retina. *J Physiol.* **404**, 323-347.
- Lee, B. B., Pokorny, J., Smith, V. C., Martin, P. R., & Valberg, A. (1990). Luminance and chromatic modulation sensitivity of macaque ganglion cells and human observers. *J Opt. Soc. Am. A.* **7**, 2223-2236.
- Lennie, P., Krauskopf, J., & Sclar, G. (1990). Chromatic mechanisms in striate cortex of macaque. *J. Neurosci.* **10**, 649-669.
- Leventhal, A. G., Rodieck, R. W., & Dreher, B. (1981). Retinal ganglion cell classes in the Old World monkey: morphology and central projections. *Science* **213**, 1139-1142.
- Livingstone, M. S. & Hubel, D. H. (1984). Anatomy and physiology of a color system in the primate visual cortex. *J Neurosci.* **4**, 309-356.
- Livingstone, M. S. & Hubel, D. H. (1987). Psychophysical evidence for separate channels for the perception of form, color, movement, and depth. *J Neurosci.* **7**, 3416-3468.
- MacAdam, D. L. (1942). Visual sensitivities to color differences in daylight. *J. Opt. Soc. Am.* **32**, 247-281.
- MacLeod, D. I. & Boynton, R. M. (1979). Chromaticity diagram showing cone excitation by stimuli of equal luminance. *J Opt. Soc. Am.* **69**, 1183-1186.
- Maddess, T., Hemmi, J. M., & James, A. C. (1998). Evidence for spatial aliasing effects in the Y-like cells of the magnocellular visual pathway. *Vision Research* **38**, 1843-1859.
- Maddess, T., James, A. C., Goldberg, I., Wine, S., & Dobinson, J. (2000). A Spatial Frequency-Doubling Illusion-Based Pattern Electroretinogram for Glaucoma. *Investigative Ophthalmology Visual Science* **41**, 3818-3826.
- Mariani, A. P. (1984). The neuronal organisation of the outer plexiform layer of the primate retina. *International Review of Cytology* 285-320.
- Martin, P. R., White, A. J., Goodchild, A. K., Wilder, H. D., & Sefton, A. E. (1997). Evidence that blue-on cells are part of the third geniculocortical pathway in primates. *Eur. J Neurosci.* **9**, 1536-1541.
- Mason C. & Kandel E.R. (1992). Central Visual Pathways. In *Principles of Neural Science*, eds. Kandel E.R., Schwartz J.H., & Jessell T.M., pp. 421-439. Prentice Hall International Inc..
- Maunsell, J. H., Nealey, T. A., & DePriest, D. D. (1990). Magnocellular and parvocellular contributions to responses in the middle temporal visual area (MT) of the macaque monkey. *J Neurosci.* **10**, 3323-3334.
- Merigan WH & Byrne CE, M. J. (1991). Does primate motion perception depend on the magnocellular pathway? *J Neurosci.* **11**, 3422-3429.

Merigan, W. H., Byrne, C. E., & Maunsell, J. H. (1991). Does primate motion perception depend on the magnocellular pathway? *J Neurosci.* **11**, 3422-3429.

Merigan, W. H. & Maunsell, J. H. (1993). How parallel are the primate visual pathways? *Annu.Rev.Neurosci.* **16**, 369-402.

Mikelberg, F. S., Schulzer, M., Drance, S. M., & Lau, W. (1986). The rate of progression of scotomas in glaucoma. *Am.J Ophthalmol* **101**, 1-6.

Minckler D.S. (1993). Neuronal damage in glaucoma. In *The optic nerve in glaucoma*, eds. Varma, R. & Spaeth, G. L., pp. 51-59. Lippincott Co., Philadelphia.

Minckler D.S. (1996). Neuronal damage in glaucoma. In *The optic nerve in glaucoma*, eds. Varma, R. & Spaeth, G. L., pp. 51-59. Lippincott Co., Philadelphia.

Minckler, D. S. (1980). The organization of nerve fiber bundles in the primate optic nerve head. *Arch.Ophthalmol* **98**, 1630-1636.

Minckler, D. S. (1986). Correlations between anatomic features and axonal transport in primate optic nerve head. *Trans.Am.Ophthalmol Soc.* **84**, 429-452.

Moreland, J. D. Analyses of Variance in Anomaloscope Matches. *Doc.Ophthalmol.Proc.Ser.* 39, 111-119. 1984.

Morgan, J., Caprioli, J., & Koseki, Y. (1999). Nitric oxide mediates excitotoxic and anoxic damage in rat retinal ganglion cells cocultured with astroglia. *Arch.Ophthalmol* **117**, 1524-1529.

Morgan, J. E. (2002). Retinal ganglion cell shrinkage in glaucoma. *J.Glaucoma.* **11**, 365-370.

Morgan, J. E., Uchida, H., & Caprioli, J. (2000). Retinal ganglion cell death in experimental glaucoma. *Br J Ophthalmol.* **84**, 303-310.

Moss, I. D., Wild, J. M., & Whitaker, D. J. (1995). The influence of age-related cataract on blue-on-yellow perimetry. *Investigative Ophthalmology & Visual Science* **36**, 764-773.

Motolko, M., Drance, S. M., & Douglas, G. R. (1982). The early psychophysical disturbances in chronic open-angle glaucoma. A study of visual functions with asymmetric disc cupping. *Arch.Ophthalmol.* **100**, 1632-1634.

Nickells, R. W. & Zack, D. J. (1996). Apoptosis in ocular disease: a molecular overview. *Ophthalmic Genet.* **17**, 145-165.

Obermayer, K. & Blasdel, G. G. (1993). Geometry of orientation and ocular dominance columns in monkey striate cortex. *J Neurosci.* **13**, 4114-4129.

Owsley, C., Sekuler, R., & Siemsen, D. (1983). Contrast sensitivity throughout adulthood. *Vision Res* **23**, 689-699.

-
- Oyster C.W (1999). *The human eye: structure and function*, 1 ed. Sinauer Associates, Sunderland, Mass.
- Pearson, P., Swanson, W. H., & Fellman, R. L. (2001). Chromatic and achromatic defects in patients with progressing glaucoma. *Vision Res.* **41**, 1215-1227.
- Perry, V. H., Oehler, R., & Cowey, A. (1984). Retinal ganglion cells that project to the dorsal lateral geniculate nucleus in the macaque monkey. *Neuroscience* **12**, 1101-1123.
- Peterson, B. B. & Dacey, D. M. (2000). Morphology of wide-field bistratified and diffuse human retinal ganglion cells. *Vis.Neurosci.* 2000.Jul.-Aug.;17.(4.):567.-78. **17**, 567-578.
- Pinckers, A. (1980). Color vision and age. *Ophthalmologica* **181**, 23-30.
- Pokorny J, Smith VC, & Lutzke M (1987). Aging of the human lens. *Applied Optics* **26**, 1437-1440.
- Pokorny, J., Smith, V. C., Verriest, G., & Pinckers, A. J. L. (1979). *Congenital and Acquired Colour Vision Defects* Grune and Stratton, New York.
- Porciatti, V., Di Bartolo, E., Nardi, N., & Fiorentini, A. (1997). Responses to chromatic and luminance contrast in glaucoma: a psychophysical and electrophysiological study. *Vision Res.* **37**, 1975-1987.
- Previc, F. H. (1990). Functional specialization in the lower and upper visual fields in humans - its ecological origins and neurophysiological implications. *Behavioural Brain Science* **13**, 519-541.
- Purpura, K., Kaplan, E., & Shapley, R. M. (1988). Background light and the contrast gain of primate P and M retinal ganglion cells. *Proc.Natl.Acad.Sci.U.S.A.* **85**, 4534-4537.
- Quigley, H. A. (1993). Open-Angle Glaucoma. *The New England Journal of Medicine* **328**, 1097-1106.
- Quigley, H. A. & Addicks, E. M. (1980). Chronic experimental glaucoma in primates. II. Effect of extended intraocular pressure elevation on optic nerve head and axonal transport. *Invest Ophthalmol Vis.Sci.* **19**, 137-152.
- Quigley, H. A., Addicks, E. M., & Green, W. R. (1982). Optic nerve damage in human glaucoma. III. Quantitative correlation of nerve fiber loss and visual field defect in glaucoma, ischemic neuropathy, papilledema, and toxic neuropathy. *Arch.Ophthalmol.* **100**, 135-146.
- Quigley, H. A., Dunkelberger, G. R., & Green, W. R. (1988). Chronic human glaucoma causing selectively greater loss of large optic nerve fibers. *Ophthalmology.* **95**, 357-363.
- Quigley, H. A., Dunkelberger, G. R., & Green, W. R. (1989). Retinal ganglion cell atrophy correlated with automated perimetry in human eyes with glaucoma. *Am.J.Ophthalmol.* **107**, 453-464.

- Quigley, H. A., Nickells, R. W., Kerrigan, L. A., Pease, M. E., Thibault, D. J., & Zack, D. J. (1995). Retinal ganglion cell death in experimental glaucoma and after axotomy occurs by apoptosis. *Invest Ophthalmol Vis.Sci.* **36**, 774-786.
- Quigley, H. A., Sanchez, R. M., Dunkelberger, G. R., L'Hernault, N. L., & Baginski, T. A. (1987). Chronic glaucoma selectively damages large optic nerve fibers. *Investigative Ophthalmology Visual Science* **28**, 913-920.
- Radius, R. L. & Bade, B. (1981). Pressure-induced optic nerve axonal transport interruption in cat eyes. *Arch.Ophthalmol* **99**, 2163-2165.
- Radius, R. L. & de Bruin, J. (1981). Anatomy of the retinal nerve fiber layer. *Invest.Ophthalmol Vis.Sci.* **21**, 745-749.
- Regan, B. C., Reffin, J. P., & Mollon, J. D. (1994). Luminance noise and the rapid determination of discrimination ellipses in colour deficiency. *Vision Res.* **34**, 1279-1299.
- Regan, D. & Neima, D. (1984). Balance between pattern and flicker sensitivities in the visual fields of ophthalmological patients. *Br.J Ophthalmol* **68**, 310-315.
- Repka, M. X. & Quigley, H. A. (1989). The effect of age on normal human optic nerve fiber number and diameter. *Ophthalmology.* **96**, 26-32.
- Rezaie, T., Child, A., Hitchings, R., Brice, G., Miller, L., Coca-Prados, M., Heon, E., Krupin, T., Ritch, R., Kreutzer, D., Crick, R. P., & Sarfarazi, M. (2002). Adult-onset primary open-angle glaucoma caused by mutations in optineurin. *Science* **295**, 1077-1079.
- Rodieck, R. W. (1998). *The first steps in seeing* Sinauer Associates Inc, Sunderland, Mass.
- Ross, J. E., Bron, A. J., & Clarke, D. D. (1984). Contrast sensitivity and visual disability in chronic simple glaucoma. *Br.J Ophthalmol* **68**, 821-827.
- Ruben, S. T., Hitchings, R. A., Fitzke, F. W., & Arden, G. B. (1994). Electrophysiology and psychophysics in ocular hypertension and glaucoma - evidence for different pathomechanisms in early glaucoma. *Eye* **8**, 516-520.
- Ruskell, G. (1988). Neurology of visual perception. In *Optometry*, ed. Edwards, K. L. R., pp. 3-24. Butterworths.
- Saari, J. (1992). The biochemistry of sensory transduction in vertebrate photoreceptors. In *Adler's physiology of the eye: clinical application*, ed. Hart W.M.Jr, pp. 460-484. Mosby, St Louis, Missouri.
- Sample, P. A., Bosworth, C. F., Blumenthal, E. Z., Girkin, C., & Weinreb, R. N. (2000). Visual function-specific perimetry for indirect comparison of different ganglion cell populations in glaucoma. *Invest.Ophthalmol Vis.Sci.* **41**, 1783-1790.

- Sample, P. A., Boynton, R. M., & Weinreb, R. (1988). Isolating the color vision loss in primary open-angle glaucoma. *Am.J.Ophthalmol.* **106**, 686-691.
- Sample, P. A., Martinez, G. A., & Weinreb, R. N. (1994). Short-wavelength automated perimetry without lens density testing. *Am.J.Ophthalmol.* **118**, 632-641.
- Sample, P. A., Taylor, J. D. N., Martinez, G. A., Lusky, M., & Weinreb, R. (1993). Short-wavelength color visual-fields in glaucoma suspects at risk. *American Journal Of Ophthalmology* **115**, 225-233.
- Sample, P. A. & Weinreb, R. (1992). Progressive color visual-field loss in glaucoma. *Investigative Ophthalmology & Visual Science* **33**, 2068-2071.
- Sample, P. A., Weinreb, R., & Boynton, R. M. (1986). Acquired dyschromatopsia in glaucoma. *Surv.Ophthalmol.* **31**, 54-64.
- Sanchez, R. M., Dunkelberger, G. R., & Quigley, H. A. (1986). The number and diameter distribution of axons in the monkey optic nerve. *Invest.Ophthalmol Vis.Sci.* **27**, 1342-1350.
- Schein, S. J. & De Monasterio, F. M. (1987). Mapping of retinal and geniculate neurons onto striate cortex of macaque. *J Neurosci.* **7**, 996-1009.
- Schiller, P. H. & Logothetis, N. K. (1990). The color-opponent and broad-band channels of the primate visual system. *Trends.Neurosci.* **13**, 392-398.
- Schiller, P. H. & Malpeli, J. G. (1978). Functional specificity of lateral geniculate nucleus laminae of the rhesus monkey. *J Neurophysiol.* **41**, 788-797.
- Sekiguchi, N., Williams, D. R., & Brainard, D. H. (1993). Efficiency in detection of isoluminant and isochromatic interference fringes. *J.Opt.Soc.Am.A* **10**, 2118-2133.
- Silveira, L. C., Lee, B. B., Yamada, E. S., Kremers, J., Hunt, D. M., Martin, P. R., & Gomes, F. L. (1999). Ganglion cells of a short-wavelength-sensitive cone pathway in New World monkeys: morphology and physiology. *Vis.Neurosci.* **16**, 333-343.
- Silverman, S. E., Trick, G. L., & Hart, W. M., Jr. (1990). Motion perception is abnormal in primary open-angle glaucoma and ocular hypertension. *Invest.Ophthalmol.Vis.Sci.* **31**, 722-729.
- Sing, N. M., Anderson, S. F., & Townsend, J. C. (2000). The normal optic nerve head. *Optom.Vis.Sci.* **77**, 293-301.
- Sokol, S., Domar, A., & Moskowitz, A. (1980). Utility of the Arden grating test in glaucoma screening: high false-positive rate in normals over 50 years of age. *Invest.Ophthalmol Vis.Sci.* **19**, 1529-1533.
- Sommer, A., Tielsch, J. M., Katz, J., Quigley, H. A., Gottsch, J. D., Javitt, J., & Singh, K. (1991). Relationship between intraocular pressure and primary open angle glaucoma among white and black Americans. The Baltimore Eye Survey. *Arch.Ophthalmol* **109**, 1090-1095.

- Spear, P. D. (1993). Neural bases of visual deficits during aging. *Vision Res.* **33**, 2589-2609.
- Sponsel, W. E., Arango, S., Trigo, Y., & Mensah, J. (1998). Clinical classification of glaucomatous visual field loss by frequency doubling perimetry. *Am.J Ophthalmol* **125**, 830-836.
- Spry, P. G. & Johnson, C. A. (2001). Senescent changes of the normal visual field: an age-old problem. *Optom. Vis. Sci.* **78**, 436-441.
- Stamper, R. L. (1989). Psychophysical changes in glaucoma. *Surv. Ophthalmol.* **33 Suppl**, 309-318.
- Stamper, R. L., Hsu-Winges, C., & Sopher, M. (1982). Arden contrast sensitivity testing in glaucoma. *Arch. Ophthalmol* **100**, 947-950.
- Steen, R., Whitaker, D., Elliott, D. B., & Wild, J. M. (1994). Age-related effects of glare on luminance and color contrast sensitivity. *Optom. Vis. Sci.* **71**, 792-796.
- Stiles, W. S. (1978). *Mechanisms of colour vision* Academic Press.
- Stone, E. M., Fingert, J. H., Alward, W. L., Nguyen, T. D., Polansky, J. R., Sunden, S. L., Nishimura, D., Clark, A. F., Nystuen, A., Nichols, B. E., Mackey, D. A., Ritch, R., Kalenak, J. W., Craven, E. R., & Sheffield, V. C. (1997). Identification of a gene that causes primary open angle glaucoma. *Science* **275**, 668-670.
- Thorell, L. G., De Valois, R. L., & Albrecht, D. G. (1984). Spatial mapping of monkey V1 cells with pure color and luminance stimuli. *Vision Res.* **24**, 751-769.
- Tielsch, J. M., Katz, J., Sommer, A., Quigley, H. A., & Javitt, J. C. (1994). Family history and risk of primary open angle glaucoma. The Baltimore Eye Survey. *Arch. Ophthalmol* **112**, 69-73.
- Tielsch, J. M., Sommer, A., Katz, J., Royall, R. M., Quigley, H. A., & Javitt, J. (1991). Racial variations in the prevalence of primary open-angle glaucoma. The Baltimore Eye Survey. *JAMA* **266**, 369-374.
- Trick, G. L. (1993). Visual dysfunction in normotensive glaucoma. *Doc. Ophthalmol.* **85**, 125-133.
- Trick, G. L., Steinman, S. B., & Amyot, M. (1995). Motion perception deficits in glaucomatous optic neuropathy. *Vision Res.* **35**, 2225-2233.
- Ts'o, D. Y. & Gilbert, C. D. (1988). The organization of chromatic and spatial interactions in the primate striate cortex. *J Neurosci.* **8**, 1712-1727.
- Tuck, M. W. & Crick, R. P. (1998). The age distribution of primary open angle glaucoma. *Ophthalmic Epidemiol.* **5**, 173-183.
- Tyler, C. W. (1981). Specific deficits of flicker sensitivity in glaucoma and ocular hypertension. *Invest. Ophthalmol Vis. Sci.* **20**, 204-212.

- van Norren, D. & Went, L. N. (1981). New test for the detection of tritan defects evaluated in two surveys. *Vision Research* **21**, 1303-1306.
- Verriest, G. (1963). Further studies on acquired deficiency of color discrimination. *Journal Of The Optical Society Of America A-Optics Image Science And Vision* **53**, 185-195.
- Verriest, G., Van Laethem, J., & Uvijls, A. (1982). A new assessment of the normal ranges of the Farnsworth-Munsell 100-hue test scores. *Am.J.Ophthalmol.* **93**, 635-642.
- Wandell B.A. (1995). *Foundations of vision* Sinauer Associates Inc, Sunderland, Mass.
- Wassle, H. & Boycott, B. B. (1991). Functional architecture of the mammalian retina. *Physiol.Rev.* **71**, 447-480.
- Weale, R. (1995). Why does the human visual system age in the way it does? *Exp.Eye Res.* **60**, 49-55.
- Weale, R. A. (1986). Retinal senescence. *Progress in Retinal Research* **5**, 53-73.
- Weinstein, J. M., Funsch, D., Page, R. B., & Brennan, R. W. (1982). Optic nerve blood flow and its regulation. *Invest.Ophthalmol Vis.Sci.* **23**, 640-645.
- Werner, J. S., Donnelly, S. K., & Kliegl, R. (1987). Aging and human macular pigment density. Appended with translations from the work of Max Schultze and Ewald Hering. *Vision Res.* **27**, 257-268.
- Werner, J. S., Peterzell, D. H., & Scheetz, A. J. (1990). Light, vision, and aging. *Optom. Vis. Sci.* **67**, 214-229.
- Westcott, M. C., Fitzke, F. W., & Hitchings, R. A. (1998). Abnormal motion displacement thresholds are associated with fine scale luminance sensitivity loss in glaucoma. *Vision Res.* **38**, 3171-3180.
- Whitaker, D. & Elliott, D. B. (1992). Simulating age-related optical changes in the human eye. *Doc Ophthalmol* **82**, 307-316.
- Wiesel, T. N. & Hubel, D. H. (1966). Spatial and chromatic interactions in the lateral geniculate body of the rhesus monkey. *J Neurophysiol.* **29**, 1115-1156.
- Wild, J. M., Moss, I. D., Whitaker, D., & Oneill, E. C. (1995). The statistical interpretation of blue-on-yellow visual-field loss. *Investigative Ophthalmology & Visual Science* **36**, 1398-1410.
- Williams, D. R., MacLeod, D. I., & Hayhoe, M. M. (1981). Foveal tritanopia. *Vision Res.* **21**, 1341-1356.
- Wojciechowski, R., Trick, G. L., & Steinman, S. B. (1995). Topography of the age-related decline in motion sensitivity. *Optom. Vis. Sci.* **72**, 67-74.

- Wood, J. L. & Lovie-Kitchin, J. E. (1993). Contrast sensitivity measurements in subjects with ocular hypertension. *Glaucoma* 110-116.
- Wright, W. D. (1952). The characteristics of Tritanopia. *J. Opt. Soc. Am.* **42**, 509-521.
- Yamagami, J., Koseki, N., & Araie, M. (1995). Color vision deficit in normal-tension glaucoma eyes. *Japanese Journal of Ophthalmology* **39**, 384-389.
- Yamazaki, Y., Drance, S. M., Lakowski, R., & Schulzer, M. (1988). Correlation between color vision and highest intraocular pressure in glaucoma patients. *Am. J. Ophthalmol.* **106**, 397-399.
- Yamazaki, Y., Lakowski, R., & Drance, S. M. (1989). A comparison of the blue color mechanism in high-tension and low-tension glaucoma. *Ophthalmology* **96**, 12-15.
- Yates, J. T., Leys, M. J., Green, M., Huang, W., Charlton, J., Reed, J., Di, B. Z., & Odom, J. V. (1998). Parallel pathways, noise masking and glaucoma detection: behavioral and electrophysiological measures. *Doc. Ophthalmol.* **95**, 283-299.
- Yu, T. C., Falcao-Reis, F. M., Spileers, W., & Arden, G. B. (1991). Peripheral color contrast - a new screening-test for preglaucomatous visual-loss. *Investigative Ophthalmology & Visual Science* **32**, 2779-2789.
- Zeki, S. M. (1973). Colour coding in rhesus monkey prestriate cortex. *Brain Res.* **53**, 422-427.
- Zeki, S. M. (1974). Functional organization of a visual area in the posterior bank of the superior temporal sulcus of the rhesus monkey. *J. Physiol.* **236**, 549-573.
- Zlatkova, M. B., Coulter, E., & Anderson, R. S. (2003). Short-wavelength acuity: blue-yellow and achromatic resolution loss with age. *Vision Res* **43**, 109-115.